



**MONASH University**

**Synthesis of Structural and Fluorescently Labelled  
Peptidic Ligands for Optical  
Imaging of G Protein-Coupled Receptors**

Mengjie Liu

Master of Pharmaceutical Sciences

A thesis submitted for the degree of Doctor of Philosophy  
at Monash University in 2016

Department of Medicinal Chemistry and Drug Action  
Monash Institute of Pharmacy and Pharmaceutical Sciences

---

# Table of Contents

Copyright Notice .....	II
Abstract.....	III
Declaration .....	V
Publications During Enrolment.....	VI
Thesis Including Published Works Declaration.....	VI
Acknowledgements .....	VIII
Abbreviations .....	IX
Amino Acid Nomenclature .....	XI

## **Copyright Notice**

© The author (2016). Except as provided in the Copyright Act 1968, this thesis may not be reproduced in any form without the written permission of the author.

I certify that I have made all reasonable efforts to secure copyright permissions for third-party content included in this thesis and have not knowingly added copyright content to my work without the owner's permission.

# Abstract

Fluorescence imaging is capable of facilitating highly specific and non-invasive investigation of cellular and molecular events both *in vitro* and *in vivo*. Fluorescently labelled peptidic ligands are useful in studying the location, distribution, trafficking and functions of G protein-coupled receptors (GPCRs). Although GPCRs are popular targets in modern target-oriented drug design, many of them have not been therapeutically exploited. An effective strategy in preparing such ligands is to conjugate fluorophores to high-affinity and selective peptide analogues that are derived from the endogenous peptides. This thesis describes the synthesis and pharmacological properties of structural and fluorescent peptide analogues that target the GPCRs of interest. Their usefulness as receptor optical imaging agents has been verified in selected analogues.

Chapter 1 describes the advantages of using fluorescently labelled peptides as optical imaging agents in studying GPCRs, and provides an overview of the key steps and considerations in designing such peptides. To support our ideas, a table containing representative examples of literature-documented fluorescently labelled peptides that target GPCRs is included.

Chapter 2 demonstrates the application of various synthesis strategies in preparing structural and fluorescent peptide analogues derived from the two endogenous neuropeptides: ghrelin and kisspeptin. Specifically, we have verified the effectiveness of standard Fmoc-based solid phase synthesis, use of orthogonal protecting groups and fluorophore conjugation in both solid and solution phase, which have resulted in fluorescently labelled ghrelin and kisspeptin analogues useful in visualising their corresponding receptors.

Chapter 3 and 4 describe utility of the verified synthesis strategies in preparing fluorescently labelled peptides that target neuropeptide Y (NPY) receptors. Chapter 3 presents synthesis and pharmacological evaluation of ligands derived from the modified NPY C-terminal 9-amino acid fragment BVD-15 scaffold (Ile-Asn-Pro-Ile-Tyr-Arg-Leu-Arg-Tyr-NH<sub>2</sub>). Fluorescence labelling



was attempted at the 3-position via propargyloxypyrrolidine, and the 2- and 4-position via Lys or Lys(azide). We have found that the 2-position labelled analogue [Lys(sCy5)<sup>2</sup>, Arg<sup>4</sup>]BVD-15 exhibited Y<sub>1</sub>R antagonism and Y<sub>4</sub>R agonism, and it represents a novel ligand useful in imaging studies of these receptors. Chapter 4 presents synthesis and pharmacological evaluation of Y<sub>4</sub> receptor ligands derived from the Y<sub>4</sub>R agonist BVD-74D, a dimeric peptide comprised of two Tyr-Arg-Leu-Arg-Tyr-NH<sub>2</sub> monomers cross-linked by a 2,7-diaminosuberoyl group. We have shown the synthesis strategies towards the two optically pure BVD-74D stereoisomers and their structural and mono-labelled fluorescent analogues, by exploiting cross metathesis between suitably protected allylglycine residues with the desired stereo-configuration. We have found that the (*R,R*)-stereoisomer exhibited stronger Y<sub>4</sub>R affinity and agonism. Importantly, the fluorescent analogue mono-sCy5-(*R,R*)-BVD-74D retained the pharmacological profiles of the unlabelled parent compound, and represents a novel ligand useful in imaging studies of Y<sub>4</sub>R.

Chapter 5 summarises the achievement presented in this thesis, and provides future directions in the relevant areas.

## Declaration

This thesis contains no material which has been accepted for the award of any other degree or diploma at any university or equivalent institution and that, to the best of my knowledge and belief, this thesis contains no material previously published or written by another person, except where due reference is made in the text of the thesis.



Signature: .....

Print Name: ..... Mengjie Liu

Date: ..... 27/09/2016

## Publications During Enrolment

- Liu, M., Richardson, R. R., Mountford, S. J., Zhang, L., Tempone, M. H., Herzog, H., Holliday, N. D., and Thompson, P. E. (2016) Identification of a Cyanine-Dye Labeled Peptidic Ligand for Y<sub>1</sub>R and Y<sub>4</sub>R, Based upon the Neuropeptide Y C-Terminal Analogue, BVD-15. *Bioconjug. Chem.* 27, 2166-2175.
- Liu, M., Mountford, S. J., Richardson, R. R., Groenen, M., Holliday, N. D., and Thompson, P. E. (2016) Optically Pure, Structural, and Fluorescent Analogues of a Dimeric Y<sub>4</sub> Receptor Agonist Derived by an Olefin Metathesis Approach. *J. Med. Chem.* 59, 6059–6069.
- Camerino, M. A., Liu, M., Moriya, S., Kitahashi, T., Mahgoub, A., Mountford, S. J., Chalmers, D. K., Soga, T., Parhar, I. S., and Thompson, P. E. (2016) Beta amino acid-modified and fluorescently labelled kisspeptin analogues with potent KISS1R activity. *J. Pept. Sci.* 22, 406-414.
- Mountford, S. J., Liu, M., Zhang, L., Groenen, M., Herzog, H., Holliday, N. D., and Thompson, P. E. (2014) Synthetic routes to the Neuropeptide Y Y<sub>1</sub> receptor antagonist 1229U91 and related analogues for SAR studies and cell-based imaging. *Org. Biomol. Chem.* 12, 3271-3281.
- Northfield, S. E., Mountford, S. J., Wielens, J., Liu, M., Zhang, L., Herzog, H., Holliday, N. D., Scanlon, M. J., Parker, M. W., Chalmers, D. K., and Thompson, P. E. (2015) Propargyloxypyrrolidine regio- and stereoisomers for click-conjugation of peptides: synthesis and application in linear and cyclic peptides. *Aust. J. Chem.* 68, 1365-1372.
- Wootten, D., Reynolds, C. A., Smith, K. J., Mobarec, J. C., Koole, C., Savage, E., Pabreja, K., Simms, J., Sridhar, R., Furness, S. G. B., Liu, M., Thompson, P. E., Miller, L. J., Christopoulos, A., and Sexton, P. M. (2016) The Extracellular Surface of the GLP-1 Receptor is a Molecular Trigger for Biased Agonism. *Cell.* 165, 1632-1643.

## Thesis Including Published Works Declaration

I hereby declare that this thesis contains no material which has been accepted for the award of any other degree or diploma at any university or equivalent institution and that, to the best of my knowledge and belief, this thesis contains no material previously published or written by another person, except where due reference is made in the text of the thesis.

This thesis includes two original papers published in peer reviewed journals. The core theme of the thesis is: Synthesis of fluorescently labelled peptidic ligands for optical imaging of G protein-coupled receptors. The ideas, development and writing up of all the papers in the thesis were the principal responsibility of myself, the student, working within the Department of Medicinal Chemistry and Drug Action, Monash Institute of Pharmacy and Pharmaceutical Sciences, Monash University, under the supervision of Assoc Prof Philip Thompson and Dr Simon Mountford.

The inclusion of co-authors reflects the fact that the work came from active collaboration between researchers and acknowledges input into team-based research.

In the case of Chapter 3 and 4, my contribution to the work involved the following:

Thesis Chapter	Publication Title	Status	Nature and % of student contribution	Co-author name(s) Nature and % of Co-author's contribution*	Co-author(s), Monash student Y/N*
3	Identification of a Cyanine-Dye Labeled Peptidic Ligand for Y <sub>1</sub> R and Y <sub>4</sub> R, Based upon the Neuropeptide Y C-Terminal Analogue, BVD-15.	Published	50% - all chemistry, writing	Rachel Richardson: 20% - pharmacological analysis, writing Simon Mountford: 2.5% - supervision, writing Lei Zhang: 2.5% - pharmacological analysis Matheus Tempone: 2.5% - pharmacological analysis Herbert Herzog: 2.5% - pharmacological analysis, supervision Nicholas Holliday: 10% - supervision, correction Philip Thompson: 10% - supervision, correction	No
4	Optically Pure, Structural, and Fluorescent Analogues of a Dimeric Y <sub>4</sub> Receptor Agonist Derived by an Olefin Metathesis Approach	Published	50% - all chemistry, writing	Simon Mountford: 15% - supervision, correction Rachel Richardson: 10% - pharmacological analysis, writing Marleen Groenen: 5% - pharmacological analysis Nicholas Holliday: 10% - supervision, correction Philip Thompson: 10% - supervision, correction	No

I have not renumbered sections of published papers in order to generate a consistent presentation within the thesis.

Student signature:

Date:

27/09/2016

The undersigned hereby certify that the above declaration correctly reflects the nature and extent of the student's and co-authors' contributions to this work. In instances where I am not the responsible author I have consulted with the responsible author to agree on the respective contributions of the authors.

Main Supervisor signature:

Date:

27/09/2016

## Acknowledgements

At the completion of my PhD, I would like to express my most sincere gratitude to my supervisors Assoc Prof Philip Thompson and Dr Simon Mountford for their continual guidance and support throughout the project. The knowledge, skills, confidence and independence they have given me will be invaluable for my future career as a researcher.

My gratitude also goes to our collaborators Dr Nicholas Holliday's group at the University of Nottingham, United Kingdom, Prof Herbert Herzog's group at the Garven Institute of Medical Research, Sydney, and Prof Ishwar Parhar's group at Monash University Sunway Campus, Malaysia. Their efforts in performing biological assays have greatly supported me in completion of my thesis as well as our publications.

I would also like to sincerely thank Prof Andrea Robinson, Dr Kade Roberts, Dr Nick Barlow, Dr Jo-Ann Pinson and Dr Ian Jennings for providing helpful experimental techniques, and Dr Jason Dang for conducting high-resolution mass spectrometry for our compounds.

I thank my former and current fellow HDR students especially Sam, Tony, Steven, Krithika, Keith, Yasmin, Krishnarjuna, Josh, Tamir, Michael, Bo, Will, Joseph and Villy, for keeping me entertained. I cherish them as lifetime friends.

Last but not least, I express my heart-felt thanks to my family members: my parents Ping Liu and Weizhuang Yin, and my wife Min (Vanessa) Chen for their unconditional love and their indispensable financial and spiritual support in completion of my degree. Their encouragement has helped me cope with the most difficult time when I almost gave up.

## Abbreviations

Alloc	Allyloxycarbonyl
Boc	<i>tert</i> -Butyloxycarbonyl
cAMP	Cyclic adenosine monophosphate
CuAAC	Copper-catalysed azide-alkyne cycloaddition
DCM	Dichloromethane
DIC	N,N-diisopropylcarbodiimide
DIPEA	N,N-diisopropylethylamine
DMB	1,3-Dimethoxybenzene
DMF	N,N-dimethylformamide
DMSO	Dimethyl sulfoxide
EDT	1,2-Ethanedithiol
ESI-MS	Electrospray ionisation mass spectroscopy
Et <sub>2</sub> O	Diethyl ether
EtOAc	Ethyl acetate
EtOH	Ethanol
Fmoc	Fluorenylmethoxycarbonyl
GnRH	Gonadotrophin releasing hormone
GPCR	G protein-coupled receptor
GPR54	G protein-coupled receptor 54
h	Hour(s)
HCTU	O-(1H-6-chlorobenzotriazol-1-yl)-N,N,N',N'-tetramethyluronium hexafluorophosphate
HRMS	High resolution mass spectrometry
KP	Kisspeptin

LCMS	Liquid chromatography mass spectroscopy
$[M+2H]^{2+}$	Doubly charged ion
$[M+3H]^{3+}$	Triply charged ion
min	Minutes
ml	Millilitres
Mtt	4-methyltrityl
NMM	N-methylmorpholine
NMR	Nuclear magnetic resonance
NPY	Neuropeptide Y
PyClock	6-Chlorobenzotriazole-1-yloxy-tris-pyrrolidinophosphonium hexafluorophosphate
RhB	Rhodamine B
RP-HPLC	Reversed-phase high performance liquid chromatography
RT	Retention time
SPPS	Solid phase peptide synthesis
THPTA	Tris(3-hydroxypropyltriazolylmethyl)amine
TFA	Trifluoroacetic acid
TIPS	Triisopropylsilane

# Amino Acid Nomenclature

One-letter Code	Three-letter Code	Full Name
A	Ala	Alanine
R	Arg	Arginine
N	Asn	Asparagine
D	Asp	Aspartic acid
C	Cys	Cysteine
(Synthetic)	Dap	2,3-Diaminopropionic acid
Q	Gln	Glutamine
E	Glu	Glutamic acid
G	Gly	Glycine
H	His	Histidine
I	Ile	Isoleucine
L	Leu	Leucine
K	Lys	Lysine
M	Met	Methionine
F	Phe	Phenylalanine
P	Pro	Proline
(Synthetic)	Pop	Propargyloxypoline
S	Ser	Serine
T	Thr	Threonine
W	Trp	Tryptophan
Y	Tyr	Tyrosine
V	Val	Valine



## CHAPTER 1 Introduction to Fluorescence Imaging and Fluorescently Labelled Peptidic Ligands

---

---

### Table of Contents

1.1	General Introduction to Optical Imaging and Fluorophores .....	1-2
1.2	G Protein-Coupled Receptors (GPCRs): Valuable Potential Drug Targets to Be Studied by Fluorescence Imaging .....	1-4
1.3	Design of Fluorescently Labelled Peptidic Ligands Targeting GPCRs .....	1-6
1.3.1	Peptides as the Receptor-Targeting Moieties .....	1-7
1.3.2	Low Molecular Weight Fluorophores as the Signalling Moieties .....	1-9
1.3.3	Fluorophore Conjugation in Respect to Positions and Chemistry .....	1-13
1.3.4	Literature Examples of Fluorescently Labelled Peptidic Ligands .....	1-18
1.4	Objectives of This Project.....	1-20
	References.....	1-31

## 1.1 General Introduction to Optical Imaging and Fluorophores

Optical imaging belongs to the family of molecular imaging technologies which have been developed to facilitate highly specific and non-invasive *in vivo* investigation of cellular and molecular events.(1) The key element in optical imaging is the ready availability and proper application of sophisticated fluorophores.(2) The term “fluorescence” refers to the property of fluorophores emitting light after absorbing photons from an external energy source, which can be ultraviolet, visible or infrared emission.(3) Following the energy absorption, the electrons within the fluorophore rise to an unstable “excitation state”, and quickly return to the original ground state while the excess energy is emitted as light.(3, 4) Due to the loss of energy, the emitted light always possesses a longer wavelength and lower intensity than the light required for excitation.(3, 5)

Since being discovered in the 19<sup>th</sup> century, fluorophores have drawn great attention in developing visualisation technologies for both scientific research and clinical settings. Various fluorophores, along with their corresponding methodologies and instruments have become commercially available.(6) This growing popularity can be attributed to several unique advantages. From the research point of view, fluorescence imaging gives high sensitivity and resolution at low fluorophore concentration, thus cost-effective measurements can be achieved at single cell level.(7-9) Compared to radioactive isotopes with limited half-lives, fluorophores can undergo repetitive excitation-emission cycles (unless they are destroyed by photobleaching in the excitation state).(5, 10) Also, their biocompatibility enables application in receptor monitoring in living whole cells,(11) while causing few occupational safety hazard and environmental concerns.(10, 12, 13) From the clinical point of view, fluorescence imaging can be performed in multichannel experiments, which allows earlier and more specific disease detection, and creates opportunities for understanding disease pathogenesis and prognosis.(14) This technology also enables

real-time monitoring of drug administration, therapeutic responses and other dynamic physiological processes without post-processing.(8, 14, 15) In addition, its non-invasive and non-radioactive nature markedly reduce associated healthcare expenditure, and patients' physiological and psychological discomfort.(16)

It also should be noted that fluorescent imaging technology possesses certain limitations. Fluorophores must be used at a low concentration in order to obtain a high specificity, thus a sensitive detector is essential.(17) Photobleaching is a particular concern when highly diluted ligands or overly strong excitation energy is used, especially with an untunable source light.(17) In addition, during the cell labelling experiment, the washing or quenching steps can potentially compromise cell viability or cause ligand dissociation.(8)

In the 21<sup>st</sup> century, fluorescent imaging technology has found its place in clinical settings. The application of intravital fluorescent stains have been reported to be successful as visual aids in neurosurgery,(18) dermatology(19) and oncology.(20) In modern target-oriented drug discovery, however, this technique is being challenged by the increasing demands for target specificity. For example, although the US Food and Drug Administration (FDA) approved fluorophore indocyanine green (ICG) has shown satisfactory sensitivity and resolution in monitoring dynamics of physiological fluids,(21-24) its non-specific nature limits its usefulness in investigating a particular biological target of interest. Moreover, although the well-established fluorescent-histochemical technique can probe a particular receptor protein by using fluorescent antibodies, it is often incapable of recognising the actual ligand binding sites owing to steric hindrance.(25)

## 1.2 G Protein-Coupled Receptors (GPCRs): Valuable Potential Drug Targets to Be Studied by Fluorescence Imaging

GPCRs comprise the largest family of transmembrane signalling molecules in the human genome.(26) This family consists of more than 800 members that are widely distributed in both human and animal physiological systems, acting as essential cellular signal transducers.(27) Their full tertiary structures were first reported by Rasmussen *et al.*, who successfully crystallised  $\beta_2$ -adrenoceptor in 2007.(28) GPCRs share a common structure comprised of seven transmembrane (7-TM)  $\alpha$ -helices linked by three extracellular and three intracellular loops.(29) The large variety of endogenous ligands for GPCRs includes peptides, proteins, lipids, ions and small molecules. In the inactive state, a G protein contains a  $G_{\beta\gamma}$  subunit associated with a  $G_\alpha$  subunit that binds to a guanine diphosphate (GDP) molecule. When stimulated by an agonist, a guanine triphosphate (GTP) molecule replaces GDP on  $G_\alpha$ , and the two subunits dissociate to interact with their corresponding effector molecules that in turn activate the intracellular signalling cascades (**Figure 1-1**).(30) G proteins have been classified into four major subclasses based on the effector molecules they stimulate.(31) The  $G_s$  G proteins promote activity of adenylyl cyclase, which in turn catalyses conversion of ATP to the second messenger cAMP,(32) while the  $G_{i/o}$  G proteins exert the opposite effects.(33) The  $G_{q/11}$  G proteins stimulate activity of the enzyme phospholipase C  $\beta$  (PLC $\beta$ ), which consequently cleaves phosphatidylinositol 4,5-biphosphate (PIP<sub>2</sub>) into the 2<sup>nd</sup> messengers inositol triphosphate (IP<sub>3</sub>) and diacylglycerol (DAG) that trigger Ca<sup>2+</sup> release from intracellular storage.(34, 35) The  $G_{12/13}$  G proteins are found to modulate RhoGTPase nucleotide exchange factors (RhoGEFs) mediated cellular events.(36) Additionally, the  $G_{\beta\gamma}$  subunits activate inward-rectifier potassium channels (GIRKs),(37) and also regulate other cellular effectors, such as PLC $\beta$ ,(38) adenylyl cyclase isoforms (39) and phosphoinositide 3 kinases (PI3Ks).(40) All these

effectors eventually trigger cellular biological responses via activating intracellular protein kinases. The receptor signalling is then terminated following hydrolysis of the  $G_{\alpha}$ -bound GTP into GDP by intrinsic GTPase activity within  $G_{\alpha}$ , and re-association of the  $G_{\alpha}$  and  $G_{\beta\gamma}$  subunits.

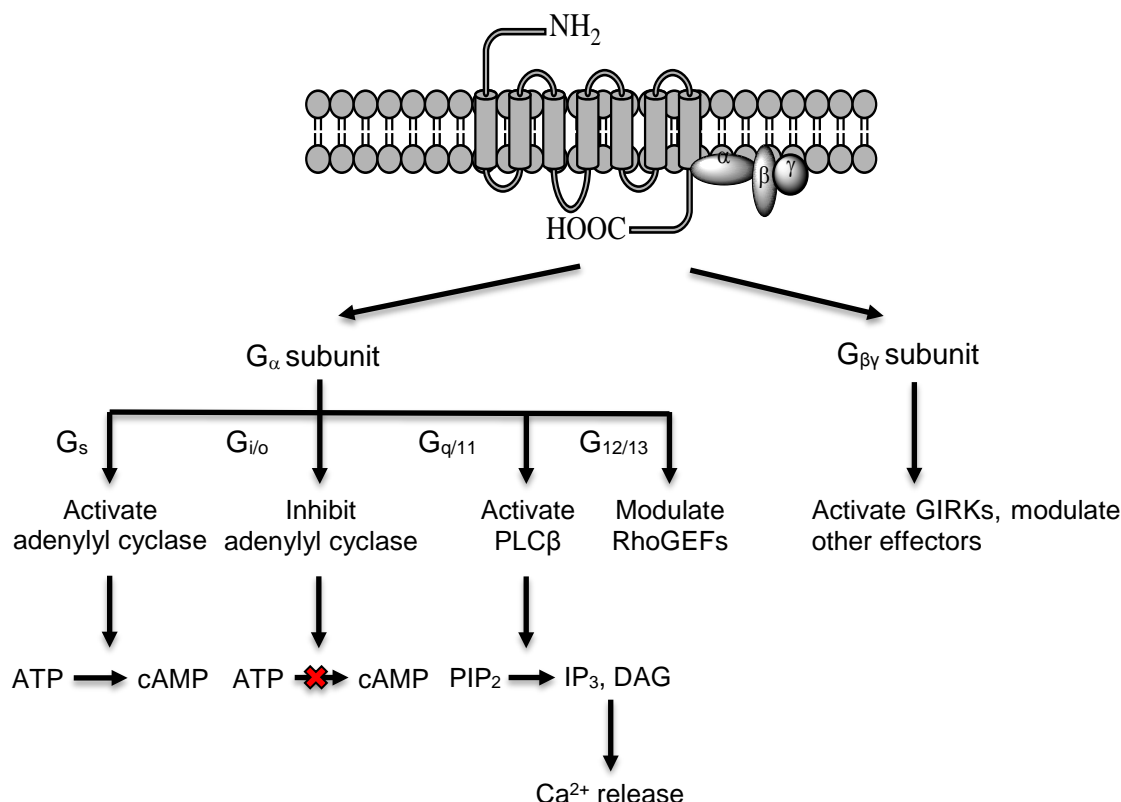


**Figure 1-1:** The general structure of GPCRs and a summary of their signalling pathways.

GPCRs have been the most extensively investigated drug targets in pharmaceutical research, owing to the fact that they are implicated in many physiological and pathophysiological processes.<sup>(10, 41-43)</sup> It was estimated that about 350 GPCRs have potential in being a drug target (excluding those olfactory receptors),<sup>(44)</sup> within which the endogenous ligands for about 200 have been identified.<sup>(42)</sup> However, although about 40-50% of commercially available drugs are GPCR-targeting,<sup>(42, 45)</sup> they only account for about 30 GPCRs. Researchers now have a large uncharted world to explore, where around 150 “orphan GPCRs” are required to be “deorphanised” by identifying their

endogenous ligands and biological functions,(46) and approximately 90% of GPCRs remain to be therapeutically exploited.(47)

Fluorescence imaging can enormously contribute to the study of GPCRs. Because of its satisfactory specificity and resolution, it is capable of optimally visualising and quantifying GPCRs in spite of their low cellular expression level.(8) Fluorescence imaging is now most commonly used for investigating GPCR localisations and differentiating expression patterns in normal and diseased tissues.(8) More applications, such as observing cell surface dynamics and receptor trafficking, studying receptor functionalities and monitoring protein-protein interactions are gradually becoming feasible.(5, 8, 48) For example, Hara *et al.* directly monitored ligand binding and interaction with the orphan receptor GPR40 for the first time using a fluorescently labelled fatty acid. They further correlated ligand binding with previously demonstrated phosphorylation of extracellular regulated kinase (ERK)-1/2 in cells that over-expressed GPR40.(49)

### **1.3 Design of Fluorescently Labelled Peptidic Ligands Targeting GPCRs**

Having the above facts in mind, one can realise that fluorescence imaging ligands that target GPCRs are produced by connecting two essential components: a fluorophore and a receptor-targeting moiety, ideally with optimised affinity and selectivity for the receptor(s) of interest.(4, 14) The receptor-targeting moiety can be either an agonist or antagonist, and is usually designed to mimic the endogenous ligand in an attempt to retain the desired pharmacological properties. In addition, as the pharmacological profiles of receptor-targeting moiety can be negatively influenced by a bulky fluorophore in close proximity,(8, 17) a spacer is often incorporated.(7, 25) That said, the following steps are typically involved in development of GPCR-targeting fluorescently labelled ligands (Flow chart in **Figure 1-2**).

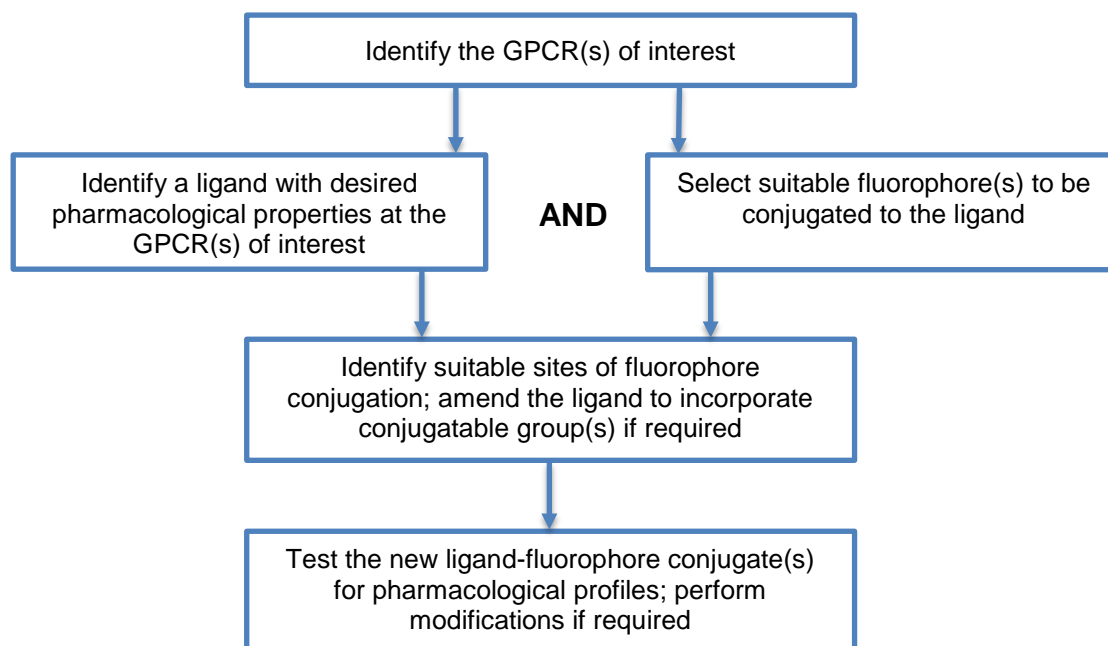


**Figure 1-2:** Typical steps involved in development of GPCR-targeting fluorescently labelled ligands.

### 1.3.1 Peptides as the Receptor-Targeting Moieties

Peptides have been utilised as new generation receptor-targeting moieties for producing fluorescent imaging agents, in addition to small molecules, fluorescent antibodies, auto-fluorescent proteins and peptide/protein tags.<sup>(50-55)</sup> The “druggability” of peptides has been attracting increasing attention after versatile solid phase peptide synthesis (SPPS) strategies became available to efficiently produce numerous analogues for pharmacological testing. By 2014, approximately 70 peptide-based pharmaceuticals have been approved by the FDA.<sup>(56)</sup>

It has been found that peptide-based ligands possess unique advantages over proteins and small-molecules. Compared to large proteins/antibodies, peptides are more tolerant to harsh synthesis conditions allowing convenient manufacture. Owing to their smaller size, they diffuse more rapidly into vasculature and target tissue, while eliciting minimal toxicity and immunogenicity.<sup>(57-65)</sup> As peptide-based ligands are often derived from the endogenous ligands of the receptors of interest, they may possess greater potency and

specificity at the target receptors.(65, 66) They are also less likely to incur systemic toxicity, because the relatively shorter half-life gives low unwanted tissue accumulation,(67) and their metabolic products are amino acids.(68) However, the “druggability” of peptides can be hindered by their low metabolic stability against endogenous proteases and peptidases.(67, 69-71) Therefore, peptide-based drugs often possess poor oral availability and need to be administered via parenteral routes, which incur higher cost and lower patient acceptance. These remain the major problems to be addressed in further pharmaceutical research.

Many of the early reported fluorescent ligands were produced based upon the endogenous peptides. Despite their good affinity and activity, endogenous peptides often fall short of metabolic stability and selectivity to the receptor subtype(s) of interest. Therefore, more recently reported ligands have been derived from truncated and systematically modified endogenous peptides after extensive investigation into the structure-activity relationships. This is done to preserve or at least only modestly sacrifice the desirable pharmacological and pharmacokinetic profiles. For example, amino acid substitutions may introduce additional molecular interactions with the receptor binding sites resulting in enhanced affinity and activity; non-proteogenic amino acids (such as D-stereoisomers) and cyclisation are useful means to enhance resistance against metabolic degradation by disrupting enzyme recognition and reducing conformational flexibility.(65, 72, 73) **Chapter appendix 1** summarises many of the reported fluorescently labelled ligands for peptide GPCRs.



### 1.3.2 Low Molecular Weight Fluorophores as the Signalling Moieties

It is fortuitous that, some of the above-mentioned drawbacks of peptides become virtues in developing fluorescent ligands. For example, rapid clearance of unbound peptides allows for a reduced background signal in imaging assays. Another key advantage over small molecules is that peptides more readily retain their pharmacological profiles after being conjugated to a bulky fluorophore, as they still account for the majority portion of the whole molecule.<sup>(25)</sup> That said, lower molecular weight fluorophores are becoming popular. They generally produce low background fluorescence from cells, cell debris, buffer components and plastic materials,<sup>(8)</sup> leading to an improved target-to-background contrast. These molecules can also be conveniently conjugated to peptidic ligands via chemically active functional groups.<sup>(8)</sup> For instance, a succinimidyl ester on a fluorescent ligand can readily form a stable amide bond with a primary amine group under alkaline conditions.

The variety of low molecular weight fluorophores is expanding rapidly. Those subclasses reported in synthesis of GPCR-targeting fluorescently labelled peptides are summarised in **Chapter appendix 2. Cyanine** and **xanthene** derivatives have been the most frequently applied fluorophores for this purpose. **Cyanine** dyes are comprised of two either symmetrical or unsymmetrical heterocyclic structures linked by a polymethine chain. They show high extinction coefficients, sharp absorption and emission profiles, and consist of the majority of fluorophores useful in *in vivo* optical imaging.<sup>(74)</sup> **Xanthene** derivatives generally show absorption and emission profiles at shorter wavelengths, therefore are less utilised in *in vivo* imaging than cyanine dyes. However, their high molar absorptivities and strong fluorescence <sup>(75)</sup> enable their utilities in labelling biomolecules for *in vitro* applications. Note that a more detailed review of these two families of dyes can be found in chapter 2 of this thesis.

**Coumarin** derivatives are popular fluorophores because of their good water solubility and cell permeability, as well as low cytotoxicity.(76) They display intrinsically high quantum yield, which can be further enhanced by placing an electron donor at the 7-position and electron withdrawing group at the 3-position.(77, 78) Their fluorescence properties are heavily dependent on surrounding chemical and biological environment, which makes them valuable environment-monitoring agents.(79, 80) However, coumarin derivatives are not recommended for *in vivo* tissue and whole-animal imaging, as their green-blue fluorescence is weakly tissue penetrating and can be blocked by autofluorescence (discussed below).

Difluoroboron dipyrromethene (commonly known as **BODIPY**) derivatives possess good photo- and chemical stability, relatively high quantum yields (between 60% and 90%), sharp fluorescence bands, good solubility in many organic solvents and low tendency to self-aggregate.(81-83) Although earlier discovered BODIPYs absorb and emit fluorescence close to the UV to blue region, a review has documented some new derivatives that operate at longer wavelengths suitable for NIR imaging *in vivo*.(83) Unlike coumarin derivatives, their fluorescence properties are relatively stable against changes in environmental factors such as *pH* and oxygen.(83-85)

**Naphthalimide** derivatives are highly fluorescent compounds with large Stokes' shift. Their emission maxima generally fall into the green spectral region. Structural modifications, such as introducing substitutions on their ring system can induce a red shift to their excitation and emission maxima. Significantly, naphthalimide derivatives have shown interesting anti-cancer properties in animal models, and some of them have entered clinical trials.(86, 87)

**Lanthanides** are the only group of inorganic fluorophores in the list. They utilise functionalised chelators based upon DOTA or DTPA to be attached to biomolecules. The chelator may also serve as a barrier to prevent water binding, which causes lanthanide deactivation.<sup>(88)</sup> The most symbolic character of these ions is their extremely high sensitivity in comparison to organic fluorophores (approx. 10,000-fold over rhodamine and BODIPY, and 5,000-fold over fluorescein).<sup>(89)</sup> In addition, they produce low background fluorescence, which can be attributed to their large Stokes' shift ( $> 200$  nm).<sup>(88)</sup> The major drawback of lanthanides is their low excitation coefficients. Therefore, they are often sensitised to boost their luminescence by another fluorophore placed in close proximity, which act as an "antenna" by absorbing and then transferring energy to the lanthanide ion.<sup>(88, 90, 91)</sup>

**Pyrene** derivatives are composed of four fused benzene rings. They display absorption and emission spectra in the ultraviolet region. Their high extinction coefficient ensures labelled biomolecules can be measured at sufficiently low concentration to obtain greater physiological relevance. Interestingly, a maleimide-functionalised pyrene displays suppressed emission and quantum yield in its uncoupled form, due to the presence of the double bond in the maleimide moiety. Pyrene's fluorescence is activated when the maleimide becomes saturated by forming a thioether with a thiol.<sup>(92, 93)</sup> One unique property of pyrene derivatives is their ability to form excited state dimers (excimers), when an electronically excited pyrene encounters a ground state pyrene in close proximity (approximately  $10 \text{ \AA}$ ).<sup>(94-96)</sup> The excimers emit at a wavelength with shift to the red spectral region ( $\sim 460 \text{ nm}$ ).<sup>(97)</sup> Therefore, labelling macromolecules with pyrene derivatives have become an efficient measure in elucidating their 3D conformations and spatial organisations.<sup>(92, 97)</sup>

The core structure of **squaraine** derivatives is a 1,3-disubstituted oxocyclobutenoate. They are characterised by the rigid, planar and electron-deficient Hückel ring. Similar to cyanine derivatives, squaraines exhibit strong absorption in the visible to NIR spectral region with high extinction coefficients.(75, 98, 99) On the other hand, their quantum yields and fluorescence lifetimes are low in aqueous environments,(100, 101) but can be markedly enhanced in hydrophobic environments such as binding to bovine serum albumin.(102, 103) To prevent loss of quantum yield and fluorescence lifetime by aggregation in aqueous environments,(104, 105) phosphonic acid-containing squaraines have been reported, where tendency to aggregate was reduced by negative charge repulsion.(106)

Selection of fluorophores for preparing labelled peptidic ligands requires collective consideration of their pharmacological profiles, optical characteristics as well as their intended experimental settings. These fluorophores, which vary in size, charge and polarity, are as likely to influence the receptor affinity and activity of the parent peptide as any other functional groups. This is true even if they are conjugated at the same position of a peptidic ligand. For example, Nouel *et al.* showed that D-Trp<sup>8</sup>-somatostatin could be labelled by fluorescein or BODIPY with only slight loss of affinity, but a Cy3.5 fluorophore resulted in reduction in affinity by almost an order of magnitude.(107, 108)

Fluorophores with minimal impact to receptor binding should ideally meet the following criteria that are frequently used to judge the optical characteristics. A high *excitation coefficient* ensures a good capability to absorb photons at a given wavelength and a greater tendency to emit light.(109, 110) A large *Stoke's shift* provides wider separation between the absorption and emission wavelength maxima, which minimises interference caused by signal overlay.(111) A high *quantum yield* (QY) gives low energy loss after absorption, which maximises fluorescence intensity.(111) Finally, a strong resistance to

photobleaching allows for repeated excitation and emission in multiple experimental sessions.

Within the frame discussed above, the preferred fluorophores must also fit the purposes of the intended experimental conditions.<sup>(112)</sup> Xanthene derivatives, e.g. fluorescein, rhodamine and their various structural analogues, show absorption and emission maxima predominantly in the visible spectrum range, and are often used for *in vitro* cellular imaging at surface level.<sup>(112)</sup> However, they only have very limited usefulness in *in vivo* deep tissue and whole animal imaging because their light penetration capability is severely compromised by tissue auto-fluorescence, reflection and refraction, as well as absorption by water, melanin, proteins and haemoglobin.<sup>(2, 14, 113, 114)</sup> On the other hand, fluorophores that absorb and emit in the near-infrared (NIR) range (650-1450 nm) are ideal choices for deep tissue and whole animal imaging.<sup>(115)</sup> While indocyanine green remains the only FDA approved NIR fluorophore, many other classes such as cyanine and squaraine derivatives have been applied in scientific research fields.

### **1.3.3 Fluorophore Conjugation in Respect to Positions and Chemistry**

Following selection of the parent peptide sequences and fluorophores, it is pivotal to collectively consider the labelling position(s) and corresponding synthesis strategies in order to attain peptides with desired pharmacological profiles. Peptide termini and amino acid side-chains are the most commonly chosen conjugation sites. However, attaching a bulky fluorophore molecule at a key receptor-binding moiety will be detrimental to the pharmacological profiles of the resulting conjugate. The process of selecting labelling positions can be guided using structure-activity relationships of the parent peptide sequence, and generally, the primary preference lies in those conjugatable amino acid residues with minor role in receptor interaction. If such options are unavailable, other

unimportant amino acid residues can be substituted to introduce new conjugation site(s). The substituents do not need to be structurally similar to preserve receptor affinity.

As briefly discussed before, fluorophores manufactured to contain a reactive or activatable group can enable rapid and convenient biomolecule conjugation. They primarily target the N-terminal  $\alpha$ -amine, C-terminal carboxylate, Lys side-chain  $\epsilon$ -amines, Cys thiol groups and alkyne groups in non-proteogenic amino acids. Consistently, fluorescently labelled peptides reported since 1960s (**Chapter appendix 1**) are mainly prepared using amide, thiourea and triazole linkages, although other strategies such as thioether, hydrazine, lanthanide chelates and fluorescent amino acids have also been demonstrated.

#### **1.3.3.1 Amine Group Conjugations**

The primary amino group has been the most popular conjugatable functionality in peptide/protein fluorescence labelling chemistry. Fluorophore conjugation can be performed either at the  $N^\alpha$ -amine or when capped or found essential in biological activities, the side-chain  $N^\epsilon$ -amine on Lys or its analogues is also used. The later strategy holds significance as Lys is the most frequently occurring conjugatable amino acid in vertebrate proteins.(116) Modern commercially available amine-oriented fluorophores are usually functionalised in a way to allow rapid conjugation under alkaline conditions in which the amine group is able to act as a nucleophile.

Isothiocyanate-containing fluorophores react with amines to form a thiourea group. This reaction involves a nucleophilic attack on the electrophilic carbon of the isothiocyanate, and subsequent electron shift to the neighbouring nitrogen (**Figure 1-3**).(117) Owing to the stability of thiourea group, this reaction is highly selective towards amines although it may also occur with other nucleophiles such as thiols and tyrosine phenolate ions.(118)

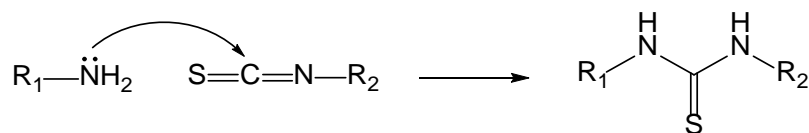


**Figure 1-3:** Reaction of a primary amine with an isothiocyanate to form thiourea.(119)

Carboxyl-containing fluorophores can be conjugated via an amide bond after being activated (e.g. forming an N-hydroxysuccinimidyl (NHS) ester) and reacting with an amine (**Figure 1-4**). Although NHS esters are predominantly selective to amines, side-reactions with hydroxyl groups on tyrosine, serine and threonine have also been reported, especially in presence of a neighbouring histidine residue.(120) These side-reactions are less prevalent in aqueous conditions where the NHS esters are more rapidly hydrolysed by water.(117)

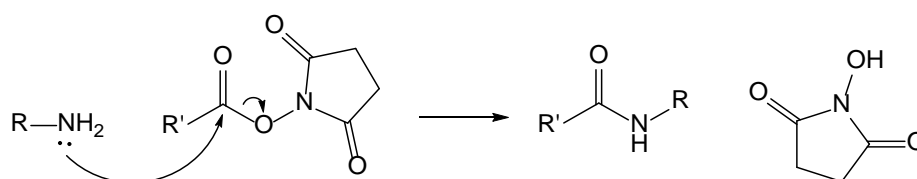


**Figure 1-4:** Reaction of a primary amine with a NHS ester to form amide.(119)

### 1.3.3.2 Cysteine Thiol Conjugations

The formation of a disulfide-like conjugate is possible, but this linkage is not commonly seen in fluorescence labelling chemistry due to its instability and the role of disulfide linkage in many peptide ligands. Instead, cysteines are often conjugated with iodoacetamides to form thioethers (**Figure 1-5**). Iodoacetamides have shown excellent tolerance to reducing agents that prevent thiol oxidation prior to labelling.(121) However, this conjugation is not specific as it can also occur on other amino acid side-chains, such as primary amines, thioethers and imidazoles,(122-126) albeit with relatively low reactivity. This problem can be minimised by using orthogonal protecting groups during peptide synthesis, or limited quantity of iodoacetamides at a slightly alkaline *pH*.(117)

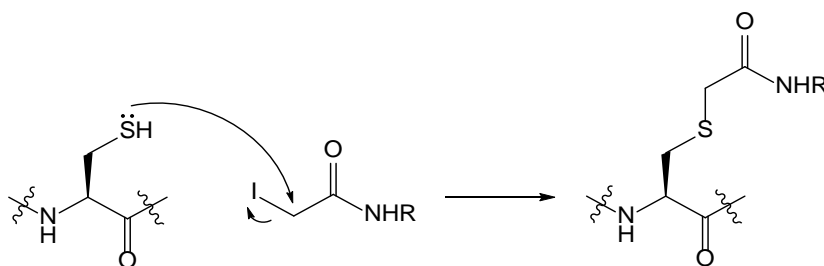


**Figure 1-5:** Reaction of cysteine thiol with iodoacetamide to form thioether.(126)

Another common example involves formation of a thioether via reaction with maleimides (**Figure 1-6**). This reaction proceeds quickly at approximately physiological *pH* via nucleophilic addition on the unsaturated maleimide residue. Compared to iodoacetamides, maleimides show no reactivity at other amino acid side-chains, allowing more specific biomolecule labelling.(117) This strategy has been successfully applied in preparing the two FDA approved antibody-cytotoxic drug conjugates, Trastuzumab-DM1 and Brentuximab vedotin.(127, 128) However, the maleimide-thiol conjugation can undergo thiol exchange in the presence of exogenous thiols in biological environment resulting in permanent fluorophore detachment (**Figure 1-7**). Moreover, succinimide ring hydrolysis in the conjugate also results in two isomeric ring-opening degradation products.(129, 130) Interestingly, Fontaine *et al.* reported their work on maleimide analogues by attaching electron-withdrawing groups at the succinimide nitrogen. The modified conjugates could be deliberately hydrolysed before administration to avoid *in vivo* thiol exchange.(129)

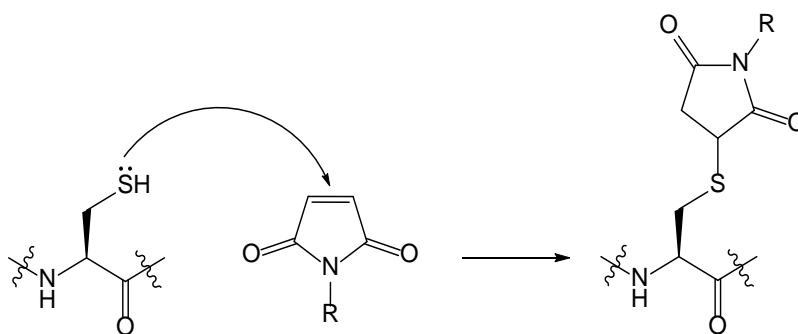


**Figure 1-6:** Reaction of cysteine thiol with maleimide to form thioether.(129)



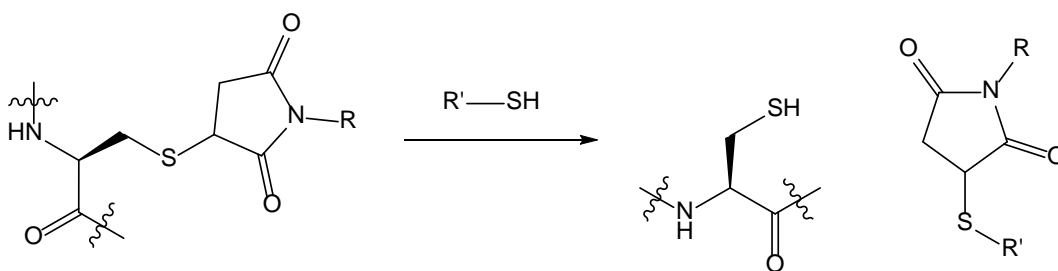


**Figure 1-7:** Undesirable thiol exchange in the presence of exogenous thiol species.

### 1.3.3.3 Copper-Catalysed Alkyne-Azide Cycloaddition (CuAAC Reaction)

The CuAAC reaction, a cyclisation reaction between an azide and an alkyne moiety to form a 1,2,3-triazole ring structure, is an important version of the Huisgen 1,3-dipolar cycloaddition first described in 1960s (**Figure 1-8A**).<sup>(131)</sup> The  $\text{Cu}^+$  ion enhances formation of the 1,4-disubstituted triazole over its 1,5-substituted regioisomer (**Figure 1-8B**).<sup>(132-134)</sup> CuAAC reaction has found its place in studies of biological systems, owing to its chemoselectivity and applicability in aqueous physiological conditions.<sup>(134-138)</sup> Thus CuAAC reaction has been a widely utilised bio-conjugation technique in activity-based enzyme profiling,<sup>(139)</sup> protein fluorescence labelling,<sup>(140)</sup> DNA silver staining,<sup>(137)</sup> and glycan visualisation via conjugation of sugar-reporting groups.<sup>(141)</sup>

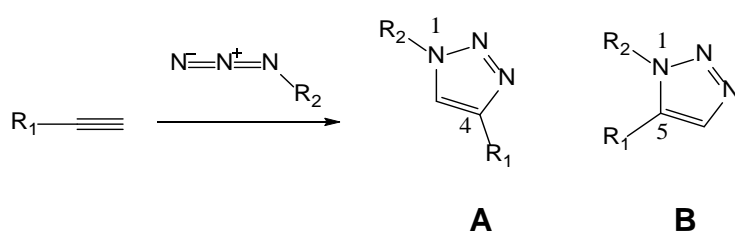


**Figure 1-8:** **A:** The desired CuAAC reaction that forms 1,4-substituted triazole; **B:** formation of 1,5-substituted regioisomer without  $\text{Cu}^+$  catalyst.

There has been a range of variant on the reaction conditions for conjugation.  $\text{Cu}^+$  catalyst is generated from  $\text{CuSO}_4 \cdot 5\text{H}_2\text{O}$  by adding sodium ascorbate (NaAsc) as the reducing agent.<sup>(142, 143)</sup> A polytriazolyamine ligand THPTA (**Figure 1-9**) further stabilises  $\text{Cu}^+$  and accelerates reaction rates by isolating any destabilising interactions.<sup>(136, 142)</sup> This ligand

also protects vulnerable amino acid residues (such as Cys, Met and His) against oxidation.(135) Lastly, aminoguanidine can be used to protect Arg and Lys side-chains against dehydroascorbate, reactive aldehydes and glyoxal formed during ascorbate oxidation.(135, 144, 145)

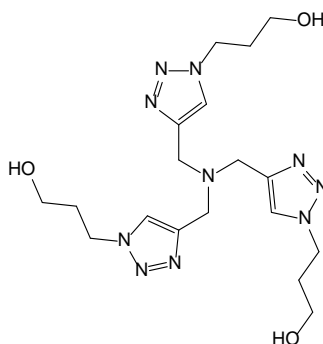


**Figure 1-9:** The structure of tris(3-hydroxypropyltriazolylmethyl)amine (THPTA).

#### 1.3.4 Literature Examples of Fluorescently Labelled Peptidic Ligands

Following the general strategies described above, research groups have been able to develop fluorescently labelled peptidic ligands for many GPCRs (**Chapter appendix 1**). These ligands have displayed not only highly desirable pharmacological properties, but also usefulness in visualisation and functional studies of the GPCR(s) they intended to target.

The list has been compiled to provide a thorough resource, but here are noted typical examples of such fluorescent ligands. First are those that were developed for the human oxytocin (OT) and vasopressin (VP) receptors. Manning's group has reported their set of ligands derived from the literature compound 1-desamino oxytocin, which displayed more potent biological activity than endogenous oxytocin.(146) To introduce a conjugatable moiety, they substituted the Leu<sup>8</sup> residue with a Lys analogue ornithine (Orn), which was in turn conjugated by a 5(6)-fluorescein via an amide bond. The resulting peptide 1-

desamino-[Orn<sup>8</sup>(5/6C-Flu)]VT was highly selective to OT receptors with nanomolar affinity, and its binding specificity was confirmed using fluorescent microscopy. Consistently, this analogue exhibited full OT agonism in inositol phosphate accumulation assays.(53) Following the readily available structure-activity relationships, they amended human vasopressin into the V<sub>1b</sub> selective ligand 1-desamino-[Leu<sup>4</sup>, Lys<sup>8</sup>]vasopressin (d[Leu<sup>4</sup>, Lys<sup>8</sup>]VP),(147-149) which then incorporated a Lys(11-aminoundecanoyl)<sup>8</sup> moiety for conjugation. The resulting ligand d[Leu<sup>4</sup>, Lys(Aud-Alexa647)<sup>8</sup>]-VP exhibited selectivity toward human V<sub>1b</sub> receptors with some affinity to OT receptors. Functional assays revealed consistent results, where it showed full agonism at V<sub>1b</sub> and partial agonism at OT receptors. Additionally, it was interesting to note that direct fluorophore conjugation without the aminoundecanoyl spacer inverted selectivity to OT receptors.(150)

Such strategies were also utilised by Chan *et al.*(151) who described a cyanine-labelled analogue based on human H2 relaxin, a double-chain insulin-like peptide cross-linked by three disulfide bonds. They first performed an alanine scan to the peptide A-chain and established structure-activity relationships at the cognate receptors RXFP1 and RXFP2. Based on these findings, an analogue with truncated residues 1 to 3 and Ala substitution at the 23-position in the A-chain displayed affinity and activity similar to endogenous H2 relaxin selectively at RXFP1.(151) An azide-functionalised Cy5.5 fluorophore was then conjugated via CuAAC reaction to a propargylglycine residue introduced to the N-terminus of B-chain.(152) In comparison to the unlabelled parent peptide, the peptide conjugate retained selectivity to RXFP1, while affinity and potency were only modestly sacrificed. Consistently, Chan *et al.* observed that this conjugate initiated drinking behaviour in rodent subjects in a similar manner to that of Cy5.5-labelled unmodified H2 relaxin. Following ICV infusion and confocal micrographs, they could also visualise CNS areas with known

distribution of RXFP1. In addition, their work held significance as relaxin has passed phase III clinical trials for treatment of acute heart failure.(153)

## 1.4 Objectives of This Project

Fluorescently labelled peptidic ligands not only are capable of studying those identified GPCRs, but also elucidating the locations, functions as well as the endogenous ligands of “orphan receptors”.(154-156) Therefore, researchers equipped with this powerful technique are able to gain a thorough understanding of various GPCR-modulated molecular events that underlie both physiology and pathophysiology,(1) which may eventually lead to discovery of new drugs and early disease detection in clinical settings.

The primary objective of this project was to synthesise high-affinity selective fluorescently labelled peptides useful for *in vitro* study of selected GPCRs, incorporating ligand-based molecule design. Taking note of the abovementioned parameters, a range of fluorophores, linkage chemistries and amino acid substitutions have been considered to identify optimised fluorescent peptides.

The following chapters have been organised to show progressively the application of these concepts. Chapter 2 briefly reviews the two classes of fluorophores (cyanine and rhodamine B derivatives) utilised in our project, and then demonstrates the application of various synthesis techniques routinely used in our laboratory in successful preparation of structural and fluorescent analogues of two GPCR-targeting neuropeptides, ghrelin and kisspeptin. Adopting these efficient synthesis strategies, our further experiments have focused on synthesis and pharmacological evaluation of ligands that target different neuropeptide Y receptor subtypes. Chapter 3 presents a group of linear fluorescently labelled ligands derived from the literature Y<sub>1</sub> receptor antagonists / Y<sub>4</sub> receptor agonist BVD-15 peptide. Chapter 4 presents our optically pure mono-fluorescently labelled dimeric

peptides based on the literature selective  $Y_4$  receptor agonist BVD-74D, prepared by exploiting alkene metathesis reactions between protected allylglycine residues with the desired stereo-configuration. The success of this work is evidenced by the identification of useful methods and reagents that can be utilised in future studies of peptide GPCR physiology and pharmacology.

**Chapter appendix 1:** Representative literature fluorescently labelled peptidic ligands. Ligand names are the same as in literature, where possible.

\* Note: this column contains the structural modifications from the endogenous peptide ligands, where 1 = Amino acid substitution, 2 = truncation, 3 = N- or C-terminal extension, 4 = spacer, 5 = C-terminal esterification and 6 = cyclisation.

Target GPCR(s)	Fluorescently labelled ligand	Structural modifications*	Linkage	Reference
<b>Adrenomedullin receptor (AM<sub>1</sub>)</b>	[K <sup>9</sup> (Tam)]ADM(1-52)	1	Amide	(157)
	[Pra <sup>9</sup> (Tam)]ADM(1-52)		Triazole	
	Tam[G <sup>14</sup> ]ADM(14-52)	1, 2	Amide	
<b>Angiotensin receptors</b>	N <sup>α</sup> -(N-fluorescein-thiocarbamoyl)-(Asp <sup>1</sup> , Ile <sup>5</sup> )-angiotensin II	1	Thiourea	(158)
	Fluorescein-angiotensin II	-		(159)
<b>Apelin receptor</b>	Lys[aminoundecanoic acyl-DY647]-apelin-13	1, 3, 4	Hydrazine	(160)
<b>Bradykinin B<sub>1</sub> receptor</b>	B-10376	1, 2, 3	Amide	(161)
	B-10378	1, 2		
<b>Calcitonin gene-related peptide (CGRP) receptor</b>	[Lys <sup>24</sup> (5-CF)]h-α-CGRP	-	Amide	(162)
<b>Chemokine receptors (multiple subtypes tested)</b>	[Dpr(Ser) <sup>73</sup> -AF647]CCL11	1	Hydrazone	(163)
	[Dpr(Ser) <sup>73</sup> -AF647]CCL19			
	[Dpr(Ser) <sup>66</sup> -AF647]CCL22			
	[Dpr(Ser) <sup>71</sup> -AF647]CXCL11			
	[Dpr(Ser) <sup>67</sup> -AF647]CXCL12			
<b>Chemokine receptor 4 (CXCR4)</b>	Ac-[dLys <sup>8</sup> (fluorescein)]TZ14011	1, 2	Amide	(164)
	Ac-[dLys <sup>8</sup> (AF488)]TZ14011			
<b>Cholecystokinin (CCK) receptors</b>	5(6)carboxy-TMR-Gly-(Nle <sup>28,31</sup> )CCK <sub>26-33</sub>	1, 2	Amide	(165)

Target GPCR(s)	Fluorescently labelled ligand	Structural modifications*	Linkage	Reference
<b>Cholecystokinin A receptor (CCK1R)</b>	Alexa <sup>488</sup> -Gly-[(D-Trp <sup>30</sup> , Nle <sup>28,31</sup> )CCK-26-32]-phenylethyl ester	1, 2, 5	Amide	(166, 167)
	Alexa <sup>488</sup> -Gly-[(Nle <sup>28,31</sup> )CCK-26-33]	1, 2		
<b>Cholecystokinin B receptor (gastrin receptor)</b>	DY-676-DGlu <sup>1</sup> -minigastrin	1, 4	Amide	(168)
	Fluorescein-Trp-Met-Asp-Phe-NH <sub>2</sub>	2	Thiourea	(169)
	Alexa <sup>488</sup> -Trp-Nle-Asp-Phe-NH <sub>2</sub>	1, 2	Amide	(170)
<b>Corticotropin-releasing factor (CRF) receptor</b>	CRF-TAMRA 1	-	Amide	(171)
<b>Endothelin-B (ET<sub>B</sub>) receptor</b>	Cy3/ET-1 Cy5/ET-1	-	(Unspecified)	(172)
<b>Follicle-stimulating hormone (FSH) receptor</b>	Fluorescein-FSH	-	Thiourea	(173)
	Sulfurhodamine B-FSH		sulfonamide	
<b>N-formyl peptide receptor</b>	TMR-N-formyl-Nle-Leu-Phe-Nle-Tyr-Lys	(derived from bacterial products)	Thiourea	(174)
	Fluorescein-fnLLFnLYK		(Unspecified)	(175)
	CHO-Met-Val-Phe-Phe-Lys(FITC)	1	Thiourea	(176)
	CHO-Met-Leu-Lys(FITC)-Phe			
	CHO-Met-Leu-Lys(ASA)-Phe		Amide	
<b>Gastrin-releasing peptide receptor</b>	AA3G-740	1, 2, 4	Amide	(177)
	Alexa Fluor 680-G-G-G-BBN[7-14]NH <sub>2</sub>	2, 4		(178)
	Cy3-GRP	3	(Unspecified)	(179)
<b>Gonadotropin-releasing-hormone (GnRH) receptor</b>	[D-Lys(TMR) <sup>6</sup> ]GnRH	1	Thiourea	(180, 181)
<b>Galanin receptor 1 (GalR1)</b>	Fluorescein-N-galanin	-	Thiourea	(182)
<b>Glucagon-like peptide-1 (GLP-1) receptor</b>	Fluorescein-Trp <sup>25</sup> -Exendin-4	-	Thioether	(183)

Target GPCR(s)	Fluorescently labelled ligand	Structural modifications*	Linkage	Reference
<b>Ghrelin receptor (GHS-R1a)</b>	[Dpr <sup>3</sup> (octanoyl), Lys <sup>19</sup> (fluorescein)]ghrelin <sub>1-19</sub>	1, 2	Thiourea	(184)
	[Dpr <sup>3</sup> (octanoyl), Lys <sup>19</sup> (Cy5)]ghrelin <sub>1-19</sub>		Amide	(185)
<b>Melanocortin receptors</b>	Rho-MTII	(Modified from α-MSH) 1, 2, 4, 6	Thiourea	(186)
	Rho-SHU-9119			
<b>Melanocortin MC<sub>4</sub> receptor</b>	HS032 HS053	(Modified from α-MSH) 1, 2, 6	Fluorescent amino acid	(187)
<b>Neurokinin 1 (NK<sub>1</sub>) receptor</b>	N <sup>α</sup> -5(6)-carboxyfluorescein-SP	-	Amide	(188)
	[Fluorescein Lys <sup>3</sup> ]SP			(189)
	[Lys <sup>3</sup> (BODIPY FI)]SP			(190)
	[Lys <sup>3</sup> (OG488)]SP			
<b>Neurokinin receptor NK<sub>2</sub></b>	Fluorescein-NKA	-	Thiourea	(191)
<b>Neurotensin receptor-1 (NTR-1)</b>	FITC-Ava-neurotensin(8-13)	2, 4	Thiourea	(192)
<b>Opioid δ-receptor</b>	Deltorphan-Alexa 488	3, 4	Thioether	(193)
	Deltorphan-BODIPY TR	3, 4		
	Pya <sup>5</sup> -Enk-OH	1	Fluorescent amino acid	(194)
	Pya <sup>5</sup> -Enk-OMe	1, 5		
	(Met-enkephalin)-NH-(CH <sub>2</sub> ) <sub>2</sub> -NH-Dns	4	(Unspecified)	(195)
	[(dAla) <sup>2</sup> -Met-enkephalin]-NH-(CH <sub>2</sub> ) <sub>2</sub> -NH-Dns	1, 4		
<b>Opioid μ-receptor</b>	Pya <sup>1</sup> -Enk-OMe	1, 5	Fluorescent amino acid	(194)
	Dermorphin-Alexa 488	1, 3, 4	Thioether	(193)
	Dermorphin-BODIPY TR			

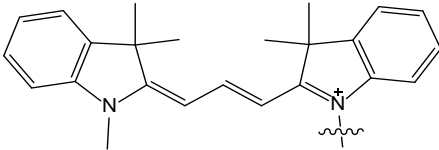
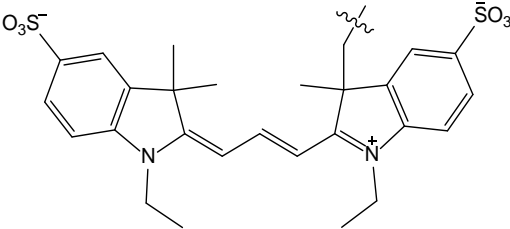
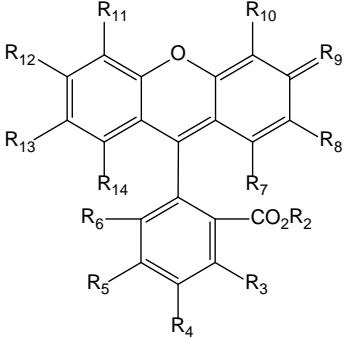
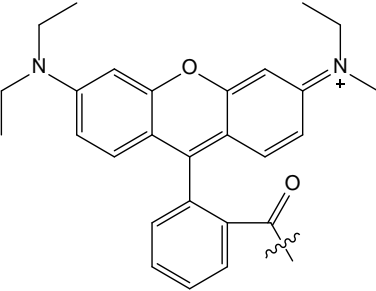
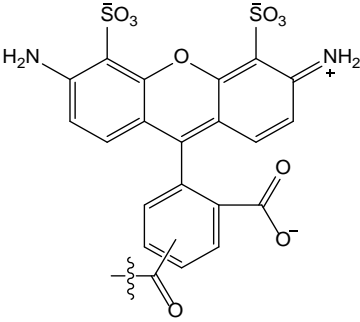
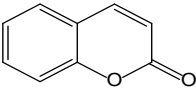
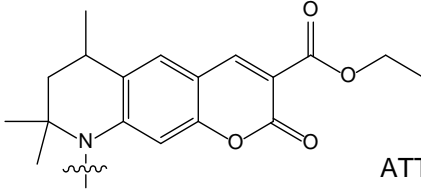


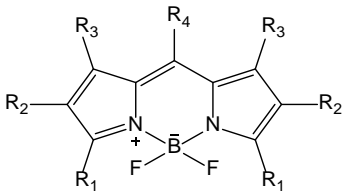
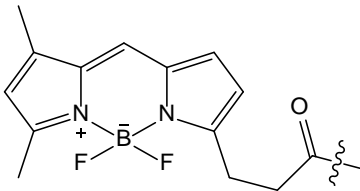
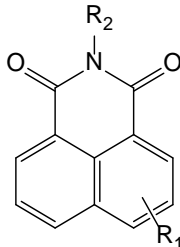
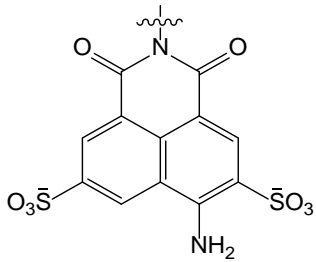
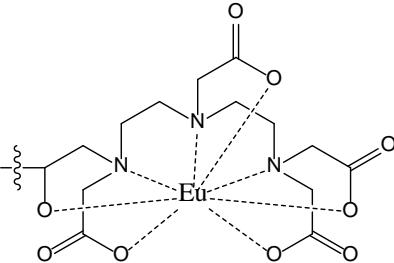
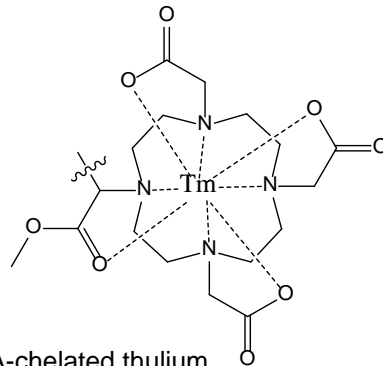
Target GPCR(s)	Fluorescently labelled ligand	Structural modifications*	Linkage	Reference
Oxytocin (OT) receptor	dThr <sup>4</sup> DHPro <sup>7</sup> Lys(Flu) <sup>8</sup> OT	1	Thiourea	(196)
	d[Orn <sup>8</sup> (5/6C-Flu)]VT		Amide	(53)
	[HO <sup>1</sup> ][Orn <sup>8</sup> (5/6C-Rhm)]VT			(197)
	NR-PEG-CBT	1, 2, 4		(198)
	SQ-PEG-CBT			
Parathyroid hormone 1 receptor (PTH1R)	PTH-TMR	-	Amide	(199)
	Rho-PTH-(1-34)	1		(200)
	Fluo-PTH-(1-34)			
	Rho-PTH-(7-34)	1, 2		
	Fluo-PTH-(7-34)			
Relaxin family peptide receptor 1 and 2 (RXFP1 and RXFP2)	Cy5.5-H2 relaxin	-	Triazole	(152)
Relaxin family peptide receptor 1 (RXFP1)	Cy5.5-H2:A(4-24)(F23A)	1, 2		
Relaxin family peptide receptor 2 (RXFP2)	Cy5.5-INSL3	-	Triazole	(151)
Relaxin family peptide receptor 3 (RXFP3)	DOTA(Eu <sup>3+</sup> )-"Easily labelled R3"	1, 4	Triazole, chelator	(201)
Secretin receptor (rat)	(Rat secretin-27)-Gly-rhodamine	3	Amide	(202)
Secretin receptor	Alexa-secretin	-	Amide	(203)
	(Lys <sup>13</sup> -Alexa)secretin	1		
	(Lys <sup>22</sup> -Alexa)secretin			
	Secretin-Gly <sup>28</sup> -(Cys <sup>29</sup> -Alexa)	3		
Somatostatin receptors (subtype unspecified)	Cyclo-cypate-[dF-cyclo(CYdWKTC)TK)-NH <sub>2</sub>	1, 2, C-terminal extension from octreotide	Amide	(204)

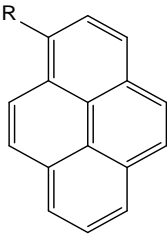
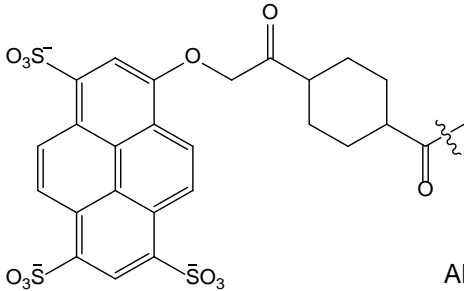
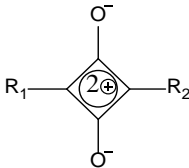
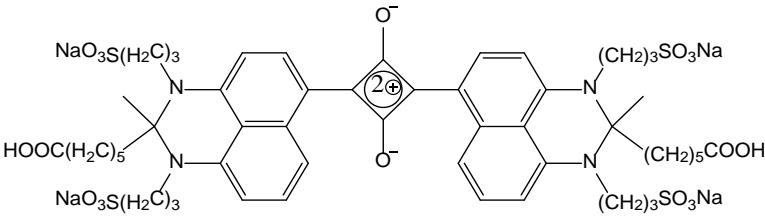
Target GPCR(s)	Fluorescently labelled ligand	Structural modifications*	Linkage	Reference
<b>Somatostatin sst<sub>1</sub> and sst<sub>2</sub> receptors</b>	$\alpha$ -Fluoresceinyl-[D-Trp <sup>8</sup> ]SRIF-14 $\alpha$ -Bodipy-[D-Trp <sup>8</sup> ]SRIF-14	1	Amide	(107)
<b>Somatostatin sst<sub>2</sub> receptor</b>	Indodicarbocyanine-octreotide	1, 2	Amide	(205)
	Indodicarbocyanine-octreotate Indotricarbocyanine-octreotate			(206)
	LS172	1, 2, C-terminal extension from octreotide		(207)
<b>Thyrotropin-releasing hormone receptor (TRHR)</b>	FL-TRH Rhod-TRH	4	Thiourea	(208, 209)
<b>Urotensin receptor (GPR14)</b>	Europium-urotensin II	-	chelator	(210)
	FITC-urotensin II		Thiourea	(210, 211)
<b>Vasopressin receptors (subtype unspecified)</b>	1-desamino-8-rhodamine-L-Lysine vasopressin	1	Thiourea	(212)
	1-deamino[3-( <i>p</i> -azidophenylalanine)]-N <sup>ε</sup> -rhodamyl-LVP			(213)
	[Mpa <sup>1</sup> , Lys(CapBio) <sup>4</sup> , Hyp <sup>7</sup> ]AVP	1, 4	Amide	(214)
<b>Vasopressin V<sub>1</sub> and V<sub>2</sub> receptors</b>	[Mpa <sup>1</sup> , Lys(carboxyfluorescein) <sup>8</sup> ]VP [Mpa <sup>1</sup> , Lys(TMR) <sup>8</sup> ]VP	1	Amide	(215, 216)
<b>Vasopressin V<sub>1a</sub> receptor</b>	PhAcAL(Mec)VP PhAcAL(Btn)VP	1, 2, cyclic to linear	Amide	(217)
<b>Vasopressin V<sub>1a</sub> and oxytocin (OT) receptors</b>	[Lys <sup>8</sup> (5C-Flu)]PVA [Lys <sup>8</sup> (5C-Rhm)]PVA	1, 2, cyclic to linear	Amide	(218)
	[Lys <sup>8</sup> (Alexa 488)]PVA			(219)
<b>Vasopressin V<sub>1b</sub> and oxytocin (OT) receptors</b>	d[Leu <sup>4</sup> , Lys(Alexa647) <sup>8</sup> ]VP	1	Amide	(150)
	d[Leu <sup>4</sup> , Lys(Aud-Alexa647) <sup>8</sup> ]VP	1, 4		
<b>Vasopressin V<sub>2</sub> receptor</b>	FL-AVP-data TR-AVP-anta	1	Thiourea	(220)

Target GPCR(s)	Fluorescently labelled ligand	Structural modifications*	Linkage	Reference
Vasotocin V <sub>1</sub> receptor	Oregon Green 488-[Arg <sup>8</sup> ]-vasotocin	1	Amide	(221)
VIP receptor	CF-VIP	-	Amide	(188)
Y receptors (subtype unspecified)	CF-NPY	-		
Y <sub>1</sub> , Y <sub>4</sub> and Y <sub>5</sub> receptors	BODIPY®TMR/FL-[Leu <sup>31</sup> , Pro <sup>34</sup> ]NPY/PYY	1	(Unspecified)	(222)
Y <sub>1</sub> , Y <sub>2</sub> , Y <sub>5</sub> receptors	Cy5-pNPY Dy630-pNPY	-	Amide	(13)
Y <sub>2</sub> and Y <sub>5</sub> receptors	BODIPY®FL-PYY(3-36)	2	(Unspecified)	(222)
Y <sub>4</sub> and Y <sub>5</sub> receptors	BODIPY®FL-hPP	-		
Y <sub>1</sub> receptor	Cy3-[Pro <sup>34</sup> ]NPY	1	(Unspecified)	(223)
	monoRhB-1229U91	1, 2, dimerisation	Amide	(224)
	[( <i>trans</i> -4-L-Ctp) <sup>3</sup> , Lys <sup>4</sup> ]BVD15	1, 2	Triazole	(225)
	[( <i>trans</i> -4-L-Ctp) <sup>3</sup> , Arg <sup>4</sup> ]BVD15			
	[( <i>cis</i> -3-L-Ctp) <sup>3</sup> , Lys <sup>4</sup> ]BVD15			
	[( <i>cis</i> -4-L-Ctp) <sup>3</sup> , Lys <sup>4</sup> ]BVD15			
	Cyclo[Glu <sup>2</sup> , <i>trans</i> -4-L-Ctp <sup>3</sup> , Dap <sup>4</sup> ]BVD-15			
	[( <i>trans</i> -4-L-R <sup>1</sup> tp) <sup>3</sup> , Arg <sup>4</sup> ]BVD15			
	[( <i>trans</i> -4-L-R <sup>2</sup> tp) <sup>3</sup> , Arg <sup>4</sup> ]BVD15			
Y <sub>1</sub> and Y <sub>4</sub> receptors	[Lys(sCy5) <sup>2</sup> , Arg <sup>4</sup> ]BVD-15	1, 2	Amide	(226)
Y <sub>2</sub> receptor	Cy3-[Ahx <sup>5-24</sup> ]NPY	1, 2	(Unspecified)	(223)
Y <sub>4</sub> receptor	Cy5-[K <sup>4</sup> ]hPP	1	Amide	(227)
	Mono-sCy5-(2 <i>R</i> ,7 <i>R</i> )-sub(YRLRY-NH <sub>2</sub> ) <sub>2</sub>	1, 2, dimerisation	Amide	(228)
Y <sub>5</sub> receptor	BODIPY®TMR-[cPP(1-7), NPY(9-23), Ala <sup>31</sup> , Aib <sup>32</sup> , Gln <sup>34</sup> ]hPP	1	(Unspecified)	(222)
	BODIPY®TMR-[hPP(1-17), Ala <sup>31</sup> , Aib <sup>32</sup> ]NPY			

## Chapter appendix 2: Commonly used fluorophores and their structures.

Chemical class	Core structure	Examples	Reference
Cyanine derivatives	$X \left[ \begin{array}{c} \text{C}=\text{C} \\   \quad   \\ \text{H} \quad \text{H} \end{array} \right]_n \text{C}=\text{Y}$		(229)
			
Xanthene derivatives			(230)
			
Coumarin derivatives			(231)

Chemical class	Core structure	Examples	Reference
<b>BODIPY derivatives</b>		 BODIPY FL	(82)
<b>Naphthalimide derivatives</b>		 Lucifer yellow	(232, 233)
<b>Lanthanides</b>	(Metal ions)	<p>DTPA-chelated europium</p>  <p>DOTA-chelated thulium</p> 	(234)

Chemical class	Core structure	Examples	Reference
Pyrene derivatives		 <p>Alexa Fluor 405</p>	(235)
Squaraines		 <p>KSQ-4-H</p>	(236, 237)

## References

- (1) Weissleder, R., and Mahmood, U. (2001) Molecular imaging. *Radiology* 219, 316-333.
- (2) Kaijzel, E. L., van der Pluijm, G., and Löwik, C. W. G. M. (2007) Whole-body optical imaging in animal models to assess cancer development and progression. *Clin. Cancer Res.* 13, 3490-3497.
- (3) Ploem, J. S. (1999) Chapter one - Fluorescence Microscopy, in *Fluorescent and Luminescent Probes for Biological Activity (Second Edition)* (Mason, W. T., Ed.) pp 3-13, Academic Press, London.
- (4) Kasten, F. H. (1999) Chapter two - Introduction to Fluorescent Probes: Properties, History and Applications, in *Fluorescent and Luminescent Probes for Biological Activity (Second Edition)* (Mason, W. T., Ed.) pp 17-39, Academic Press, London.
- (5) Daly, C. J., and McGrath, J. C. (2003) Fluorescent ligands, antibodies, and proteins for the study of receptors. *Pharmacol. Ther.* 100, 101-118.
- (6) Haustein, E., and Schwille, P. (2004) Single-molecule spectroscopic methods. *Curr. Opin. Struct. Biol* 14, 531-540.
- (7) Bai, M., and Bornhop, D. J. (2012) Recent advances in receptor-targeted fluorescent for *in vivo* cancer imaging. *Curr. Med. Chem.* 19, 4742-4758.
- (8) Böhme, I., and Beck-Sickinger, A. (2009) Illuminating the life of GPCRs. *Cell Commun. Signal.* 7, 16.
- (9) Vernall, A. J., Stoddart, L. A., Briddon, S. J., Hill, S. J., and Kellam, B. (2012) Highly potent and selective fluorescent antagonists of the human adenosine A<sub>3</sub> receptor based on the 1,2,4-triazolo[4,3-*a*]quinoxalin-1-one scaffold. *J. Med. Chem.* 55, 1771-1782.
- (10) Hanson, G. T., and Hanson, B. J. (2008) Fluorescent probes for cellular assays. *Comb. Chem. High T. Scr.* 11, 505-513.
- (11) Ma, Z., Du, L., and Li, M. (2014) Toward fluorescent probes for G-protein-coupled receptors (GPCRs). *J. Med. Chem.* 57, 8187-8203.
- (12) Cottet, M., Faklaris, O., Zwier, J. M., Trinquet, E., Pin, J.-P., and Durroux, T. (2011) Original fluorescent ligand-based assays open new perspectives in G-protein coupled receptor drug screening. *Pharmaceuticals* 4, 202-214.
- (13) Schneider, E., Mayer, M., Ziemek, R., Li, L., Hutzler, C., Bernhardt, G., and Buschauer, A. (2006) A simple and powerful flow cytometric method for the simultaneous determination of multiple parameters at G protein-coupled receptor subtypes. *ChemBioChem* 7, 1400-1409.
- (14) Sheth, R. A., and Mahmood, U. (2010) Optical molecular imaging and its emerging role in colorectal cancer. *Am. J. Physiol. Gastrointest. Liver Physiol.* 299, G807-G820.

- 
- (15) Rudin, M., and Weissleder, R. (2003) Molecular imaging in drug discovery and development. *Nat. Rev. Drug Discov.* 2, 123-131.
- (16) de Haller, E. B. (1996) Time-resolved transillumination and optical tomography. *J. Biomed. Opt.* 1, 7-17.
- (17) McGrath, J. C., Arribas, S., and Daly, C. J. (1996) Fluorescent ligands for the study of receptors. *Trends Pharmacol. Sci.* 17, 393-399.
- (18) Sanai, N., Eschbacher, J., Hattendorf, G., Coons, S. W., Preul, M. C., Smith, K. A., Nakaji, P., and Spetzler, R. F. (2001) Intraoperative confocal microscopy for brain tumors: a feasibility analysis in humans. *Neurosurgery* 68, 282-290.
- (19) Jonak, C., Skvara, H., Kunstfeld, R., Trautinger, F., and Schmid, J. A. (2011) Intradermal indocyanine green for *in vivo* fluorescence laser scanning microscopy of human skin: a pilot study. *PLoS ONE* 6, e23972.
- (20) Astner, S., Dietterle, S., Otberg, N., Rowert-Huber, H.-J., Stockfleth, E., and Lademann, J. (2008) Clinical applicability of *in vivo* fluorescence confocal microscopy for noninvasive diagnosis and therapeutic monitoring of nonmelanoma skin cancer. *J. Biomed. Opt.* 13, 014003.
- (21) Marshall, M. V., Rasmussen, J. C., Tan, I. C., Aldrich, M. B., Adams, K. E., Wang, X., Fife, C. E., Maus, E. A., Smith, L. A., and Sevic-Muraca, E. M. (2010) Near-infrared fluorescence imaging in humans with indocyanine green: A review and update. *Open Surg. Oncol. J.* 2, 12-25.
- (22) Unno, N., Inuzuka, K., Suzuki, M., Yamamoto, N., Sagara, D., Nishiyama, M., and Konno, H. (2007) Preliminary experience with a novel fluorescence lymphography using indocyanine green in patients with secondary lymphedema. *J. Vasc. Surg.* 45, 1016-1021.
- (23) Unno, N., Nishiyama, M., Suzuki, M., Yamamoto, N., Inuzuka, K., Sagara, D., Tanaka, H., and Konno, H. (2008) Quantitative lymph imaging for assessment of lymph function using indocyanine green fluorescence lymphography. *Eur. J. Vasc. Endovasc. Surg.* 36, 230-236.
- (24) Dorshow, R. B., Bugaj, J. E., Burleigh, B. D., Duncan, J. R., Johnson, M. A., and Jones, W. B. (1998) Noninvasive fluorescence detection of hepatic and renal function. *J. Biomed. Opt.* 3, 340-345.
- (25) Leopoldo, M., Lacivita, E., Berardi, F., and Perrone, R. (2009) Developments in fluorescent probes for receptor research. *Drug Discov. Today* 14, 706-712.
- (26) Venter, J. C., Adams, M. D., Myers, E. W., Li, P. W., Mural, R. J., Sutton, G. G., Smith, H. O., Yandell, M., Evans, C. A., Holt, R. A., Gocayne, J. D., Amanatides, P., Ballew, R. M., Huson, D. H., Wortman, J. R., Zhang, Q., Kodira, C. D., Zheng, X. H., Chen, L., Skupski, M., Subramanian, G., Thomas, P. D., Zhang, J., Gabor Miklos, G. L., Nelson, C., Broder, S., Clark, A. G., Nadeau, J., McKusick, V. A., Zinder, N., Levine, A. J., Roberts, R. J., Simon, M., Slayman, C., Hunkapiller, M., Bolanos, R., Delcher, A., Dew, I., Fasulo, D., Flanigan, M., Florea, L., Halpern, A., Hannenhalli, S., Kravitz, S., Levy, S., Mobarry, C., Reinert, K.,



- Remington, K., Abu-Threideh, J., Beasley, E., Biddick, K., Bonazzi, V., Brandon, R., Cargill, M., Chandramouliswaran, I., Charlab, R., Chaturvedi, K., Deng, Z., Francesco, V. D., Dunn, P., Eilbeck, K., Evangelista, C., Gabrielian, A. E., Gan, W., Ge, W., Gong, F., Gu, Z., Guan, P., Heiman, T. J., Higgins, M. E., Ji, R.-R., Ke, Z., Ketchum, K. A., Lai, Z., Lei, Y., Li, Z., Li, J., Liang, Y., Lin, X., Lu, F., Merkulov, G. V., Milshina, N., Moore, H. M., Naik, A. K., Narayan, V. A., Neelam, B., Nusskern, D., Rusch, D. B., Salzberg, S., Shao, W., Shue, B., Sun, J., Wang, Z. Y., Wang, A., Wang, X., Wang, J., Wei, M.-H., Wides, R., Xiao, C., Yan, C., et al. (2001) The sequence of the human genome. *Science* 291, 1304-1351.
- (27) Lagerstrom, M. C., and Schioth, H. B. (2008) Structural diversity of G protein-coupled receptors and significance for drug discovery. *Nat. Rev. Drug Discov.* 7, 339-357.
- (28) Rasmussen, S. G. F., Choi, H.-J., Rosenbaum, D. M., Kobilka, T. S., Thian, F. S., Edwards, P. C., Burghammer, M., Ratnala, V. R. P., Sanishvili, R., Fischetti, R. F., Schertler, G. F. X., Weis, W. I., and Kobilka, B. K. (2007) Crystal structure of the human beta2 adrenergic G-protein-coupled receptor. *Nature* 450, 383-387.
- (29) Bockaert, J., and Philippe Pin, J. (1999) Molecular tinkering of G protein-coupled receptors: an evolutionary success. *EMBO J.* 18, 1723-1729.
- (30) Klabunde, T., and Hessler, G. (2002) Drug design strategies for targeting G-protein-coupled receptors. *ChemBioChem* 3, 928-944.
- (31) Williams, C., and Hill, S. J. (2009) GPCR signaling: understanding the pathway to successful drug discovery, in *G Protein-Coupled Receptors in Drug Discovery* (Leifert, R. W., Ed.) pp 39-50, Humana Press, Totowa, NJ.
- (32) Lodish, H., Berk, A., Zipursky, S. L., Matsudaira, P., Baltimore, D., and Darnell, J. (2000) Section 20.3 G protein-coupled receptors and their effectors, in *Molecular Cell Biology 4th Edition*, New York: W.H. Freeman; Basingstoke: Macmillan.
- (33) Katada, T., Bokoch, G. M., Northup, J. K., Ui, M., and Gilman, A. G. (1984) The inhibitory guanine nucleotide-binding regulatory component of adenylate cyclase. Properties and function of the purified protein. *J. Biol. Chem.* 259, 3568-3577.
- (34) Falkenburger, B. H., Dickson, E. J., and Hille, B. (2013) Quantitative properties and receptor reserve of the DAG and PKC branch of G<sub>q</sub>-coupled receptor signaling. *J. Gen. Physiol.* 141, 537-555.
- (35) Berridge, M. J. (1998) Neuronal Calcium Signaling. *Neuron* 21, 13-26.
- (36) Siehler, S. (2009) Regulation of RhoGEF proteins by G<sub>12/13</sub>-coupled receptors. *Br. J. Pharmacol.* 158, 41-49.
- (37) Mark, M. D., and Herlitze, S. (2000) G-protein mediated gating of inward-rectifier K<sup>+</sup> channels. *Eur. J. Biochem.* 267, 5830-5836.
- (38) Camps, M., Carozzi, A., Schnabel, P., Scheer, A., Parker, P. J., and Gierschik, P. (1992) Isozyme-selective stimulation of phospholipase C- $\beta$ 2 by G protein  $\beta\gamma$ -subunits. *Nature* 360, 684-686.

- 
- (39) Tang, W. J., and Gilman, A. G. (1991) Type-specific regulation of adenylyl cyclase by G protein beta gamma subunits. *Science* 254, 1500-1503.
- (40) Fruman, D. A., Meyers, R. E., and Cantley, L. C. (1998) Phosphoinositide kinases. *Annu. Rev. Biochem.* 67, 481-507.
- (41) Ma, P., and Zimmel, R. (2002) Value of novelty? *Nat. Rev. Drug Discov.* 1, 571-572.
- (42) Filmore, D. (2004) It's a GPCR world. *Modern Drug Discovery* 7, 24-28.
- (43) Drews, J. (2000) Drug discovery: A historical perspective. *Science* 287, 1960-1964.
- (44) Fredriksson, R., Lagerström, M. C., Lundin, L.-G., and Schiöth, H. B. (2003) The G-protein-coupled receptors in the human genome form five main families. Phylogenetic analysis, paralogon groups, and fingerprints. *Mol. Pharmacol.* 63, 1256-1272.
- (45) Tautermann, C. S. (2014) GPCR structures in drug design, emerging opportunities with new structures. *Bioorg. Med. Chem. Lett.* 24, 4073-4079.
- (46) Davenport, A. P., Alexander, S. P. H., Sharman, J. L., Pawson, A. J., Benson, H. E., Monaghan, A. E., Liew, W. C., Mpamhanga, C. P., Bonner, T. I., Neubig, R. R., Pin, J. P., Spedding, M., and Harmar, A. J. (2013) International union of basic and clinical pharmacology. LXXXVIII. G protein-coupled receptor list: recommendations for new pairings with cognate ligands. *Pharmacol. Rev.* 65, 967-986.
- (47) Garland, S. L. (2013) Are GPCRs still a source of new targets? *J. Biomol. Screen.* 18, 947-966.
- (48) Vernall, A. J., Hill, S. J., and Kellam, B. (2013) The evolving small-molecule fluorescent-conjugate toolbox for class A GPCRs. *Br. J. Pharmacol.* In Press.
- (49) Hara, T., Hirasawa, A., Sun, Q., Koshimizu, T.-a., Itsubo, C., Sadakane, K., Awaji, T., and Tsujimoto, G. (2009) Flow cytometry-based binding assay for GPR40 (FFAR1; Free Fatty Acid Receptor 1). *Mol. Pharmacol.* 75, 85-91.
- (50) Yates, A. S., Doughty, S. W., Kendall, D. A., and Kellam, B. (2005) Chemical modification of the naphthoyl 3-position of JWH-015: In search of a fluorescent probe to the cannabinoid CB2 receptor. *Bioorg. Med. Chem. Lett.* 15, 3758-3762.
- (51) Bai, M., Sexton, M., Stella, N., and Bornhop, D. J. (2008) MBC94, a conjugable ligand for cannabinoid CB2 receptor imaging. *Bioconjug. Chem.* 19, 988-992.
- (52) Fahrenholz, F., Jurzak, M., Gerstberger, R., and Haase, W. (1993) Renal and central vasopressin receptors: Immunocytochemical localization. *Ann. N. Y. Acad. Sci.* 689, 194-206.
- (53) Terrillon, S., Cheng, L. L., Stoev, S., Mouillac, B., Barberis, C., Manning, M., and Durroux, T. (2002) Synthesis and characterization of fluorescent antagonists and agonists for human oxytocin and vasopressin V1a receptors. *J. Med. Chem.* 45, 2579-2588.

- 
- (54) Böhme, I., Mörl, K., Bamming, D., Meyer, C., and Beck-Sickinger, A. G. (2007) Tracking of human Y receptors in living cells-A fluorescence approach. *Peptides* 28, 226-234.
- (55) Los, G. V., Encell, L. P., McDougall, M. G., Hartzell, D. D., Karassina, N., Zimprich, C., Wood, M. G., Learish, R., Ohana, R. F., Urh, M., Simpson, D., Mendez, J., Zimmerman, K., Otto, P., Vidugiris, G., Zhu, J., Darzins, A., Klaubert, D. H., Bulleit, R. F., and Wood, K. V. (2008) HaloTag: A novel protein labeling technology for cell imaging and protein analysis. *ACS Chem. Biol.* 3, 373-382.
- (56) Fosgerau, K., and Hoffmann, T. (2015) Peptide therapeutics: current status and future directions. *Drug Discov. Today* 20, 122-128.
- (57) Bellmann-Sickert, K., and Beck-Sickinger, A. G. (2010) Peptide drugs to target G protein-coupled receptors. *Trends Pharmacol. Sci.* 31, 434-441.
- (58) Beck-Sickinger, A. G., and Khan, I. U. (2008) Targeted tumor diagnosis and therapy with peptide hormones as radiopharmaceuticals. *Anticancer Agents Med. Chem.* 8, 186-199.
- (59) Liu, S., and Edwards, D. S. (2002) Fundamentals of receptor-based diagnostic metalloradiopharmaceuticals, in *Contrast Agents II* (Krause, W., Ed.) pp 259-278, Springer Berlin Heidelberg.
- (60) Ambrosini, V., Fani, M., Fanti, S., Forrer, F., and Maecke, H. R. (2011) Radiopeptide imaging and therapy in Europe. *J. Nucl. Med.* 52, 42S-55S.
- (61) Okarvi, S. M. (2001) Recent progress in fluorine-18 labelled peptide radiopharmaceuticals. *Eur. J. Nucl. Med.* 28, 929-938.
- (62) Bugaj, J. E., Achilefu, S., Dorshow, R. B., and Rajagopalan, R. (2001) Novel fluorescent contrast agents for optical imaging of *in vivo* tumors based on a receptor-targeted dye-peptide conjugate platform. *J. BioMed. Opt.* 6, 122-133.
- (63) Goldsmith, S. J. (1997) Receptor imaging: Competitive or complementary to antibody imaging? *Semin. Nucl. Med.* 27, 85-93.
- (64) McGregor, D. P. (2008) Discovering and improving novel peptide therapeutics. *Curr. Opin. Pharmacol.* 8, 616-619.
- (65) Sato, A. K., Viswanathan, M., Kent, R. B., and Wood, C. R. (2006) Therapeutic peptides: technological advances driving peptides into development. *Curr. Opin. Pharmacol.* 17, 638-642.
- (66) Marx, V. (2005) Watching peptide drugs grow up. *Chem. Eng. News Archive* 83, 17-24.
- (67) Vlieghe, P., Lisowski, V., Martinez, J., and Khrestchatisky, M. (2010) Synthetic therapeutic peptides: science and market. *Drug Discov. Today* 15, 40-56.
- (68) Loffet, A. (2002) Peptides as drugs: is there a market? *J. Pept. Sci.* 8, 1-7.

- 
- (69) McAfee, J. G., and Neumann, R. D. (1996) Radiolabeled peptides and other ligands for receptors overexpressed in tumor cells for imaging neoplasms. *Nucl. Med. Biol.* 23, 673-676.
- (70) Zwanziger, D., and Beck-Sickinger, A. G. (2008) Radiometal targeted tumor diagnosis and therapy with peptide hormones. *Curr. Pharm. Des.* 14, 2385-2400.
- (71) Hruby, V. J. (2002) Designing peptide receptor agonists and antagonists. *Nat. Rev. Drug Discov.* 1, 847-858.
- (72) Dooley, C. T., Chung, N. N., Wilkes, B. C., Schiller, P. W., Bidlack, J. M., Pasternak, G. W., and Houghten, R. A. (1994) An all D-amino acid opioid peptide with central analgesic activity from a combinatorial library. *Science* 266, 2019-2022.
- (73) Ahrens, V. M., Bellmann-Sickert, K., and Beck-Sickinger, A. G. (2012) Peptides and peptide conjugates: therapeutics on the upward path. *Future Med. Chem.* 4, 1567-1586.
- (74) Chen, H., Lin, W., Cui, H., and Jiang, W. (2015) Development of unique xanthene-cyanine fused near-infrared fluorescent fluorophores with superior chemical stability for biological fluorescence imaging. *Chemistry* 21, 733-745.
- (75) Gonçalves, M. S. T. (2009) Fluorescent labeling of biomolecules with organic probes. *Chem. Rev.* 109, 190-212.
- (76) Li, J., Zhang, C.-F., Ming, Z.-Z., Yang, W.-C., and Yang, G.-F. (2013) Novel coumarin-based sensitive and selective fluorescent probes for biothiols in aqueous solution and in living cells. *RSC Advances* 3, 26059-26065.
- (77) Wheelock, C. E. (1959) The fluorescence of some coumarins. *J. Am. Chem. Soc.* 81, 1348-1352.
- (78) Lin, W., Long, L., and Tan, W. (2010) A highly sensitive fluorescent probe for detection of benzenethiols in environmental samples and living cells. *Chem. Commun.* 46, 1503-1505.
- (79) Pajk, S. (2014) Synthesis and fluorescence properties of environment-sensitive 7-(diethylamino)coumarin derivatives. *Tetrahedron Lett.* 55, 6044-6047.
- (80) Li, J., Zhang, C.-F., Yang, S.-H., Yang, W.-C., and Yang, G.-F. (2014) A coumarin-based fluorescent probe for selective and sensitive detection of thiophenols and its application. *Anal. Chem.* 86, 3037-3042.
- (81) Boens, N., Leen, V., and Dehaen, W. (2012) Fluorescent indicators based on BODIPY. *Chem. Soc. Rev.* 41, 1130-1172.
- (82) Ulrich, G., Ziessel, R., and Harriman, A. (2008) The chemistry of fluorescent bodipy dyes: versatility unsurpassed. *Angew. Chem. Int. Ed.* 47, 1184-1201.
- (83) Loudet, A., and Burgess, K. (2007) BODIPY dyes and their derivatives: syntheses and spectroscopic properties. *Chem. Rev.* 107, 4891-4932.

- 
- (84) Johnson, I. D., Kang, H. C., and Haugland, R. P. (1991) Fluorescent membrane probes incorporating dipyrrometheneboron difluoride fluorophores. *Anal. Biochem.* 198, 228-237.
- (85) Karolin, J., Johansson, L. B. A., Strandberg, L., and Ny, T. (1994) Fluorescence and absorption spectroscopic properties of dipyrrometheneboron difluoride (BODIPY) derivatives in liquids, lipid membranes, and proteins. *J. Am. Chem. Soc.* 116, 7801-7806.
- (86) Brana, M. F., and Ramos, A. (2001) Naphthalimides as anticancer agents: synthesis and biological activity. *Curr. Med. Chem. Anticancer Agents* 1, 237-255.
- (87) Ingrassia, L., Lefranc, F., Kiss, R., and Mijatovic, T. (2009) Naphthalimides and azonafides as promising anti-cancer agents. *Curr. Med. Chem.* 16, 1192-1213.
- (88) Handl, H. L., and Gillies, R. J. (2005) Lanthanide-based luminescent assays for ligand-receptor interactions. *Life Sci.* 77, 361-371.
- (89) Inglese, J., Samama, P., Patel, S., Burbaum, J., Stroke, I. L., and Appell, K. C. (1998) Chemokine receptor-ligand interactions measured using time-resolved fluorescence. *Biochemistry* 37, 2372-2377.
- (90) Yip, Y.-W., Wen, H., Wong, W.-T., Tanner, P. A., and Wong, K.-L. (2012) Increased antenna effect of the lanthanide complexes by control of a number of terdentate N-donor pyridine ligands. *Inorg. Chem.* 51, 7013-7015.
- (91) Leif, R. C., Vallarino, L. M., Becker, M. C., and Yang, S. (2006) Increasing the luminescence of lanthanide complexes. *Cytometry Part A* 69A, 767-778.
- (92) Bains, G. K., Kim, S. H., Sorin, E. J., and Narayanaswami, V. (2012) The extent of pyrene excimer fluorescence emission is a reflector of distance and flexibility: analysis of the segment linking the LDL receptor-binding and tetramerization domains of apolipoprotein E3. *Biochemistry* 51, 6207-6219.
- (93) (2010) Thiol-reactive probes, in *Molecular probes handbook, a guide to fluorescent probes and labeling technologies 11th Edition* (Johnson, I., and Spence, M. T. Z., Eds.), Invitrogen.
- (94) Förster, T. (1969) Excimers. *Angew. Chem. Int. Ed.* 8, 333-343.
- (95) Winnik, F. M. (1993) Photophysics of preassociated pyrenes in aqueous polymer solutions and in other organized media. *Chem. Rev.* 93, 587-614.
- (96) Van der Horst, D. J., and Ryan, R. O. (2012) 9 - Lipid Transport A2 - Gilbert, Lawrence I, in *Insect Molecular Biology and Biochemistry* pp 317-345, Academic Press, San Diego.
- (97) Hammarström, P., Kalman, B., Jonsson, B.-H., and Carlsson, U. (1997) Pyrene excimer fluorescence as a proximity probe for investigation of residual structure in the unfolded state of human carbonic anhydrase II. *FEBS Lett.* 420, 63-68.
- (98) Hu, L., Yan, Z., and Xu, H. (2013) Advances in synthesis and application of near-infrared absorbing squaraine dyes. *RSC Advances* 3, 7667-7676.

- 
- (99) Yagi, S., and Nakazumi, H. (2006) Chapter 6 - Syntheses and application of squarylium dyes A2 - Kim, Sung-Hoon, in *Functional Dyes* pp 215-255, Elsevier Science, Amsterdam.
- (100) Song, B., Zhang, Q., Ma, W.-H., Peng, X.-J., Fu, X.-M., and Wang, B.-S. (2009) The synthesis and photostability of novel squarylium indocyanine dyes. *Dyes Pigm.* 82, 396-400.
- (101) Tatarets, A. L., Fedyunyayeva, I. A., Dyubko, T. S., Povrozin, Y. A., Doroshenko, A. O., Terpetschnig, E. A., and Patsenker, L. D. (2006) Synthesis of water-soluble, ring-substituted squaraine dyes and their evaluation as fluorescent probes and labels. *Anal. Chim. Acta* 570, 214-223.
- (102) Oswald, B., Patsenker, L., Duschl, J., Szmackinski, H., Wolfbeis, O. S., and Terpetschnig, E. (1999) Synthesis, spectral properties, and detection limits of reactive squaraine dyes, a new class of diode laser compatible fluorescent protein labels. *Bioconjug. Chem.* 10, 925-931.
- (103) Volkova, K. D., Kovalska, V. B., Tatarets, A. L., Patsenker, L. D., Kryvorotenko, D. V., and Yarmoluk, S. M. (2007) Spectroscopic study of squaraines as protein-sensitive fluorescent dyes. *Dyes Pigm.* 72, 285-292.
- (104) Chen, H., Farahat, M. S., Law, K.-Y., and Whitten, D. G. (1996) Aggregation of surfactant squaraine dyes in aqueous solution and microheterogeneous media: correlation of aggregation behavior with molecular structure. *J. Am. Chem. Soc.* 118, 2584-2594.
- (105) Xu, Y., Li, Z., Malkovskiy, A., Sun, S., and Pang, Y. (2010) Aggregation control of squaraines and their use as near-infrared fluorescent sensors for protein. *J. Phys. Chem. B* 114, 8574-8580.
- (106) Reddington, M. V. (2007) Synthesis and properties of phosphonic acid containing cyanine and squaraine dyes for use as fluorescent labels. *Bioconjug. Chem.* 18, 2178-2190.
- (107) Nouel, D., Gaudriault, G., Houle, M., Reisine, T., Vincent, J.-P., Mazella, J., and Beaudet, A. (1997) Differential internalization of somatostatin in COS-7 cells transfected with SST1 and SST2 receptor subtypes: a confocal microscopic study using novel fluorescent somatostatin derivatives. *Endocrinology* 138, 296-306.
- (108) Beaudet, A., Nouel, D., Stroh, T., Vandenbulcke, F., Dan-Farra, C., and Vincent, P. (1998) Fluorescent ligands for studying neuropeptide receptors by confocal microscopy. *Braz. J. Med. Biol. Res.* 31, 1479-1489.
- (109) Taylor, D. L. (1988) Chapter 13 Basic Fluorescence Microscopy, in *Methods in Cell Biology* (Yu-Li Wang, D. L. T., and Jeon, K. W., Eds.) pp 207-237, Academic Press.
- (110) Zhang, H. (1990) Approximate calculation of extinction coefficient. *J. Phys. D: Appl. Phys.* 23, 1735-1737.
- (111) Hermanson, G. T. (2008) Chapter 9 - Fluorescent Probes, in *Bioconjugate Techniques (Second Edition)* pp 396-497, Academic Press, New York.

- (112) Lee, S., Xie, J., and Chen, X. (2010) Peptide-based probes for targeted molecular imaging. *Biochemistry* 49, 1364-1376.
- (113) Weissleder, R. (2001) A clearer vision for in vivo imaging. *Nat. Biotech.* 19, 316-317.
- (114) Fukumura, D., Xavier, R., Sugiura, T., Chen, Y., Park, E.-C., Lu, N., Selig, M., Nielsen, G., Taksir, T., Jain, R. K., and Seed, B. (1998) Tumor induction of VEGF promoter activity in stromal cells. *Cell* 94, 715-725.
- (115) Pansare, V. J., Hejazi, S., Faenza, W. J., and Prud'homme, R. K. (2012) Review of long-wavelength optical and NIR imaging materials: contrast agents, fluorophores, and multifunctional nano carriers. *Chem. Mater.* 24, 812-827.
- (116) Sullivan, R. (2012) Bayesian Statistics, in *Introduction to Data Mining for the Life Sciences* pp 303-361, Humana Press, Totowa, NJ.
- (117) Hermanson, G. T. (2013) Chapter 3 - The Reactions of Bioconjugation, in *Bioconjugate Techniques (Third edition)* pp 229-258, Academic Press, Boston.
- (118) Podhradsky, D., Drobnica, L., and Kristian, P. (1979) Reactions of cysteine, its derivatives, glutathione, coenzyme A, and dihydrolipoic acid with isothiocyanates. *Experientia* 35, 154.
- (119) Tabujew, I., and Peneva, K. (2015) CHAPTER 1 Functionalization of Cationic Polymers for Drug Delivery Applications, in *Cationic Polymers in Regenerative Medicine* pp 1-29, The Royal Society of Chemistry.
- (120) Mädler, S., Bich, C., Touboul, D., and Zenobi, R. (2009) Chemical cross-linking with NHS esters: a systematic study on amino acid reactivities. *J. Mass. Spectrom.* 44, 694-706.
- (121) Toseland, C. P. (2013) Fluorescent labeling and modification of proteins. *J. Chem. Biol.* 6, 85-95.
- (122) Crestfield, A. M., Stein, W. H., and Moore, S. (1963) Alkylation and identification of the histidine residues at the active site of ribonuclease. *J. Biol. Chem.* 238, 2413-2419.
- (123) Stark, G. R., and Stein, W. H. (1964) Alkylation of the methionine residues of ribonuclease in 8 M urea. *J. Biol. Chem.* 239, 3755-3761.
- (124) Lang, S., Spratt, D. E., Guillemette, J. G., and Palmer, M. (2005) Dual-targeted labeling of proteins using cysteine and selenomethionine residues. *Anal. Biochem.* 342, 271-279.
- (125) Jullien, M., and Garel, J. R. (1981) Fluorescent probe of ribonuclease A conformation. *Biochemistry* 20, 7021-7026.
- (126) Yang, Z., and Attygalle, A. B. (2007) LC/MS characterization of undesired products formed during iodoacetamide derivatization of sulfhydryl groups of peptides. *J. Mass. Spectrom.* 42, 233-243.

- (127) Senter, P. D., and Sievers, E. L. (2012) The discovery and development of brentuximab vedotin for use in relapsed Hodgkin lymphoma and systemic anaplastic large cell lymphoma. *Nat. Biotech.* 30, 631-637.
- (128) Lewis Phillips, G. D., Li, G., Dugger, D. L., Crocker, L. M., Parsons, K. L., Mai, E., Blättler, W. A., Lambert, J. M., Chari, R. V. J., Lutz, R. J., Wong, W. L. T., Jacobson, F. S., Koeppen, H., Schwall, R. H., Kenkare-Mitra, S. R., Spencer, S. D., and Sliwkowski, M. X. (2008) Targeting HER2-positive breast cancer with Trastuzumab-DM1, an antibody-cytotoxic drug conjugate. *Cancer Res.* 68, 9280-9290.
- (129) Fontaine, S. D., Reid, R., Robinson, L., Ashley, G. W., and Santi, D. V. (2015) Long-term stabilization of maleimide-thiol conjugates. *Bioconjug. Chem.* 26, 145-152.
- (130) Knight, P. (1979) Hydrolysis of p-NN'-phenylenebismaleimide and its adducts with cysteine. Implications for cross-linking of proteins. *Biochem. J.* 179, 191-197.
- (131) Huisgen, R. (1963) Kinetic and mechanism of 1,3-dipolar cycloadditions. *Angew. Chem. Int. Ed.* 2, 633-645.
- (132) Rostovtsev, V. V., Green, L. G., Fokin, V. V., and Sharpless, K. B. (2002) A stepwise huisgen cycloaddition process: copper(I)-catalyzed regioselective "ligation" of azides and terminal alkynes. *Angew. Chem. Int. Ed.* 41, 2596-2599.
- (133) Huisgen, R. (1984), in *1,3-Dipolar Cycloaddition Chemistry* (A., P., Ed.) pp 1-176, Wiley, New York.
- (134) Tornøe, C. W., Christensen, C., and Meldal, M. (2002) Peptidotriazoles on solid phase: [1,2,3]-triazoles by regiospecific copper(I)-catalyzed 1,3-dipolar cycloadditions of terminal alkynes to azides. *J. Org. Chem.* 67, 3057-3064.
- (135) Hong, V., Presolski, S. I., Ma, C., and Finn, M. G. (2009) Analysis and optimization of copper-catalyzed azide-alkyne cycloaddition for bioconjugation. *Angew. Chem. Int. Ed.* 48, 9879-9883.
- (136) Wang, Q., Chan, T. R., Hilgraf, R., Fokin, V. V., Sharpless, K. B., and Finn, M. G. (2003) Bioconjugation by copper(I)-catalyzed azide-alkyne [3 + 2] cycloaddition. *J. Am. Chem. Soc.* 125, 3192-3193.
- (137) Gierlich, J., Gutmiedl, K., Gramlich, P. M. E., Schmidt, A., Burley, G. A., and Carell, T. (2007) Synthesis of highly modified DNA by a combination of PCR with alkyne-bearing triphosphates and click chemistry. *Chem-Eur. J.* 13, 9486-9494.
- (138) Breinbauer, R., and Köhn, M. (2003) Azide-alkyne coupling: A powerful reaction for bioconjugate chemistry. *ChemBioChem* 4, 1147-1149.
- (139) Speers, A. E., and Cravatt, B. F. (2004) Profiling enzyme activities *in vivo* using click chemistry methods. *Chem. Biol.* 11, 535-546.
- (140) Beatty, K. E., Xie, F., Wang, Q., and Tirrell, D. A. (2005) Selective dye-labeling of newly synthesized proteins in bacterial cells. *J. Am. Chem. Soc.* 127, 14150-14151.



- 
- (141) Hsu, T.-L., Hanson, S. R., Kishikawa, K., Wang, S.-K., Sawa, M., and Wong, C.-H. (2007) Alkynyl sugar analogs for the labeling and visualization of glycoconjugates in cells. *Proc. Natl. Acad. Sci.* **104**, 2614-2619.
- (142) Chan, T. R., Hilgraf, R., Sharpless, K. B., and Fokin, V. V. (2004) Polytriazoles as copper(I)-stabilizing ligands in catalysis. *Org. Lett.* **6**, 2853-2855.
- (143) Davies, M. B. (1992) Reactions of L-ascorbic acid with transition metal complexes. *Polyhedron* **11**, 285-321.
- (144) Shangari, N., Chan, T. S., Chan, K., Huai Wu, S., and O'Brien, P. J. (2007) Copper-catalyzed ascorbate oxidation results in glyoxal/AGE formation and cytotoxicity. *Mol. Nutr. Food. Res.* **51**, 445-455.
- (145) Thornalley, P. J. (1998) Glutathione-dependent detoxification of  $\alpha$ -oxoaldehydes by the glyoxalase system: involvement in disease mechanisms and antiproliferative activity of glyoxalase I inhibitors. *Chem. Biol. Interact.* **111-112**, 137-151.
- (146) Hope, D. B., Murti, V. V. S., and du Vigneaud, V. (1962) A highly potent analogue of oxytocin, desamino-oxytocin. *J. Biol. Chem.* **237**, 1563-1566.
- (147) Pena, A., Murat, B., Trueba, M., Ventura, M. A., Bertrand, G., Cheng, L. L., Stoev, S., Szeto, H. H., Wo, N., Brossard, G., Gal, C. S.-L., Manning, M., and Guillon, G. (2007) Pharmacological and physiological characterization of d[Leu<sup>4</sup>, Lys<sup>8</sup>]vasopressin, the first V<sub>1b</sub>-selective agonist for rat vasopressin/oxytocin receptors. *Endocrinology* **148**, 4136-4146.
- (148) Cheng, L. L., Stoev, S., Manning, M., Derick, S., Pena, A., Mimoun, M. B., and Guillon, G. (2004) Design of potent and selective agonists for the human vasopressin V<sub>1b</sub> receptor based on modifications of [deamino-Cys]arginine vasopressin at position 4. *J. Med. Chem.* **47**, 2375-2388.
- (149) Pena, A., Murat, B., Trueba, M., Ventura, M. A., Wo, N. C., Szeto, H. H., Cheng, L. L., Stoev, S., Guillon, G., and Manning, M. (2007) Design and synthesis of the first selective agonists for the rat vasopressin V<sub>1b</sub> receptor: based on modifications of deamino-[Cys]arginine vasopressin at positions 4 and 8. *J. Med. Chem.* **50**, 835-847.
- (150) Corbani, M., Trueba, M., Stoev, S., Murat, B., Mion, J., Boulay, V., Guillon, G., and Manning, M. (2011) Design, synthesis, and pharmacological characterization of fluorescent peptides for imaging human V<sub>1b</sub> vasopressin or oxytocin receptors. *J. Med. Chem.* **54**, 2864-2877.
- (151) Chan, L. J., Rosengren, K. J., Layfield, S. L., Bathgate, R. A. D., Separovic, F., Samuel, C. S., Hossain, M. A., and Wade, J. D. (2012) Identification of key residues essential for the structural fold and receptor selectivity within the A-chain of human gene-2 (H2) relaxin. *J. Biol. Chem.* **287**, 41152-41164.
- (152) Chan, L. J., Smith, C. M., Chua, B. E., Lin, F., Bathgate, R. A. D., Separovic, F., Gundlach, A. L., Hossain, M. A., and Wade, J. D. (2013) Synthesis of fluorescent analogs of relaxin family peptides and their preliminary in vitro and in vivo characterization. *Front. Chem.* **1**, 30.
-

- 
- (153) Teerlink, J. R., Cotter, G., Davison, B. A., Felker, G. M., Filippatos, G., Greenberg, B. H., Ponikowski, P., Unemori, E., Voors, A. A., Adams Jr, K. F., Dorobantu, M. I., Grinfeld, L. R., Jondeau, G., Marmor, A., Masip, J., Pang, P. S., Werdan, K., Teichman, S. L., Trapani, A., Bush, C. A., Saini, R., Schumacher, C., Severin, T. M., and Metra, M. (2013) Serelaxin, recombinant human relaxin-2, for treatment of acute heart failure (RELAX-AHF): a randomised, placebo-controlled trial. *Lancet* 381, 29-39.
- (154) Flower, D. R. (1999) Modelling G-protein-coupled receptors for drug design. *Biochim. Biophys. Acta.* 1422, 207-234.
- (155) Cheng, Z., Garvin, D., Paguio, A., Stecha, P., Wood, K., and Fan, F. (2010) Luciferase reporter assay system for deciphering GPCR pathways. *Curr. Chem. Genomics* 4, 84-91.
- (156) Krucker, T., and Sandanaraj, B. S. (2011) Optical imaging for the new grammar of drug discovery. *Philos. Trans. A. Math. Phys. Eng. Sci.* 369, 4651-4665.
- (157) Schönauer, R., Kaiser, A., Holze, C., Babilon, S., Köbberling, J., Riedl, B., and Beck-Sickinger, A. G. (2015) Fluorescently labeled adrenomedullin allows real-time monitoring of adrenomedullin receptor trafficking in living cells. *J. Pept. Sci.* 21, 905-912.
- (158) Barnes, L. D., Guy, M. N., Roberson, G. M., and Osgood, R. W. (1982) Synthesis, characterization, and biological activity of  $N^{\alpha}$ -(*N*-fluoresceinthiocarbamoyl)-(Asp<sup>1</sup>, Ile<sup>5</sup>)-angiotensin II. *Arch. Biochem. Biophys.* 214, 239-247.
- (159) Hein, L., Meinel, L., Pratt, R. E., Dzau, V. J., and Kobilka, B. K. (1997) Intracellular Trafficking of Angiotensin II and its AT1 and AT2 Receptors: Evidence for Selective Sorting of Receptor and Ligand. *Mol. Endocrinol.* 11, 1266-1277.
- (160) Margathe, J. F., Iturrioz, X., Regenass, P., Karpenko, I. A., Humbert, N., de Rocquigny, H., Hibert, M., Llorens-Cortes, C., and Bonnet, D. (2016) Convenient access to fluorescent probes by chemoselective acylation of hydrazinopeptides: application to the synthesis of the first far-red ligand for apelin receptor imaging. *Chemistry* 22, 1399-1405.
- (161) Bawolak, M.-T., Gera, L., Morissette, G., Bouthillier, J., Stewart, J. M., Gobeil, L.-A., Lodge, R., Adam, A., and Marceau, F. (2009) Fluorescent ligands of the bradykinin B<sub>1</sub> receptors: pharmacologic characterization and application to the study of agonist-induced receptor translocation and cell surface receptor expression. *J. Pharmacol. Exp. Ther.* 329, 159-168.
- (162) Fuente-Moreno, M., Oddo, A., Sheykhzade, M., Pickering, D. S., and Hansen, P. R. (2015) in *24<sup>th</sup> American Peptide Symposium* (Srivastava, V., Yudin, A., and Lebl, M., Eds.) pp 264-265, Orlando, America.
- (163) Strong, A. E., Thierry, A.-C., Cousin, P., Moulon, C., and Demotz, S. (2006) Synthetic chemokines directly labeled with a fluorescent dye as tools for studying chemokine and chemokine receptor interactions. *Eur. Cytokine Netw.* 17, 49-59.
- (164) Oishi, S., Masuda, R., Evans, B., Ueda, S., Goto, Y., Ohno, H., Hirasawa, A., Tsujimoto, G., Wang, Z., Peiper, S. C., Naito, T., Kodama, E., Matsuoka, M., and Fujii, N. (2008) Synthesis

- and application of fluorescein- and biotin-labeled molecular probes for the chemokine receptor CXCR4. *ChemBioChem* 9, 1154-1158.
- (165) Roettger, B. F., Rentsch, R. U., Pinon, D. I., Holicky, E., Hadac, E., Larkin, J. M., and Miller, L. J. (1995) Dual pathways of internalization of the cholecystokinin receptor. *J. Cell Biol.* 128, 1029-1041.
- (166) Cawston, E. E., Harikumar, K. G., and Miller, L. J. (2012) Ligand-induced internalization of the type 1 cholecystokinin receptor independent of recognized signaling activity. *Am. J. Physiol. Cell. Physiol.* 302, C615-27.
- (167) Harikumar, K. G., Pinon, D. I., Wessels, W. S., Prendergast, F. G., and Miller, L. J. (2002) Environment and mobility of a series of fluorescent reporters at the amino terminus of structurally related peptide agonists and antagonists bound to the cholecystokinin receptor. *J. Biol. Chem.* 277, 18552-18560.
- (168) Laabs, E., Béhé, M., Kossatz, S., Frank, W., Kaiser, W. A., and Hilger, I. (2011) Optical imaging of CCK2/gastrin receptor-positive tumors with a minigastrin near-infrared probe. *Invest. Radiol.* 46, 196-201.
- (169) Sachatello, C. R., Sedwick, J., Moriarty, C. L., Grahl-Nielsen, O., and Tritsch, G. L. (1971) Synthesis and secretagogue activity of a potent fluorescent analog of the gastrin peptides. *Endocrinology* 88, 1300-1302.
- (170) Harikumar, K. G., Clain, J., Pinon, D. I., Dong, M., and Miller, L. J. (2005) Distinct molecular mechanisms for agonist peptide binding to types A and B cholecystokinin receptors demonstrated using fluorescence spectroscopy. *J. Biol. Chem.* 280, 1044-1050.
- (171) Hubbard, C. S., Dolence, E. K., Shires, J. A., and Rose, J. D. (2009) Identification of brain target neurons using a fluorescent conjugate of corticotropin-releasing factor. *J. Chem. Neuroanat.* 37, 245-253.
- (172) Oksche, A., Boese, G., Horstmeyer, A., Papsdorf, G., Furkert, J., Beyermann, M., Bienert, M., and Rosenthal, W. (2000) Evidence for downregulation of the endothelin-B-receptor by the use of fluorescent endothelin-1 and a fusion protein consisting of the endothelin-B-receptor and the green fluorescent protein. *J. Cardiovasc. Pharmacol.* 36, S44-S77.
- (173) Mancini, R. E., Castro, A., and Seiguer, A. C. (1967) Histologic localization of follicle-stimulating and luteinizing hormones in the rat testis. *J. Histochem. Cytochem.* 15, 516-525.
- (174) Niedel, J. E., Kahane, I., and Cuatrecasas, P. (1979) Receptor-mediated internalization of fluorescent chemotactic peptide by human neutrophils. *Science* 205, 1412-1414.
- (175) Loitto, V.-M., Rasmusson, B., and Magnusson, K.-E. (2001) Assessment of neutrophil N-formyl peptide receptors by using antibodies and fluorescent peptides. *J. Leukoc. Biol.* 69, 762-771.

- 
- (176) Vilven, J. C., Domalewski, M., Prossnitz, E. R., Ye, R. D., Muthukumaraswamy, N., Harris, R. B., Freer, R. J., and Sklar, L. A. (1998) Strategies for positioning fluorescent probes and crosslinkers on formyl peptide ligands. *J. Recept. Signal Transduct. Res.* 18, 187-221.
- (177) Levi, J., Sathirachinda, A., and Gambhir, S. S. (2014) A high-affinity, high-stability photoacoustic agent for imaging gastrin-releasing peptide receptor in prostate cancer. *Clin. Cancer Res.* 20, 3721-3729.
- (178) Ma, L., Yu, P., Veerendra, B., Rold, T. L., Retzlöff, L., Prasanphanich, A., Sieckman, G., Hoffman, T. J., Volkert, W. A., and Smith, C. J. (2007) In vitro and in vivo evaluation of Alexa Fluor 680-bombesin[7-14]NH<sub>2</sub> peptide conjugate, a high-affinity fluorescent probe with high selectivity for the gastrin-releasing peptide receptor. *Mol. Imaging* 6.
- (179) Grady, E. F., Slice, L. W., Brant, W. O., Walsh, J. H., Payan, D. G., and Bunnett, N. W. (1995) Direct observation of endocytosis of gastrin releasing peptide and its receptor. *J. Biol. Chem.* 270, 4603-4611.
- (180) Naor, Z., Atlas, D., Clayton, R. N., Forman, D. S., Amsterdam, A., and Catt, K. J. (1981) Interaction of fluorescent gonadotropin-releasing hormone with receptors in cultured pituitary cells. *J. Biol. Chem.* 256, 3049-3052.
- (181) Hazum, E., Cuatrecasas, P., Marian, J., and Conn, P. M. (1980) Receptor-mediated internalization of fluorescent gonadotropin-releasing hormone by pituitary gonadotropes. *Proc. Natl. Acad. Sci. USA* 77, 6692-6695.
- (182) Wang, S., Clemmons, A., Strader, C., and Bayne, M. (1998) Evidence for hydrophobic interaction between galanin and the GalR1 galanin receptor and GalR1-mediated ligand internalization: fluorescent probing with a fluorescein-galanin. *Biochemistry* 37, 9528-9535.
- (183) Chicchi, G. G., Cascieri, M. A., Graziano, M. P., Calahan, T., and Tota, M. R. (1997) Fluorescein-Trp<sup>25</sup>-exendin-4, a biologically active fluorescent probe for the human GLP-1 receptor. *Peptides* 18, 319-321.
- (184) McGirr, R., McFarland, M. S., McTavish, J., Luyt, L. G., and Dhanvantari, S. (2011) Design and characterization of a fluorescent ghrelin analog for imaging the growth hormone secretagogue receptor 1a. *Regul. Pept.* 172, 69-76.
- (185) Douglas, G. A. F., McGirr, R., Charlton, C. L., Kagan, D. B., Hoffman, L. M., Luyt, L. G., and Dhanvantari, S. (2014) Characterization of a far-red analog of ghrelin for imaging GHS-R in P19-derived cardiomyocytes. *Peptides* 54, 81-88.
- (186) Cai, M., Stankova, M., Pond, S. J. K., Mayorov, A. V., Perry, J. W., Yamamura, H. I., Trivedi, D., and Hruby, V. J. (2004) Real time differentiation of G-protein coupled receptor (GPCR) agonist and antagonist by two photon fluorescence laser microscopy. *J. Am. Chem. Soc.* 126, 7160-7161.
- (187) Fernandez, R. M., Ito, A. S., Schiöth, H. B., and Lamy, M. T. (2003) Structural study of melanocortin peptides by fluorescence spectroscopy: identification of  $\beta$ -(2-naphthyl)-D-alanine as a fluorescent probe. *Biochim. Biophys. Acta.* 1623, 13-20.

- 
- (188) Fabry, M., Cabrele, C., Höcker, H., and Beck-Sickinger, A. G. (2000) Differently labeled peptide ligands for rapid investigation of receptor expression on a new human glioblastoma cell line. *Peptides* 21, 1885-1893.
- (189) Tota, M. R., Daniel, S., Sirotina, A., Mazina, K. E., Fong, T. M., Longmore, J., and Strader, C. D. (1994) Characterization of a fluorescent substance P analog. *Biochemistry* 33, 13079-13086.
- (190) Bennett, V. J., and Simmons, M. A. (2001) Analysis of fluorescently labeled substance P analogs: binding, imaging and receptor activation. *BMC Chem. Biol.* 1, 1-12.
- (191) Ceszowski, K., and Chollet, A. (1992) Synthesis of fluoresceinyl-neurokinin-A, a biologically active probe for NK2 receptors. *Bioorg. Med. Chem. Lett.* 2, 609-612.
- (192) Maes, V., Hultsch, C., Kohl, S., Bergmann, R., Hanke, T., and Tourwé, D. (2006) Fluorescein-labeled stable neurotensin derivatives. *J. Pept. Sci.* 12, 505-508.
- (193) Arttamangkul, S., Alvarez-Maubecin, V., Thomas, G., Williams, J. T., and Grandy, D. K. (2000) Binding and internalization of fluorescent opioid peptide conjugates in living cells. *Mol. Pharmacol.* 58, 1570-1580.
- (194) Mihara, H., Lee, S., Shimohigashi, Y., Aoyagi, H., Kato, T., Izumiya, N., and Costa, T. (1987) Synthesis, receptor binding activity and fluorescence property of fluorescent enkephalin analogs containing L-1-pyrenylalanine. *Int. J. Pept. Protein Res.* 30, 605-612.
- (195) Guyon-Gruaz, A., Demonte, J. P., Fournie-Zaluski, M. C., Englert, A., and Roques, B. P. (1981) Conformational studies of dansylated enkephalins by fluorescence transfer measurements. Proton nuclear magnetic resonance spectroscopy and theoretical calculations. *Biochemistry* 20, 6677-6683.
- (196) Buku, A., Yamin, N., and Gazis, D. (1988) Fluorescent, photoaffinity, and biotinyl analogs of oxytocin. *Peptides* 9, 783-786.
- (197) Karpenko, I. A., Kreder, R., Valencia, C., Villa, P., Mendre, C., Mouillac, B., Mély, Y., Hibert, M., Bonnet, D., and Klymchenko, A. S. (2014) Red fluorescent turn-on ligands for imaging and quantifying G protein-coupled receptors in living cells. *ChemBioChem* 15, 359-363.
- (198) Karpenko, I. A., Klymchenko, A. S., Gioria, S., Kreder, R., Shulov, I., Villa, P., Mély, Y., Hibert, M., and Bonnet, D. (2015) Squaraine as a bright, stable and environment-sensitive far-red label for receptor-specific cellular imaging. *Chem. Commun.* 51, 2960-2963.
- (199) Guo, J., Song, L., Liu, M., and Mahon, M. J. (2012) Fluorescent ligand-directed co-localization of the parathyroid hormone 1 receptor with the brush-border scaffold complex of the proximal tubule reveals hormone-dependent changes in ezrin immunoreactivity consistent with inactivation. *Biochim. Biophys. Acta.* 1823, 2243-2253.

- 
- (200) Ferrari, S. L., Behar, V., Chorev, M., Rosenblatt, M., and Bisello, A. (1999) Endocytosis of ligand-human parathyroid hormone receptor 1 complexes is protein kinase C-dependent and involves  $\beta$ -arrestin2. *J. Biol. Chem.* 274, 29968-29975.
- (201) Zhang, W.-J., Luo, X., Song, G., Wang, X.-Y., Shao, X.-X., and Guo, Z.-Y. (2012) Design, recombinant expression and convenient A-chain N-terminal europium-labelling of a fully active human relaxin-3 analogue. *FEBS J.* 279, 1505-1512.
- (202) Holtmann, M. H., Roettger, B. F., Pinon, D. I., and Miller, L. J. (1996) Role of receptor phosphorylation in desensitization and internalization of the secretin receptor. *J. Biol. Chem.* 271, 23566-23571.
- (203) Harikumar, K. G., Hosohata, K., Pinon, D. I., and Miller, L. J. (2006) Use of probes with fluorescence indicator distributed throughout the pharmacophore to examine the peptide agonist-binding environment of the family B G protein-coupled secretin receptor. *J. Biol. Chem.* 281, 2543-2550.
- (204) Ye, Y., Li, W. P., Anderson, C. J., Kao, J., Nikiforovich, G. V., and Achilefu, S. (2003) Synthesis and characterization of a macrocyclic near-infrared optical scaffold. *J. Am. Chem. Soc.* 125, 7766-7767.
- (205) Licha, K., Hassenius, C., Becker, A., Henklein, P., Bauer, M., Wisniewski, S., Wiedenmann, B., and Semmler, W. (2001) Synthesis, characterization, and biological properties of cyanine-labeled somatostatin analogues as receptor-targeted fluorescent probes. *Bioconjug. Chem.* 12, 44-50.
- (206) Becker, A., Hassenius, C., Licha, K., Ebert, B., Sukowski, U., Semmler, W., Wiedenmann, B., and Grötzinger, C. (2001) Receptor-targeted optical imaging of tumors with near-infrared fluorescent ligands. *Nat. Biotech.* 19, 327-331.
- (207) Edwards, W. B., Xu, B., Akers, W., Cheney, P. P., Liang, K., Rogers, B. E., Anderson, C. J., and Achilefu, S. (2008) Agonist-antagonist dilemma in molecular imaging: evaluation of a monomolecular multimodal imaging agent for the somatostatin receptor. *Bioconjug. Chem.* 19, 192-200.
- (208) Halpern, J., and Hinkle, P. M. (1981) Direct visualization of receptors for thyrotropin-releasing hormone with a fluorescein-labeled analog. *Proc. Natl. Acad. Sci. USA* 78, 587-591.
- (209) Ashworth, R., Yu, R., Nelson, E. J., Dermer, S., Gershengorn, M. C., and Hinkle, P. M. (1995) Visualization of the thyrotropin-releasing hormone receptor and its ligand during endocytosis and recycling. *Proc. Natl. Acad. Sci. USA* 92, 512-516.
- (210) Oh, K.-S., Lee, S., and Lee, B. H. (2011) Development of filtration-based time-resolved fluorescence assay for the high-throughput screening of urotensin II receptor antagonist. *Assay. Drug. Dev. Technol.* 9, 514-521.
- (211) Doan, N. D., Nguyen, T. T. M., Létourneau, M., Turcotte, K., Fournier, A., and Chatenet, D. (2012) Biochemical and pharmacological characterization of nuclear urotensin-II binding sites in rat heart. *Br. J. Pharmacol.* 166, 243-257.

- 
- (212) Kirk, K. L., Buku, A., and Eggena, P. (1987) Cell specificity of vasopressin binding in renal collecting duct: computer-enhanced imaging of a fluorescent hormone analog. *Proc. Natl. Acad. Sci. USA* 84, 6000-6004.
- (213) Buku, A., Schwartz, I. L., Gazis, D., Ma, C. L., and Eggena, P. (1985) Synthesis and biological activities of a fluorescent photoaffinity analog of vasopressin. *Endocrinology* 117, 196-200.
- (214) Buku, A., and Gazis, D. (1990) Probes for vasopressin receptors: Attachment of affinity and fluorescent groups in vasopressin. *Int. J. Pept. Protein Res.* 35, 128-132.
- (215) Lutz, W. H., Londowski, J. M., and Kumar, R. (1990) The synthesis and biological activity of four novel fluorescent vasopressin analogs. *J. Biol. Chem.* 265, 4657-4663.
- (216) Lutz, W., Sanders, M., Salisbury, J., and Kumar, R. (1990) Internalization of vasopressin analogs in kidney and smooth muscle cells: evidence for receptor-mediated endocytosis in cells with V<sub>2</sub> or V<sub>1</sub> receptors. *Proc. Natl. Acad. Sci. USA* 87, 6507-6511.
- (217) Howl, J., Wang, X., Kirk, C. J., and Wheatley, M. (1993) Fluorescent and biotinylated linear peptides as selective bifunctional ligands for the V<sub>1a</sub> vasopressin receptor. *Eur. J. Biochem.* 213, 711-719.
- (218) Durroux, T., Peter, M., Turcatti, G., Chollet, A., Balestre, M.-N., Barberis, C., and Seyer, R. (1999) Fluorescent pseudo-peptide linear vasopressin antagonists: design, synthesis, and applications. *J. Med. Chem.* 42, 1312-1319.
- (219) Albizu, L., Teppaz, G., Seyer, R., Bazin, H., Ansanay, H., Manning, M., Mouillac, B., and Durroux, T. (2007) Toward efficient drug screening by homogeneous assays based on the development of new fluorescent vasopressin and oxytocin receptor ligands. *J. Med. Chem.* 50, 4976-4985.
- (220) Pavo, I., Jans, D. A., Peters, R., Penke, B., and Fahrenholz, F. (1994) Lateral mobility of the antagonist-occupied V<sub>2</sub> vasopressin receptor in membranes of renal epithelial cells. *Biochim. Biophys. Acta.* 1223, 240-246.
- (221) Lewis, C. M., Dolence, E. K., Zhang, Z., and Rose, J. D. (2004) Fluorescent vasotocin conjugate for identification of the target cells for brain actions of vasotocin. *Bioconjug. Chem.* 15, 909-914.
- (222) Dumont, Y., Gaudreau, P., Mazzuferi, M., Langlois, D., Chabot, J.-G., Fournier, A., Simonato, M., and Quirion, R. (2005) BODIPY®-conjugated neuropeptide Y ligands: new fluorescent tools to tag Y<sub>1</sub>, Y<sub>2</sub>, Y<sub>4</sub> and Y<sub>5</sub> receptor subtypes. *Br. J. Pharmacol.* 146, 1069-1081.
- (223) Ingenhoven, N., and Beck-Sickinger, A. G. (1997) Fluorescent labelled analogues of neuropeptide Y for the characterization of cells expressing NPY receptor subtypes. *J. Recept. Signal Transduct. Res.* 17, 407-418.
- (224) Mountford, S. J., Liu, M., Zhang, L., Groenen, M., Herzog, H., Holliday, N. D., and Thompson, P. E. (2014) Synthetic routes to the Neuropeptide Y Y<sub>1</sub> receptor antagonist

- 1229U91 and related analogues for SAR studies and cell-based imaging. *Org. Biomol. Chem.* 12, 3271-3281.
- (225) Northfield, S. E., Mountford, S. J., Wielens, J., Liu, M., Zhang, L., Herzog, H., Holliday, N. D., Scanlon, M. J., Parker, M. W., Chalmers, D. K., and Thompson, P. E. (2015) Propargyloxypyrroline regio- and stereoisomers for click-conjugation of peptides: Synthesis and application in linear and cyclic peptides. *Aust. J. Chem.* 68, 1365.
- (226) Liu, M., Richardson, R. R., Mountford, S. J., Zhang, L., Tempone, M. H., Herzog, H., Holliday, N. D., and Thompson, P. E. (2016) Identification of a cyanine-dye labeled peptidic ligand for Y<sub>1</sub>R and Y<sub>4</sub>R, based upon the neuropeptide Y C-terminal analogue, BVD-15. *Bioconjug. Chem.* 27, 2166-2175.
- (227) Ziemek, R., Schneider, E., Kraus, A., Cabrele, C., Beck-Sickinger, A., Bernhardt, G., and Buschauer, A. (2007) Determination of affinity and activity of ligands at the human neuropeptide Y Y<sub>4</sub> receptor by flow cytometry and aequorin luminescence. *J. Recept. Signal Transduct. Res.* 27, 217-233.
- (228) Liu, M., Mountford, S. J., Richardson, R. R., Groenen, M., Holliday, N. D., and Thompson, P. E. (2016) Optically pure, structural, and fluorescent analogues of a dimeric Y<sub>4</sub> receptor agonist derived by an olefin metathesis approach. *J. Med. Chem.* 59, 6059-6069.
- (229) Hermanson, G. T. (2013) Chapter 10 - Fluorescent Probes, in *Bioconjugate Techniques (Third edition)* pp 395-463, Academic Press, Boston.
- (230) Robertson, T. A., Bunel, F., and Roberts, M. S. (2013) Fluorescein derivatives in intravital fluorescence imaging. *Cells* 2, 591-606.
- (231) Kim, D.-C., Rho, S.-H., Kim, D., Kim, S. I., Jang, C.-S., Ryu, J. K., Kim, B. W., Kweon, C. O., Kim, H.-k., and Lee, S. J. (2013) Coumarin, a lead compound of warfarin, inhibits melanogenesis via blocking adenylyl cyclase. *Am. J. Biomed. Res.* 1, 43-47.
- (232) Banerjee, S., Veale, E. B., Phelan, C. M., Murphy, S. A., Tocci, G. M., Gillespie, L. J., Frimannsson, D. O., Kelly, J. M., and Gunnlaugsson, T. (2013) Recent advances in the development of 1,8-naphthalimide based DNA targeting binders, anticancer and fluorescent cellular imaging agents. *Chem. Soc. Rev.* 42, 1601-1618.
- (233) Hanani, M. (2011) Lucifer yellow - an angel rather than the devil. *J. Cell. Mol. Med.* 16, 22-31.
- (234) Josan, J. S., De Silva, C. R., Yoo, B., Lynch, R. M., Pagel, M. D., Vagner, J., and Hruby, V. J. (2011) Fluorescent and lanthanide labeling for ligand screens, assays, and imaging. *Methods Mol. Biol.* 716, 89-126.
- (235) Aguilera-Sigalat, J., Sanchez-SanMartín, J., Agudelo-Morales, C. E., Zaballos, E., Galian, R. E., and Pérez-Prieto, J. (2012) Further insight into the photostability of the pyrene fluorophore in halogenated solvents. *ChemPhysChem* 13, 835-844.



- (236) Yesudas, K., Chaitanya, G. K., Prabhakar, C., Bhanuprakash, K., and Rao, V. J. (2006) Structure, bonding, and lowest energy transitions in unsymmetrical squaraines: a computational study. *J. Phys. Chem. A* **110**, 11717-11729.
- (237) Umezawa, K., Citterio, D., and Suzuki, K. (2008) Water-soluble NIR fluorescent probes based on squaraine and their application for protein labeling. *Anal. Sci.* **24**, 213-217.

## CHAPTER 2 Methodologies of Peptide Synthesis and Fluorescence Labelling – Ghrelin and Kisspeptin Analogues as Examples

### Table of Contents

2.1	General Introduction and Objectives .....	2-3
2.2	Cyanine and Rhodamine Fluorophores.....	2-3
2.2.1	Cyanine Derivatives .....	2-3
2.2.2	Rhodamine Derivatives .....	2-5
2.3	Synthesis of Fluorescently Labelled Human Ghrelin Analogues .....	2-7
2.3.1	Introduction .....	2-7
2.3.2	Results and Discussion .....	2-9
2.3.2.1	Chemistry.....	2-9
2.3.2.2	Pharmacology .....	2-11
2.3.3	Summary – Ghrelin Analogues.....	2-15
2.4	Synthesis of Fluorescently Labelled Human and Tilapia Kisspeptin analogues ...	2-15
2.4.1	Introduction .....	2-15
2.4.2	Results and Discussion .....	2-18
2.4.2.1	Human Kisspeptin Analogues .....	2-18
2.4.2.1.1	Chemistry .....	2-18
2.4.2.1.2	Pharmacology.....	2-20
2.4.2.2	Tilapia Kisspeptin Analogues .....	2-23
2.4.2.2.1	Chemistry .....	2-23
2.4.2.2.2	Pharmacology.....	2-24
2.4.3	Summary – Kisspeptin Analogues.....	2-25
2.5	Experimental Methods.....	2-26
2.5.1	Materials .....	2-26
2.5.2	Peptide Synthesis .....	2-27
2.5.2.1	Analogue 2A: [K <sup>19</sup> (RhB)]hGhrelin <sub>1-19</sub> .....	2-27
2.5.2.2	Analogue 2B: [dY <sup>1</sup> ]hKP-10 .....	2-28
2.5.2.3	Analogue 2C: [dY <sup>1</sup> , Pop <sup>4</sup> ]hKP-10 .....	2-28
2.5.2.4	Analogue 2D: [RhB-1]-hKP-10 .....	2-28

---

2.5.2.5	Analogue 2E: [Cy5.5]-hKP-10 .....	2-28
2.5.2.6	Analogue 2F: [dY <sup>1</sup> , Pop <sup>4</sup> (RhB-4)]hKP-10.....	2-28
2.5.2.7	Analogue 2G: Kiss1 .....	2-29
2.5.2.8	Analogue 2H: Kiss2.....	2-29
2.5.2.9	Analogue 2I: [dY <sup>1</sup> ]Kiss1.....	2-29
2.5.2.10	Analogue 2J: [dF <sup>1</sup> ]Kiss2.....	2-29
2.5.2.11	Analogue 2K: [RhB-1]-Kiss1.....	2-29
2.5.2.12	Analogue 2L: [RhB-1]-Kiss2.....	2-30
2.5.3	Dual-luciferase Reporter Assays .....	2-30
References.....		2-31

## **2.1 General Introduction and Objectives**

Efficient peptide synthesis and fluorophore conjugation techniques are key to successful development of GPCR-targeting fluorescently labelled peptides. The widely utilised modern Fmoc-based solid phase peptide synthesis (SPPS) strategies allow robust and fully automated sequence assembly in high yield. N-terminal Fmoc deprotection and amino acid coupling can be performed under alkaline conditions, orthogonal to the acidolytic conditions during resin and protecting group cleavage. Fluorescence labelling is generally performed following peptide backbone synthesis, and can be achieved in either solid or solution phase.

In this chapter, we first introduce the two classes of fluorophores used in the thesis, and then demonstrate the application of various synthesis strategies for preparing peptide conjugates. Broadly, these strategies include linear peptide synthesis, use of orthogonal protecting groups, and conjugate labelling in both solid and solution phase. This resulted in successful preparation of fluorescent analogues of two GPCR-targeting neuropeptides, ghrelin and kisspeptin. This work has contributed to collaborative projects with researchers interested in the pharmacology and physiology of the target receptors.

## **2.2 Cyanine and Rhodamine Fluorophores**

### **2.2.1 Cyanine Derivatives**

The cyanine family of dyes have been widely used in labelling biomolecules, such as labelling nucleotides in DNA sequencing,(1) quantification of fibrillar proteins,(2) detecting cellular production of reactive oxygen species (3) and discriminating different biologically important biothiol molecules.(4) Their applications as environmental *pH* sensors have also been reported.(5, 6) Cyanine based fluorophores consist of two either symmetrical or unsymmetrical cationic nitrogen-containing ring structures linked by a polymethine chain

(Figure 2-1).(7-9) The number of carbon atoms in the polymethine chain determines the nomenclature of cyanine derivatives. For example, Cy5 represents a 5-carbon intermediate chain.(7)

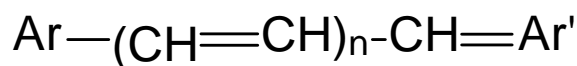


**Figure 2-1:** The general structure of cyanine derivatives. Ar and Ar' represent ring structures.

The optical properties (e.g. absorption and emission maxima, and photostability) of cyanine derivatives can be manipulated by varying the ring structures and the length of polymethine chain, while retaining high extinction coefficients up to  $200,000 \text{ M}^{-1}\text{cm}^{-1}$ .(7, 8, 10) By increasing the length of their polymethine chains, their absorption and emission spectra can be shifted further toward the NIR region in favour of *in vivo* tissue imaging. However, this comes at a cost of reducing their quantum yield.(11, 12) Cyanine derivatives are now widely used as long-wavelength fluorophores, where the excitation and emission wavelength vary in the mid-500 nm to mid-700 nm range, but may also increase to 900 nm depending on the modifications.(7, 13, 14) They also produce sharp absorption bands and emission profiles, as well as stable fluorescence under various biological pH conditions.(15) In addition, the excitation and emission spectra of Cy5 and Cy5.5 possess sufficiently low blood and tissue absorption to enable a clear imaging.(15)

Due to the presence of multiple ring structures, earlier generation of cyanine derivatives are more hydrophobic in nature thus likely to cause biomolecule aggregation, precipitation and even fluorescence quenching by dye-dye hydrophobic interactions. This problem was later resolved by introducing multiple sulfate groups to the aromatic rings so as to improve aqueous solubility.(16) The major demerit of cyanine dyes is their relatively low resistance to photobleaching,(17, 18) which can potentially be improved by structural modifications.(19, 20) For instance, placing a rigid cyclohexenyl structure in the middle of

the polymethine chain has been found to markedly enhance both the photostability and quantum yield of cyanine dyes.(21, 22)

Cyanine derivatives are often functionalised with a spacer-attached conjugatable group at one of their nitrogen atoms.(8, 9) In this thesis, Cy5.5 (as the commercially available Cy5.5 N-hydroxysuccinimidyl ester, Cy5.5-NHS ester, **Figure 2-2A**) and its hydrophilic variant sulfo-Cy5 (sCy5, **Figure 2-2B**) have been used to prepare peptide conjugates via amide bond formation.

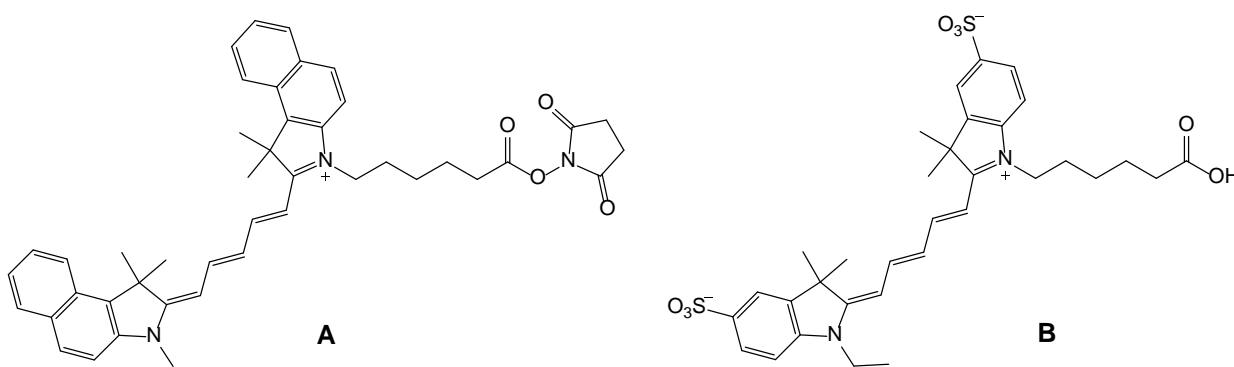


**Figure 2-2:** The chemical structures of cyanine dye utilised in this project. **A:** Cy5.5-NHS ester and **B:** sulfo-Cy5 (sCy5)

## 2.2.2 Rhodamine Derivatives

Rhodamine derivatives belong to the xanthene family.(23) Many members of this family have been synthesised and studied since fluorescein was reported in 1870s.(24) Rhodamine derivatives are characterised by their multi-aromatic structure, which is responsible for their fluorescence properties (**Figure 2-3A**).

Rhodamine derivatives can be excited at low- to high-500 nm range depending on the particular structure, and their emission falls in mid- to high-500 nm range.(13) Replacing the oxygen atom in the top middle ring with a dimethylsilyl group can shift their absorption and emission maxima further to the NIR region.(25). Although their quantum yield is

relatively low (~25%), they are more resistant to degradation during prolonged storage and light exposure compared to their structural analogues fluorescein derivatives.(7) They also show satisfactory chemical stability, photostability and photophysical properties, which warrant their applications in many scientific fields.(23, 26) However, the small Stokes shift (about 20-30 nm) limits their usefulness in some instances.(13, 27)

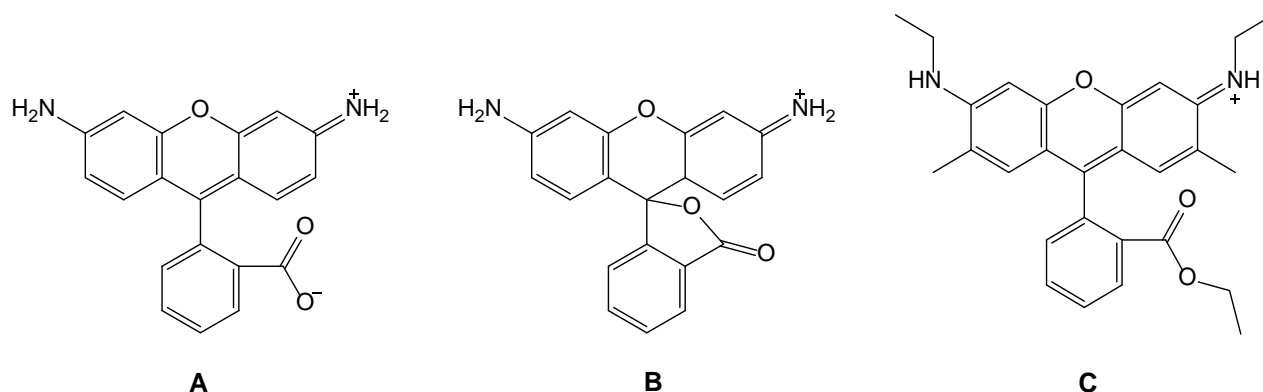


**Figure 2-3:** The basic chemical structure of: **A:** Rhodamine derivatives; **B:** Undesired lactone formation; **C:** Rhodamine 6G.

It is important to note that in alkaline solutions, the carboxylic group can be deprotonated to form a zwitterion.(23) This in turn causes a reduction in extinction coefficient, and a shift of absorption and fluorescence maxima to shorter wavelength.(26) In addition, zwitterion formation often causes a reversible lactone formation (**Figure 2-3B**) especially in relatively less polar organic solvents, leading to decrease in quantum yield or even loss of fluorescence.(23, 26) Therefore, rhodamine derivatives are often modified to protect their carboxylic group. For example, rhodamine 6G is not susceptible to the lactone-forming reaction owing to its esterified carboxylic group (**Figure 2-3C**). (16, 26)

Attachment of reactive conjugatable groups for rhodamine derivatives is usually achieved at the 5- or 6-carbon on their lower ring.(16) Such derivatives have been found useful in a number of applications, including investigating behaviour of microtubules and actin filaments in living embryos (using 5-carboxytetramethylrhodamine N-succinimidyl

ester),(28) and studying protein conformational changes (using tetramethylrhodamine 5-iodoacetamide).(29) Rhodamine-conjugated peptides (using an isothiocyanate derivative) for studying cell lineages in leech embryonic cells has also been described.(30)

Modified rhodamine B (RhB) derivatives that incorporate a piperazine ring were reported by Nguyen *et al.*(31) This modification prevents lactone formation and provides a secondary amine available for further derivatisation. A series of RhB derivatives that incorporated various reactive groups were prepared in our laboratory and have been utilised in this study (**Figure 2-4**).(32) RhB-1 includes a carboxylic group for amide bond formation. RhB-2 and RhB-3 are both functionalised by an alkyne for conjugation to peptides with azido groups via the click reaction, but incorporate hydrocarbon side-chains of difference length. Lastly, RhB-4 incorporates an azide moiety specifically for conjugation to alkyne-containing partners.

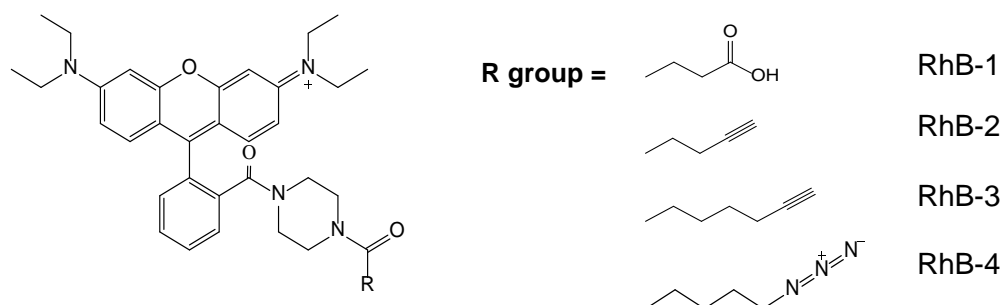


**Figure 2-4:** Structures of rhodamine B derivatives used in our project.

## 2.3 Synthesis of Fluorescently Labelled Human Ghrelin Analogues

### 2.3.1 Introduction

Ghrelin is a peptide hormone that plays important roles in physiological energy homeostasis, governing body thermoregulation, fat intake and metabolism.(33, 34) Human ghrelin is a 28-amino acid polypeptide acylated at Ser<sup>3</sup> by a hydrophobic *n*-octanoyl moiety, which is essential for its endocrine activity (**Figure 2-5**).(35-40) This acylation is



catalysed by ghrelin-O-acyltransferase (GOAT) that has been identified mainly in stomach and intestine.(41) Ghrelin is predominantly produced and secreted from X/A-like cells in stomach,(37) but also present in small amount in other human organs, such as lungs,(42) placenta,(43) pituitary,(44) kidney,(45) foetal thyroid(46) and testis.(47) The physiological functions of ghrelin are mediated by growth-hormone secretagogue receptor type 1a (GHS-R1a, also called ghrelin receptor GRLN-R).(37, 48) It belongs to the GPCR superfamily, triggering the  $G_{\alpha/11}$ -coupled signalling pathway upon activation.(48) Interestingly, adenosine can also activate GHS-R1a as a partial agonist at a distinct binding site and trigger  $G_s$ -coupled signalling pathway.(49) Lately, a splice variant of GHS-R1a was discovered and named GHS-R1b, which was proposed to terminate constitutive signalling of GHS-R1a by forming heterodimers.(50, 51) However, GHS-R1b showed no affinity to ghrelin or ghrelin mimetics, and its biological significance remains unclear.(48)

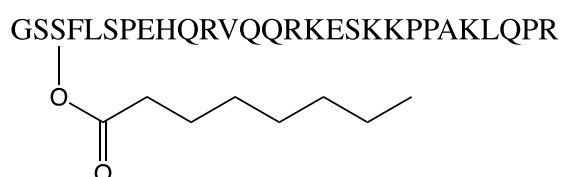


**Figure 2-5:** The structure of human ghrelin.

Activation of GHS-R1a was found to promote food intake and fat deposition,(52-54) but reduce appetite during stressful conditions.(55) Its functions in regulating insulin secretion remain controversial.(56, 57) Ghrelin also facilitates immunological responses,(58) and plays pathophysiological roles in cardiovascular diseases.(59-61) The more abundantly circulating ghrelin variant, des-acyl ghrelin, was found to exert some counteracting functions, such as increasing insulin sensitivity and promoting expression of genes relevant to glucose and fat metabolism.(62, 63) However, it (and some of its fragments) also shares common functions with acylated ghrelin, such as preventing  $\beta$ -cell destruction induced by interferon and serum starvation.(64, 65)

Although some truncated and radiolabelled ghrelin analogues have been developed,(39, 66, 67) fluorescently labelled analogues remained unavailable until McGirr *et al.* reported a novel compound derived from the truncated analogue ghrelin<sub>1-19</sub>.(68) It incorporated a fluorescein moiety at Lys<sup>19</sup> and an isosteric amide replacement of the octanoyl ester at Ser<sup>3</sup>. Albeit a 7-fold reduction in affinity compared to the unlabelled ghrelin<sub>1-19</sub>, this analogue showed nanomolar affinity with an IC<sub>50</sub> of  $9.5 \pm 2.6$  nM. The later reported sCy5-containing derivative showed a slightly sacrificed affinity (IC<sub>50</sub> =  $25.8 \pm 3.4$  nM).(69)

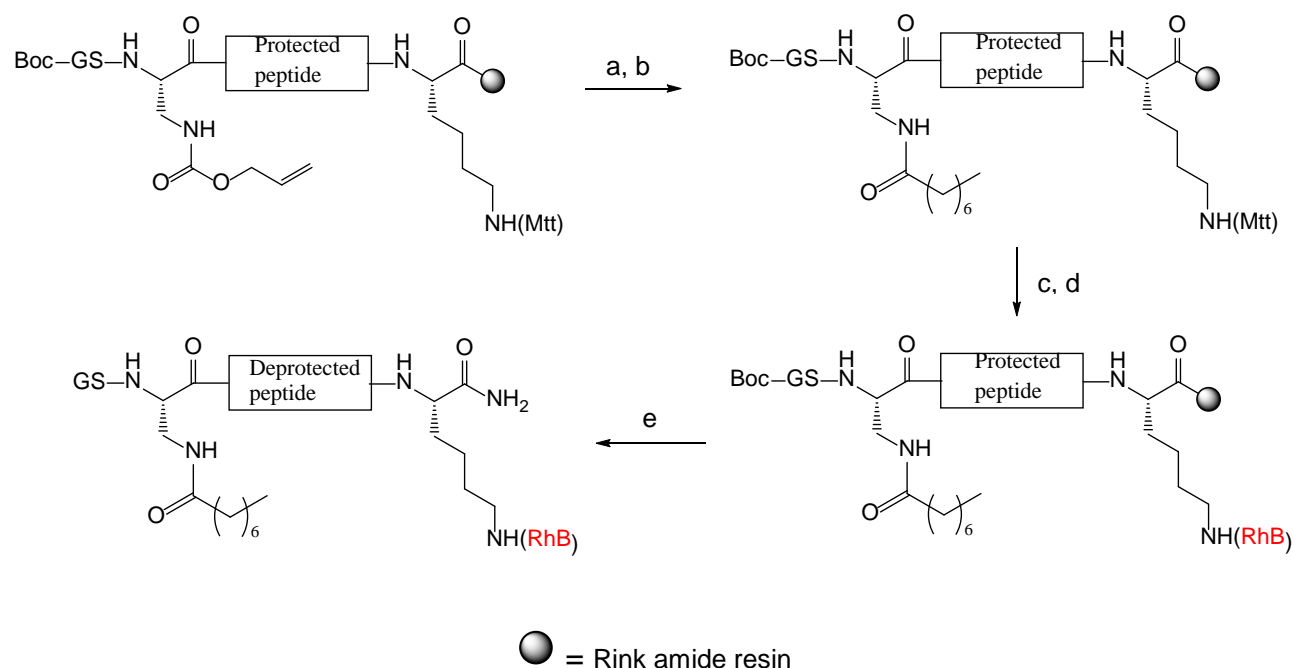
The aim of our work was to develop fluorescently labelled ghrelin analogues for pharmacological studies in the laboratories of our collaborator John Furness at the University of Melbourne. We here attempted to replicate the strategy of McGirr *et al.* to include the RhB-1 fluorophore at the same position for characterisation of GHS-R1a in whole cells.

## **2.3.2 Results and Discussion**

### **2.3.2.1 Chemistry**

The synthesis of the rhodamine labelled acyl ghrelin analogues **2A** was achieved as follows and is presented in detail as a generalised representation of standard solid phase peptide synthesis as carried out in this thesis. The synthesis of the linear peptide backbone followed the standard Fmoc-based solid phase peptide synthesis (SPPS) strategy.(70) The peptide was constructed on Rink amide resin to afford the C-terminal amide. Each N<sup>α</sup>-Fmoc protected amino acid was activated by HCTU and DIPEA, and coupled to the exposed N-terminal primary amine of the growing resin-bound peptide chain. The new N-terminus was then deprotected using piperidine (20%) in DMF before the next coupling. These processes were repeated for all amino acids until completion of

the linear sequence, which was then subject to post-synthesis modifications and finally acidolytic cleavage.



**Scheme 2-1:** Orthogonal deprotection of Alloc and Mtt groups to enable different conjugations. Reagents and conditions: **a.**  $\text{PhSiH}_3$ ,  $\text{Pd(PPh}_3)_4$  in DCM, 30 min; **b.** octanoic acid, PyClock, DIPEA in DMF, overnight; **c.** TFA 2% and TIPS 5% in DCM, 2 ml  $\times$  2 min  $\times$  10; **d.** RhB-1, PyClock, DIPEA in DMF, overnight; **e.** TFA, TIPS, DMB, 3 h.

In the case of analogue **2A** (Scheme 2-1), Alloc and 4-methyltrityl (Mtt) protecting groups were incorporated for Dap<sup>3</sup> and Lys<sup>19</sup> respectively. Significantly, these groups are orthogonal to each other, enabling selective deprotection and side-chain conjugation in solid phase.<sup>(71, 72)</sup> After assembling the linear sequence with an intact N-terminal Boc group on Rink amide resin, the Alloc-protected Dap<sup>3</sup> residue was deprotected on resin by treating with  $\text{PhSiH}_3$  and  $\text{Pd(PPh}_3)_4$  in a neutral condition,<sup>(71)</sup> and the octanoic acid chain was coupled in presence of the coupling reagents PyClock and DIPEA. As a phosphonium salt, PyClock has been found favourable over the uronium reagent HCTU when prolonged reaction is required, as it does not terminate peptide chain growth by forming guanidinium derivatives.<sup>(73)</sup> The Mtt-protected Lys was then deprotected in a mildly acidic condition (2% TFA) and subsequently coupled by the RhB-1 fluorophore. Finally, the peptide

conjugate was cleaved using TFA in presence of TIPS and DMB as scavengers, to yield the crude product for RP-HPLC purification.

The analytical data of analogue **2A** are summarised in **Table 2-1**. As illustrated by the HPLC chromatographs (**Figure 2-6**), conjugations at side-chains of Dap<sup>3</sup> and Lys<sup>19</sup> had both proceeded efficiently, which showed the efficiency of PyClock in preparing peptide conjugates. The desired product was the predominant species and readily purified. A minor component was identified as an Arg deletion product.

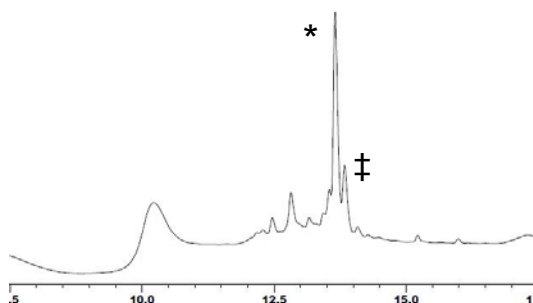


**Figure 2-6:** HPLC chromatograph of analogue **2A**. \* = Desired product; ‡ = by-product with Arg deletion.

**Table 2-1:** Fluorescently labelled ghrelin analogue **2A** and its analytical data.

Code	Sequence	HPLC RT <sup>a</sup> (min)	MW (Calc)	m/z [M+3H] <sup>3+</sup> (found)	Purity (%)
<b>2A</b>	RhB-Ghrelin <sub>1-19</sub>	13.58	2946.9	983.3	97

<sup>a</sup> HPLC retention time using a Phenomenex Luna C-8 column (100Å, 3µm, 100×2.00mm). The gradient is composed of 100% H<sub>2</sub>O (0.1% TFA) for 4 min, 0-60% acetonitrile in H<sub>2</sub>O (0.1% TFA) over 10 min and isocratic 60% acetonitrile in H<sub>2</sub>O (0.1% TFA) for 1 min.

### 2.3.2.2 Pharmacology

The fluorescently labelled ghrelin analogue **2A** is being utilised in a range of studies conducted by John Furness's group at the University of Melbourne, Australia. The characterisation of the peptide *in vitro* in recombinant cell lines is presented here to demonstrate the receptor binding affinity, agonist efficacy and specificity, which are all comparable to ghrelin itself.

First, **2A** was assayed for its ability to specifically label human embryonic kidney 293 (HEK293) cells transfected to express human GHS-R1a receptors (**Figure 2-7**). When treated with **2A** at a concentration of 100 nM, cells with GHS-R1a expression exhibited strong fluorescence, which was absent in cells without tetracycline-induced receptor expression. Binding of analogue **2A** was then competed using the endogenous ligand human ghrelin (hGhrelin) at increasing concentrations up to 10  $\mu$ M. While the labelled cells retained weak fluorescence in presence of 3x concentration (300 nM) of competing ligand, 10x concentration (1  $\mu$ M) was able to fully displace **2A** from the receptors. On the other hand, binding of **2A** could not be displaced by the inactive analogue des-acyl ghrelin at concentrations up to 30  $\mu$ M (**Figure 2-8**). These findings strongly suggested that **2A** bound to GHS-R1a with high specificity.

Analogue **2A** was then analysed with  $\text{Ca}^{2+}$  mobilisation assays for its GHS-R1a agonism (**Figure 2-9**). **2A** elicited a dose-dependent response (red curve) showing comparable efficacy and potency to endogenous ghrelin, at both human GHS-R1a ( $\text{EC}_{50}$  = 4.62 nM vs. 11.9 nM respectively) and rat GHS-R1a ( $\text{EC}_{50}$  = 13.45 nM vs. 9 nM respectively). The dose-response curve was shifted rightwards upon addition of increasing concentration of the GHS-R1a antagonist YIL781,(74) reflecting highly specific activity of **2A** at this receptor. Finally, using fluorescence imaging assays, the usefulness of **2A** as a fluorescent ligand was verified by the absence of fluorescence in cells without tetracycline-induced GHS-R1a expression, and the weakened signal in presence of the antagonist YIL781 (**Figure 2-10**).

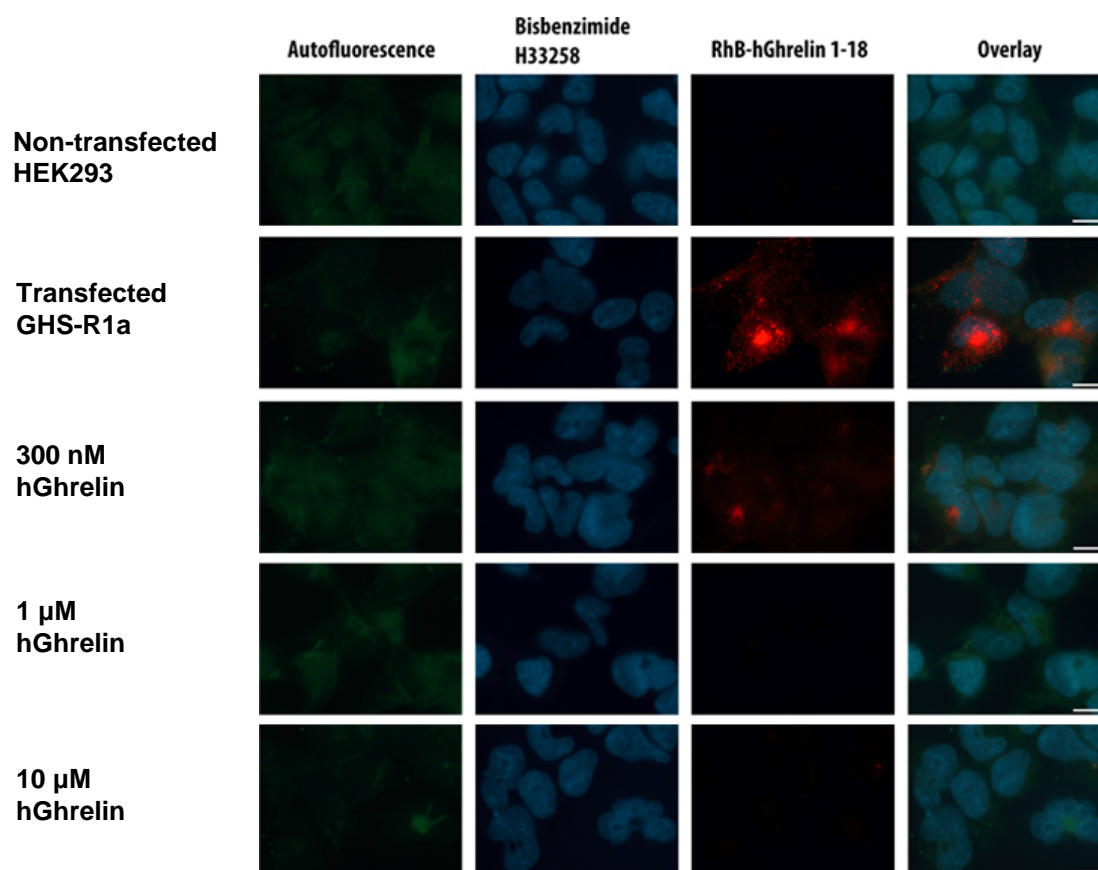


**Figure 2-7:** GHS-R1a binding assays by imaging using bisbenzimidide (H33258) as the counterstain.(75) HEK293 cells were incubated with analogue **2A** 100 nM, in the absence of transfected GHS-R1a (control, first row), or presence of transfected GHS-R1a with increasing concentration of endogenous hGhrelin. Scale bar 10  $\mu$ m.

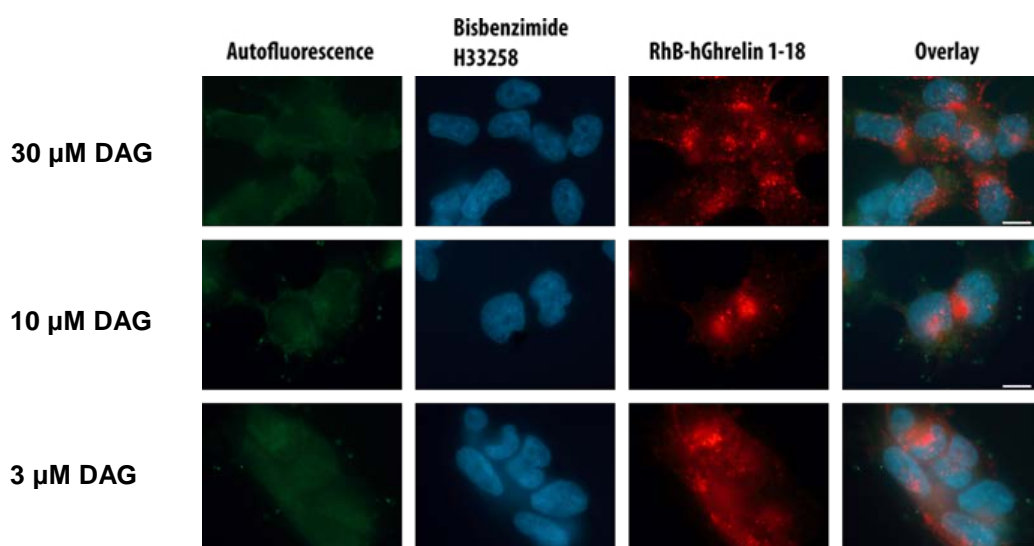


**Figure 2-8:** **2A** bound to GHS-R1a was not displaced by addition of des-acyl hGhrelin. Scale bar 10  $\mu$ m.

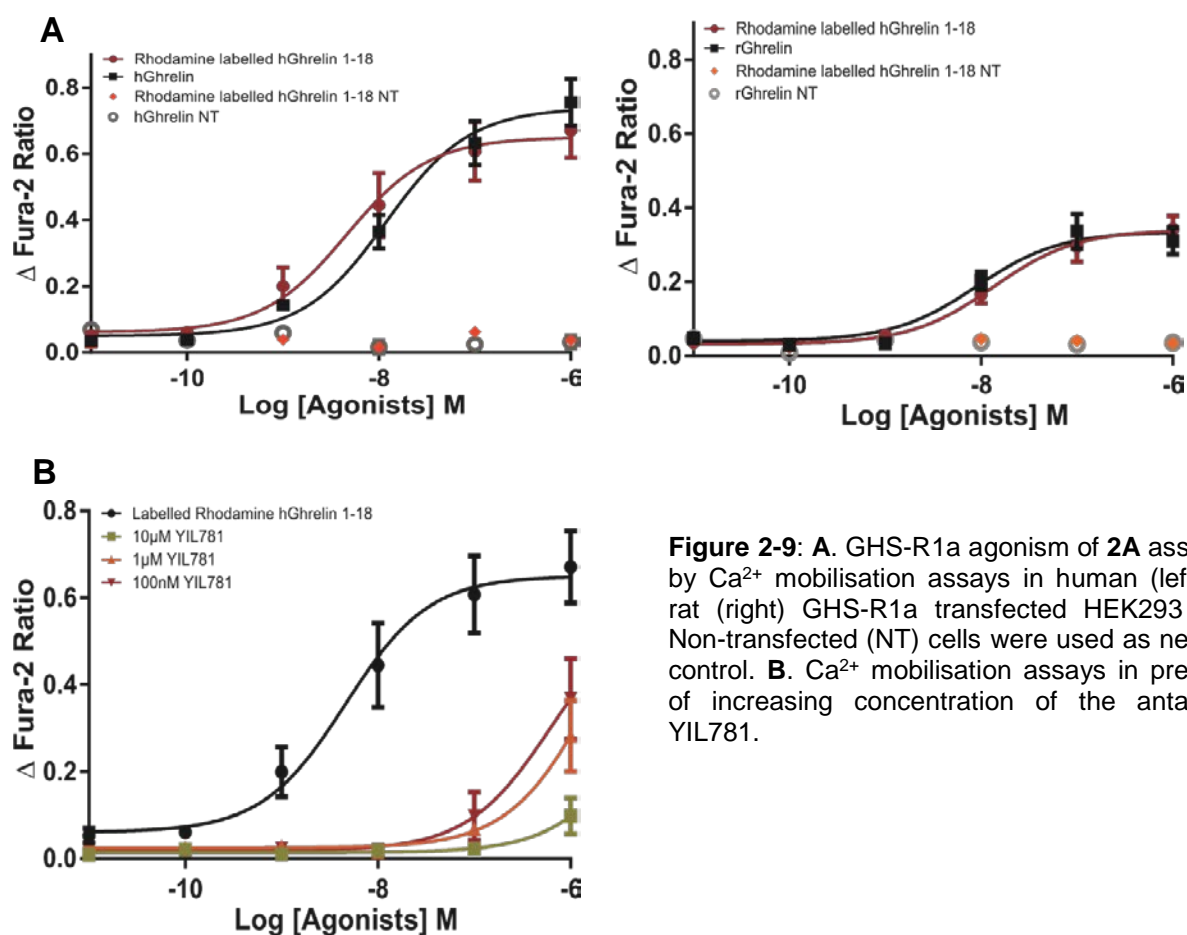


**Figure 2-9: A.** GHS-R1a agonism of **2A** assessed by  $\text{Ca}^{2+}$  mobilisation assays in human (left) and rat (right) GHS-R1a transfected HEK293 cells. Non-transfected (NT) cells were used as negative control. **B.**  $\text{Ca}^{2+}$  mobilisation assays in presence of increasing concentration of the antagonist YIL781.

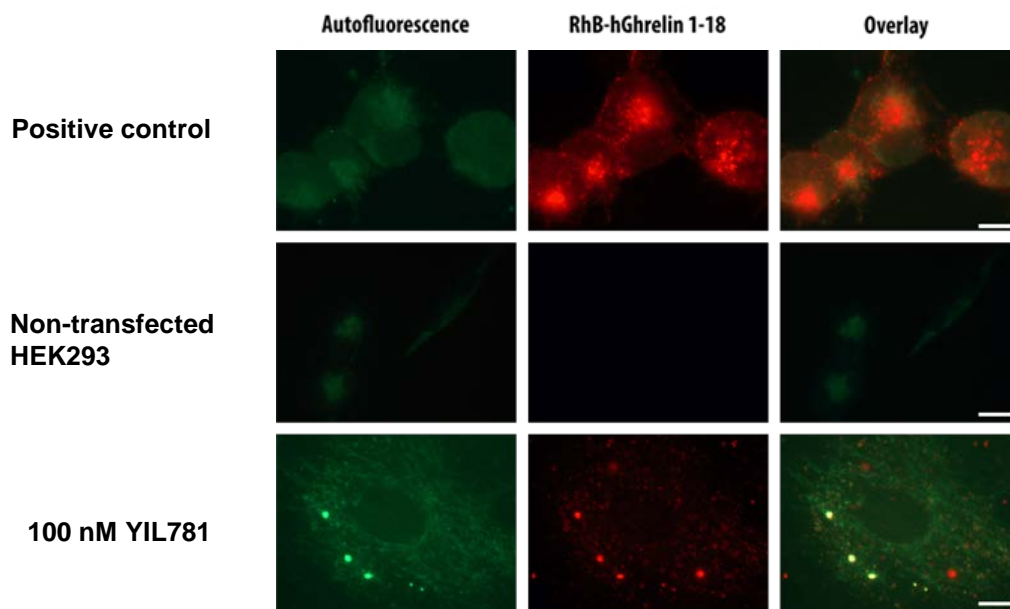


**Figure 2-10: 2A** as a fluorescent GHS-R1a ligand. Panels illustrate the lack of fluorescent ligand binding in control cells without GHS-R1a transfection, and weakened fluorescence in presence of the GHS-R1a antagonist YIL781 (100 nM). Scale bar 10  $\mu$ m.

### 2.3.3 Summary – Ghrelin Analogues

The total synthesis of our 19-position RhB labelled hGhrelin<sub>1-19</sub> analogue (RhB-Ghrelin<sub>1-19</sub>) was achieved by an Fmoc-based SPPS strategy. The most important feature of our synthetic route was that the three susceptible primary amines at the N-terminus, Dap<sup>3</sup> and Lys<sup>19</sup> were all orthogonally protected (by Boc, Alloc and Mtt group respectively) to enable selective solid phase deprotection and conjugation. Using receptor imaging and Ca<sup>2+</sup> mobilisation assays, we have shown that RhB-Ghrelin<sub>1-19</sub> bound to GHS-R1a receptor with high specificity, and appeared to be an agonist exhibiting similar efficacy and potency to that of endogenous human ghrelin. Its suitability as a fluorescent GHS-R1a ligand has also been verified by imaging assays. The peptide continues to be used for the characterisation of GHS-R1a in native tissue samples as the physiology of this important hormone's tissue expression and biological function is examined.

For this work, the effectiveness of our peptide synthesis strategies in preparing high-affinity, specific and biologically active fluorescently labelled peptides has been exemplified.

## 2.4 Synthesis of Fluorescently Labelled Human and Tilapia Kisspeptin analogues

### 2.4.1 Introduction

The human kisspeptin peptide family consists of four bioactive members (54-, 14-, 13- and 10-amino acid sequence) that are all C-terminal amidated (**Table 2-2**).<sup>(76)</sup> They are generated by post-translational proteolytic cleavage from a 145-amino acid precursor protein coded by the *KISS1* gene.<sup>(76, 77)</sup> All kisspeptins contain a common C-terminal “RF-motif” that is also found in many other GPCR-targeting neuropeptides.<sup>(78)</sup> All kisspeptins exhibit similar affinity and potency at their cognate receptor KISSR1



(commonly known as GPR54),<sup>1</sup>(76, 79) which belongs to the G<sub>q/11</sub> protein-coupled GPCR subfamily.(80-82) GPR54 is abundantly expressed in both central and peripheral nervous systems, including hypothalamus, amygdala, pituitary, spinal cord, placenta, pancreas, lung and stomach.(76, 77, 80, 83-85)

**Table 2-2:** Amino acid sequences of human endogenous kisspeptin-54, -14, -13 and -10.

Kisspeptin	Sequence
<b>KP-54</b>	G <sup>1</sup> TSLSPPPES <sup>10</sup> SGSRQQPGLS <sup>20</sup> APHSRQIPAP <sup>30</sup> QGAVLVQ REK <sup>40</sup> DLPNY <sup>45</sup> NWNSF <sup>50</sup> GLRF <sup>54</sup> -NH <sub>2</sub>
<b>KP-14</b>	DLPNY <sup>45</sup> NWNSFGLRF <sup>54</sup> -NH <sub>2</sub>
<b>KP-13</b>	LPNY <sup>45</sup> NWNSFGLRF <sup>54</sup> -NH <sub>2</sub>
<b>KP-10</b>	Y <sup>45</sup> NWNSFGLRF <sup>54</sup> -NH <sub>2</sub>

Human kisspeptin-GPR54 signalling system plays a pivotal role in puberty initiation and reproductive system development probably by stimulating a GnRH resurgence that subsequently boosts release of follicle-stimulating hormone (FSH) and luteinizing hormone (LH).(86-91) This is supported by clinical evidence that mutations of GPR54 receptor gene were present in patients with isolated hypogonadotropic hypogonadism,(86, 92, 93) a syndrome characterised by low plasma GnRH level, impaired gonadotropin secretion, growth retardation and permanent sexual infantilism.(91, 94) An activating mutation on the other hand was associated with central precocious puberty.(95) Moreover, the involvement of kisspeptin-GPR54 signalling system in tumour metastasis has opened a new perspective in anti-cancer drug development. Indeed, loss of kisspeptin-GPR54 expression has been identified in, for example, deeply invasive melanomas,(96) bladder tumours(97) and gastric cancers.(98) However opposite findings have also been reported in other cancers such as hepatocellular and renal cell carcinomas.(99-101)

<sup>1</sup> For consistency with our publication, the receptor KISSR1 will be named GPR54 from here onwards.

Orthologues of Kisspeptin-GPR54 signalling system have also been identified in teleosts, where its expression exhibits significant species dependency.(102) While some teleosts possess two types of GPR54's (Kiss-R1 and Kiss-R2) and two kisspeptin derivatives (Kiss1 and Kiss2),(103-109) many others have only Kiss-R2 and Kiss2.(110) The first non-human GPR54 orthologue was identified in tilapia brain by our collaborator Ishwar Parhar's research group (Monash University Sunway Campus, Malaysia) using laser-captured microdissection.(111) This receptor belongs to the Kiss-R2 subfamily and was found to co-localise in GnRH-expressing neurons.(110-112) Notably, the concomitant expression pattern of Kiss-R2 and GnRH in tilapia and other teleosts strongly supports the roles of kisspeptin as a regulator of puberty and reproduction in piscine species.(113, 114) Parhar's group predicted two tilapia kisspeptin sequences from genomic data: Kiss1 (YSLFSFGLRY-NH<sub>2</sub>) and Kiss2 (FNYNPLSLRF-NH<sub>2</sub>),(115) however they only detected Kiss2 mRNA expression in tilapia brain tissues. Fluorescently labelled tilapia kisspeptin analogues are therefore capable of providing useful insight to the involvement of GPR54 signalling in growth and reproduction, which is in turn of significant benefits for the agricultural industry needs.

Although modified peptidic ligands are gradually becoming available (summarised in our publication, full paper available in Appendix),(116) to date only a few of fluorescent analogues derived from the bioactive KP-52 and KP-14 sequences have been reported.(117) They incorporated either tetramethylrhodamine or rhodamine green at the N-terminus via amide or triazole linkage respectively. Here we report our work on preparation of a series of human and tilapia kisspeptin analogues derived from the endogenous bioactive 10-amino acid sequences.

## 2.4.2 Results and Discussion

### 2.4.2.1 Human Kisspeptin Analogues

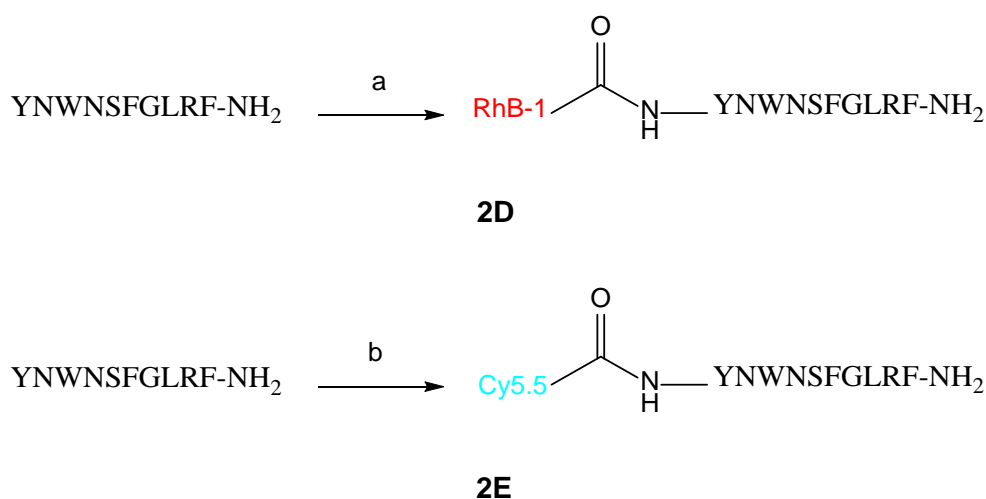
Our design of human kisspeptins was guided by the previously reported SAR information on KP-10. Briefly, alanine scans showed retained activity at the 3- and 5-position.(83, 118, 119) A D-Tyr<sup>1</sup> substitution resulted in enhanced potency *in vivo*.(120) Residue at the 6-position is crucial for receptor binding and activity,(78, 83, 119, 121) however some hydrophobic substitutions can be tolerated, such as Trp and cyclohexylalanine.(78, 119) While the importance of Arg<sup>9</sup>,(78, 119, 122) Phe<sup>10</sup>(83, 118, 119) and the C-terminal amide (76, 78, 82, 118, 119) has been well established, substituting Phe<sup>10</sup> with Trp or Tyr retained activity.(78, 119) Here we produced a series of analogues fluorescently labelled at the N-terminus as well as the 4-position via the Pro structural analogue propargyloxypyrrolidine (synthesis described in chapter 3 and in more detail in our publication).(32)

#### 2.4.2.1.1 Chemistry

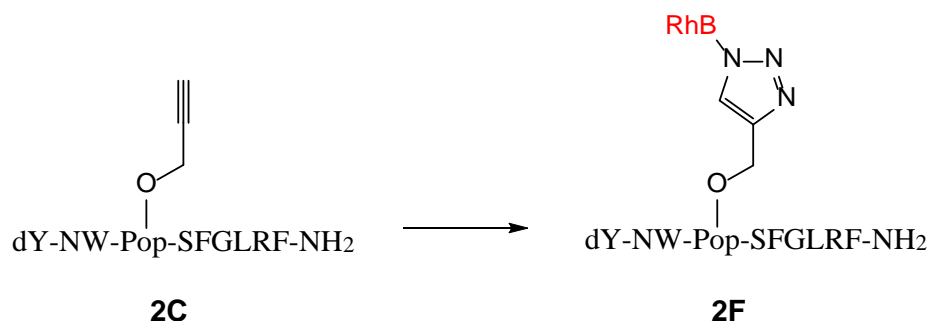
All peptide backbones were synthesised on Rink amide resin adopting the standard Fmoc-based SPPS strategy as described for the ghrelin analogue **2A**. The potent human GPR54 agonist [D-Tyr<sup>1</sup>]KP-10 (**2B**) were prepared as a reference.(120) **2B** was further amended to include a Pop<sup>4</sup> as a click-conjugatable group and this afforded analogue **2C**.

Labelling via condensation reactions as in **2D** and **2E** was achieved in solution without need of orthogonal protection, considering only one primary amine moiety was present. Notably, we here utilised mild organic bases in favour of selectively deprotonating the N<sup>α</sup>-amine without affecting other ionisable side-chains such as Tyr phenol and Arg guanidinium. That said, **2D** (**Figure 2-11**) was prepared by treating the endogenous KP-10 (synthesised by other group members) with RhB-1 in presence of PyClock and N-

methylmorpholine (NMM), while **2E** was prepared by treating with molar equivalent of the Cy5.5-NHS ester in presence of 2,4,6-trimethylpyridine (TMP) (**Scheme 2-2**). The triazole-conjugated analogue **2F** (**Figure 2-11**) was prepared by treating with the azide-bearing RhB-4 following the CuAAC strategy as reviewed in chapter 1 (**Scheme 2-3**). With respect to chemical synthesis, CuAAC demonstrated advantages over condensation reactions, where it rapidly proceeded to completion (within 1 h), and its aqueous reaction mixture could be directly purified by RP-HPLC without need for a lyophilisation step. The analytical data of these analogues are summarised in **Table 2-3**.



**Scheme 2-2:** Fluorescence labelling by condensation reactions in **2D** and **2E**. Reagents and conditions: a. RhB-1 (1.2 eq.), PyClock (2 eq.), NMM (12 eq.) in DMF, overnight; b. Cy5.5-NHS ester (1.2 eq.), TMP (12 eq.) in DMF, overnight.



**Scheme 2-3:** Fluorescence labelling by CuAAC reaction in **2F**. Reagents and conditions: RhB-4 (2 eq.), CuSO<sub>4</sub> (0.5 eq.), THPTA (2.5 eq.), aminoguanidine (25 eq.), NaAsc (25 eq.), DMSO (2%) in potassium phosphate buffer (0.1 M, pH = 7.4), 1 h.

**Table 2-3:** Synthesised human KP-10 analogues and their analytical data.

Code	Sequence	HPLC RT (min)	MW (Calc)	m/z (found)	Purity (%)
<b>2B</b>	dY-NWNSFGLRF-NH <sub>2</sub>	12.91 <sup>a</sup>	1302.4	652.2 <sup>c</sup>	99
<b>2C</b>	dY-NW-Pop-SFGLRF-NH <sub>2</sub>	13.51 <sup>a</sup>	1339.5	670.6 <sup>c</sup>	97
<b>2D</b>	(RhB-1)-YNWNSFGLRF-NH <sub>2</sub>	14.94 <sup>a</sup>	1896.2	948.9 <sup>c</sup>	99
<b>2E</b>	Cy5.5-YNWNSFGLRF-NH <sub>2</sub>	12.83 <sup>b</sup>	1868.2	934.8 <sup>c</sup>	99
<b>2F</b>	dY-NW-Pop(RhB-4)SFGLRF-NH <sub>2</sub>	14.42 <sup>a</sup>	1976.3	659.7 <sup>d</sup>	96

<sup>a</sup> HPLC retention time using a Phenomenex Luna C-8 column (100Å, 3µm, 100x2.00mm).

The gradient is composed of 100% H<sub>2</sub>O (0.1% TFA) for 4 min, 0-60% acetonitrile in H<sub>2</sub>O (0.1% TFA) over 10 min and isocratic 60% acetonitrile in H<sub>2</sub>O (0.1% TFA) for 1 min.

<sup>b</sup> For analogue **2E**, the gradient is composed of 100% H<sub>2</sub>O (0.1% TFA) for 4 min, 20-100% acetonitrile in H<sub>2</sub>O (0.1% TFA) over 10 min and isocratic 100% acetonitrile in H<sub>2</sub>O (0.1% TFA) for 1 min.

<sup>c</sup> ESI-MS base peak corresponds to [M+2H]<sup>2+</sup>.

<sup>d</sup> ESI-MS base peak corresponds to [M+3H]<sup>3+</sup>.

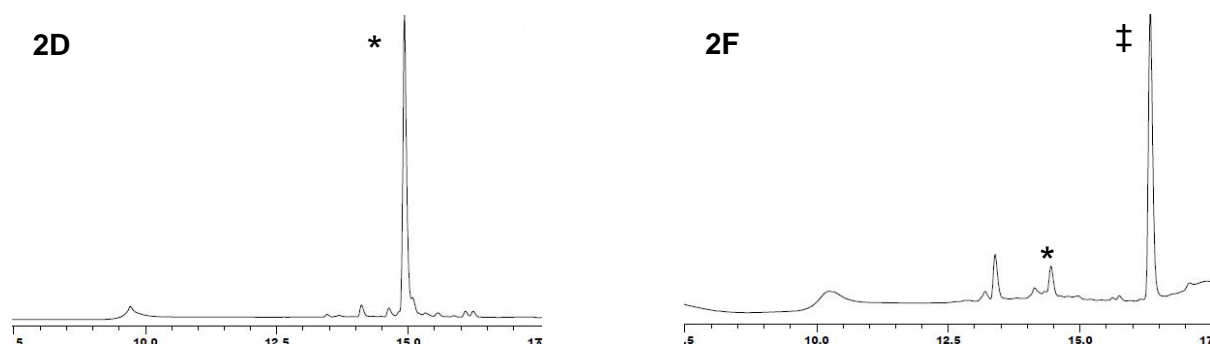


**Figure 2-11:** HPLC chromatographs (crude) of analogues fluorescently labelled in solution phase by condensation reaction (**2D**) and CuAAC reaction (**2F**). \* = Desired product, ‡ = excess RhB-4 derivative.

#### 2.4.2.1.2 Pharmacology

The human kisspeptin analogues were assessed for their GPR54 activity by our collaborator Ishwar Parhar's group using *in-vitro* dual-luciferase reporter assays. This assay system utilised two luciferase-catalysed bioluminescence reactions without cross-reactivity.<sup>(123)</sup> The first is a firefly luciferase reaction as the experimental reporter that emits light in the yellow-green region (550-557 nm).<sup>(124, 125)</sup> The second is a renilla luciferase reaction used as an internal control to reduce possible inherent variabilities,<sup>(126)</sup> which emits light in the green-blue region peaking at around 480 nm.<sup>(123)</sup> In our experiments, HEK cells were transfected with four plasmid DNAs that

coded for the two luciferases, the kisspeptin receptor of interest and the transcription factor NFAT. When an agonist activated kisspeptin receptors, its  $G_{q/11}$  subunit subsequently activated the intracellular signalling cascade, which eventually triggered expression of both luciferases. First, adding a reagent containing the firefly luciferin started the firefly luciferase reaction (**Figure 2-12**).<sup>(125, 126)</sup> Once the reading was collected, the renilla luciferase reaction was started by adding a coelenterazine-containing mixture (**Figure 2-13**),<sup>(126)</sup> which also simultaneously quenched the firefly luciferase luminescence. The ratio between the two readings was obtained as the normalised result.

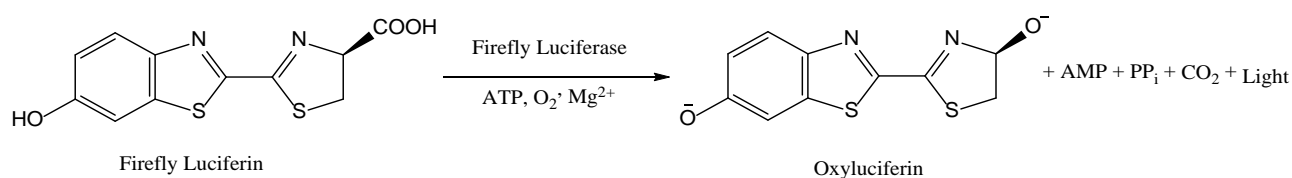


**Figure 2-12:** Firefly luciferase luminescence reaction.

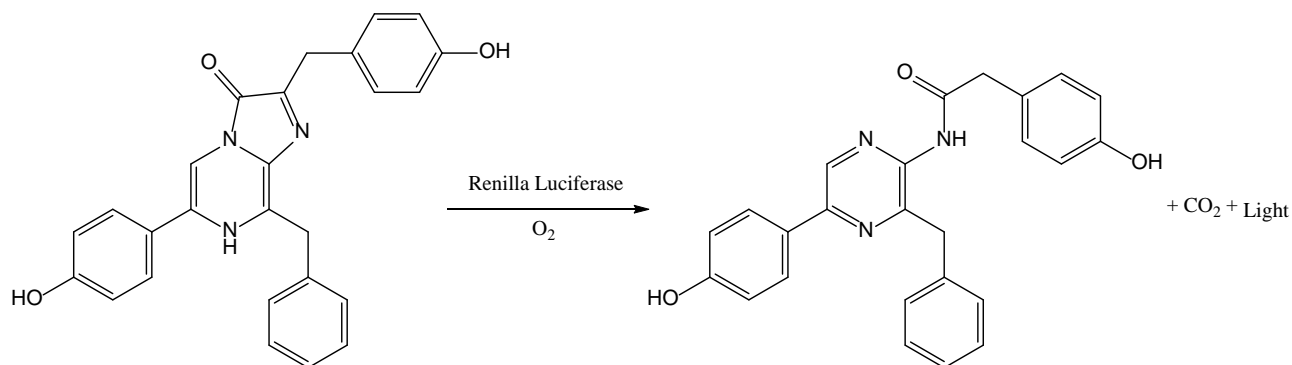


**Figure 2-13:** Renilla luciferase luminescence reaction.

The resulting pharmacological data of human KP-10 analogues (**Table 2-4**) have been published by our group in Journal of Peptide Science (full paper available in Appendix).<sup>(116)</sup> In the following section, other relevant analogues reported in the paper are listed for convenient comparison. The endogenous KP-10 displayed a potent agonistic activity with  $EC_{50}$  of  $13 \pm 1.9$  nM. A nanomolar potency was observed for its D-Tyr<sup>1</sup>

containing analogue **2B**, which was in good agreement with the literature.<sup>(120)</sup> As deletion of Tyr<sup>1</sup> residue has been found to markedly compromise potency,<sup>(80)</sup> this observation might be attributed to either stronger ligand-receptor binding, or enhanced metabolic stability due to the D-amino acid stereoisomer.

As we expected, the potency of those fluorescently labelled analogues was a function of both the labelling site and the type of fluorophore. The N-terminal RhB-1 labelled **2D** essentially retained receptor activity compared to the parent peptide KP-10, showing an EC<sub>50</sub> of 31 ± 19.2 nM. The type of conjugation linker appeared to be unimportant, as replacement with a thiourea group (compound **14** in the paper, synthesised using RhB-isothiocyanate) did not significantly alter receptor activity. However, a more hydrophobic Cy5.5 conjugated at the same position (**2E**) resulted in a completely inactive compound. Both the Pop-containing analogue **2C** and its RhB labelled derivative **2F** were also inactive, likely to reflect an unfavourable conformational alternation caused by this turn-inducing Pro analogue.

**Table 2-4:** Synthesised human KP-10 analogues and their pharmacological data.

Code	Code in publication	Sequence	EC <sub>50</sub> (nM)
-	<b>1</b>	YNWNSFGLRF-NH <sub>2</sub>	13±1.9
<b>2B</b>	<b>2</b>	dY-NWNSFGLRF-NH <sub>2</sub>	5.3±1.23
<b>2C</b>	-	dY-NW-Pop-SFGLRF-NH <sub>2</sub>	Inactive
<b>2D</b>	<b>12</b>	(RhB-1)-YNWNSFGLRF-NH <sub>2</sub>	31±19.2
<b>2E</b>	<b>13</b>	Cy5.5-YNWNSFGLRF-NH <sub>2</sub>	Inactive
-	<b>14</b>	RhB(NHCS)-YNWNSFGLRF-NH <sub>2</sub>	10±11.0
<b>2F</b>	<b>15</b>	dY-NW-Pop(RhB-4)SFGLRF-NH <sub>2</sub>	Inactive

\* Data taken from Camerino, M.A., Liu, M. *et al.*, *J. Pept. Sci.* 2016; 22: 406-414.  
NHCS in **14** = isothiocyanate linkage

### 2.4.2.2 Tilapia Kisspeptin Analogues

#### 2.4.2.2.1 Chemistry

The tilapia kisspeptin analogues were prepared using similar strategies as described for their human orthologues. The Kiss1 and Kiss2 sequences as predicted from tilapia genomic data (115) were both synthesised as reference compounds (**2G** and **2H**) following the standard Fmoc-based SPPS. We then adopted the modification strategy as seen in the human orthologue **2B**, where both Kiss1 and Kiss2 were substituted to contain N-terminal D-amino acid and this resulted in analogues **2I** and **2J**. Lastly, both kisspeptin sequences were N-terminally labelled via solution phase condensation reactions, which were achieved by treating with RhB-1 in presence of PyClock and NMM to give analogues **2K** and **2L** in high yield (Figure 2-14). The analytical data for all synthesised analogues are summarised in **Table 2-5**.

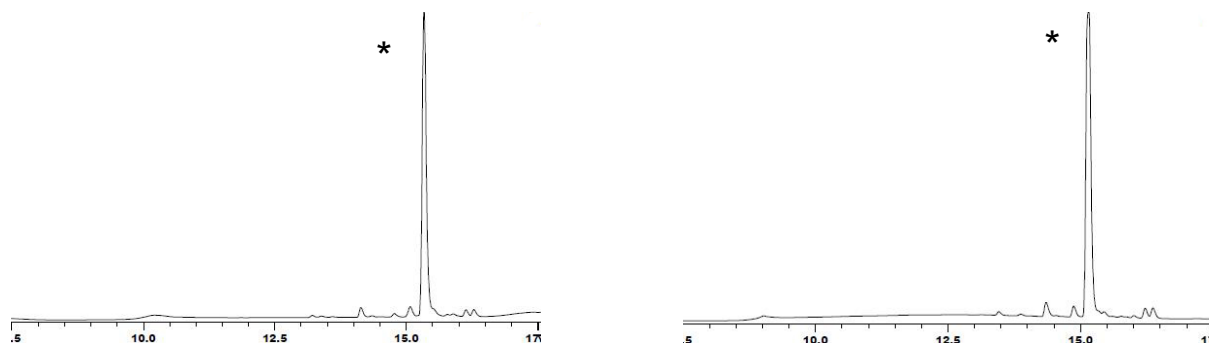


**Figure 2-14:** HPLC chromatographs (crude) of analogues **2K** and **2L**. \* = Desired product.



**Table 2-5:** Synthesised tilapia Kiss1 and Kiss2 analogues and their analytical data.

Code	Sequence	HPLC RT <sup>a</sup> (min)	MW (Calc)	m/z (found) <sup>b</sup>	Purity (%)
<b>2G</b>	YSLFSFGLRY-NH <sub>2</sub>	13.38	1251.5	626.6	99
<b>2H</b>	FNYNPLSLRF-NH <sub>2</sub>	12.85	1269.5	635.7	99
<b>2I</b>	dY-SLFSFGLRY-NH <sub>2</sub>	13.30	1251.5	626.6	99
<b>2J</b>	dF-NYNPLSLRF-NH <sub>2</sub>	12.82	1269.5	635.6	99
<b>2K</b>	(RhB-1)-YSLFSFGLRY-NH <sub>2</sub>	15.35	1845.2	923.4	99
<b>2L</b>	(RhB-1)-FNYNPLSLRF-NH <sub>2</sub>	15.07	1863.2	932.4	99

<sup>a</sup> LC/MS retention time using a Phenomenex Luna C-8 column (100Å, 3µm, 100×2.00mm).

The gradient is composed of 100% H<sub>2</sub>O (0.1% TFA) for 4 min, 0-60% acetonitrile in H<sub>2</sub>O (0.1% TFA) over 10 min and isocratic 60% acetonitrile in H<sub>2</sub>O (0.1% TFA) for 1 min.

<sup>b</sup> ESI-MS base peak corresponds to [M+2H]<sup>2+</sup>.

#### 2.4.2.2.2 Pharmacology

**Table 2-6:** Synthesised tilapia Kiss1 and Kiss2 analogues and their pharmacological data.

Code	Sequence	EC <sub>50</sub> (nM)
<b>2G</b>	YSLFSFGLRY-NH <sub>2</sub>	Inactive
<b>2H</b>	FNYNPLSLRF-NH <sub>2</sub>	1.3
<b>2I</b>	dY-SLFSFGLRY-NH <sub>2</sub>	(not determined)
<b>2J</b>	dF-NYNPLSLRF-NH <sub>2</sub>	0.85
<b>2K</b>	(RhB-1)-YSLFSFGLRY-NH <sub>2</sub>	Inactive
<b>2L</b>	(RhB-1)-FNYNPLSLRF-NH <sub>2</sub>	6.6

The tilapia Kiss1 and Kiss2 analogues were analysed using the same assay procedures on HEK cells transfected with tilapia GPR54 receptors, where the PhD candidate has contributed by analysing **2G**, **2H** and **2J** (Table 2-6). Overall, markedly different receptor activities were observed with the two paralogous peptides. Kiss1 (**2G**) and its labelled analogue **2K** were both completely inactive at tilapia GPR54, therefore the D-Tyr<sup>1</sup> containing analogue **2I** was not pursued further. On the contrary, the endogenous Kiss2 (**2H**) and its D-Phe<sup>1</sup> analogue **2J** both displayed highly potent agonism with EC<sub>50</sub> of 1.3 and 0.85 nM respectively. The RhB moiety caused 5-fold reduction in activity (**2L**), but still displayed nanomolar EC<sub>50</sub>, implying that the N-terminus of Kiss2 was not essential for receptor interaction. The strong selectivity of tilapia GPR54 towards Kiss2 suggests that

another unidentified receptor for Kiss1 probably exists, provided that Kiss1 mRNA encodes functional Kiss1 peptide in the peripheral tissues of tilapia.<sup>2</sup> Significantly, **2L** represents a potentially useful fluorescent kisspeptin analogue, which has been utilised in mapping GPR54 receptors in GnRH neurons in tilapia pituitary gland (unpublished data).

### **2.4.3 Summary – Kisspeptin Analogues**

In this section, we have demonstrated the synthesis of structural and fluorescently labelled human and tilapia kisspeptin analogues.

The human analogues were derived from the endogenous 10-amino acid peptide KP-10. Using dual-luciferase reporter assays, we have shown that RhB labelling at the N-terminus via either amide or thiourea group essentially retained receptor agonism, while Cy5.5 resulted in complete inactivity. In addition, the Pop<sup>4</sup> modified analogues were also inactive, suggesting possible 3D conformational changes incurred by this rigid cyclic amino acid.

The tilapia analogues were derived from two predicted 10-amino acid peptides Kiss1 and Kiss2, however only Kiss2 analogues were active at GPR54. In particular, the RhB-1 labelled Kiss2 exhibited only slightly sacrificed agonism in comparison to the unlabelled parent peptide and [D-Phe<sup>1</sup>]Kiss2. Therefore, this analogue holds potential as a novel fluorescent ligand for studying tilapia GPR54, and such application has been demonstrated in our preliminary imaging experiments.

---

<sup>2</sup> Personal communication with Dr Satoshi Ogawa, Parhar's group.

## 2.5 Experimental Methods

### 2.5.1 Materials

Protected amino acids were purchased from Chemimpex, Mimotopes and Auspep. Rink amide resin (0.53 mmol/g, 100-200 mesh), HCTU and PyClock were purchased from Chemimpex. TFA, DIPEA, NMM, TIPS, DMB, octanoic acid, piperidine, CuSO<sub>4</sub>, aminoguanidine, NaASc, DMSO, PhSiH<sub>3</sub> and Pd(PPh<sub>3</sub>)<sub>4</sub> were obtained from Sigma-Aldrich. THPTA was a gift from Dr Bim Graham's group, Monash University. The Cy5.5-NHS ester was obtained from Lumiprobe. The rhodamine B analogue was from Sigma-Aldrich and modified as reported to produce four piperazine-containing analogues as described in 2.2.2. All solvents were obtained from Merck and of analytical grade. All chemicals were used without further purification.

Molecular mass of the peptides was determined by ESI-MS using a Shimadzu LCMS2020 instrument that incorporates a Phenomenex Luna C-8 column (100 Å, 3 µm, 100 × 2.00 mm). The system used 0.05% TFA in Milli-Q water as the aqueous buffer and 0.05% TFA in acetonitrile as the organic buffer. The eluting profile was a linear gradient of 0-60% acetonitrile in water over 10 min at 0.2 ml/min.

Crude peptides were purified on a Phenomenex Luna C-8 column (100 Å, 10 µm, 250 × 21.2 mm) utilising a Waters 600 semi-preparative RP-HPLC that incorporates a Waters 486 UV detector. The detection wavelength was set at 230 nm. The system used 0.1% TFA in Milli-Q water as the aqueous buffer, and 0.1% TFA in acetonitrile as the organic buffer. The eluting profile was a linear gradient of 0-80% acetonitrile in water over 60 min at 10 ml/min.

## 2.5.2 Peptide Synthesis

The purity of all final products exceeded 96% according to HPLC chromatographs produced by the ESI-MS method described above.

**General Method 1:** Linear peptides (0.1 mmol scale) were synthesised following the standard Fmoc-based solid phase peptide synthesis (SPPS) strategy.<sup>(127-129)</sup> A 3-channel serial peptide synthesiser ("PS3", Protein Technologies Inc.) automated the processes. Fmoc deprotection was achieved by 20% v/v piperidine in DMF for 2 × 5 min. N<sup>α</sup>-Fmoc protected amino acids (3 eq.) were coupled using DMF as solvent, and HCTU (3 eq.) with DIPEA in DMF (7% v/v) as the activating agent for 50 min.

**General Method 2:** The completed peptide sequences were cleaved off resin by TIPS (2.5%) and DMB (5%) in TFA (5 ml) for 3 h. The mixture was then filtered, concentrated by stream of N<sub>2</sub>, precipitated in cold Et<sub>2</sub>O and centrifuged at 3000 rpm for 5 min. The crude product was precipitated and centrifuged for two more times, and then diluted with H<sub>2</sub>O-ACN (50%:50%) for lyophilisation.

### 2.5.2.1 Analogue 2A: [K<sup>19</sup>(RhB)]hGhrelin<sub>1-19</sub>

The linear backbone was prepared by General Method 1. The Alloc group at Dap<sup>3</sup> was removed using PhSiH<sub>3</sub> and Pd(PPh<sub>3</sub>)<sub>4</sub> in DCM under N<sub>2</sub>, and the free amine was conjugated by treating with octanoic acid (3 eq.), PyClock (3 eq.) in DIPEA (5 eq.) in DMF (5 ml) overnight. The Mtt group at Lys<sup>19</sup> was removed using TFA (2%) and TIPS (5%) in DCM (2 ml × 2 min × 10) to allow conjugation of RhB-1 (3 eq.) using the same method as for octanoic acid. The finished peptide was cleaved following General Method 2. After purification, **2A** was obtained as a fluffy magenta powder (2.0 mg). HPLC RT 13.58 min. ESI-MS: 983.3 (M+3H)<sup>3+</sup>.

**2.5.2.2 Analogue 2B: [dY<sup>1</sup>]hKP-10**

The peptide was synthesised on Rink amide resin using General Method 1 followed by 2. After purification, **2B** was obtained as a fluffy white powder (2.5 mg). HPLC RT 12.91 min. ESI-MS: 652.2 (M+2H)<sup>2+</sup>.

**2.5.2.3 Analogue 2C: [dY<sup>1</sup>, Pop<sup>4</sup>]hKP-10**

The peptide was synthesised on Rink amide resin using General Method 1 followed by 2. After purification, **2C** was obtained as a fluffy white powder (2.6 mg). HPLC RT 13.51 min. ESI-MS: 670.6 (M+2H)<sup>2+</sup>.

**2.5.2.4 Analogue 2D: [RhB-1]-hKP-10**

The peptide backbone was synthesised on Rink amide resin using General Method 1 followed by 2. Fluorescence labelling was achieved by treating the backbone (20 mg) with RhB-1 (1.2 eq.), PyClock (2 eq.) and NMM (12 eq.) in DMF (0.6 ml) overnight. After purification, **2D** was obtained as a fluffy magenta powder (10 mg). HPLC RT 14.94 min. ESI-MS: 948.9 (M+2H)<sup>2+</sup>.

**2.5.2.5 Analogue 2E: [Cy5.5]-hKP-10**

The peptide backbone was synthesised on Rink amide resin using General Method 1 followed by 2. Fluorescence labelling was achieved by treating the backbone (10 mg) with Cy5.5-NHS ester (1.2 eq.) and 2,4,6-trimethylpyridine (12 eq.) in DMF (0.6 ml) overnight. After purification, **2E** was obtained as a fluffy blue powder (1.2 mg). HPLC RT 12.83 min. ESI-MS: 934.8 (M+2H)<sup>2+</sup>.

**2.5.2.6 Analogue 2F: [dY<sup>1</sup>, Pop<sup>4</sup>(RhB-4)]hKP-10**

The peptide backbone was synthesised on Rink amide resin using General Method 1 followed by 2. Fluorescence labelling was achieved by treating the backbone (15 mg) with

RhB-4 (2 eq.), CuSO<sub>4</sub> (0.5 eq.), THPTA (2.5 eq.), aminoguanidine (25 eq.), sodium ascorbate (25 eq.) and DMSO (2%) in potassium phosphate buffer (0.1 M, pH = 7.4) for 1 h. After purification, **2F** was obtained as a fluffy magenta powder (1.1 mg). HPLC RT 14.42 min. ESI-MS: 659.7 (M+3H)<sup>3+</sup>.

#### **2.5.2.7 Analogue 2G: Kiss1**

The peptide was synthesised on Rink amide resin using General Method 1 followed by 2. After purification, **2G** was obtained as a fluffy white powder (39 mg). HPLC RT 13.38 min. ESI-MS: 626.6 (M+2H)<sup>2+</sup>.

#### **2.5.2.8 Analogue 2H: Kiss2**

The peptide was synthesised on Rink amide resin using General Method 1 followed by 2. After purification, **2H** was obtained as a fluffy white powder (42.6 mg). HPLC RT 12.85 min. ESI-MS: 635.7 (M+2H)<sup>2+</sup>.

#### **2.5.2.9 Analogue 2I: [dY<sup>1</sup>]Kiss1**

The peptide was synthesised on Rink amide resin using General Method 1 followed by 2. After purification, **2I** was obtained as a fluffy white powder (19.8 mg). HPLC RT 13.30 min. ESI-MS: 626.6 (M+2H)<sup>2+</sup>.

#### **2.5.2.10 Analogue 2J: [dF<sup>1</sup>]Kiss2**

The peptide was synthesised on Rink amide resin using General Method 1 followed by 2. After purification, **2J** was obtained as a fluffy white powder (72 mg). HPLC RT 12.82 min. ESI-MS: 635.6 (M+2H)<sup>2+</sup>.

#### **2.5.2.11 Analogue 2K: [RhB-1]-Kiss1**

The peptide backbone was synthesised on Rink amide resin using General Method 1 followed by 2. Fluorescence labelling was achieved by treating the backbone (15 mg) with

RhB-1 (1.2 eq.), PyClock (2 eq.) and NMM (12 eq.) in DMF (0.6 ml) overnight. After purification, **2K** was obtained as a fluffy magenta powder (5.6 mg). HPLC RT 15.35 min. ESI-MS: 923.4 (M+2H)<sup>2+</sup>.

#### **2.5.2.12 Analogue 2L: [RhB-1]-Kiss2**

The peptide was synthesised on Rink amide resin using General Method 1 followed by 2. Fluorescence labelling was achieved by treating the backbone (15 mg) with RhB-1 (1.2 eq.), PyClock (2 eq.) and NMM (12 eq.) in DMF (0.6 ml) overnight. After purification, **2L** was obtained as a fluffy magenta powder (6.0 mg). HPLC RT 15.07 min. ESI-MS: 932.4 (M+2H)<sup>2+</sup>.

### **2.5.3 Dual-luciferase Reporter Assays**

The details of this assay system have been described in our publication in Journal of Peptide Science (full paper available in Appendix).(116)

## References

- (1) Mitra, R. D., Shendure, J., Olejnik, J., Edyta Krzymanska, O., and Church, G. M. (2003) Fluorescent in situ sequencing on polymerase colonies. *Anal. Biochem.* 320, 55-65.
- (2) Volkova, K. D., Kovalska, V. B., Segers-Nolten, G. M., Veldhuis, G., Subramaniam, V., and Yarmoluk, S. M. (2009) Explorations of the application of cyanine dyes for quantitative  $\alpha$ -synuclein detection. *Biotech. Histochem.* 84, 55-61.
- (3) Oushiki, D., Kojima, H., Terai, T., Arita, M., Hanaoka, K., Urano, Y., and Nagano, T. (2010) Development and application of a near-infrared fluorescence probe for oxidative stress based on differential reactivity of linked cyanine dyes. *J. Am. Chem. Soc.* 132, 2795-2801.
- (4) Guo, Z., Nam, S., Park, S., and Yoon, J. (2012) A highly selective ratiometric near-infrared fluorescent cyanine sensor for cysteine with remarkable shift and its application in bioimaging. *Chem. Sci.* 3, 2760-2765.
- (5) Briggs, M. S., Burns, D. D., Cooper, M. E., and Gregory, S. J. (2000) A pH sensitive fluorescent cyanine dye for biological applications. *Chem. Commun.*, 2323-2324.
- (6) Cooper, M. E., Gregory, S., Adie, E., and Kalinka, S. (2002) pH-Sensitive cyanine dyes for biological applications. *J. Fluoresc.* 12, 425-429.
- (7) Hermanson, G. T. (2008) Chapter 9 - Fluorescent Probes, in *Bioconjugate Techniques (Second Edition)* pp 396-497, Academic Press, New York.
- (8) Ernst, L. A., Gupta, R. K., Mujumdar, R. B., and Waggoner, A. S. (1989) Cyanine dye labeling reagents for sulfhydryl groups. *Cytometry* 10, 3-10.
- (9) Mujumdar, R. B., Ernst, L. A., Mujumdar, S. R., Lewis, C. J., and Waggoner, A. S. (1993) Cyanine dye labeling reagents: Sulfoindocyanine succinimidyl esters. *Bioconjug. Chem.* 4, 105-111.
- (10) Bremer, C., Ntziachristos, V., and Weissleder, R. (2003) Optical-based molecular imaging: contrast agents and potential medical applications. *Eur. Radiol.* 13, 231-43.
- (11) Haughland, R. P. (2002) *Molecular Probes 9th Edition*, Molecular Probes Inc., Eugene, OR.
- (12) Mojzych, M., and Henary, M. (2008) Synthesis of cyanine dyes, in *Heterocyclic Polymethine Dyes: Synthesis, Properties and Applications* (Strekowski, L., Ed.) pp 1-9, Springer Berlin Heidelberg, Berlin, Heidelberg.
- (13) Formica, M., Fusi, V., Giorgi, L., and Micheloni, M. (2012) New fluorescent chemosensors for metal ions in solution. *Coord. Chem. Rev.* 256, 170-192.
- (14) Gonçalves, M. S. T. (2009) Fluorescent labeling of biomolecules with organic probes. *Chem. Rev.* 109, 190-212.



- 
- (15) Ballou, B., Fisher, G. W., Waggoner, A. S., Farkas, D. L., Reiland, J. M., Jaffe, R., Mujumdar, R. B., Mujumdar, S. R., and Hakala, T. R. (1995) Tumor labeling *in vivo* using cyanine-conjugated monoclonal antibodies. *Cancer Immunol Immunother* 41, 257-263.
- (16) Hermanson, G. T. (2013) Chapter 10 - Fluorescent Probes, in *Bioconjugate Techniques (Third edition)* pp 395-463, Academic Press, Boston.
- (17) Pawley, J. B. (1995) *Handbook of Confocal Microscopy*, 2nd ed., Plenum Press, New York.
- (18) Berlier, J. E., Rothe, A., Buller, G., Bradford, J., Gray, D. R., Filanoski, B. J., Telford, W. G., Yue, S., Liu, J., Cheung, C.-Y., Chang, W., Hirsch, J. D., Beechem Rosaria P. Haugland, J. M., and Haugland, R. P. (2003) Quantitative comparison of long-wavelength Alexa Fluor dyes to Cy dyes: fluorescence of the dyes and their bioconjugates. *J. Histochem. Cytochem.* 51, 1699-1712.
- (19) Renikuntla, B. R., Rose, H. C., Eldo, J., Waggoner, A. S., and Armitage, B. A. (2004) Improved photostability and fluorescence properties through polyfluorination of a cyanine dye. *Org. Lett.* 6, 909-912.
- (20) Samanta, A., Vendrell, M., Das, R., and Chang, Y.-T. (2010) Development of photostable near-infrared cyanine dyes. *Chem. Commun.* 46, 7406-7408.
- (21) Górecki, T., Patonay, G., Strekowski, L., Chin, R., and Salazar, N. (1996) Synthesis of novel near-infrared cyanine dyes for metal ion determination. *J. Heterocyclic Chem.* 33, 1871-1876.
- (22) Patonay, G., Antoine, M. D., Devanathan, S., and Strekowski, L. (1991) Near-infrared probe for determination of solvent hydrophobicity. *Appl. Spectrosc.* 45, 457-461.
- (23) Beija, M., Afonso, C. A. M., and Martinho, J. M. G. (2009) Synthesis and applications of Rhodamine derivatives as fluorescent probes. *Chem. Soc. Rev.* 38, 2410-2433.
- (24) Baeyer, A. (1876) Phthalic acid-phenol compounds. *Justus Liebigs Ann. Chem.* 183, 1-74.
- (25) Egawa, T., Koide, Y., Hanaoka, K., Komatsu, T., Terai, T., and Nagano, T. (2011) Development of a fluorescein analogue, TokyoMagenta, as a novel scaffold for fluorescence probes in red region. *Chem. Commun.* 47, 4162-4164.
- (26) Drexhage, K. H. (1976) Fluorescence efficiency of laser dyes. *J. Res. Natl. Bur. Stand.* 80A, 421-428.
- (27) Ma, Z., Du, L., and Li, M. (2014) Toward fluorescent probes for G-protein-coupled receptors (GPCRs). *J. Med. Chem.* 57, 8187-8203.
- (28) Kellogg, D. R., Mitchison, T. J., and Alberts, B. M. (1988) Behaviour of microtubules and actin filaments in living *Drosophila* embryos. *Development* 103, 675-686.
- (29) Heuck, A. P., Savva, C. G., Holzenburg, A., and Johnson, A. E. (2007) Conformational changes that effect oligomerization and initiate pore formation are triggered

- throughout perfringolysin O upon binding to cholesterol. *J. Biol. Chem.* 282, 22629-22637.
- (30) Weisblat, D. A., Zackson, S. L., Blair, S. S., and Young, J. D. (1980) Cell lineage analysis by intracellular injection of fluorescent tracers. *Science* 209, 1538-1541.
  - (31) Nguyen, T., and Francis, M. B. (2003) Practical Synthetic Route to Functionalized Rhodamine Dyes. *Org. Lett.* 5, 3245-3248.
  - (32) Northfield, S. E., Mountford, S. J., Wielens, J., Liu, M., Zhang, L., Herzog, H., Holliday, N. D., Scanlon, M. J., Parker, M. W., Chalmers, D. K., and Thompson, P. E. (2015) Propargyloxypyrroline regio- and stereoisomers for click-conjugation of peptides: synthesis and application in linear and cyclic peptides. *Aust. J. Chem.* 68, 1365-1372.
  - (33) Ma, X., Lin, L., Qin, G., Lu, X., Fiorotto, M., Dixit, V. D., and Sun, Y. (2011) Ablations of ghrelin and ghrelin receptor exhibit differential metabolic phenotypes and thermogenic capacity during aging. *PLoS ONE* 6, e16391.
  - (34) Zigman, J. M., Nakano, Y., Coppari, R., Balthasar, N., Marcus, J. N., Lee, C. E., Jones, J. E., Deysher, A. E., Waxman, A. R., White, R. D., Williams, T. D., Lachey, J. L., Seeley, R. J., Lowell, B. B., and Elmquist, J. K. (2005) Mice lacking ghrelin receptors resist the development of diet-induced obesity. *J. Clin. Invest.* 115, 3564-3572.
  - (35) Tomasetto, C., Karam, S. M., Ribieras, S., Masson, R., Lefèbvre, O., Staub, A., Alexander, G., Chenard, M.-P., and Rio, M.-C. (2000) Identification and characterization of a novel gastric peptide hormone: The motilin-related peptide. *Gastroenterology* 119, 395-405.
  - (36) Kojima, M., Hosoda, H., Date, Y., Nakazato, M., Matsuo, H., and Kangawa, K. (1999) Ghrelin is a growth-hormone-releasing acylated peptide from stomach. *Nature* 402, 656-660.
  - (37) De Vriese, C., and Delporte, C. (2008) Ghrelin: A new peptide regulating growth hormone release and food intake. *Int. J. Biochem. Cell Biol.* 40, 1420-1424.
  - (38) Hosoda, H., Kojima, M., Mizushima, T., Shimizu, S., and Kangawa, K. (2003) Structural divergence of human ghrelin: Identification of multiple ghrelin-derived molecules produced by post-translational processing. *J. Biol. Chem.* 278, 64-70.
  - (39) Matsumoto, M., Hosoda, H., Kitajima, Y., Morozumi, N., Minamitake, Y., Tanaka, S., Matsuo, H., Kojima, M., Hayashi, Y., and Kangawa, K. (2001) Structure-activity relationship of ghrelin: Pharmacological study of ghrelin peptides. *Biochem. Biophys. Res. Commun.* 287, 142-146.
  - (40) Großauer, J., Kosol, S., Schrank, E., and Zangger, K. (2010) The peptide hormone ghrelin binds to membrane-mimetics via its octanoyl chain and an adjacent phenylalanine. *Bioorg. Med. Chem.* 18, 5483-5488.
  - (41) Yang, J., Brown, M. S., Liang, G., Grishin, N. V., and Goldstein, J. L. (2008) Identification of the acyltransferase that octanoylates ghrelin, an appetite-stimulating peptide hormone. *Cell* 132, 387-396.

- 
- (42) Volante, M., Fulcheri, E., Allia, E., Cerrato, M., Pucci, A., and Papotti, M. (2002) Ghrelin expression in fetal, infant, and adult human lung. *J. Histochem. Cytochem.* 50, 1013-1021.
- (43) Gualillo, O., Caminos, J. E., Blanco, M., García-Caballero, T., Kojima, M., Kangawa, K., Dieguez, C., and Casanueva, F. F. (2001) Ghrelin, a novel placental-derived hormone. *Endocrinology* 142, 788-794.
- (44) Korbonits, M., Bustin, S. A., Kojima, M., Jordan, S., Adams, E. F., Lowe, D. G., Kangawa, K., and Grossman, A. B. (2001) The expression of the growth hormone secretagogue receptor ligand ghrelin in normal and abnormal human pituitary and other neuroendocrine tumors. *J. Clin. Endocrinol. Metab.* 86, 881-887.
- (45) Mori, K., Yoshimoto, A., Takaya, K., Hosoda, K., Ariyasu, H., Yahata, K., Mukoyama, M., Sugawara, A., Hosoda, H., Kojima, M., Kangawa, K., and Nakao, K. (2000) Kidney produces a novel acylated peptide, ghrelin. *FEBS Lett.* 486, 213-216.
- (46) Volante, M., Allia, E., Fulcheri, E., Cassoni, P., Ghigo, E., Muccioli, G., and Papotti, M. (2003) Ghrelin in fetal thyroid and follicular tumors and cell lines: Expression and effects on tumor growth. *Am. J. Pathol.* 162, 645-654.
- (47) Gaytan, F., Barreiro, M. L., Caminos, J. E., Chopin, L. K., Herington, A. C., Morales, C., Pinilla, L., Paniagua, R., Nistal, M., Casanueva, F. F., Aguilar, E., Diéguez, C., and Tena-Sempere, M. (2004) Expression of ghrelin and its functional receptor, the type 1a growth hormone secretagogue receptor, in normal human testis and testicular tumors. *J. Clin. Endocrinol. Metab.* 89, 400-409.
- (48) Howard, A. D., Feighner, S. D., Cully, D. F., Arena, J. P., Liberator, P. A., Rosenblum, C. I., Hamelin, M., Hreniuk, D. L., Palyha, O. C., Hamelin, M., Hreniuk, D. L., Palyha, O. C., Anderson, J., Paress, P. S., Diaz, C., Chou, M., Liu, K. K., McKee, K. K., Pong, S.-S., Chaung, L.-Y., Elbrecht, A., Dashkevich, M., Heavens, R., Rigby, M., Sirinathsinghji, D. J. S., Dean, D. C., Melillo, D. G., Patchett, A. A., Nargund, R., Griffin, P. R., DeMartino, J. A., Gupta, S. K., Schaeffer, J. M., Smith, R. G., and Ploeg, L. H. T. v. d. (1996) A receptor in pituitary and hypothalamus that functions in growth hormone release. *Science* 273, 974-977.
- (49) Carreira, M. C., Camina, J. P., Smith, R. G., and Casanueva, F. F. (2004) Agonist-specific coupling of growth hormone secretagogue receptor type 1a to different intracellular signalling systems. *Neuroendocrinology* 79, 13-25.
- (50) Leung, P.-K., Chow, K. B. S., Lau, P.-N., Chu, K.-M., Chan, C.-B., Cheng, C. H. K., and Wise, H. (2007) The truncated ghrelin receptor polypeptide (GHS-R1b) acts as a dominant-negative mutant of the ghrelin receptor. *Cell. Signal.* 19, 1011-1022.
- (51) Chow, K. B. S., Sun, J., Man Chu, K., Tai Cheung, W., Cheng, C. H. K., and Wise, H. (2012) The truncated ghrelin receptor polypeptide (GHS-R1b) is localized in the endoplasmic reticulum where it forms heterodimers with ghrelin receptors (GHS-R1a) to attenuate their cell surface expression. *Mol. Cell Endocrinol.* 348, 247-254.
- (52) Tschöp, M., Smiley, D. L., and Heiman, M. L. (2000) Ghrelin induces adiposity in rodents. *Nature* 407, 908-913.
-

- 
- (53) Nakazato, M., Murakami, N., Date, Y., Kojima, M., Matsuo, H., Kangawa, K., and Matsukura, S. (2001) A role for ghrelin in the central regulation of feeding. *Nature* 409, 194-198.
- (54) Asakawa, A., Inui, A., Kaga, T., Katsuura, G., Fujimiya, M., Fujino, M. A., and Kasuga, M. (2003) Antagonism of ghrelin receptor reduces food intake and body weight gain in mice. *Gut* 52, 947-952.
- (55) Patterson, Z. R., Ducharme, R., Anisman, H., and Abizaid, A. (2010) Altered metabolic and neurochemical responses to chronic unpredictable stressors in ghrelin receptor-deficient mice. *Eur. J. Neurosci.* 32, 632-639.
- (56) Date, Y., Nakazato, M., Hashiguchi, S., Dezaki, K., Mondal, M. S., Hosoda, H., Kojima, M., Kangawa, K., Arima, T., Matsuo, H., Yada, T., and Matsukura, S. (2002) Ghrelin is present in pancreatic  $\alpha$ -cells of humans and rats and stimulates insulin secretion. *Diabetes* 51, 124-129.
- (57) Saad, M. F., Bernaba, B., Hwu, C.-M., Jinagouda, S., Fahmi, S., Kogosov, E., and Boyadjian, R. (2002) Insulin regulates plasma ghrelin concentration. *J. Clin. Endocrinol. Metab.* 87, 3997-4000.
- (58) Waseem, T., Duxbury, M., Ito, H., Ashley, S. W., and Robinson, M. K. (2008) Exogenous ghrelin modulates release of pro-inflammatory and anti-inflammatory cytokines in LPS-stimulated macrophages through distinct signaling pathways. *Surgery* 143, 334-342.
- (59) Nagaya, N., Miyatake, K., Uematsu, M., Oya, H., Shimizu, W., Hosoda, H., Kojima, M., Nakanishi, N., Mori, H., and Kangawa, K. (2001) Hemodynamic, renal, and hormonal effects of ghrelin infusion in patients with chronic heart failure. *J. Clin. Endocrinol. Metab.* 86, 5854-5859.
- (60) Beiras-Fernandez, A., Kreth, S., Weis, F., Ledderose, C., Pöttinger, T., Dieguez, C., Beiras, A., and Reichart, B. (2010) Altered myocardial expression of ghrelin and its receptor (GHSR-1a) in patients with severe heart failure. *Peptides* 31, 2222-2228.
- (61) Katugampola, S. D., Pallikaros, Z., and Davenport, A. P. (2001) [ $^{125}$ I-His $^9$ ]-Ghrelin, a novel radioligand for localizing GHS orphan receptors in human and rat tissue; up-regulation of receptors with atherosclerosis. *Br. J. Pharm* 134, 143-149.
- (62) Gauna, C., Meyler, F. M., Janssen, J. A. M. J. L., Delhanty, P. J. D., Abribat, T., van Koetsveld, P., Hofland, L. J., Broglio, F., Ghigo, E., and van Der Lely, A.-J. (2004) Administration of acylated ghrelin reduces insulin sensitivity, whereas the combination of acylated plus unacylated ghrelin strongly improves insulin sensitivity. *J. Clin. Endocrinol. Metab.* 89, 5035-5042.
- (63) Delhanty, P. J. D., Sun, Y., Visser, J. A., van Kerkwijk, A., Huisman, M., van Ijcken, W. F. J., Swagemakers, S., Smith, R. G., Themmen, A. P. N., and van der Lely, A.-J. (2010) Unacylated ghrelin rapidly modulates lipogenic and insulin signaling pathway gene expression in metabolically active tissues of GHSR deleted mice. *PLoS ONE* 5, e11749.

- (64) Granata, R., Settanni, F., Biancone, L., Trovato, L., Nano, R., Bertuzzi, F., Destefanis, S., Annunziata, M., Martinetti, M., Catapano, F., Ghè, C., Isgaard, J., Papotti, M., Ghigo, E., and Muccioli, G. (2007) Acylated and unacylated ghrelin promote proliferation and inhibit apoptosis of pancreatic  $\beta$ -cells and human islets: involvement of 3',5'-cyclic adenosine monophosphate/protein kinase A, extracellular signal-regulated kinase 1/2, and phosphatidylinositol 3-kinase/Akt signaling. *Endocrinology* 148, 512-529.
- (65) Granata, R., Settanni, F., Julien, M., Nano, R., Togliatto, G., Trombetta, A., Gallo, D., Piemonti, L., Brizzi, M. F., Abribat, T., van Der Lely, A.-J., and Ghigo, E. (2012) Des-acyl ghrelin fragments and analogues promote survival of pancreatic  $\beta$ -cells and human pancreatic islets and prevent diabetes in streptozotocin-treated rats. *J. Med. Chem.* 55, 2585-2596.
- (66) Bednarek, M. A., Feighner, S. D., Pong, S.-S., McKee, K. K., Hreniuk, D. L., Silva, M. V., Warren, V. A., Howard, A. D., Van der Ploeg, L. H. Y., and Heck, J. V. (2000) Structure-function studies on the new growth hormone-releasing peptide, ghrelin: minimal sequence of ghrelin necessary for activation of growth hormone secretagogue receptor 1a. *J. Med. Chem.* 43, 4370-4376.
- (67) Rosita, D., DeWit, M. A., and Luyt, L. G. (2009) Fluorine and rhenium substituted ghrelin analogues as potential imaging probes for the growth hormone secretagogue receptor. *J. Med. Chem.* 52, 2196-2203.
- (68) McGirr, R., McFarland, M. S., McTavish, J., Luyt, L. G., and Dhanvantari, S. (2011) Design and characterization of a fluorescent ghrelin analog for imaging the growth hormone secretagogue receptor 1a. *Regul. Pept.* 172, 69-76.
- (69) Douglas, G. A. F., McGirr, R., Charlton, C. L., Kagan, D. B., Hoffman, L. M., Luyt, L. G., and Dhanvantari, S. (2014) Characterization of a far-red analog of ghrelin for imaging GHS-R in P19-derived cardiomyocytes. *Peptides* 54, 81-88.
- (70) Chan, W., and White, P. (2000) *Fmoc solid phase peptide synthesis - a practical approach*, Oxford: Oxford University Press.
- (71) Thieriet, N., Alsina, J., Giralt, E., Guibé, F., and Albericio, F. (1997) Use of Alloc-amino acids in solid-phase peptide synthesis. Tandem deprotection-coupling reactions using neutral conditions. *Tetrahedron Lett.* 38, 7275-7278.
- (72) Aletras, A., Barlos, K., Gatos, D., Koutsogianni, S., and Mamos, P. (1995) Preparation of the very acid-sensitive Fmoc-Lys(Mtt)-OH Application in the synthesis of side-chain to side-chain cyclic peptides and oligolysine cores suitable for the solid-phase assembly of MAPs and TASP. *Int. J. Pept. Protein Res.* 45, 488-496.
- (73) Dubey, L. V., and Dubey, I. Y. (2005) Side reactions of onium coupling reagents BOP and HBTU in the synthesis of silica polymer supports. *Ukrainica Bioorganica Acta* 1, 13-19.
- (74) Esler, W. P., Rudolph, J., Claus, T. H., Tang, W., Barucci, N., Brown, S.-E., Bullock, W., Daly, M., DeCarr, L., Li, Y., Milardo, L., Molstad, D., Zhu, J., Gardell, S. J., Livingston, J. N., and Sweet, L. J. (2007) Small-molecule ghrelin receptor antagonists improve glucose tolerance, suppress appetite, and promote weight loss. *Endocrinology* 148, 5175-5185.

- 
- (75) Schnell, S. A., and Wessendorf, M. W. (1995) Bisbenzimidazole: a fluorescent counterstain for tissue autoradiography. *Histochem. Cell Biol.* 103, 111-114.
- (76) Kotani, M., Detheux, M., Vandenbogaerde, A., Communi, D., Vanderwinden, J.-M., Poul, E. L., Brézillon, S., Tyldesley, R., Suarez-Huerta, N., Vandeput, F., Blanpain, C., Schiffmann, S. N., Vassart, G., and Parmentier, M. (2001) The metastasis suppressor gene KiSS-1 encodes kisspeptins, the natural ligands of the orphan G protein-coupled receptor GPR54. *J. Biol. Chem.* 276, 34631-34636.
- (77) Lee, J.-H., Miele, M. E., Hicks, D. J., Philips, K. K., Trent, J. M., Weissman, B. E., and Welch, D. R. (1996) KiSS-1, a novel human malignant melanoma metastasis-suppressor gene. *J. Natl. Cancer Inst.* 88, 1731-1737.
- (78) Tomita, K., Niida, A., Oishi, S., Ohno, H., Cluzeau, J., Navenot, J.-M., Wang, Z.-x., Peiper, S. C., and Fujii, N. (2006) Structure-activity relationship study on small peptidic GPR54 agonists. *Bioorgan. Med. Chem.* 14, 7595-7603.
- (79) Mikkelsen, J. D., Bentsen, A. H., Ansel, L., Simonneaux, V., and Juul, A. (2009) Comparison of the effects of peripherally administered kisspeptins. *Regul. Pept.* 152, 95-100.
- (80) Muir, A. I., Chamberlain, L., Elshourbagy, N. A., Michalovich, D., Moore, D. J., Calamari, A., Szekeres, P. G., Sarau, H. M., Chambers, J. K., Murdock, P., Steplewski, K., Shabon, U., Miller, J. E., Middleton, S. E., Darker, J. G., Larminie, C. G. C., Wilson, S., Bergsma, D. J., Emson, P., Faull, R., Philpott, K. L., and Harrison, D. C. (2001) AXOR12, a novel human G protein-coupled receptor, activated by the peptide KiSS-1. *J. Biol. Chem.* 276, 28969-28975.
- (81) Stafford, L. J., Xia, C., Ma, W., Cai, Y., and Liu, M. (2002) Identification and characterization of mouse metastasis-suppressor KiSS1 and its G-protein-coupled receptor. *Cancer Res.* 62, 5399-5404.
- (82) Ohtaki, T., Shintani, Y., Honda, S., Matsumoto, H., Hori, A., Kanehashi, K., Terao, Y., Kumano, S., Takatsu, Y., Masuda, Y., Ishibashi, Y., Watanabe, T., Asada, M., Yamada, T., Suenaga, M., Kitada, C., Usuki, S., Kurokawa, T., Onda, H., Nishimura, O., and Fujino, M. (2001) Metastasis suppressor gene KiSS-1 encodes peptide ligand of a G-protein-coupled receptor. *Nature* 411, 613-617.
- (83) Niida, A., Wang, Z., Tomita, K., Oishi, S., Tamamura, H., Otaka, A., Navenot, J.-M., Broach, J. R., Peiper, S. C., and Fujii, N. (2006) Design and synthesis of downsized metastatin (45-54) analogs with maintenance of high GPR54 agonistic activity. *Bioorg. Med. Chem. Lett.* 16, 134-137.
- (84) Makri, A., Pissimissis, N., Lembessis, P., Polychronakos, C., and Koutsilieris, M. (2008) The kisspeptin (KiSS-1)/GPR54 system in cancer biology. *Cancer Treat. Rev.* 34, 682-692.
- (85) Thompson, E. L., Patterson, M., Murphy, K. G., Smith, K. L., Dhillon, W. S., Todd, J. F., Ghatei, M. A., and Bloom, S. R. (2004) Central and peripheral administration of kisspeptin-10 stimulates the hypothalamic-pituitary-gonadal axis. *J. Neuroendocrinol.* 16, 850-858.

- 
- (86) Seminara, S. B., Messenger, S., Chatzidaki, E. E., Thresher, R. R., Acierno, J. S., Shagoury, J. K., Bo-Abbas, Y., Kuohung, W., Schwinof, K. M., Hendrick, A. G., Zahn, D., Dixon, J., Kaiser, U. B., Slaugenhaupt, S. A., Gusella, J. F., O'Rahilly, S., Carlton, M. B. L., Crowley, W. F., Aparicio, S. A. J. R., and Colledge, W. H. (2003) The GPR54 gene as a regulator of puberty. *N. Engl. J. Med.* 349, 1614-1627.
- (87) Shahab, M., Mastronardi, C., Seminara, S. B., Crowley, W. F., Ojeda, S. R., and Plant, T. M. (2005) Increased hypothalamic GPR54 signaling: A potential mechanism for initiation of puberty in primates. *Proc. Natl. Acad. Sci.* 102, 2129-2134.
- (88) Popa, S. M., Clifton, D. K., and Steiner, R. A. (2005) A KiSS to remember. *Trends Endocrinol. Metab.* 16, 249-250.
- (89) Navarro, V. M., Castellano, J. M., Fernández-Fernández, R., Tovar, S., Roa, J., Mayen, A., Barreiro, M. L., Casanueva, F. F., Aguilar, E., Dieguez, C., Pinilla, L., and Tena-Sempere, M. (2005) Effects of KiSS-1 peptide, the natural ligand of GPR54, on follicle-stimulating hormone secretion in the rat. *Endocrinology* 146, 1689-1697.
- (90) Navarro, V. M., Fernández-Fernández, R., Castellano, J. M., Roa, J., Mayen, A., Barreiro, M. L., Gaytan, F., Aguilar, E., Pinilla, L., Dieguez, C., and Tena-Sempere, M. (2004) Advanced vaginal opening and precocious activation of the reproductive axis by KiSS-1 peptide, the endogenous ligand of GPR54. *J. Physiol.* 561, 379-386.
- (91) Seminara, S. B. (2005) Metastin and its G protein-coupled receptor, GPR54: Critical pathway modulating GnRH secretion. *Front. Neuroendocrinol.* 26, 131-138.
- (92) Silveira, L. G., Noel, S. D., Silveira-Neto, A. P., Abreu, A. P., Brito, V. N., Santos, M. G., Bianco, S. D. C., Kuohung, W., Xu, S., Gryngarten, M., Escobar, M. E., Arnhold, I. J. P., Mendonca, B. B., Kaiser, U. B., and Latronico, A. C. (2010) Mutations of the KISS1 gene in disorders of puberty. *J. Clin. Endocrinol. Metab.* 95, 2276-2280.
- (93) Roux, N. d., Genin, E., Carel, J.-C., Matsuda, F., Chaussain, J.-L., and Milgrom, E. (2003) Hypogonadotropic hypogonadism due to loss of function of the KiSS1-derived peptide receptor GPR54. *Proc. Natl. Acad. Sci.* 100, 10972-10976.
- (94) Dungan, H. M., Clifton, D. K., and Steiner, R. A. (2006) Minireview: kisspeptin neurons as central processors in the regulation of gonadotropin-releasing hormone secretion. *Endocrinology* 147, 1154-1158.
- (95) Teles, M. G., Bianco, S. D. C., Brito, V. N., Trarbach, E. B., Kuohung, W., Xu, S., Seminara, S. B., Mendonca, B. B., Kaiser, U. B., and Latronico, A. C. (2008) A GPR54-activating mutation in a patient with central precocious puberty. *N. Engl. J. Med.* 358, 709-715.
- (96) Shirasaki, F., Takata, M., Hatta, N., and Takehara, K. (2001) Loss of expression of the metastasis suppressor gene KiSS1 during melanoma progression and its association with LOH of chromosome 6q16.3-q23. *Cancer Res.* 61, 7422-7425.
- (97) Sanchez-Carbayo, M., Capodieci, P., and Cordon-Cardo, C. (2003) Tumor suppressor role of KiSS-1 in bladder cancer: loss of KiSS-1 expression is associated with bladder cancer progression and clinical outcome. *Am. J. Pathol.* 162, 609-617.

- 
- (98) Dhar, D. K., Naora, H., Kubota, H., Maruyama, R., Yoshimura, H., Tonomoto, Y., Tachibana, M., Ono, T., Otani, H., and Nagasue, N. (2004) Downregulation of KiSS-1 expression is responsible for tumor invasion and worse prognosis in gastric carcinoma. *Int. J. Cancer* 111, 868-872.
- (99) Schmid, K., Wang, X., Haitel, A., Sieghart, W., Peck-Radosavljevic, M., Bodingbauer, M., Rasoul-Rockenschaub, S., and Wrba, F. (2007) KiSS-1 overexpression as an independent prognostic marker in hepatocellular carcinoma: an immunohistochemical study. *Virchows Arch* 450, 143-149.
- (100) Ikeguchi, M., Hirooka, Y., and Kaibara, N. (2003) Quantitative reverse transcriptase polymerase chain reaction analysis for KiSS-1 and orphan G-protein-coupled receptor (hOT7T175) gene expression in hepatocellular carcinoma. *J Cancer Res Clin Oncol* 129, 531-535.
- (101) Shoji, S., Tang, X. Y., Umemura, S., Itoh, J., Takekoshi, S., Shima, M., Usui, Y., Nagata, Y., Uchida, T., Osamura, R. Y., and Terachi, T. (2009) Metastin inhibits migration and invasion of renal cell carcinoma with overexpression of metastin receptor. *Eur. Urol.* 55, 441-451.
- (102) Gopurappilly, R., Ogawa, S., and Parhar, I. S. (2013) Functional significance of GnRH and kisspeptin, and their cognate receptors in teleost reproduction. *Front. Endocrinol. (Lausanne)* 4, 24.
- (103) Mechaly, A. S., Viñas, J., and Piferrer, F. (2009) Identification of two isoforms of the kisspeptin-1 receptor (kiss1r) generated by alternative splicing in a modern teleost, the senegalese sole (*solea senegalensis*). *Biol. Reprod.* 80, 60-69.
- (104) Li, S., Zhang, Y., Liu, Y., Huang, X., Huang, W., Lu, D., Zhu, P., Shi, Y., Cheng, C. H. K., Liu, X., and Lin, H. (2009) Structural and functional multiplicity of the kisspeptin/GPR54 system in goldfish (*Carassius auratus*). *J. Endocrinol.* 201, 407-418.
- (105) Biran, J., Ben-Dor, S., and Levavi-Sivan, B. (2008) Molecular identification and functional characterization of the kisspeptin/kisspeptin receptor system in lower vertebrates. *Biol. Reprod.* 79, 776-786.
- (106) Lee, Y. R., Tsunekawa, K., Moon, M. J., Um, H. N., Hwang, J.-I., Osugi, T., Otaki, N., Sunakawa, Y., Kim, K., Vaudry, H., Kwon, H. B., Seong, J. Y., and Tsutsui, K. (2009) Molecular evolution of multiple forms of kisspeptins and GPR54 receptors in vertebrates. *Endocrinology* 150, 2837-2846.
- (107) Kanda, S., Akazome, Y., Matsunaga, T., Yamamoto, N., Yamada, S., Tsukamura, H., Maeda, K.-i., and Oka, Y. (2008) Identification of KiSS-1 product kisspeptin and steroid-sensitive sexually dimorphic kisspeptin neurons in medaka (*Oryzias latipes*). *Endocrinology* 149, 2467-2476.
- (108) van Aerle, R., Kille, P., Lange, A., and Tyler, C. R. (2008) Evidence for the existence of a functional Kiss1/Kiss1 receptor pathway in fish. *Peptides* 29, 57-64.
- (109) Kitahashi, T., Ogawa, S., and Parhar, I. S. (2009) Cloning and expression of kiss2 in the zebrafish and medaka. *Endocrinology* 150, 821-831.
-



- 
- (110) Tena-Sempere, M., Felip, A., Gómez, A., Zanuy, S., and Carrillo, M. (2012) Comparative insights of the kisspeptin/kisspeptin receptor system: Lessons from non-mammalian vertebrates. *Gen. Comp. Endocrinol.* 175, 234-243.
- (111) Parhar, I. S., Ogawa, S., and Sakuma, Y. (2004) Laser-captured single digoxigenin-labeled neurons of gonadotropin-releasing hormone types reveal a novel G protein-coupled receptor (Gpr54) during maturation in cichlid fish. *Endocrinology* 145, 3613-3618.
- (112) Um, H. N., Han, J. M., Hwang, J.-I., Hong, S. I., Vaudry, H., and Seong, J. Y. (2010) Molecular coevolution of kisspeptins and their receptors from fish to mammals. *Ann. N. Y. Acad. Sci.* 1200, 67-74.
- (113) Nocillado, J. N., Levavi-Sivan, B., Carrick, F., and Elizur, A. (2007) Temporal expression of G-protein-coupled receptor 54 (GPR54), gonadotropin-releasing hormones (GnRH), and dopamine receptor D2 (drd2) in pubertal female grey mullet, *Mugil cephalus*. *Gen. Comp. Endocrinol.* 150, 278-287.
- (114) Mohamed, J. S., Benninghoff, A. D., Holt, G. J., and Khan, I. A. (2007) Developmental expression of the G protein-coupled receptor 54 and three GnRH mRNAs in the teleost fish cobia. *J. Mol. Endocrinol.* 38, 235-244.
- (115) Ogawa, S., Ng, K. W., Xue, X., Ramadasan, P. N., Sivalingam, M., Li, S., Levavi-Sivan, B., Lin, H., Liu, X., and Parhar, I. S. (2013) Thyroid hormone upregulates hypothalamic kiss2 gene in the male Nile tilapia, *Oreochromis niloticus*. *Front. Endocrinol.* 4, 184.
- (116) Camerino, M. A., Liu, M., Moriya, S., Kitahashi, T., Mahgoub, A., Mountford, S. J., Chalmers, D. K., Soga, T., Parhar, I. S., and Thompson, P. E. (2016) Beta amino acid-modified and fluorescently labelled kisspeptin analogues with potent KISS1R activity. *J. Pept. Sci.* 22, 406-414.
- (117) Kaneda, M., Misu, R., Ohno, H., Hirasawa, A., Ieda, N., Uenoyama, Y., Tsukamura, H., Maeda, K.-i., Oishi, S., and Fujii, N. (2014) Design and synthesis of fluorescent probes for GPR54. *Bioorg. Med. Chem.* 22, 3325-3330.
- (118) Lee, J. Y., Moon, J. S., Eu, Y.-J., Lee, C. W., Yang, S.-T., Lee, S. K., Jung, H. H., Kim, H. H., Rhim, H., Seong, J. Y., and Kim, J. I. (2009) Molecular interaction between kisspeptin decapeptide analogs and a lipid membrane. *Arch. Biochem. Biophys.* 485, 109-114.
- (119) Orsini, M. J., Klein, M. A., Beavers, M. P., Connolly, P. J., Middleton, S. A., and Mayo, K. H. (2007) Metastin (KiSS-1) mimetics identified from peptide structure-activity relationship-derived pharmacophores and directed small molecule database screening. *J. Med. Chem.* 50, 462-471.
- (120) Curtis, A. E., Cooke, J. H., Baxter, J. E., Parkinson, J. R. C., Bataveljic, A., Ghatei, M. A., Bloom, S. R., and Murphy, K. G. (2010) A kisspeptin-10 analog with greater in vivo bioactivity than kisspeptin-10. *Am. J. Physiol. Endocrinol. Metab.* 298, E296-E303.
- (121) Gutiérrez-Pascual, E., Leprince, J., Martínez-Fuentes, A. J., Ségalas-Milazzo, I., Pineda, R., Roa, J., Duran-Prado, M., Guilhaudis, L., Desperrois, E., Lebreton, A., Pinilla, L., Tonon, M.-C., Malagón, M. M., Vaudry, H., Tena-Sempere, M., and Castaño, J. P. (2009) *In vivo*

- and *in vitro* structure-activity relationships and structural conformation of kisspeptin-10-related peptides. *Mol. Pharmacol.* 76, 58-67.
- (122) Asami, T., Nishizawa, N., Ishibashi, Y., Nishibori, K., Horikoshi, Y., Matsumoto, H., Ohtaki, T., and Kitada, C. (2012) Trypsin resistance of a decapeptide KISS1R agonist containing an N<sup>ω</sup>-methylarginine substitution. *Bioorg. Med. Chem. Lett.* 22, 6328-6332.
- (123) Bhaumik, S., and Gambhir, S. S. (2002) Optical imaging of Renilla luciferase reporter gene expression in living mice. *Proc. Natl. Acad. Sci.* 99, 377-382.
- (124) Seliger, H. H., Buck, J. B., Fastie, W. G., and McElroy, W. D. (1964) The spectral distribution of firefly light. *J. Gen. Physiol.* 48, 95-104.
- (125) Marques, S. M., and Esteves da Silva, J. C. G. (2009) Firefly bioluminescence: A mechanistic approach of luciferase catalyzed reactions. *IUBMB Life* 61, 6-17.
- (126) Sherf, B. A., Navarro, S. L., Hannah, R. R., and Wood, K. V. (1996) Dual-luciferase<sup>TM</sup> reporter assay: an advanced co-reporter technology integrating firefly and renilla luciferase assays. *Promega Notes Magazine* 57, 2.
- (127) Merrifield, R. B. (1963) Solid phase peptide synthesis. I. The synthesis of a tetrapeptide. *J. Am. Chem. Soc.* 85, 2149-2154.
- (128) Carpino, L. A., and Han, G. Y. (1970) 9-Fluorenylmethoxycarbonyl function, a new base-sensitive amino-protecting group. *J. Am. Chem. Soc.* 92, 5748-5749.
- (129) Carpino, L. A., and Han, G. Y. (1972) The 9-fluorenylmethoxycarbonyl amino-protecting group. *J. Org. Chem.* 37, 3404-3409.

---

## CHAPTER 3      Synthesis of Fluorescently Labelled Peptidic Ligands Targeting Neuropeptide Y Y<sub>1</sub> Receptors Based on the Y<sub>1</sub>R Antagonist / Y<sub>4</sub>R Agonist BVD-15 Scaffold

---

### Table of Contents

3.1	General Introduction to Neuropeptide Y and Y receptors .....	3-2
3.2	Physiological Functions and Clinical Relevance of Y <sub>1</sub> Receptors .....	3-5
3.2.1	Y <sub>1</sub> Receptors in Feeding Regulation .....	3-5
3.2.2	Y <sub>1</sub> Receptors in Ethanol Consumption .....	3-5
3.2.3	Y <sub>1</sub> Receptors in Neurological Functions .....	3-6
3.2.4	Y <sub>1</sub> Receptors in Vasoconstriction .....	3-7
3.2.5	Y <sub>1</sub> Receptors in Cancers .....	3-7
3.3	Synthesis of Y <sub>1</sub> R-Targeting Fluorescent Ligands.....	3-8
3.4	Objectives.....	3-9
3.5	Results and Discussion .....	3-9
3.5.1	BVD-15 Analogues Fluorescently Labelled at the 3-Position.....	3-9
3.5.2	Identification of a Cyanine-Dye Labeled Peptidic Ligand for Y <sub>1</sub> R and Y <sub>4</sub> R, Based upon the Neuropeptide Y C-terminal Analogue, BVD-15 .....	3-14
3.6	Summary .....	3-25
	References.....	3-27

### 3.1 General Introduction to Neuropeptide Y and Y receptors

Neuropeptide Y (NPY) was first isolated by Tatemoto's group from porcine brain in 1982. It is a 36-amino acid C-terminal amidated polypeptide, expressed abundantly in both central and peripheral nervous systems.(1, 2) NPY shares 70% and 50% amino acid sequence homology with peptide YY (PYY)(3) and pancreatic polypeptide (PP)(4) respectively, and these three peptides collectively form the NPY peptide family (**Table 3-1**).(2, 5, 6) NPY also shows a high degree of sequence conservation across species.(7) The physiological functions of NPY are mediated by Y receptors. At least seven subtypes have been identified: Y<sub>1</sub>R, Y<sub>2</sub>R, Y<sub>4</sub>R, Y<sub>5</sub>R, y<sub>6</sub>R, Y<sub>7</sub>R and Y<sub>8</sub>R, where y<sub>6</sub>R is a pseudogene identified only in mice and rabbits, Y<sub>7</sub>R is found in fish and chicken, and Y<sub>8</sub>R has been discovered in teleost tetraploidisation as a receptor gene.(8-10) These subtypes all belong to the rhodopsin-like G<sub>i</sub> coupled GPCR family. Since functional y<sub>6</sub>R, Y<sub>7</sub>R and Y<sub>8</sub>R are not present in mammal, physiological and pathophysiological studies have predominantly focused on the Y<sub>1</sub>R, Y<sub>2</sub>R, Y<sub>4</sub>R and Y<sub>5</sub>R subtypes. Their general distribution in human physiological system is briefly summarised in **Table 3-2**.(8, 11-14)

**Table 3-1:** Amino acid sequences of human neuropeptide Y, peptide YY and pancreatic polypeptide. All three are 36-amino acid, C-terminal amidated polypeptides.

Peptide Name	Sequence
Neuropeptide Y	Y <sup>1</sup> PSKPDNPGE <sup>10</sup> DAPAEDMARY <sup>20</sup> YSALRHYINL <sup>30</sup> ITRQRY <sup>36</sup> -NH <sub>2</sub>
Peptide YY	Y <sup>1</sup> PIKPEAPGE <sup>10</sup> DASPEELNRY <sup>20</sup> YASLRHYLNL <sup>30</sup> VTRQRY <sup>36</sup> -NH <sub>2</sub>
Pancreatic polypeptide	A <sup>1</sup> PLEPVYPGD <sup>10</sup> NATPEQMAQY <sup>20</sup> AADLRRYINM <sup>30</sup> LTRPRY <sup>36</sup> -NH <sub>2</sub>

**Table 3-2:** General distribution of Y receptor subtypes in human physiological system.

Y receptor subtype	Examples of locations
Y <sub>1</sub> R	Cerebral cortex, amygdala, thalamus, blood vessels
Y <sub>2</sub> R	Hippocampus, breast tissue, nerve endings
Y <sub>4</sub> R	Heart, intestine, prostate, lung, testis
Y <sub>5</sub> R	Paraventricular nucleus, hypothalamus

NPY, PYY and PP all exhibit cross-reactivity at the four mammal Y receptor subtypes. It was found that Y<sub>1</sub>R and Y<sub>2</sub>R display similar affinity to NPY and PYY, but lower affinity to PP; Y<sub>4</sub>R preferentially binds to PP while showing lower affinity to NPY and PYY, and all three peptides bind to Y<sub>5</sub>R with similar affinity.(15, 16) To prepare fluorescently labelled peptides that specifically target the desired Y receptor subtype(s), high-affinity selective analogues derived from the endogenous peptides were sought and are summarised in **Table 3-3**. These peptides all contain amino acid substitutions and sequence truncation – proven useful strategies in optimising peptides for desired pharmacological profiles (as summarised in **Chapter 1**). In regards to Y<sub>1</sub>R, Leu<sup>31</sup> and Pro<sup>34</sup> substitutions in human NPY and PYY introduced Y<sub>1</sub>R selectivity with little influence on affinity. The first small truncated Y<sub>1</sub>R agonist [Pro<sup>30</sup>, Nle<sup>31</sup>, Bpa<sup>32</sup>, Leu<sup>34</sup>]hNPY<sub>28–36</sub> suggested the importance of NPY C-terminal amino acids in maintaining Y<sub>1</sub>R affinity. The small-molecule antagonists BIBP3226 and BIBO3304 (**Figure 3-1**), derived from NPY C-terminal sequence, also displayed satisfactory Y<sub>1</sub>R pharmacological profiles and were utilised in preparing pyridinium- and cyanine-labelled fluorescent analogues.(17-21)

Our laboratory has a continuous interest in developing fluorescently labelled Y<sub>1</sub>R ligands for imaging studies. Here we took particular note of two peptidic Y<sub>1</sub>R antagonists, which have been amended in our project as the parent compounds for fluorescence labelling. The first was the BVD-15 (or BW1911U90) scaffold, a 9-amino acid C-terminal amidated polypeptide systematically modified from the NPY C-terminal fragment NPY<sub>28–36</sub>. Its amino

acid sequence is Ile-Asn-Pro-Ile-Tyr-Arg-Leu-Arg-Tyr-NH<sub>2</sub>.<sup>(22)</sup> This peptide exhibited moderate competitive Y<sub>1</sub>R antagonism and Y<sub>4</sub>R agonism with similar potency.<sup>(22-24)</sup> The second was the homodimeric Y<sub>1</sub>R antagonist 1229U91 (or GR231118) scaffold, comprised of two units of [Glu<sup>2</sup>, Dap<sup>4</sup>]BVD-15 cross-linked by (2,4') and (2',4) lactam bridges (**Figure 3-2**).<sup>1(25)</sup> Comparing to BVD-15, 1229U91 exhibited more potent Y<sub>1</sub>R competitive antagonism and Y<sub>4</sub>R agonism.<sup>(24-27)</sup>

**Table 3-3:** Representative Y receptor-targeting peptidic ligands with selectivity.

Y receptor peptidic ligands	Targeting receptor(s)	Reference
[Phe <sup>7</sup> , Pro <sup>34</sup> ]pNPY	Y <sub>1</sub> R selective agonist	(28)
[Leu <sup>31</sup> , Pro <sup>34</sup> ]hNPY	Y <sub>1</sub> R selective agonist	(29)
[Leu <sup>31</sup> , Pro <sup>34</sup> ]hPYY	Y <sub>1</sub> R selective agonist	(30)
[Pro <sup>30</sup> , Nle <sup>31</sup> , Bpa <sup>32</sup> , Leu <sup>34</sup> ]hNPY <sub>28-36</sub>	Y <sub>1</sub> R selective agonist	(31)
BVD-15 (or BW1911U90)	Y <sub>1</sub> R antagonist, Y <sub>4</sub> R agonist	(22)
1229U91 (or GR231118)	Y <sub>1</sub> R antagonist, Y <sub>4</sub> R agonist	(25)
hNPY <sub>13-36</sub>	Y <sub>2</sub> R selective agonist	(32)
hPYY <sub>3-36</sub>	Y <sub>2</sub> R selective agonist	(33)
[Gln <sup>34</sup> ]hPP (or TM30338)	Y <sub>2</sub> R and Y <sub>4</sub> R agonist	(34)
BVD-74D	Y <sub>4</sub> R selective agonist	(35)
VD-11	Y <sub>4</sub> R selective antagonist	(36)
[Ala <sup>31</sup> , Aib <sup>32</sup> ]pNPY	Y <sub>5</sub> R selective agonist	(37)
[cPP <sub>1-7</sub> , NPY <sub>19-23</sub> , Ala <sup>31</sup> , Aib <sup>32</sup> , Gln <sup>34</sup> ]hPP	Y <sub>5</sub> R agonist with Y <sub>1</sub> R affinity	(38, 39)

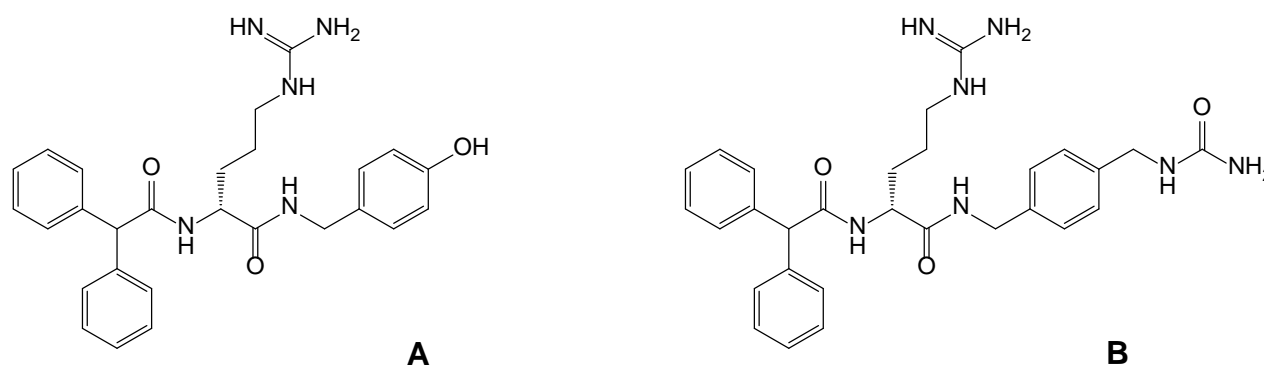


**Figure 3-1:** Structures of **A**: BIBP3226 and **B**: BIBO3304.

<sup>1</sup> Dap represents diaminopropionic acid. It is also abbreviated Dpr in some literature.



expression was observed in ethanol withdrawal.(46) Further, centrally administered NPY caused reduction in ethanol consumption in rats predisposed to ethanol but elicited no effect in control subjects.(47, 48) By using receptor knockout mice, it has been found that central Y<sub>1</sub>R activation stimulated ethanol intake, while Y<sub>2</sub>R activation counteracted this effect.(49, 50) These results imply that compounds targeting central Y<sub>1</sub>R and/or Y<sub>2</sub>R may have potential in controlling severe alcoholism in addition to psychological therapies.

### **3.2.3 Y<sub>1</sub> Receptors in Neurological Functions**

Activation of Y<sub>1</sub>R in the central nucleus of the amygdala elicited an anxiolytic response that was dissociated with Y<sub>1</sub>R-induced food intake.(51, 52) Therefore, Y<sub>1</sub>R neurons responsible for these functions may be located in different CNS regions. Desai *et al.* showed that anxiety and depression induced by cholecystokinin-4 were attenuated by pre-treatment with NPY or the Y<sub>1</sub>R selective agonist [Leu<sup>31</sup>, Pro<sup>34</sup>]NPY.(53) Another study showed anxiety-like behaviour in rats when Y<sub>1</sub>R expression was reduced by antisense oligodeoxynucleotides.(54) Moreover, exogenously administered NPY and Y<sub>1</sub>R agonists stimulated neurogenesis and neuron differentiation in the hippocampus, the central brain region responsible for learning, memory and general cognition. This raised the probability that Y<sub>1</sub>R agonists may serve as neuroprotective agents for cognitive impairments such as schizophrenia, and neurodegenerative conditions such as Alzheimer's disease.(55-57) Finally, some studies have collectively shown that Y<sub>1</sub>R's in the dentate gyrus of hippocampus stimulated seizures, while those in extrahippocampal regions exerted an inhibitory effect. However, these findings required further investigations as involvement of Y<sub>2</sub>R and Y<sub>5</sub>R could not be ruled out.(58)



### 3.2.4 Y<sub>1</sub> Receptors in Vasoconstriction

Y<sub>1</sub>R mediates vasoconstriction by directly contracting vascular smooth muscles and indirectly potentiating noradrenergic nervous activity mediated via  $\alpha_1$ -adrenoceptors.(11, 59, 60) Consistently, these effects were absent in Y<sub>1</sub>R knockout mice.(61) Y<sub>1</sub>R-mediated vasoconstriction is manifested both centrally and peripherally. For example, NPY and the Y<sub>1</sub>R agonist [Pro<sup>34</sup>]NPY were found to potently contract human cerebral arteries *in vitro*.(59) Moreover, NPY counteracted arterial vasodilation and loss of vascular contractility in portal hypertension, and these effects were diminished by co-administering the Y<sub>1</sub>R antagonist BIBP3226.(62) In pulmonary hypertension, increased NPY-ergic innervation and consequent Y<sub>1</sub>R up-regulation at pulmonary arteries were observed. The resultant hypersensitivity to NPY stimulation may further cause pulmonary artery remodelling that lead to vascular blockage.(63)

### 3.2.5 Y<sub>1</sub> Receptors in Cancers

Tumours that over-express certain receptors can enlarge and metastasise when stimulated by the corresponding neurotransmitters or neurohormones. For instance, Y<sub>1</sub>R activation promotes proliferation of prostate cancer cells.(64) Reubi *et al.* showed that 85% of cases for primary breast carcinomas and 100% of cases for lymph node metastases predominantly over-expressed Y<sub>1</sub>R, whereas the Y<sub>2</sub>R subtype was preferentially expressed in normal breast tissues.(13, 65) Additionally, a dose-dependent inhibition of cancerous cell growth induced by NPY was also observed.(13) Although not fully understood, Y<sub>1</sub>R are speculated to elicit tumour proliferation, apoptosis, metastasis and angiogenesis.(66)

### 3.3 Synthesis of Y<sub>1</sub>R-Targeting Fluorescent Ligands

With Y<sub>1</sub>R identified as a valuable target of potential pharmaceuticals, some corresponding fluorescently labelled peptides have been reported (summarised in **Table 1-2 of Chapter 1**). These ligands are generally derived from full-length endogenous peptide ligands, which may suffer from metabolic instability and low selectivity to the Y receptor subtype(s) of interest. As a different approach, our project utilised the truncated NPY C-terminal fragment BVD-15 as the starting compound. To amend the BVD-15 peptide to conjugation, Guérin *et al.* introduced a  $\epsilon$ -amine at the 4-position resulting in [Lys<sup>4</sup>]BVD-15 with enhanced Y<sub>1</sub>R affinity.<sup>(67)</sup> This analogue could incorporate bifunctional chelators DOTA<sup>2</sup> and NOTA<sup>3</sup> to produce models of radiolabelled peptidic ligands.<sup>(67, 68)</sup> Based on their findings, we demonstrated that the 4-position could also tolerate other basic residues. As a representative example, it was shown that the residue at the 4-position could be changed to Arg,<sup>(69)</sup> which in turn allowed substitution at the 2-position with new conjugates such as Lys(NOTA).<sup>(70)</sup> Additionally, Zwanziger's group and we both showed that modification at the 5-position was tolerated with 4-substituted phenylalanine derivatives.<sup>(31, 70)</sup>

As a different approach, we have also previously utilised 1229U91 as a starting compound, where robust synthesis strategies towards its structural and fluorescent analogues have been demonstrated (published in Organic and Biomolecular Chemistry, full paper available in Appendix).<sup>(71)</sup> These results have provided us with useful insight for our further projects, especially in orthogonal protections and mono-labelling of dimeric peptide analogues.

---

<sup>2</sup> DOTA: 1,4,7,10-tetraazacyclododecane-1,4,7,10-tetraacetic acid

<sup>3</sup> NOTA: 1,4,7-triazacyclononane-1,4,7-triacetic acid

### 3.4 Objectives

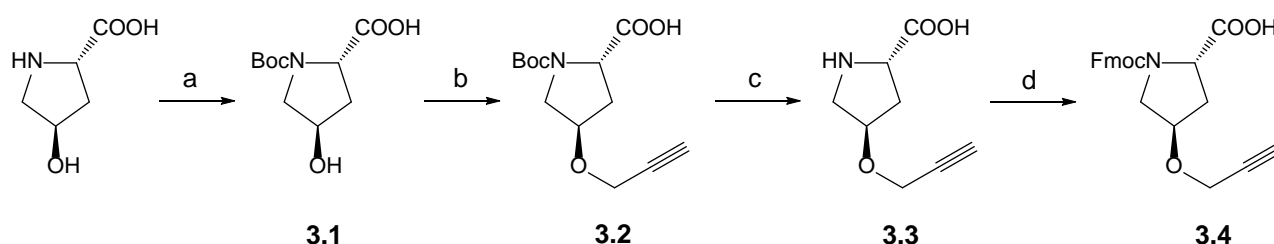
The physiological and pathophysiological involvements of Y<sub>1</sub>R remain far from being conclusive. A typical example is that feeding behaviour and the associated obesity appear to be regulated by multiple subtypes in highly complicated cooperating or counteracting mechanisms. Therefore, high-affinity, specific traceable peptidic ligands are preferential in this regard. Building on previous valuable structure-activity relationships, our present work has explored the 2-, 3- and 4-positions as potential sites of conjugation in preparing fluorescently labelled BVD-15 analogues for *in vitro* studies of Y<sub>1</sub>R. Significantly, we have identified a peptide conjugate with high affinity at Y<sub>1</sub>R and moderate affinity at Y<sub>4</sub>R, which was found useful in performing fluorescent imaging studies of these two subtypes in intact living cells.

### 3.5 Results and Discussion

#### 3.5.1 BVD-15 Analogues Fluorescently Labelled at the 3-Position

This section describes the preparation of BVD-15 analogues containing Pro derivatives at the 3-position. The underpinning rationale for development of Pro derivatives is that Pro has inherent conformational restriction and that by derivatising through the ring we might preserve the bioactive peptide conformation, something that is less likely with the less restricted  $\alpha$ -amino acids. In order to do this our group had developed a series of propargyloxyproline (Pop) derivatives with different stereo- and regio-configurations and the synthesis strategies of these were described in our publication in Australian Journal of Chemistry (full paper available in Appendix).(72) The PhD candidate has contributed to these by synthesising the Fmoc-protected *trans*-4-L-propargyloxyproline (Fmoc-*trans*-4-L-Pop-OH, **Scheme 3-1**). The starting compound unprotected 4-hydroxy-L-proline was treated with Boc anhydride (Boc<sub>2</sub>O) in the presence of triethylamine (Et<sub>3</sub>N) to afford N<sup>α</sup>-

Boc protection (**3.1**) in 92% crude yield. **3.1** was then treated with propargyl bromide in a strong anhydrous alkaline condition (with NaH) under nitrogen to generate Boc-4-L-propargyloxyproline (**3.2**, 91% crude yield). To achieve Fmoc protection, the Boc group was removed by TFA to obtain the intermediate **3.3**, which was then treated with Fmoc-succinimide (Fmoc-OSu) in a mild alkaline condition (with Na<sub>2</sub>CO<sub>3</sub>) to afford the desired product **3.4** in 30% yield after column chromatography.



**Scheme 3-1:** Synthesis of Fmoc-*trans*-4-L-Pop-OH. Reagents and conditions: **a.** Boc<sub>2</sub>O, Et<sub>3</sub>N in MeOH, reflux 3.5 h then RT overnight; **b.** propargyl bromide (80% w/v in toluene), NaH (60% in mineral oil) in anhydrous DMF under N<sub>2</sub>, 0°C, 2 h; **c.** TFA (50%) in DCM, 45 min; **d.** Fmoc-OSu, Na<sub>2</sub>CO<sub>3</sub> in dioxane, 0°C for 1 h then RT overnight.

The resulting Fmoc-*trans*-4-L-Pop-OH was then incorporated in the synthesis of peptide analogues **3A-3C**, where the analytical data are summarised in **Table 3-4**. The linear parent peptide IN-*trans*-4-L-Pop-RYRLRY-NH<sub>2</sub> (**3A**) was prepared by standard Fmoc-based SPPS on Rink amide resin as described in the previous chapter. The synthesis proceeded straightforward, where the product was obtained in relatively good yield and high purity after HPLC (**Figure 3-3**). The fluorescent analogue **3B** was obtained from **3A** using a CuAAC reaction, making use of the readily available azide-functionalised coumarin derivative (**Figure 3-4**). Notably, the CuAAC condition was modified from that reported in **Chapter 2**, where the reaction was performed in a DMF-H<sub>2</sub>O mixture (75%:25%) in the absence of THPTA and aminoguanidine. As illustrated by the HPLC chromatograph, this simplified condition also resulted in efficient fluorophore conjugation with the desired product well separated from the excess coumarin and other impurities (**Figure 3-3**). Conjugation of analogue **3A** with two RhB derivatives was completed by our other group

members and the resulting fluorescent variants were reported as **16** and **17** in our publication.(72)

**Table 3-4:** BVD-15 analogues fluorescently labelled at the 3-position and their analytical data.

Code	Sequence <sup>a</sup>	HPLC RT (min) <sup>b</sup>	MW (Calc)	m/z (found)	Purity (%)
<b>3A</b>	IN- <i>trans</i> -4-L-Pop-RYRLRY-NH <sub>2</sub>	11.03	1303.5	652.7 <sup>c</sup>	94
<b>3B</b>	IN- <i>trans</i> -4-L-Ctp-RYRLRY-NH <sub>2</sub>	11.48	1519.7	507.8 <sup>d</sup>	98
<b>3C</b>	I-cyc[E- <i>trans</i> -4-L-Pop-Dap]-YRLRY-NH <sub>2</sub>	11.72	1230.4	616.3 <sup>c</sup>	- <sup>e</sup>

<sup>a</sup> Ctp = coumarin-triazole-proline.

<sup>b</sup> HPLC retention time using a Phenomenex Luna C-8 column (100Å, 3µm, 100×2.00mm).

The gradient is composed of 100% H<sub>2</sub>O (0.1% TFA) for 4min, 0-60% acetonitrile in H<sub>2</sub>O (0.1% TFA) over 10min and isocratic 60% acetonitrile in H<sub>2</sub>O (0.1% TFA) for 1min.

<sup>c</sup> ESI-MS base peak corresponds to [M+2H]<sup>2+</sup>.

<sup>d</sup> ESI-MS base peak corresponds to [M+3H]<sup>3+</sup>.

<sup>e</sup> Crude **3C** was directly used in fluorophore conjugation without purification.

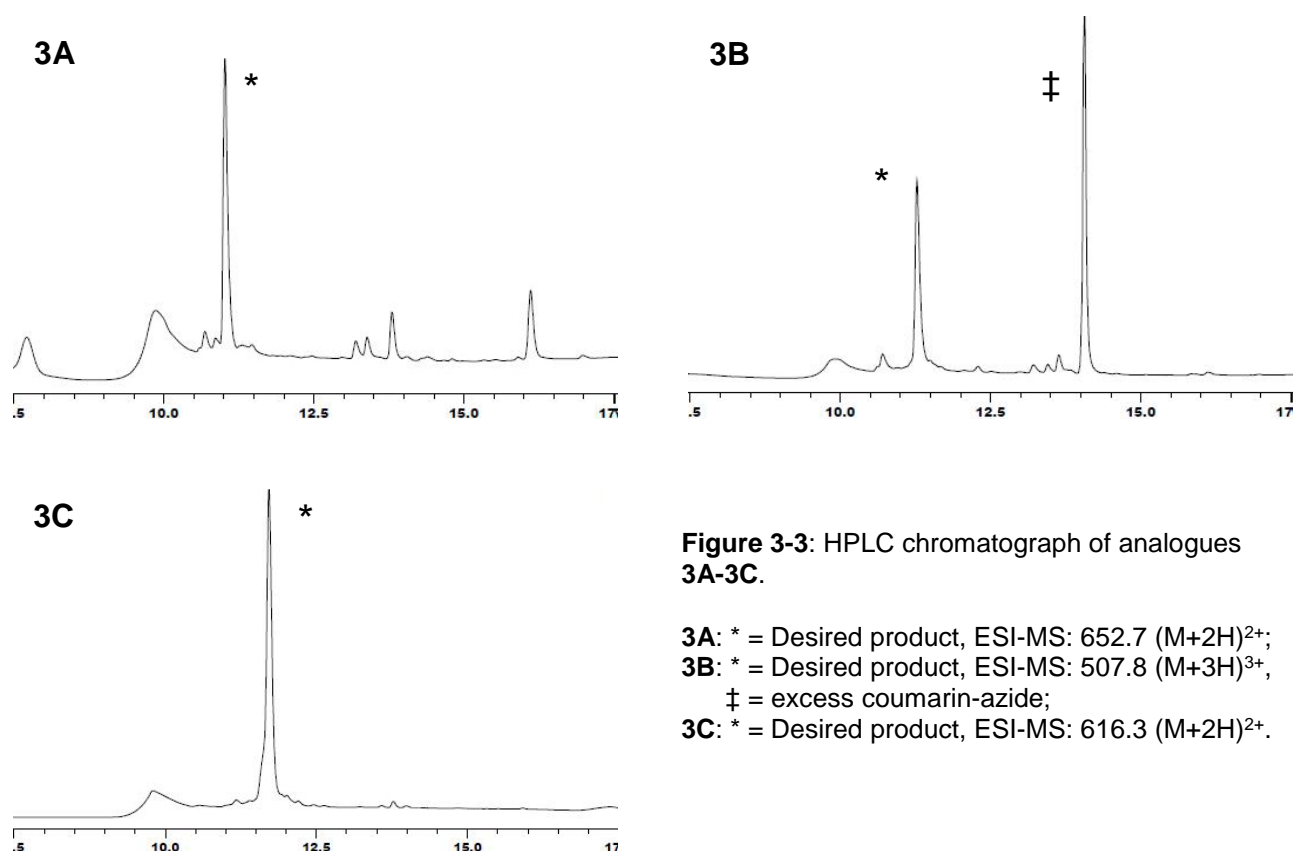


**Figure 3-3:** HPLC chromatograph of analogues **3A-3C**.

**3A:** \* = Desired product, ESI-MS: 652.7 (M+2H)<sup>2+</sup>;

**3B:** \* = Desired product, ESI-MS: 507.8 (M+3H)<sup>3+</sup>,

† = excess coumarin-azide;

**3C:** \* = Desired product, ESI-MS: 616.3 (M+2H)<sup>2+</sup>.

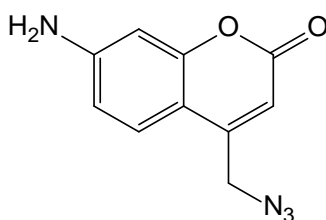
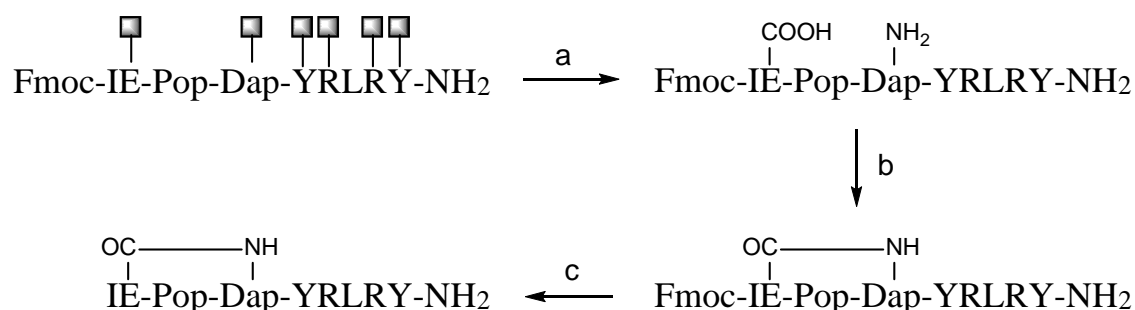


**Figure 3-4:** Structure of the coumarin-azide derivative used in this project.

The cyclic analogue **3C**, which can be considered a derivative of the cyclic monomeric form of 1229U91, was also prepared (**Scheme 3-2**). The linear precursor peptide was first assembled and cleaved off resin following the standard procedures, where the N-terminal Fmoc group was left intact. Subsequently, cyclisation was achieved in solution by treating with PyClock in the presence of NMM. Importantly, the reaction mixture was diluted to a concentration of 1.0 mg peptide per ml considering that intermolecular dimerisation might occur at higher concentration. The N-terminal Fmoc group was then deprotected in solution using 20% piperidine, and the crude product was readily recovered by adding minimal TFA then precipitating with excess Et<sub>2</sub>O. As illustrated by HPLC, the cyclisation reaction proceeded to completion without any observable trace of linear precursor, and the crude product was sufficiently pure for utility in direct fluorophore conjugation performed by our other group members.



**Scheme 3-2:** Synthesis of the cyclic monomer **3C**. Reagents and conditions: **a.** TFA, TIPS, DMB, 3 h; **b.** PyClock, NMM in DMF, overnight; **c.** piperidine (20%) in DMF, 1 h.

Analogues **3A**, **3B** and **3C** were assessed for their Y<sub>1</sub>R affinity by our collaborator Herbert Herzog's group at the Garvan Institute of Medical Research, Sydney. This assay system adopted the previously reported procedures which involved competition binding against <sup>125</sup>I-labelled human PYY ([<sup>125</sup>I]hPYY) in brain membrane preparations from Y<sub>2</sub>Y<sub>4</sub> knockout mice.<sup>(73)</sup> The RhB-conjugated analogues **16** and **17** were assayed for Y<sub>1</sub>R affinity by our collaborator Nicholas Holliday's group at the University of Nottingham, UK, using competition binding against [<sup>125</sup>I]hPYY on membranes expressing recombinant GFP-tagged Y<sub>1</sub>R.<sup>(74, 75)</sup> In both assays, compound INPKYRLRY-NH<sub>2</sub> was included as a reference. Their pharmacological data (**Table 3-5**) have contributed to our publication in Australian Journal of Chemistry (full paper available in Appendix).<sup>(72)</sup> In the following discussion, other relevant analogues have been taken from the paper for convenient comparison.

With respect to all 3-position fluorescently labelled analogues reported in our publication, most displayed comparable Y<sub>1</sub>R affinity to the parent compounds in nanomolar range (**Table 3-5**). Comparing with the reference analogues [Lys<sup>4</sup>]BVD-15 (**1**) and [Arg<sup>4</sup>]BVD-15 (**2**), the coumarin-containing analogues **3B** (**11**) and **14** both retained strong Y<sub>1</sub>R affinity with IC<sub>50</sub> of 6.0 nM and 1.9 nM respectively. Analogues **16** and **17** contained two different RhB derivatives, where **16** was without the piperazine ring spacer. Both displayed consistent results where the affinity (10 nM and 18 nM respectively) was in comparable range with that of the reference compound [Lys<sup>4</sup>]BVD-15 (**1**).

**Table 3-5:** BVD-15 analogues fluorescently labelled at the 3-position and their pharmacological data.

Code	Code in publication	Sequence <sup>a</sup>	IC <sub>50</sub> (nM) Y <sub>2</sub> Y <sub>4</sub> KO
(Reference)	1	INPKYRLRY-NH <sub>2</sub>	0.9
(Reference)	2	INPRYRLRY-NH <sub>2</sub>	1.3
3A	5	IN- <i>trans</i> -4-L-Pop-RYRLRY-NH <sub>2</sub>	-
3C	8	l-cyc[E- <i>trans</i> -4-L-Pop-Dap]-YRLRY-NH <sub>2</sub>	-
3B	11	IN- <i>trans</i> -4-L-Ctp-RYRLRY-NH <sub>2</sub>	6.0
	14	l-cyc[E- <i>trans</i> -4-L-Ctp-Dap]-YRLRY-NH <sub>2</sub>	1.9
			IC <sub>50</sub> (nM) Y <sub>1</sub> -HEK293
	1	INPKYRLRY-NH <sub>2</sub>	7.9
	16	IN- <i>trans</i> -4-L-R <sup>1</sup> tp-RYRLRY-NH <sub>2</sub>	10
	17	IN- <i>trans</i> -4-L-R <sup>2</sup> tp-RYRLRY-NH <sub>2</sub>	18

<sup>a</sup> R<sup>1</sup>tp and R<sup>2</sup>tp represent rhodamine B-conjugated Pop, where the structures can be found in our publication.

Collectively, our data suggested that the active 3D conformation maintained by the turn-inducing residue Pro was not markedly influenced by neither conjugating groups nor a cyclised peptide chain and so substitution at the 3-position with a proline derivative is supported. However, the range of fluorophores accessible through click chemistry is somewhat limited by reagents and expense. We therefore extended our focus to the 2- and 4-positions using rhodamine B and cyanine derivatives as fluorophores.

### 3.5.2 Identification of a Cyanine-Dye Labeled Peptidic Ligand for Y<sub>1</sub>R and Y<sub>4</sub>R, Based upon the Neuropeptide Y C-terminal Analogue, BVD-15

The complete work on synthesising BVD-15 analogues fluorescently labelled at the 2- and 4-positions has been published in Bioconjugate Chemistry (full paper attached below).



# Identification of a Cyanine-Dye Labeled Peptidic Ligand for Y<sub>1</sub>R and Y<sub>4</sub>R, Based upon the Neuropeptide Y C-Terminal Analogue, BVD-15

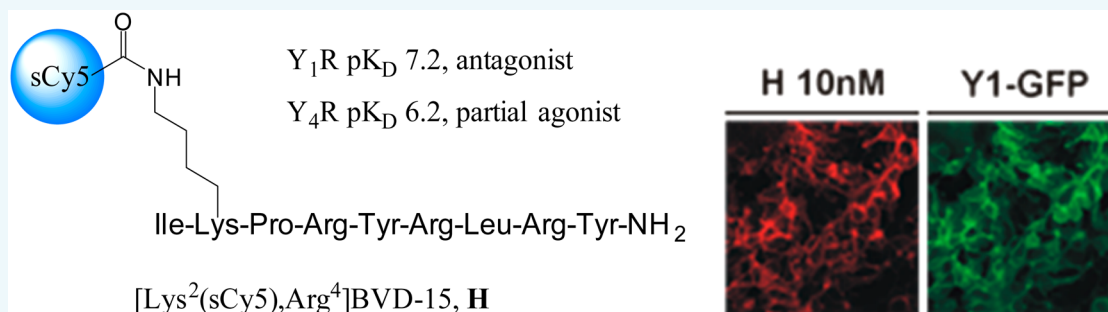
Mengjie Liu,<sup>†</sup> Rachel R. Richardson,<sup>§</sup> Simon J. Mountford,<sup>†</sup> Lei Zhang,<sup>‡</sup> Matheus H. Tempone,<sup>§</sup> Herbert Herzog,<sup>‡</sup> Nicholas D. Holliday,<sup>\*,§</sup> and Philip E. Thompson<sup>\*,†</sup>

<sup>†</sup>Medicinal Chemistry, Monash Institute of Pharmaceutical Sciences, Monash University, 381 Royal Parade, Parkville, VIC 3052, Australia

<sup>‡</sup>Neuroscience Division, Garvan Institute of Medical Research, St. Vincent's Hospital, Darlinghurst, NSW 2010, Australia

<sup>§</sup>Cell Signalling Research Group, School of Life Sciences, University of Nottingham, Queen's Medical Centre, Nottingham, NG7 2UH, United Kingdom

## S Supporting Information



**ABSTRACT:** Traceable truncated Neuropeptide Y (NPY) analogues with Y<sub>1</sub> receptor (Y<sub>1</sub>R) affinity and selectivity are highly desirable tools in studying receptor location, regulation, and biological functions. A range of fluorescently labeled analogues of a reported Y<sub>1</sub>R/Y<sub>4</sub>R preferring ligand BVD-15 have been prepared and evaluated using high content imaging techniques. One peptide, [Lys<sup>2</sup>(sCy5), Arg<sup>4</sup>]BVD-15, was characterized as an Y<sub>1</sub>R antagonist with a pK<sub>D</sub> of 7.2 measured by saturation analysis using fluorescent imaging. The peptide showed 8-fold lower affinity for Y<sub>4</sub>R (pK<sub>D</sub> = 6.2) and was a partial agonist at this receptor. The suitability of [Lys<sup>2</sup>(sCy5), Arg<sup>4</sup>]BVD-15 for Y<sub>1</sub>R and Y<sub>4</sub>R competition binding experiments was also demonstrated in intact cells. The nature of the label was shown to be critical with replacement of sCy5 by the more hydrophobic Cy5.5 resulting in a switch from Y<sub>1</sub>R antagonist to Y<sub>1</sub>R partial agonist.

## INTRODUCTION

Neuropeptide Y (NPY) is a 36-amino-acid, C-terminal amidated polypeptide first isolated from porcine brain by Tatemoto's group in 1982.<sup>1</sup> It is a member of the NPY peptide family along with pancreatic polypeptide (PP, isolated in 1983)<sup>2</sup> and peptide YY (PYY, isolated in 1980),<sup>3</sup> which both share a high degree of homology in amino acid sequence. The physiological functions of NPY are mediated by Y receptors, belonging to the rhodopsin-like G<sub>i</sub> coupled G protein-coupled receptor (GPCR) family and four subtypes, Y<sub>1</sub>R, Y<sub>2</sub>R, Y<sub>4</sub>R, and Y<sub>5</sub>R have been identified in humans.<sup>4–6</sup> Y<sub>1</sub>R is expressed abundantly in both central and peripheral sympathetic nervous systems, and the NPY/Y<sub>1</sub>R signaling cascade is implicated in various physiological responses, including regulation of feeding behavior,<sup>7,8</sup> stimulation of ethanol intake,<sup>9,10</sup> vasoconstriction,<sup>11,12</sup> and initiation of anxiety and depression.<sup>13,14</sup> In addition, breast carcinomas, including primary tumors and lymph node metastases, have also been found to overexpress Y<sub>1</sub>R.<sup>15</sup> This suggests that Y<sub>1</sub>R may be responsible in tumor proliferation, apoptosis, metastasis and angiogenesis.<sup>16</sup>

With Y<sub>1</sub>R being a potential drug target, traceable high affinity Y<sub>1</sub>R ligands are highly desirable tools for studying the localization, regulation, and functions of this receptor. Lys<sup>4</sup>(sCy5)-NPY was shown to be an agonist of Y<sub>1</sub>R, Y<sub>2</sub>R, and Y<sub>4</sub>R receptors, and of utility in the development of FACS-based functional assays of complex cell-based assay systems.<sup>17</sup> Another approach has been to derive fluorescent or radio-labeled analogues of the Y<sub>1</sub>R arginamide antagonist series (BIBP3226, BIBO3304),<sup>18</sup> including pyridinium and cyanine based BIBP3226 derivatives suitable for fluorescent imaging.<sup>19,20</sup> An alternative starting point has made use of smaller NPY derived peptide ligands, such as the competitive Y<sub>1</sub>R antagonist/Y<sub>4</sub>R agonist BVD-15 (or BW1911U90), a non-peptide modified from the NPY C-terminal fragment (Figure 1).<sup>21</sup> This peptide has been amenable to conjugation with a variety of radiolabels and fluorophores. In particular, Guérin et

Received: July 12, 2016

Revised: August 8, 2016

Published: August 11, 2016



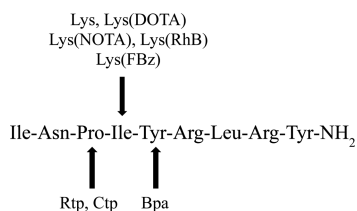


**Figure 1.** Amino acid sequence of BVD-15 scaffold and reported conjugated amino acid replacements. FBz = 4-fluorobenzoyl, Rtp = rhodamine B-triazolyl-proline, Ctp = coumarin-triazolyl-proline, Bpa = 4-benzoylphenylalanine.

al. showed that the Ile<sup>4</sup> residue could be substituted by conjugated Lys to incorporate DOTA, NOTA or fluorine moieties,<sup>22,23</sup> and we extended this result to include a rhodamine fluorophore.<sup>24</sup> No less notably, the Lys<sup>4</sup> substitution itself resulted in increased affinity,<sup>23</sup> and other basic residues were also well tolerated.<sup>24</sup> This prompted us to examine such analogues with Pro<sup>3</sup> as a point of conjugation and we have recently described propargyloxypyrrolidine containing Lys<sup>4</sup>- and Arg<sup>4</sup>-BVD-15 that could incorporate rhodamine B and 7-aminocoumarin fluorophores.<sup>25</sup> The tyrosine at the 5-position has been also shown to be capable of replacement with a conjugate group.<sup>26</sup>

Noting that the position and nature of the conjugated group and its linkage could have a significant influence on the pharmacology of the resulting peptide, here we have examined the 2- and 4-position as the points of conjugation, and identified a number of potent novel fluorescently labeled Y<sub>1</sub>R-targeting peptidic ligands. We have explored the utility of one of these and found it to be an excellent reagent for performing fluorescent imaging of recombinant cells transfected with Y<sub>1</sub>R or Y<sub>4</sub>R, allowing the development of receptor binding studies in intact living cells.

## RESULTS AND DISCUSSION

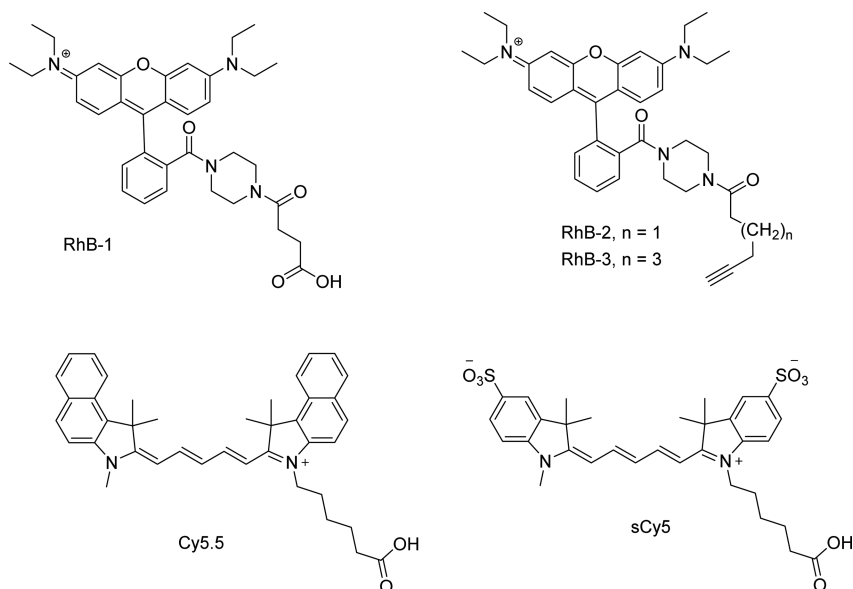
**Chemistry.** We began by expanding our pool of conjugate precursors to include a variety of rhodamine B (RhB) conjugates (Figure 2), taking advantage of the capacity to

generate different linkers from a common, inexpensive precursor,<sup>27</sup> as well as two cyanine dyes (Figure 2) Cy5.5 and sulfo-Cy5 (sCy5). We extended the types of conjugates included at Lys<sup>4</sup>, but also encompassed substitutions at Asn<sup>2</sup>. While a lysine residue at the 2-position had been shown to be detrimental to Y<sub>1</sub>R activity,<sup>23</sup> the influence of subsequent conjugation had not been tested.

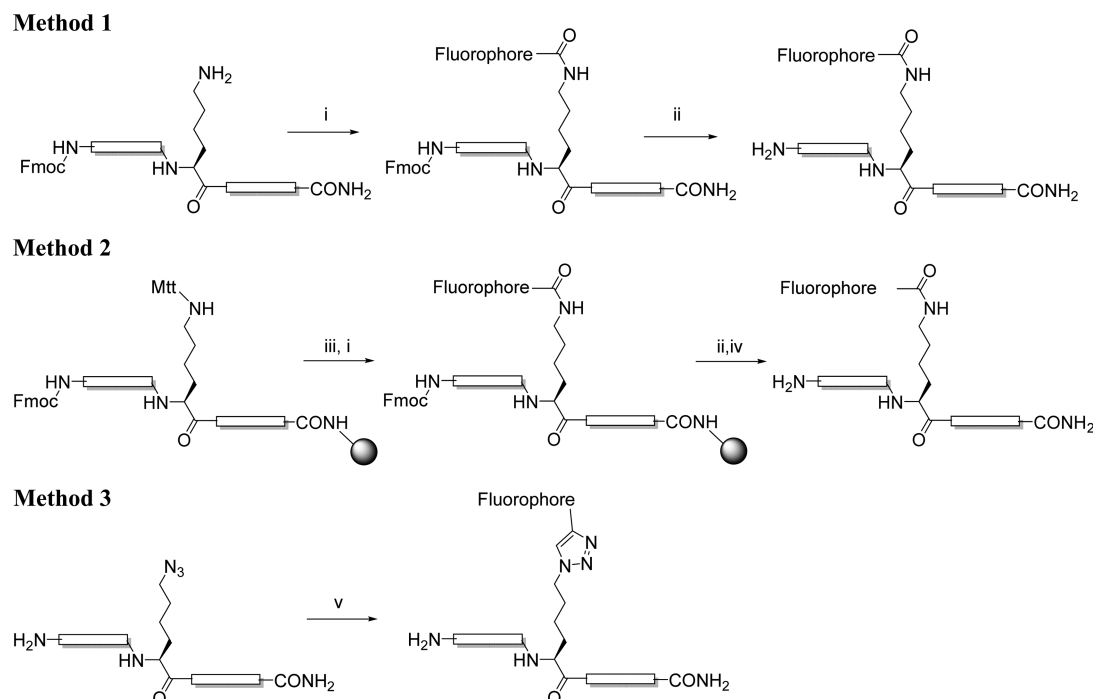
The synthesis of the conjugated BVD-15 analogues was achieved by one of three distinct methods. While all peptide backbones were prepared by adapting standard Fmoc-based solid phase peptide synthesis (SPPS) strategies, both solid and solution phase side-chain labeling were attempted. To facilitate chemoselective derivatization at the 2-position, the 4-position was substituted by an Arg residue, which retains high affinity for Y<sub>1</sub>R receptors.<sup>25</sup>

In the first instance, linear peptides were synthesized with N-terminal Fmoc protection and amide coupling in solution was achieved using carboxyl-functionalized fluorophores, followed by Fmoc-deprotection to yield the target peptides (analogues A, D, F, and H, using Method 1 in Scheme 1). In Method 2, selective  $\epsilon$ -amine modification on solid phase was achieved by incorporating  $\epsilon$ -Mtt-protected Lys as an orthogonal protection. The Mtt group was selectively cleaved off by treating with 25% HFIP and 5% TIPS, and then the Cy5.5 fluorophore was coupled as an N-succinimidyl ester. The N-terminal Fmoc group was removed by 20% piperidine prior to the final acidolytic cleavage, giving analogues E and G. In order to prepare analogues B and C where conjugates are linked by the 1,2,3-triazole group, Fmoc-Lys(azide)-OH was incorporated at the 4-position. Labeling was then achieved by solution phase CuAAC reaction using the alkyne-containing RhB-2 and RhB-3, in the presence of CuSO<sub>4</sub> and sodium ascorbate as the catalysts (Method 3).<sup>25</sup> The synthesized analogues with their analytical data are summarized in Table 1.

**Pharmacological Analysis of NPY Analogues.** We examined the functional properties of the BVD-15 analogues as antagonists of NPY-induced Y<sub>1</sub>R engagement with  $\beta$ -arrestin2, a GPCR effector protein involved in G protein independent signaling and agonist induced receptor desensiti-



**Figure 2.** Fluorescent dye conjugates utilized in this study.

Scheme 1. Fluorescent Labeling of BVD-15 Analogues<sup>a</sup>


<sup>a</sup>Reagents and Conditions: (i) fluorophore-COOH (1.2 equiv), PyClox (2 equiv), NMM (12 equiv), DMF, overnight (Note that for E and G, Cy5.5, was coupled as an N-succinimidyl ester); (ii) Piperidine (20%) in DMF, 5 min × 2; (iii) HFIP (25%) and TIPS (5%) in DCM, 30 min; (iv) TFA-TIPS-DMB (92.5%:2.5%:5%), 3 h; (v) RhB-alkyne (2 equiv), CuSO<sub>4</sub> (0.5 equiv), THPTA (2.5 equiv), aminoguanidine (25 equiv), sodium ascorbate (25 equiv), DMSO 2% in potassium phosphate buffer (0.1 M, pH = 7.4), 1 h.

**Table 1. Fluorescently Labeled BVD-15 Analogues and Their Analytical Data**

code	sequence	MW (Calc.)	ESI-MS <i>m/z</i> <sup>a</sup>	LC/MS <sup>b</sup> RT (min)	HPLC purity (%)
A	INPK(RhB-1) YRLRY-NH <sub>2</sub>	1815.2	605.9	10.24 <sup>c</sup>	93
B	INP(K-N <sub>3</sub> -RhB-2) YRLRY-NH <sub>2</sub>	1839.3	613.9	13.42	99
C	INP(K-N <sub>3</sub> -RhB-3) YRLRY-NH <sub>2</sub>	1867.3	623.3	13.58	99
D	IK(RhB-1) PRYRLRY-NH <sub>2</sub>	1857.3	620.1	13.09	99
E	INPK(Cy5.5) YRLRY-NH <sub>2</sub>	1786.5	596.6	14.12 <sup>d</sup>	94
F	INPK(sCy5) YRLRY-NH <sub>2</sub>	1859.3	621.2	12.72	98
G	IK(Cy5.5) PRYRLRY-NH <sub>2</sub>	1829.3	610.6	14.11 <sup>d</sup>	99
H	IK(sCy5) PRYRLRY-NH <sub>2</sub>	1901.3	635.4	12.06	98

<sup>a</sup>ESI-MS base peak corresponds to [M+3H]<sup>3+</sup>. <sup>b</sup>HPLC retention time using a Phenomenex Luna C-8 column (100 Å, 3 μm, 100 × 2.00 mm). The gradient is composed of 100% H<sub>2</sub>O (0.1% TFA) for 4 min, 0–60% acetonitrile in H<sub>2</sub>O (0.1% TFA) over 10 min, and isocratic 60% acetonitrile in H<sub>2</sub>O (0.1% TFA) for 1 min. Detection wavelength = 214 nm. <sup>c</sup>For analogue A, the gradient is composed of 100% H<sub>2</sub>O (0.1% TFA) for 4 min, 20–100% acetonitrile in H<sub>2</sub>O (0.1% TFA) over 10 min, and isocratic 100% acetonitrile (0.1% TFA) for 1 min. <sup>d</sup>For analogue E and G, the gradient is composed of 100% H<sub>2</sub>O (0.1% TFA) for 4 min, 0–80% acetonitrile in H<sub>2</sub>O (0.1% TFA) over 10 min, and isocratic 80% acetonitrile (0.1% TFA) for 1 min.

zation and internalization.<sup>28</sup> This assay gives a strong functional readout consistent with other second messenger assays, and the limited receptor reserve allows discrimination of agonist efficacy

via changes in  $R_{\max}$  as compared to standard second messenger assays.<sup>20,21,28–30</sup> Unlabeled [Lys<sup>4</sup>]BVD-15<sup>23,24</sup> behaved as a competitive reversible antagonist of NPY stimulated responses, as indicated by Schild analysis (Figure 3A) with a  $pA_2$  of 7.5, and all but one of the labeled ligands showed comparable high affinity antagonism.  $pK_b$  values were calculated from NPY concentration response curve shifts in the presence of a single antagonist concentration (100 or 300 nM; Figure S1), and ranged from 6.9 to 7.9 with the rhodamine-linked triazole compound B showing highest affinity (Table 2). Of the four cyanine labeled derivatives, three were antagonists (Table 2) with compound H [Lys<sup>2</sup>(sCy5), Arg<sup>4</sup>]BVD-15 showing highest affinity, and shared the surmountable antagonist characteristics of [Lys<sup>4</sup>]BVD-15 (Figure 3B). Interestingly, substitution of the sCy5 fluorophore for Cy5.5 at the same 2-position led to compound G showing partial agonism in the Y<sub>1</sub>R arrestin recruitment assay, with a  $pEC_{50}$  of  $7.04 \pm 0.19$  and a maximal response of  $52.8 \pm 4.8\%$  compared to that elicited by 1 μM NPY ( $n = 3$ ; Figure S2). In contrast, analogues E, F (both cyanine labeled at 4-position) and H showed no agonism at concentrations up to 1 μM.

We screened the fluorescent BVD-15 analogues for their ability to specifically label 293TR cells stably expressing the GFP-tagged Y<sub>1</sub>R. In plate-reader based imaging assays, RhB labeled derivatives (e.g., A, Figure 4) exhibited specific Y<sub>1</sub>R receptor binding, predominantly localized to the plasma membrane that was inhibited by NPY and the nonpeptide Y<sub>1</sub>R antagonist BIBO3304. Cy5.5 analogues (E, G) displayed significant nonspecific binding in addition to cellular labeling and were not pursued further. However, compound H displayed specific plasma membrane labeling of Y<sub>1</sub>R-GFP cells at concentrations as low as 1 nM (Figure 5A), and specific

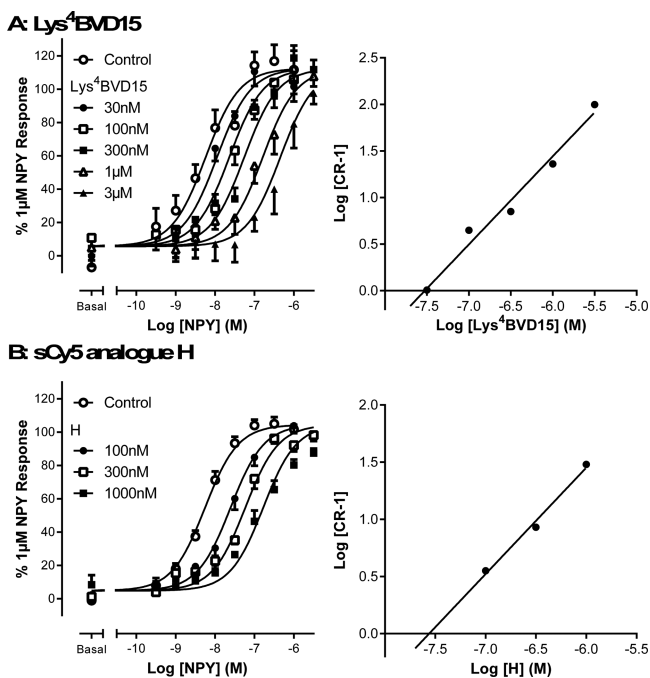


**Figure 3.** Surmountable antagonism of NPY stimulated  $\text{Y}_1\text{R}$  activation by unlabeled [ $\text{Lys}^4$ ]BVD15 (Panel A) and sCy5-labeled derivative H (Panel B). Stably transfected HEK293  $\text{Y}_1\text{R}$ - $\beta$ -arrestin2 cells were pretreated for 30 min with the antagonist peptide at the indicated concentrations, prior to 1 h NPY stimulation.  $\beta$ -arrestin2 recruitment was quantified by high content imaging complementation assay as described in [Experimental Methods](#). Pooled data from 5 (A) or 4–7 experiments (B), globally fitted to obtain NPY  $\text{pEC}_{50}$  estimates, were used for Schild analysis in the right-hand panels. These derived  $\text{pA}_2$  affinity estimates of 7.53 (analogue A) and 7.56 (analogue H) and respective slopes of 0.95 and 0.93, indicative of competitive reversible antagonism.

**Table 2.** Affinity Estimates for BVD-15 Analogues Derived from Functional Measurements or [ $^{125}\text{I}$ ]PYY Competition Binding

code	sequence	$\text{pK}_b^a$	$\text{pK}_i$ ( $\pm\text{SEM}$ )
[ $\text{Lys}^4$ ] BVD-15 <sup>24</sup>	INPKYRLRY-NH <sub>2</sub>	7.5 $\pm$ 0.1	8.6 $\pm$ 0.1
A	INPK(RhB-1)YRLRY-NH <sub>2</sub>	7.6 $\pm$ 0.2	9.5 $\pm$ 0.2
B	INP(K-N <sub>3</sub> -RhB-2)YRLRY-NH <sub>2</sub>	7.9 $\pm$ 0.2	9.6 $\pm$ 0.1
C	INP(K-N <sub>3</sub> -RhB-3)YRLRY-NH <sub>2</sub>	7.6 $\pm$ 0.2	9.4 $\pm$ 0.1
D	IK(RhB-1)PRYRLRY-NH <sub>2</sub>	6.9 $\pm$ 0.4	9.2 $\pm$ 0.1
E	INPK(Cy5.5)YRLRY-NH <sub>2</sub>	7.3 $\pm$ 0.1	8.4 $\pm$ 0.2
F	INPK(sCy5)YRLRY-NH <sub>2</sub>	7.3 $\pm$ 0.1	N.D. <sup>c</sup>
G	IK(Cy5.5)PRYRLRY-NH <sub>2</sub>	agonist <sup>b</sup>	8.8 $\pm$ 0.3
H	IK(sCy5)PRYRLRY-NH <sub>2</sub>	7.5 $\pm$ 0.2	9.4 $\pm$ 0.1

<sup>a</sup> $\text{pK}_b$  estimates derived from pooled data using the  $\text{Y}_1\text{R}$ - $\beta$ -arrestin2 recruitment assay presented in [Figure S1](#) ( $n = 4$  or greater). For comparison,  $\text{pK}_i$  estimates ( $n = 3$ , except compound B  $n = 2$ ) are derived from [ $^{125}\text{I}$ ]PYY binding studies in  $\text{Y}_1\text{R}$ -GFP membranes, performed under low sodium conditions in the absence of guanine nucleotides. <sup>b</sup> $\text{pEC}_{50} = 7.0 \pm 0.2$ , partial agonist ([Figure S2](#)). <sup>c</sup>N.D. = not determined

binding was fully inhibited by unlabeled competitors such as NPY or BIBO3304.

Peptide H was therefore chosen to develop a plate-reader imaging based  $\text{Y}_1\text{R}$  binding assay, using living whole cells.

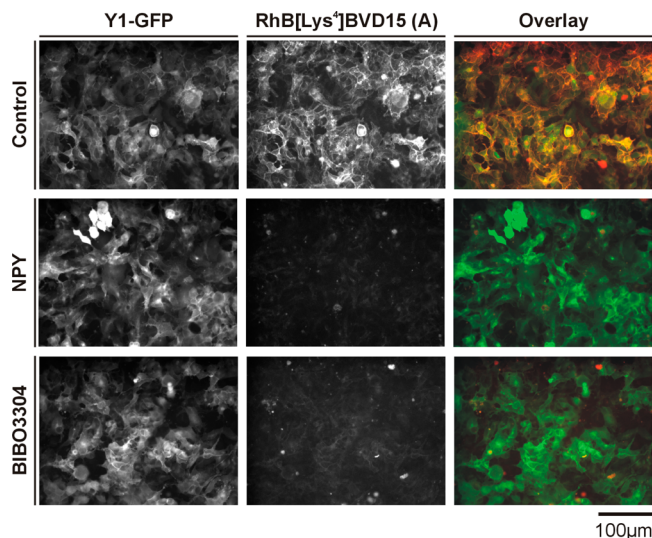


**Figure 4.** Cellular labeling of  $\text{Y}_1\text{R}$ -GFP by [ $\text{Lys}^4(\text{RhB})$ ]BVD-15 (A). 293TR  $\text{Y}_1\text{R}$ -GFP cells were incubated for 30 min at 37 °C with 10 nM A in the absence (control) or presence of 100 nM NPY or 100 nM BIBO3304. Representative IX Micro images (from one of three experiments) of GFP (left) or RhB fluorescence (center) are indicated, demonstrating extensive cell surface labeling using ligand A and colocalization with the GFP-tagged  $\text{Y}_1\text{R}$ .

Peptide H displayed fluorescence consistent with the sCy5 labeling, with excitation and emission maxima at 653 and 667 nm, respectively, and a relative quantum yield of 127% compared to sCy5-NHS alone ([SI Figure 4](#)). Based on optimized incubation conditions of 30 min at 37 °C, saturation analysis demonstrated one site binding and derived a  $\text{Y}_1\text{R}$   $\text{pK}_D$  for H of  $7.16 \pm 0.06$  ( $n = 4$ ) ([Figure 5B](#)), an estimate of affinity that was not significantly different from the  $\text{pK}_i$  derived by functional analysis ([Figure 3](#)). Furthermore, initial BIBO3304 competition data compared a family of curves at different H concentrations (1, 10, and 100 nM), yielding BIBO3304  $\text{pIC}_{50}$  values of  $9.06 \pm 0.07$ ,  $8.69 \pm 0.07$ , and  $8.31 \pm 0.07$ , respectively ( $n = 4$ , [Figure 5B](#)). The proportionate shift in competing ligand  $\text{IC}_{50}$  was consistent with equilibrium conditions and the Cheng-Prusoff relationship. Additional affinity estimates for BIBO3304 ( $\text{pK}_i = 8.9$ ) and H ( $\text{pK}_i = 7.3$ ) determined by this method were consistent with our other whole cell data.

Peptide H was employed in the study of a range of known Y receptor agonists, antagonists, as well as a series of analogues prepared in related studies ([Table 3](#)).<sup>29,31</sup> The expected  $\text{Y}_1$ -like pharmacology in the competition assay was observed for agonist peptides ([Figure 5D](#);  $\text{NPY} = [\text{Leu}31, \text{Pro}34]\text{NPY} \geq \text{PYY} > \text{PYY}3-36 = \text{PP}$ ), as previously described for many  $\text{Y}_1$  receptor systems,<sup>32</sup> and also antagonists, such as the dimeric peptide 1229U91.<sup>29</sup> The order of affinity based on  $\text{pK}_i$  values from these experiments was consistent with [ $^{125}\text{I}$ ]PYY binding assays for representative ligands performed in  $\text{Y}_1\text{R}$ -GFP cell membranes (and previously described data from  $\text{Y}_2\text{Y}_4$  receptor knockout mice).<sup>29</sup> For the nonpeptide antagonist BIBO3304 there was good correspondence between affinities measured in these formats, and also functional measurements previously reported.<sup>28</sup> For the peptide ligands the actual  $\text{pK}_i$  values for the whole cell assays were consistently lower than for membrane based assays ([Table 4](#)). The reason for this discrepancy is not obvious, but note that there is a closer correlation between the competition binding ( $\text{pK}_i$ ) and the functional antagonism in the



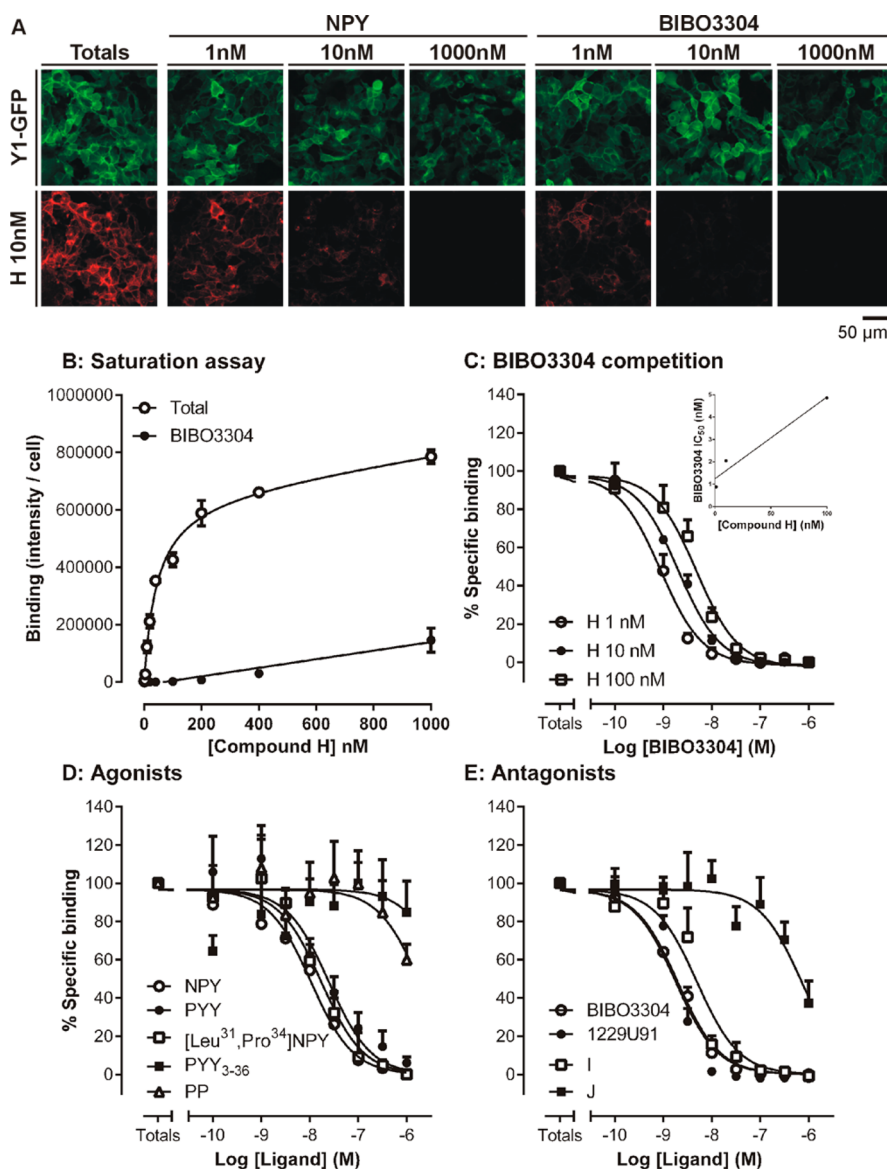


**Figure 5.**  $Y_1$ R binding assays using sCy5 labeled analogue **H**. Images from the IX Ultra platereader (Panel A,  $400 \times 400$  pixels from original  $1000 \times 1000$  acquisition) show binding of 10 nM **H** (red channel) to live 293TR  $Y_1$ R-GFP cells in the absence or presence of different NPY or BIBO3304 concentrations (30 min, with  $Y_1$ R-GFP images (green) also presented for comparison). Saturation analysis (Panel B) was performed in the absence (total) or presence of 1  $\mu$ M BIBO3304 (example experiment representative of 4). Pooled competition binding data (Panels C–E, at least 3 experiments) were derived from granularity analysis of the ligand images, normalized to total specific binding (100%). In C, BIBO3304 competition curves were performed at three **H** concentrations; the plot of the BIBO3304  $IC_{50}$  versus ligand concentration (inset) provides additional  $K_i$  affinity estimates for both BIBO3304 and **H** quoted in text (see [Experimental Methods](#)).  $pK_i$  estimates were also obtained for a range of agonist peptides (Panel D) and antagonists (Panel E), as indicated in Table 4.

whole cell system. The difference may be due to the buffer conditions in routine  $Y$  receptor membrane binding assays (low sodium and absence of guanine nucleotides) that are designed to promote the high affinity ternary receptor complex, and maximize radiolabeled agonist peptide binding.<sup>33</sup> The non-physiological buffer cation concentrations might also directly affect peptide ligand binding to the receptor. Thus, one of the important advantages of our measurements using fluorescent antagonist binding to whole cells, in physiological buffer, is that the affinities obtained should closely correspond to observations from functional data, particularly for agonists. Indeed, the estimates of agonist affinity by this route (Figure 5D) do closely correspond with their potencies in  $Y_1$ R-arrestin recruitment assay previously reported,<sup>28</sup> as anticipated for a response with

limited receptor reserve.<sup>33</sup> We also assayed compounds for which we had membrane competition binding data spanning a range of affinities, including analogues of 1229U91, **I** and **J** (Figure 5E; Table 3)<sup>29</sup> and some unlabeled BVD-15 analogues **K**–**N** (Table 3) and found the same trends (Table 4, Figure S3).

Compound **H** displayed moderate affinity for  $Y_4$ R (Figure 6), with saturation binding assays yielding a  $pK_D$  for **H** of  $6.26 \pm 0.11$  ( $n = 4$ ), 8-fold lower than for  $Y_1$ R. It did not bind cells expressing  $Y_2$ R or  $Y_5$ R (data not shown) at up to 1  $\mu$ M, as might be predicted from the reported selectivity profile for BVD-15.<sup>35</sup> In contrast to its actions at the  $Y_1$ R, **H** was a  $Y_4$ R partial agonist, a property shared by BVD-15, in the  $\beta$ -arrestin2 recruitment assay (Figure 6;  $pEC_{50} = 7.10 \pm 0.19$ , 1  $\mu$ M

**Table 3. Analytical Data of Dimeric 1229U91 Analogues and Other Unlabeled BVD-15 Analogues**

code	sequence	MW (Calc.)	ESI-MS $m/z$	LC/MS RT. (min) <sup>c</sup>	HPLC purity (%)
I	Bis(Lys <sup>4</sup> ) 1229U91 <sup>29</sup>	2436.9	851.6 <sup>a</sup>	11.16	98
J	Bis(des-Ile <sup>1</sup> ) 1229U91 <sup>29</sup>	2126.4	748.1 <sup>a</sup>	11.00	99
K	FBz- INPKYRLRY- NH <sub>2</sub>	1343.6	672.8 <sup>b</sup>	12.30	97
L	INPOYRLRY- NH <sub>2</sub> <sup>24</sup>	1207.4	604.7 <sup>b</sup>	10.55	98
M	FBz- INPRF*RLRY- NH <sub>2</sub>	1506.7	754.2 <sup>b</sup>	12.93	99
N	INPRF*RLRY- NH <sub>2</sub>	1384.6	693.2 <sup>b</sup>	11.51	98

<sup>a</sup>ESI-MS base peak corresponds to  $[M+TFA+3H]^{3+}$ . Note that  $[M+3H]^{3+}$  peaks were observed at lower intensity. <sup>b</sup>ESI-MS base peak corresponds to  $[M+2H]^{2+}$ . <sup>c</sup>HPLC retention time using a Phenomenex Luna C-8 column (100 Å, 3  $\mu$ m, 100  $\times$  2.00 mm). The gradient is composed of 100% H<sub>2</sub>O (0.1% TFA) for 4 min, 0–60% acetonitrile in H<sub>2</sub>O (0.1% TFA) over 10 min, and isocratic 60% acetonitrile in H<sub>2</sub>O (0.1% TFA) for 1 min. Detection wavelength = 214 nm. FBz = 4-fluorobenzoyl, O = ornithine, F\* = Phe(4-CH<sub>2</sub>NH-FBz).

response  $59.0 \pm 3.6\%$ , 100 nM PP,  $n = 6$ ); other cyanine BVD-15 analogues E–G displayed limited Y<sub>4</sub>R agonism at the highest concentration tested (1  $\mu$ M). At 100 nM, H selectively labeled 293TR cells expressing Y<sub>4</sub>R-GFP (Figure 6A), enabling competition binding studies to derive  $pK_i$  estimates for human PP, 1229U91, and its analogues I and J (Figure 6C; Table 4). As previously discussed, these estimates were lower than those previously reported for [<sup>125</sup>I]PP agonist binding studies in Y<sub>4</sub>R containing membranes.<sup>34</sup> However, the estimates of PP and 1229U91 affinity in whole cells by this route closely corresponded with their potencies in the arrestin recruitment assay (PP  $pEC_{50} = 8.77 \pm 0.07$ ,  $n = 5$ ; 1229U91 weak partial agonist  $pEC_{50} = 7.43 \pm 0.41$ ,  $n = 4$ ; Figure 6D). Comparisons of Y<sub>1</sub>R/Y<sub>4</sub>R binding affinities of 1229U91 analogues demonstrated that I had equivalent Y<sub>1</sub>R/Y<sub>4</sub>R selectivity as 1229U91 (16–30-fold selective for Y<sub>1</sub>R), while removal of the terminal Ile residues in J reversed the selectivity profile between these

subtypes (approximately 8-fold higher affinity for Y<sub>4</sub>R over Y<sub>1</sub>R).

In summary, our studies of fluorescent labeling of the BVD-15 scaffold has allowed us to identify some new features of the peptides' structure–activity relationships. First, we confirmed the general tolerance for modification at the 4-position, with retention of antagonistic activity at levels similar to the parent peptide in the presence of rhodamine derivatives and cyanine dyes. Second, we showed for the first time that the Asn residue at 2-position, in combination with introduction of an Arg at 4-position, yields peptides with retained affinity. However, while the sulfated Cy5 (sCy5) ligand is an antagonist, the more hydrophobic Cy5.5 label has agonist properties. This is significant as only one other example of a truncated NPY analogue has been shown to be an agonist.<sup>26</sup> We have also shown that analogue H is an excellent ligand for performing receptor binding studies at Y<sub>1</sub>R in intact cells using high content imaging, with low levels of nonspecific binding. Finally, we also show that analogue H has Y<sub>4</sub>R agonism, albeit at a lower level of affinity compared to Y<sub>1</sub>R binding. Thus, analogue H is also a suitable ligand for conducting competition binding and functional assays against Y<sub>4</sub>R and has been applied recently in structure–activity studies of the dimeric Y<sub>4</sub> agonist, BVD-74D.<sup>36,37</sup> The ready synthesis of this fluorescent ligand and its favorable properties will be of great utility in the development of new ligands for these two important receptors.

## EXPERIMENTAL METHODS

**Material.** N<sup>α</sup>-Fmoc protected amino acids were purchased from Auspep, Chemimpex and Mimotopes. Rink amide resin (0.53 mequiv/g, 100–200 mesh), HCTU and PyClock were obtained from Chemimpex. TFA, TIPS, DMB, HFIP, DIPEA, piperidine, CuSO<sub>4</sub>, aminoguanidine, sodium ascorbate, and DMSO were purchased from Sigma-Aldrich. All solvents were obtained from Merck. Cyanine dyes were purchased from Lumiprobe and W&J PharmaChem. THPTA was a gift from Dr Bim Graham's group (Monash Institute of Pharmaceutical Sciences, Monash University). The Rhodamine B derivatives were prepared in-house from the commercially available product (Sigma-Aldrich), according to Nguyen and Francis.<sup>27</sup> All solvents were of analytical grade, and all chemicals were used without further purification.

**Table 4. Competition Binding Assays at Y<sub>1</sub>R and Y<sub>4</sub>R Using Compound H as a Competing Ligand, In Comparison to Radioligand Binding Data**

peptide	Y <sub>1</sub> R ( $pK_i$ ) <sup>a</sup> live cell imaging (H)	Y <sub>1</sub> R ( $pK_i$ ) [ <sup>125</sup> I]PYY membranes	Y <sub>4</sub> R ( $pK_i$ ) <sup>a</sup> live cell imaging (H)	Y <sub>4</sub> R ( $pK_i$ ) [ <sup>125</sup> I]PP membranes
NPY	$7.95 \pm 0.12$	$9.75 \pm 0.16$	-	-
PYY	$7.67 \pm 0.10$	$9.50 \pm 0.23$	-	-
Leu <sup>31</sup> , Pro <sup>34</sup> -NPY	$7.82 \pm 0.11$	-	-	-
PYY(3–36)	<6.0	-	-	-
PP	<6.0	-	$8.69 \pm 0.11$	$10.1 \pm 0.21$ <sup>34</sup>
BIBO3304	$8.76 \pm 0.04$	$9.25 \pm 0.11$	-	-
1229U91	$8.80 \pm 0.07$	$9.90 \pm 0.06$	$7.21 \pm 0.10$	$9.6 \pm 0.11$ <sup>34</sup>
I	$8.35 \pm 0.12$	$10.18 \pm 0.12$	$7.20 \pm 0.10$	-
J	$6.03 \pm 0.59$	$8.91 \pm 0.08$	$6.91 \pm 0.11$	-
K	$6.48 \pm 0.17$	$9.10 \pm 0.08$	-	-
L	$7.69 \pm 0.09$	$9.73 \pm 0.01$	-	-
M	$6.23 \pm 0.11$	$8.62 \pm 0.19$	-	-
N	$7.59 \pm 0.10$	$9.74 \pm 0.08$	-	-

<sup>a</sup> $pK_i$  estimates from  $n = 3$ –4 whole cell competition binding (H) in Y<sub>1</sub>R-GFP or Y<sub>4</sub>R-GFP cells, using the Cheng-Prusoff correction based on H  $pK_D$  derived from saturation analysis in imaging studies.  $pK_i$  estimates derived from [<sup>125</sup>I]PYY binding to 293TR Y<sub>1</sub>R-GFP membranes ( $n = 2$ –6).

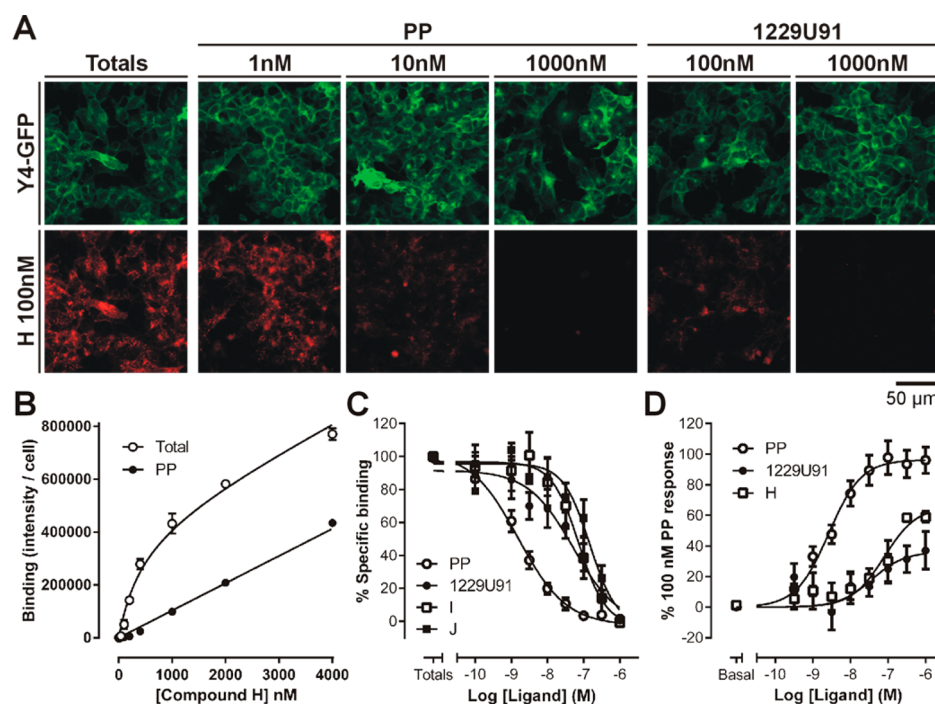


**Figure 6.** [Lys<sup>2</sup>(sCy5), Arg<sup>4</sup>]BVD-15 (H) is also a Y<sub>4</sub>R fluorescent ligand. Panel A illustrates representative images of 100 nM H binding (red) to 293TR Y<sub>4</sub>R-GFP cells (green) in the absence or presence of the endogenous peptide PP or 1229U91. Quantification of these data obtained saturation data for H ( $pK_D$  6.26), in which nonspecific binding was assessed in the presence of 1  $\mu$ M PP (Panel B, experiment representative of 4), and competition curves in Panel C (pooled from 4 to 7 experiments), from which the  $pK_i$  estimates in Table 4 were determined. In the Y<sub>4</sub>R- $\beta$ -arrestin2 recruitment assay (Panel D), H was a partial agonist compared to PP, but of higher relative efficacy than 1229U91 (pooled data 4–10 experiments).

Molecular mass of peptides was determined by ESI-MS using a Shimadzu LCMS2020 instrument, incorporating a Phenomenex Luna C-8 column (100 Å, 3  $\mu$ m, 100  $\times$  2.00 mm). Detection wavelength was set at 214 nm. This system used 0.05% TFA in Milli-Q water as the aqueous buffer, and 0.05% TFA in acetonitrile as the organic buffer. The eluting profile was a linear gradient of 0–60% acetonitrile in water over 10 min at 0.2 mL/min.

Crude peptides were purified on a Phenomenex Luna C-8 column (100 Å, 10  $\mu$ m, 250  $\times$  21.2 mm) utilizing a Waters 600 semipreparative RP-HPLC that incorporates a Waters 486 UV detector. Detection wavelength was set at 230 nm. This system used 0.1% TFA in Milli-Q water as the aqueous buffer, and 0.1% TFA in acetonitrile as the organic buffer. The eluting profile was a linear gradient of 0–80% acetonitrile in water over 60 min at 10 mL/min.

**Peptide Synthesis. General Synthesis.** Linear peptides (0.1 mmol scale) were synthesized on Rink amide resin using a 3-channel serial automated peptide synthesizer ("PS3", Protein Technologies Inc.), which adopted standard Fmoc-based solid-phase synthesis strategy. Fmoc deprotection was performed by piperidine (20% v/v) in DMF for 2  $\times$  5 min. Fmoc protected amino acids (3 equiv) were coupled using DMF as solvent, and DIPEA in DMF (7% v/v) with HCTU (3 equiv) as the activating agent for 50 min.

Protected peptidyl-resins were cleaved by treating with a cocktail (5 mL) composed of TFA-TIPS-DMB (92.5%:2.5%:5%) for 3 h. The cleavage mixture was then filtered, concentrated by stream of N<sub>2</sub>, precipitated in cold Et<sub>2</sub>O, and centrifuged at 3000 rpm for 5 min. The crude product was dissolved in water–acetonitrile mixture (50%:50%) and lyophilized.

**Labeling Methods. Method 1.** The N<sup>α</sup>-Fmoc protected linear peptide dissolved in DMF (0.6 mL) was treated with carboxyl-functionalized fluorophore of interest (1.2 equiv), PyClock (2 equiv), and NMM (12 equiv) overnight. After DMF was removed in vacuo, the product was washed by TFA (1 mL), precipitated by cold Et<sub>2</sub>O, and centrifuged at 3000 rpm for 5 min. The N<sup>α</sup>-Fmoc group was then removed by piperidine (20%) in DMF (5 mL) for 30 min and the reagents were evaporated in vacuo. The product was redissolved in water–acetonitrile (50%:50%) and lyophilized.

**Method 2.** The protected peptidyl-resin containing a Lys(Mtt) residue was treated with HFIP (25%) and TIPS (5%) in DCM (5 mL) for 30 min to selectively remove the Mtt group. Cy5.5 (as an N-succinimidyl ester) was conjugated by treating overnight in an alkaline condition created by DIPEA (10 equiv).

**Method 3.** Linear peptide containing a Lys(azide) residue (15 mg) was labeled by treating with a mixture of RhB-alkyne (2 equiv), CuSO<sub>4</sub> (0.5 equiv), THPTA (2.5 equiv), sodium ascorbate (25 equiv), and aminoguanidine (25 equiv) in a potassium phosphate buffer containing 2% DMSO, where the final concentration of linear peptide was 0.2 mM. The mixture was stirred for 1 h and lyophilized.

Peptides were purified by RP-HPLC as described above. The purity of all peptides are  $\geq$ 93% according to the HPLC chromatographs produced by the ESI-MS method described above, and MS data corresponded to the expected  $m/z$  values. Additional details are provided in Table 1, Table 3, and Supporting Information.

**Cell Culture.** HEK293T and 293TR cells (Invitrogen) were cultured in Dulbecco's modified Eagle's medium (DMEM, Sigma-Aldrich) supplemented with 10% fetal bovine serum,



293TR cell lines inducibly expressing Y<sub>1</sub>R or Y<sub>4</sub>R tagged with C-terminal GFP, and dual HEK293 cells coexpressing Y receptor-Yc and  $\beta$ -arrestin2-Yn (where Yc and Yn are complementary fragments of YFP) are as previously reported.<sup>28,38</sup>

#### [<sup>125</sup>I]PYY Competition Binding Studies in Membranes.

Competition binding assays were carried out as described previously.<sup>28,38</sup> Using membranes from the 293TR Y<sub>1</sub>R-GFP cells, competition binding assays were performed for 90 min at 21 °C in buffer (25 mM HEPES, 2.5 mM CaCl<sub>2</sub>, 1.0 mM MgCl<sub>2</sub>, 0.1% bovine serum albumin, 0.1 mg/mL bacitracin; pH = 7.4), increasing concentrations of unlabeled ligands (10<sup>-12</sup> M to 10<sup>-6</sup> M, duplicate) and [<sup>125</sup>I]PYY (15 pM). Nonspecific binding in these experiments comprised less than 5% of total counts, and was subtracted from the data.

In both sets of data, IC<sub>50</sub> values were calculated from displacement curves (repeated 2–3 times for each peptide, fitted using nonlinear least-squares regression in GraphPad Prism v 6 (GraphPad software, San Diego CA, U.S.A.). They were converted to pK<sub>i</sub> estimates using the Cheng-Prusoff relationship

$$K_i = \frac{IC_{50}}{1 + [RL]/K_{RL}}$$

where [RL] and K<sub>RL</sub> represent the concentration and equilibrium dissociation constant of [<sup>125</sup>I]PYY, respectively.

**Y Receptor- $\beta$ -Arrestin Recruitment Assays.** Bimolecular fluorescence complementation (BiFC) based detection of Y receptor- $\beta$ -arrestin2 association was performed as described previously.<sup>28,38</sup> The Y receptor arrestin BiFC cell lines were seeded at 40 000 cells/well onto poly(D-lysine)-coated Greiner 655090 imaging plates, and experiments performed 24 h later. Stimulation with human NPY (Y<sub>1</sub>R) or PP (Y<sub>4</sub>R; Bachem, St. Helens, U.K.), or other ligands was performed in HEPES-buffered saline solution (HBSS) including 0.1% BSA (10<sup>-10</sup> M–10<sup>-6</sup> M) for 60 min at 37 °C, with antagonist preincubations (30 min, 37 °C) if required. Incubations were terminated by fixation with 3% paraformaldehyde in phosphate buffered saline (PBS, 10 min at 21 °C), the cells were washed once with PBS and the cell nuclei were stained for 15 min with H33342 (2  $\mu$ g/mL in PBS, Sigma). H33342 was then removed by a final PBS wash. Images (4 central sites/well) were acquired automatically on the IX Ultra confocal platereader, using 405 nm/488 nm laser lines for H33342 and complemented YFP excitation, respectively.

A granularity algorithm (MetaXpress 5.3) identified internal fluorescent compartments within these images of at least 3  $\mu$ m diameter (range set to 3–12  $\mu$ m), on the basis of granule intensity thresholds set with reference to the vehicle or positive plate controls (e.g., 1  $\mu$ M NPY). The response for each data point (duplicate data) was quantified as mean granule average intensity/cell, normalized to the reference agonist response. Concentration response curves were fitted to the pooled data by nonlinear least-squares regression (GraphPad Prism), yielding estimates of agonist potency as pEC<sub>50</sub> and maximum response (R<sub>max</sub>). Where appropriate, the Gaddum equation was used to calculate an estimate of antagonist affinity:

$$pK_b = \log[CR - 1] - \log[B]$$

where CR is the concentration ratio (NPY EC<sub>50</sub> in the presence of antagonist/control NPY EC<sub>50</sub>), and [B] is the antagonist concentration used. To assess NPY concentration response

curves in the absence and presence of multiple antagonist concentrations ([Lys<sup>4</sup>]BVD-15 or compound H), Schild analysis was performed by global fitting of the curve families in GraphPad Prism; the Schild plot of log[CR - 1] versus log[B] illustrated the antagonist affinity estimate (pA<sub>2</sub>) as the X-intercept of the fitted line.

#### Y Receptor Saturation and Competition Fluorescent Ligand Binding Assays.

293TR Y<sub>1</sub>R-GFP or Y<sub>4</sub>R-GFP cells were seeded at 20 000 cells/well in poly(D-lysine) coated 96-well Greiner 655090 imaging plates, treated as required with 1  $\mu$ g/mL tetracycline for 18–21 h and then used in experiments at confluence. Incubations were performed in HBSS/0.1% BSA, the permeable nuclear dye H33342 (2  $\mu$ g/mL, Sigma), and competitor ligands as appropriate (10<sup>-10</sup> M to 10<sup>-5</sup> M) for 2 min, prior to the addition of fluorescent ligand at the concentration indicated. In saturation studies, nonspecific binding was assessed in the presence of 1  $\mu$ M BIBO3304 (Y<sub>1</sub>R) or PP (Y<sub>4</sub>R). After 30 min at 37 °C the media was replaced with HBSS/0.1% BSA and plates were immediately imaged (2 sites/well). For cyanine analogues (e.g., H) an IX Ultra confocal platereader (Molecular Devices, Sunnyvale CA, U.S.A.) used laser excitation/emission filter settings appropriate for H33342 (DAPI), Y receptor-GFP (FITC), and fluorescent ligand (Cy5). For rhodamine B derivatives an IX Micro epifluorescence platereader (Molecular Devices) acquired the images using the TRITC excitation/emission filter set.

For fluorescent ligand binding using H, bound ligand fluorescence was quantified by granularity analysis (2–3- $\mu$ m-diameter granules; MetaXpress 5.3, Molecular Devices). Competition data were normalized to positive (totals 100%) and negative (0%, in the presence of either 1  $\mu$ M NPY or 100 nM PP as appropriate) controls. For saturation studies, total and nonspecific binding data were globally fitted using a one site binding model whereby

$$\text{Total binding} = B_{\max} \cdot \frac{[FL]}{[FL] + K_D} + NS \times [FL]$$

$$\text{Nonspecific binding} = NS \times [FL]$$

[FL] is the fluorescent ligand concentration, B<sub>max</sub> represents the maximum specific binding, NS is the gradient of the nonspecific binding relationship, and K<sub>D</sub> is the equilibrium dissociation constant for compound H.

pIC<sub>50</sub> values for unlabeled ligands were then determined from the pooled data using GraphPad Prism, and converted to pK<sub>i</sub> using the Cheng-Prusoff relationship described above and the fluorescent ligand K<sub>D</sub> estimated from saturation data. In competition experiments in which compound H concentration [FL] in the assay was varied, the plot of BIBO3304 IC<sub>50</sub> versus [FL] was fitted by linear regression using the relationship derived from the Cheng-Prusoff equation

$$IC_{50} = \frac{K_i}{K_D} \times [FL] + K_i$$

The y intercept for this fit derives an estimate of K<sub>i</sub> for the competing ligand, BIBO3304, and the slope (K<sub>i</sub>/K<sub>D</sub>) also yields a further measurement of affinity of the fluorescent ligand H (K<sub>D</sub>).



## ■ ASSOCIATED CONTENT

### ■ Supporting Information

The Supporting Information is available free of charge on the ACS Publications website at DOI: 10.1021/acs.bioconjchem.6b00376.

Detailed synthesis procedures as well as additional supplementary figures showing dose–response curves for Y<sub>1</sub>R binding by peptides, fluorescence excitation/emission spectra for compound **H**, and HPLC profiles for synthesized peptides (PDF)

## ■ AUTHOR INFORMATION

### Corresponding Authors

\*E-mail: [nicholas.holliday@nottingham.ac.uk](mailto:nicholas.holliday@nottingham.ac.uk), Tel: +44 115 82 30084, Fax: +44 115 82 30081.

\*E-mail: [philip.thompson@monash.edu](mailto:philip.thompson@monash.edu), Tel: +61 3 99039672, Fax: +61 3 99039582.

### Notes

The authors declare no competing financial interest.

## ■ ACKNOWLEDGMENTS

This work was supported by CRC for Biomedical Imaging Development (CRC-BID), Australia. M.L. was supported by an Australian Postgraduate Award scholarship. RRR was supported by the Nottingham-Monash PhD program.

## ■ ABBREVIATIONS

DCM, dichloromethane; DIPEA, *N,N*-diisopropylethylamine; DMB, 1,3-dimethoxybenzene; DMF, *N,N*-dimethylformamide; HCTU, *O*-(1*H*-6-chlorobenzotriazol-1-yl)-*N,N,N',N'*-tetramethyluronium hexafluorophosphate; HFIP, hexafluoroisopropanol; NMM, *N*-methylmorpholine; RhB, Rhodamine B; TFA, trifluoroacetic acid; THPTA, tris(3-hydroxypropyltriethylmethyl)amine; TIPS, triisopropylsilane

## ■ REFERENCES

- (1) Tatemoto, K. (1982) Neuropeptide Y: Complete amino acid sequence of the brain peptide. *Proc. Natl. Acad. Sci. U. S. A.* 79, 5485–5489.
- (2) Hoffmann, J. A., and Chance, R. E. (1983) Crystallization of bovine pancreatic polypeptide. *Biochem. Biophys. Res. Commun.* 116, 830–835.
- (3) Tatemoto, K., and Mutt, V. (1980) Isolation of two novel candidate hormones using a chemical method for finding naturally occurring polypeptides. *Nature* 285, 417–418.
- (4) Blomqvist, A. G., and Herzog, H. (1997) Y-receptor subtypes - how many more? *Trends Neurosci.* 20, 294–298.
- (5) Bromée, T., Sjödin, P., Fredriksson, R., Boswell, T., Larsson, T. A., Salaneck, E., Zoorob, R., Mohell, N., and Larhammar, D. (2006) Neuropeptide Y-family receptors Y<sub>6</sub> and Y<sub>7</sub> in chicken. *FEBS J.* 273, 2048–2063.
- (6) Salaneck, E., Larsson, T. A., Larson, E. T., and Larhammar, D. (2008) Birth and death of neuropeptide Y receptor genes in relation to the teleost fish tetraploidization. *Gene* 409, 61–71.
- (7) Kanatani, A., Mashiko, S., Murai, N., Sugimoto, N., Ito, J., Fukuroda, T., Fukami, T., Morin, N., MacNeil, D. J., Van der Ploeg, L. H. T., Saga, Y., Nishimura, S., and Ihara, M. (2000) Role of the Y<sub>1</sub> receptor in the regulation of neuropeptide Y-mediated feeding: comparison of wild-type, Y<sub>1</sub> receptor-deficient, and Y<sub>5</sub> receptor-deficient mice. *Endocrinology* 141, 1011–1016.
- (8) Kanatani, A., Ishihara, A., Asahi, S., Tanaka, T., Ozaki, S., and Ihara, M. (1996) Potent neuropeptide Y Y<sub>1</sub> receptor antagonist, 1229U91: blockade of neuropeptide Y-induced and physiological food intake. *Endocrinology* 137, 3177–3182.
- (9) Thiele, T. E., Koh, M. T., and Pedrazzini, T. (2002) Voluntary alcohol consumption is controlled via the neuropeptide Y Y<sub>1</sub> receptor. *J. Neurosci.* 22, RC208.
- (10) Thorsell, A. (2007) Neuropeptide Y (NPY) in alcohol intake and dependence. *Peptides* 28, 480–483.
- (11) Nilsson, T., Cantera, L., and Edvinsson, L. (1996) Presence of neuropeptide Y Y<sub>1</sub> receptor mediating vasoconstriction in human cerebral arteries. *Neurosci. Lett.* 204, 145–148.
- (12) Edvinsson, L., Ekblad, E., Håkanson, R., and Wahlestedt, C. (1984) Neuropeptide Y potentiates the effect of various vasoconstrictor agents on rabbit blood vessels. *Br. J. Pharmacol.* 83, 519–525.
- (13) Desai, S. J., Borkar, C. D., Nakhate, K. T., Subhedar, N. K., and Kokare, D. M. (2014) Neuropeptide Y attenuates anxiety- and depression-like effects of cholecystokinin-4 in mice. *Neuroscience* 277, 818–830.
- (14) Wahlestedt, C., Pich, E. M., Koob, G. F., Yee, F., and Heilig, M. (1993) Modulation of anxiety and neuropeptide Y-Y<sub>1</sub> receptors by antisense oligodeoxynucleotides. *Science* 259, 528–531.
- (15) Reubi, J., Gugger, M., and Waser, B. (2002) Co-expressed peptide receptors in breast cancer as a molecular basis for in vivo multireceptor tumour targeting. *Eur. J. Nucl. Med. Mol. Imaging* 29, 855–862.
- (16) Körner, M., and Reubi, J. C. (2006) Chapter 62 - Somatostatin and NPY, in *Handbook of Biologically Active Peptides* (Abba, J. K., Ed.) pp 435–441, Academic Press, Burlington.
- (17) Schneider, E., Mayer, M., Ziemek, R., Li, L., Hutzler, C., Bernhardt, G., and Buschauer, A. (2006) A simple and powerful flow cytometric method for the simultaneous determination of multiple parameters at G protein-coupled receptor subtypes. *ChemBioChem* 7, 1400–1409.
- (18) Wieland, H. A., Engel, W., Eberlein, W., Rudolf, K., and Doods, H. N. (1998) Subtype selectivity of the novel nonpeptide neuropeptide Y Y<sub>1</sub> receptor antagonist BIBO 3304 and its effect on feeding in rodents. *Br. J. Pharmacol.* 125, 549–555.
- (19) Schneider, E., Keller, M., Brennauer, A., Hoefelschweiger, B. K., Gross, D., Wolfbeis, O. S., Bernhardt, G., and Buschauer, A. (2007) Synthesis and characterization of the first fluorescent nonpeptide NPY Y<sub>1</sub> receptor antagonist. *ChemBioChem* 8, 1981–1988.
- (20) Keller, M., Erdmann, D., Pop, N., Pluym, N., Teng, S., Bernhardt, G., and Buschauer, A. (2011) Red-fluorescent arginamide-type NPY Y<sub>1</sub> receptor antagonists as pharmacological tools. *Bioorg. Med. Chem.* 19, 2859–2878.
- (21) Leban, J. J., Heyer, D., Landavazo, A., Matthews, J., Aulabaugh, A., and Daniels, A. J. (1995) Novel modified carboxy terminal fragments of neuropeptide Y with high affinity for Y<sub>2</sub>-type receptors and potent functional antagonism at the Y<sub>1</sub>-type receptor. *J. Med. Chem.* 38, 1150–1157.
- (22) Guérin, B., Ait-Mohand, S., Tremblay, M.-C., Dumulon-Perreault, V. r., Fournier, P., and Bénard, F. (2010) Total solid-phase synthesis of NOTA-functionalized peptides for PET imaging. *Org. Lett.* 12, 280–283.
- (23) Guérin, B., Dumulon-Perreault, V., Tremblay, M.-C., Ait-Mohand, S., Fournier, P., Dubuc, C., Authier, S., and Bénard, F. (2010) [Lys(DOTA\*)]BVD15, a novel and potent neuropeptide Y analog designed for Y<sub>1</sub> receptor-targeted breast tumor imaging. *Bioorg. Med. Chem. Lett.* 20, 950–953.
- (24) Liu, M., Mountford, S. J., Zhang, L., Lee, I.-C., Herzog, H., and Thompson, P. E. (2013) Synthesis of BVD15 peptide analogues as models for radioligands in tumour imaging. *Int. J. Pept. Res. Ther.* 19, 33–41.
- (25) Northfield, S. E., Mountford, S. J., Wielens, J., Liu, M., Zhang, L., Herzog, H., Holliday, N. D., Scanlon, M. J., Parker, M. W., Chalmers, D. K., and Thompson, P. E. (2015) Propargyloxypyrrolidine regio- and stereoisomers for click-conjugation of peptide: synthesis and application in linear and cyclic peptides. *Aust. J. Chem.* 68, 1365.
- (26) Zwanziger, D., Böhme, I., Lindner, D., and Beck-Sickingler, A. G. (2009) First selective agonist of the neuropeptide Y<sub>1</sub>-receptor with reduced size. *J. Pept. Sci.* 15, 856–866.

- (27) Nguyen, T., and Francis, M. B. (2003) Practical synthetic route to functionalized rhodamine dyes. *Org. Lett.* 5, 3245–3248.
- (28) Kilpatrick, L. E., Briddon, S. J., Hill, S. J., and Holliday, N. D. (2010) Quantitative analysis of neuropeptide Y receptor association with  $\beta$ -arrestin2 measured by bimolecular fluorescence complementation. *Br. J. Pharmacol.* 160, 892–906.
- (29) Mountford, S. J., Liu, M., Zhang, L., Groenen, M., Herzog, H., Holliday, N. D., and Thompson, P. E. (2014) Synthetic routes to the Neuropeptide Y Y<sub>1</sub> receptor antagonist 1229U91 and related analogues for SAR studies and cell-based imaging. *Org. Biomol. Chem.* 12, 3271–3281.
- (30) Holliday, N. D., Michel, M. C., and Cox, H. M. (2004) NPY receptor subtypes and their signal transduction, in *Neuropeptide Y and Related Peptides* (Michel, M. C., Ed.) pp 45–73, Springer, Berlin.
- (31) Liu, M. J., Mountford, S. J., Zhang, L., Lee, I. C., Herzog, H., and Thompson, P. E. (2013) Synthesis of BVD15 peptide analogues as models for radioligands in tumour imaging. *Int. J. Pept. Res. Ther.* 19, 33–41.
- (32) Michel, M. C., Beck-Sickinger, A., Cox, H., Doods, H. N., Herzog, H., Larhammar, D., Quirion, R., Schwartz, T., and Westfall, T. (1998) XVI. International Union of Pharmacology recommendations for the nomenclature of neuropeptide Y, peptide YY, and pancreatic polypeptide receptors. *Pharmacol. Rev.* 50, 143–50.
- (33) Stott, L. A., Hall, D. A., and Holliday, N. D. (2016) Unravelling intrinsic efficacy and ligand bias at G protein coupled receptors: A practical guide to assessing functional data. *Biochem. Pharmacol.* 101, 1–12.
- (34) Parker, E. M., Babij, C. K., Balasubramaniam, A., Burrier, R. E., Guzzi, M., Hamud, F., Gitali, M., Rudinski, M. S., Tao, Z., Tice, M., Xia, L., Mullins, D. E., and Salisbury, B. G. (1998) GR231118 (1229U91) and other analogues of the C-terminus of neuropeptide Y are potent neuropeptide Y Y<sub>1</sub> receptor antagonists and neuropeptide Y Y<sub>4</sub> receptor agonists. *Eur. J. Pharmacol.* 349, 97–105.
- (35) Balasubramaniam, A., Dhawan, V. C., Mullins, D. E., Chance, W. T., Sheriff, S., Guzzi, M., Prabhakaran, M., and Parker, E. M. (2001) Highly selective and potent neuropeptide Y (NPY) Y<sub>1</sub> receptor antagonists based on [Pro(30), Tyr(32), Leu(34)]NPY(28–36)-NH<sub>2</sub> (BW1911U90). *J. Med. Chem.* 44, 1479–1482.
- (36) Liu, M., Mountford, S. J., Richardson, R. R., Groenen, M., Holliday, N. D., and Thompson, P. E. (2016) Optically Pure, Structural, and Fluorescent Analogues of a Dimeric Y<sub>4</sub> Receptor Agonist Derived by an Olefin Metathesis Approach. *J. Med. Chem.* 59, 6059–6069.
- (37) Kuhn, K. K., Ertl, T., Dukorn, S., Keller, M., Bernhardt, G., Reiser, O., and Buschauer, A. (2016) High Affinity Agonists of the Neuropeptide Y (NPY) Y<sub>4</sub> Receptor Derived from the C-Terminal Pentapeptide of Human Pancreatic Polypeptide (hPP): Synthesis, Stereochemical Discrimination, and Radiolabeling. *J. Med. Chem.* 59, 6045–6058.
- (38) Kilpatrick, L. E., Briddon, S. J., and Holliday, N. D. (2012) Fluorescence correlation spectroscopy, combined with bimolecular fluorescence complementation, reveals the effects of  $\beta$ -arrestin complexes and endocytic targeting on the membrane mobility of neuropeptide Y receptors. *Biochim. Biophys. Acta, Mol. Cell Res.* 1823, 1068–1081.

### 3.6 Summary

This chapter has described the chemical synthesis and pharmacological properties of a series of fluorescently labelled peptides derived from the NPY C-terminal 9-amino acid fragment, Y<sub>1</sub>R antagonist / Y<sub>4</sub>R agonist BVD-15 peptide. Specifically, we have amended the 2-, 3- and 4-positions to include amino acids with reactive groups to study their potential as sites of fluorophore conjugations.

To prepare the 3-position labelled ligands, we have successfully synthesised a series of Fmoc-protected propargyloxypyrrolidine derivatives with different stereo- and regio-configurations, which were incorporated as a substitution of the Pro<sup>3</sup> residue to enable labelling with azide-bearing coumarin and rhodamine B derivatives. Competition binding assays have revealed that the majority of resulting peptide conjugates exhibited strong Y<sub>1</sub>R affinity, suggesting that conjugating groups at the 3-position did not significantly disturb the peptide active 3D conformations. The usefulness of these ligands in Y<sub>1</sub>R imaging studies remains to be confirmed.

We have also prepared a group of BVD-15 analogues that incorporated cyanine or rhodamine B derivatives at the 2- or 4-position, where labelling was achieved either in solution or on-resin with application of orthogonal protecting groups. We have demonstrated that fluorophore conjugations at the 4-position could be well tolerated, resulting in comparable antagonistic activity to the unlabelled parent compound. We also showed that a conjugated Lys<sup>2</sup> in combination with an Arg<sup>4</sup> retained Y<sub>1</sub>R affinity; interestingly, while [Lys<sup>2</sup>(Cy5.5), Arg<sup>4</sup>]BVD-15 showed unexpected partial Y<sub>1</sub>R agonism, other 2-position labelled analogues were found to be antagonists. Most importantly, the sulfated Cy5 (sCy5) containing ligand [Lys<sup>2</sup>(sCy5), Arg<sup>4</sup>]BVD-15 exhibited both competitive Y<sub>1</sub>R antagonism and Y<sub>4</sub>R partial agonism with lower affinity, and its applicability in

imaging-based competition binding assays has been demonstrated in living whole cells. Therefore, [Lys<sup>2</sup>(sCy5), Arg<sup>4</sup>]BVD-15 represents a novel fluorescently labelled Y<sub>1</sub>R/Y<sub>4</sub>R peptidic ligand with great potential in receptor visualisation and new ligand analysis in regards to these GPCRs.

## References

- (1) Dumont, Y., Martel, J.-C., Fournier, A., St-Pierre, S., and Quirion, R. (1992) Neuropeptide Y and neuropeptide Y receptor subtypes in brain and peripheral tissues. *Prog. Neurobiol.* 38, 125-167.
- (2) Tatemoto, K. (1982) Neuropeptide Y: Complete amino acid sequence of the brain peptide. *Proc. Natl. Acad. Sci.* 79, 5485-5489.
- (3) Tatemoto, K., and Mutt, V. (1980) Isolation of two novel candidate hormones using a chemical method for finding naturally occurring polypeptides. *Nature* 285, 417-418.
- (4) Hoffmann, J. A., and Chance, R. E. (1983) Crystallization of bovine pancreatic polypeptide. *Biochem. Biophys. Res. Co.* 116, 830-835.
- (5) Larhammar, D. (1996) Evolution of neuropeptide Y, peptide YY and pancreatic polypeptide. *Regul. Pept.* 62, 1-11.
- (6) Brothers, S. P., and Wahlestedt, C. (2010) Therapeutic potential of neuropeptide Y (NPY) receptor ligands. *EMBO Mol. Med.* 2, 429-439.
- (7) Blomqvist, A. G., Söderberg, C., Lundell, I., Milner, R. J., and Larhammar, D. (1992) Strong evolutionary conservation of neuropeptide Y: sequences of chicken, goldfish, and *Torpedo marmorata* DNA clones. *Proc. Natl. Acad. Sci. USA* 89, 2350-2354.
- (8) Blomqvist, A. G., and Herzog, H. (1997) Y-receptor subtypes - how many more? *Trends Neurosci.* 20, 294-298.
- (9) Bromée, T., Sjödin, P., Fredriksson, R., Boswell, T., Larsson, T. A., Salaneck, E., Zoorob, R., Mohell, N., and Larhammar, D. (2006) Neuropeptide Y-family receptors Y<sub>6</sub> and Y<sub>7</sub> in chicken. *FEBS J.* 273, 2048-2063.
- (10) Salaneck, E., Larsson, T. A., Larson, E. T., and Larhammar, D. (2008) Birth and death of neuropeptide Y receptor genes in relation to the teleost fish tetraploidization. *Gene* 409, 61-71.
- (11) Grundemar, L., Jonas, S. E., Mörner, N., Högestätt, E. D., Wahlestedt, C., and Håkanson, R. (1992) Characterization of vascular neuropeptide Y receptors. *Br. J. Pharmacol.* 105, 45-50.
- (12) Gerald, C., Walker, M. W., Vaysse, P. J.-J., He, C., Branchek, T. A., and Weinshank, R. L. (1995) Expression cloning and pharmacological characterization of a human hippocampal neuropeptide Y/peptide YY Y<sub>2</sub> receptor subtype. *J. Biol. Chem.* 270, 26758-26761.
- (13) Reubi, J. C., Gugger, M., Waser, B., and Schaer, J.-C. (2001) Y<sub>1</sub>-mediated effect of neuropeptide Y in cancer: breast carcinomas as targets. *Cancer Res.* 61, 4636-4641.
- (14) Nichol, K. A., Morey, A., Couzens, M. H., Shine, J., Herzog, H., and Cunningham, A. M. (1999) Conservation of expression of neuropeptide Y<sub>5</sub> receptor between human and

- rat hypothalamus and limbic regions suggests an integral role in central neuroendocrine control. *J. Neurosci.* 19, 10295-10304.
- (15) Balasubramaniam, A. (2003) Neuropeptide Y (NPY) family of hormones: Progress in the development of receptor selective agonists and antagonists. *Curr. Pharm. Des.* 9, 1165-1175.
  - (16) Parker, M. S., Sah, R., Balasubramaniam, A., Sallee, F. R., Zerbe, O., and Parker, S. L. (2011) Non-specific binding and general cross-reactivity of Y receptor agonists are correlated and should importantly depend on their acidic sectors. *Peptides* 32, 258-265.
  - (17) Rudolf, K., Eberlein, W., Engel, W., Wieland, H. A., Willim, K. D., Entzeroth, M., Wienen, W., Beck-Sickinge, A. G., and Doods, H. N. (1994) The first highly potent and selective non-peptide neuropeptide Y Y<sub>1</sub> receptor antagonist: BIBP3226. *Eur. J. Pharmacol.* 271, R11-R13.
  - (18) Doods, H. N., Wieland, H. A., Engel, W., Eberlein, W., Willim, K.-D., Entzeroth, M., Wienen, W., and Rudolf, K. (1996) BIBP 3226, the first selective neuropeptide Y<sub>1</sub> receptor antagonist: a review of its pharmacological properties. *Regul. Pept.* 65, 71-77.
  - (19) Dumont, Y., St-Pierre, J.-A., and Quirion, R. (1996) Comparative autoradiographic distribution of neuropeptide Y Y-1 receptors visualized with the Y<sub>1</sub> receptor agonist [<sup>125</sup>I][Leu<sup>31</sup>, Pro<sup>34</sup>]PYY and the non-peptide antagonist [<sup>3</sup>H]BIBP3226. *NeuroReport* 7, 901-904.
  - (20) Malmström, R. E. (2000) Neuropeptide Y Y<sub>1</sub> receptor mediated mesenteric vasoconstriction in the pig in vivo. *Regul. Pept.* 95, 59-63.
  - (21) Mollereau, C., Mazarguil, H., Marcus, D., Quelven, I., Kotani, M., Lannoy, V., Dumont, Y., Quirion, R., Detheux, M., Parmentier, M., and Zajac, J.-M. (2002) Pharmacological characterization of human NPFF(1) and NPFF(2) receptors expressed in CHO cells by using NPY Y<sub>1</sub> receptor antagonists. *Eur. J. Pharmacol.* 451, 245-256.
  - (22) Leban, J. J., Heyer, D., Landavazo, A., Matthews, J., Aulabaugh, A., and Daniels, A. J. (1995) Novel modified carboxy terminal fragments of neuropeptide Y with high affinity for Y<sub>2</sub>-type receptors and potent functional antagonism at the Y<sub>1</sub>-type receptor. *J. Med. Chem.* 38, 1150-1157.
  - (23) Balasubramaniam, A., Dhawan, V. C., Mullins, D. E., Chance, W. T., Sherif, S., Guzzi, M., Prabhakaran, M., and Parker, E. M. (2001) Highly selective and potent neuropeptide Y (NPY) Y<sub>1</sub> receptor antagonists based on [Pro(30), Tyr(32), Leu(34)]NPY(28-36)-NH<sub>2</sub> (BW1911U90). *J. Med. Chem.* 44, 1479-1482.
  - (24) Parker, E. M., Babij, C. K., Balasubramaniam, A., Burrier, R. E., Guzzi, M., Hamud, F., Gitali, M., Rudinski, M. S., Tao, Z., Tice, M., Xia, L., Mullins, D. E., and Salisbury, B. G. (1998) GR231118 (1229U91) and other analogues of the C-terminus of neuropeptide Y are potent neuropeptide Y Y<sub>1</sub> receptor antagonists and neuropeptide Y Y<sub>4</sub> receptor agonists. *Eur. J. Pharmacol.* 349, 97-105.

- 
- (25) Daniels, A., Matthews, J., Slepetis, R., Jansen, M., Viveros, O., Tadepalli, A., Harrington, W., Heyer, D., Landavazo, A., and Leban, J. (1995) High-affinity neuropeptide Y receptor antagonists. *Proc. Natl. Acad. Sci.* 92, 9067-9071.
- (26) Matthews, J. E., Jansen, M., Lyster, D., Cox, R., Chen, W.-J., Koller, K. J., and Daniels, A. J. (1997) Pharmacological characterization and selectivity of the NPY antagonist GR231118 (1229U91) for different NPY receptors. *Regul. Pept.* 72, 113-119.
- (27) Schober, D. A., Gackenhimer, S. L., Heiman, M. L., and Gehlert, D. R. (2000) Pharmacological characterization of 125I-1229U91 binding to Y1 and Y4 neuropeptide Y/peptide YY receptors. *J. Pharmacol. Exp. Ther.* 293, 275-280.
- (28) Söll, R. M., Dinger, M. C., Lundell, I., Larhammer, D., and Beck-Sickinger, A. G. (2001) Novel analogues of neuropeptide Y with a preference for the Y<sub>1</sub>-receptor. *Eur. J. Biochem.* 268, 2828-2837.
- (29) Fuhlendorff, J., Gether, U., Aakerlund, L., Langeland-Johansen, N., Thøgersen, H., Melberg, S. G., Olsen, U. B., Thastrup, O., and Schwartz, T. W. (1990) [Leu<sup>31</sup>, Pro<sup>34</sup>]neuropeptide Y: a specific Y1 receptor agonist. *Proc. Natl. Acad. Sci.* 87, 182-186.
- (30) Dumont, Y., Fournier, A., St-Pierre, S., and Quirion, R. (1995) Characterization of neuropeptide Y binding sites in rat brain membrane preparations using [<sup>125</sup>I][Leu<sup>31</sup>,Pro<sup>34</sup>]peptide YY and [<sup>125</sup>I]peptide YY<sub>3-36</sub> as selective Y<sub>1</sub> and Y<sub>2</sub> radioligands. *J. Pharmacol. Exp. Ther.* 272, 673-80.
- (31) Zwanziger, D., Böhme, I., Lindner, D., and Beck-Sickinger, A. G. (2009) First selective agonist of the neuropeptide Y<sub>1</sub>-receptor with reduced size. *J. Pept. Sci.* 15, 856-866.
- (32) Schwippert, W. W., Röttgen, A., and Ewert, J. P. (1998) Neuropeptide Y (NPY) or fragment NPY 13-36, but not NPY 18-36, inhibit retinotectal transfer in cane toads *Bufo marinus*. *Neurosci. Lett.* 253, 33-36.
- (33) Batterham, R. L., Cowley, M. A., Small, C. J., Herzog, H., Cohen, M. A., Dakin, C. L., Wren, A. M., Brynes, A. E., Low, M. J., Ghatei, M. A., Cone, R. D., and Bloom, S. R. (2002) Gut hormone PYY<sub>3-36</sub> physiologically inhibits food intake. *Nature* 418, 650-654.
- (34) Kamiji, M. M., and Inui, A. (2007) NPY Y2 and Y4 receptors selective ligands: promising anti-obesity drugs? *Curr. Top. Med. Chem.* 7, 1734-1742.
- (35) Balasubramaniam, A., Mullins, D. E., Lin, S., Zhai, W., Tao, Z., Dhawan, V. C., Guzzi, M., Knittel, J. J., Slack, K., Herzog, H., and Parker, E. M. (2006) Neuropeptide Y (NPY) Y4 receptor selective agonists based on NPY(32-36): development of an anorectic Y4 receptor selective agonist with picomolar affinity. *J. Med. Chem.* 49, 2661-2665.
- (36) Parker, M. S., Sah, R., Sheriff, S., Balasubramaniam, A., and Parker, S. L. (2005) Internalization of cloned pancreatic polypeptide receptors is accelerated by all types of Y4 agonists. *Regul. Pept.* 132, 91-101.
- (37) Cabrele, C., Langer, M., Bader, R., Wieland, H. A., Doods, H. N., Zerbe, O., and Beck-Sickinger, A. G. (2000) The first selective agonist for the neuropeptide Y Y5 receptor increases food intake in rats. *J. Biol. Chem.* 275, 36043-36048.

- 
- (38) Dumont, Y., Thakur, M., Beck-Sickinger, A., Fournier, A., and Quirion, R. Characterization of a new neuropeptide Y Y<sub>5</sub> agonist radioligand: [<sup>125</sup>I][cPP(1-7), NPY(19-23), Ala<sup>31</sup>, Aib<sup>32</sup>, Gln<sup>34</sup>]hPP. *Neuropeptides* 38, 163-174.
- (39) Lecklin, A., Lundell, I., Salmela, S., Männistö, P. T., Beck-Sickinger, A. G., and Larhammar, D. (2003) Agonists for neuropeptide Y receptors Y<sub>1</sub> and Y<sub>5</sub> stimulate different phases of feeding in guinea pigs. *Br. J. Pharm* 139, 1433-1440.
- (40) Kalra, S. P., Dube, M. G., Pu, S., Xu, B., Horvath, T. L., and Kalra, P. S. (1999) Interacting appetite-regulating pathways in the hypothalamic regulation of body weight. *Endocr. Rev.* 20, 68-100.
- (41) Kanatani, A., Ishihara, A., Asahi, S., Tanaka, T., Ozaki, S., and Ihara, M. (1996) Potent neuropeptide Y Y<sub>1</sub> receptor antagonist, 1229U91: blockade of neuropeptide Y-induced and physiological food intake. *Endocrinology* 137, 3177-3182.
- (42) Kanatani, A., Ito, J., Ishihara, A., Iwaasa, H., Takahiro, F., Fukami, T., J. MacNeil, D., Van der Ploeg, L. H. T., and Ihara, M. (1998) NPY-induced feeding involves the action of a Y<sub>1</sub>-like receptor in rodents. *Regul. Pept.* 75-76, 409-415.
- (43) Kanatani, A., Mashiko, S., Murai, N., Sugimoto, N., Ito, J., Fukuroda, T., Fukami, T., Morin, N., MacNeil, D. J., Van der Ploeg, L. H. Y., Saga, Y., Nishimura, S., and Ihara, M. (2000) Role of the Y<sub>1</sub> receptor in the regulation of neuropeptide Y-mediated feeding: comparison of wild-type, Y<sub>1</sub> receptor-deficient, and Y<sub>5</sub> receptor-deficient mice. *Endocrinology* 141, 1011-1016.
- (44) Thiele, T. E., and Badia-Elder, N. E. (2003) A role for neuropeptide Y in alcohol intake control: evidence from human and animal research. *Physiology & Behavior* 79, 95-101.
- (45) Clark, J., Keaton, A., Sahu, A., Kaira, S., Mahajan, S., and Gudger, J. (1998) Neuropeptide Y (NPY) levels in alcoholic and food restricted male rats: implications for site selective function. *Regul. Pept.* 25, 335-345.
- (46) Roy, A., and Pandey, S. C. (2002) The decreased cellular expression of neuropeptide Y protein in rat brain structures during ethanol withdrawal after chronic ethanol exposure. *Alcohol. Clin. Exp. Res.* 26, 796-803.
- (47) Badia-Elder, N. E., Stewart, R. B., Powrozek, T. A., Roy, K. F., Murphy, J. M., and Li, T. K. (2001) Effect of neuropeptide Y (NPY) on oral ethanol intake in wistar, alcohol-preferring (P), and -nonpreferring (NP) rats. *Alcohol. Clin. Exp. Res.* 25, 386-390.
- (48) Thorsell, A. (2007) Neuropeptide Y (NPY) in alcohol intake and dependence. *Peptides* 28, 480-483.
- (49) Thiele, T. E., Koh, M. T., and Pedrazzini, T. (2002) Voluntary alcohol consumption is controlled via the neuropeptide Y Y<sub>1</sub> receptor. *J. Neurosci.* 22, RC208.
- (50) Thiele, T. E., Naveilhan, P., and Ernfors, P. (2000) Mutant mice lacking the Y<sub>2</sub> neuropeptide Y (NPY) receptor consume less ethanol than wild-type mice. *Alcohol. Clin. Exp. Res.* 2000, 97A.
-



- 
- (51) Heilig, M. (2004) The NPY system in stress, anxiety and depression. *Neuropeptides* 38, 213-224.
  - (52) Heilig, M., McLeod, S., Brot, M., Heinrichs, S. C., Menzaghi, F., Koob, G. F., and Britton, K. T. (1993) Anxiolytic-like action of neuropeptide Y: mediation by Y1 receptors in amygdala, and dissociation from food Intake effects. *Neuropsychopharmacology* 8, 357-363.
  - (53) Desai, S. J., Borkar, C. D., Nakhate, K. T., Subhedar, N. K., and Kokare, D. M. (2014) Neuropeptide Y attenuates anxiety- and depression-like effects of cholecystokinin-4 in mice. *Neuroscience* 277, 818-830.
  - (54) Wahlestedt, C., Pich, E., Koob, G., Yee, F., and Heilig, M. (1993) Modulation of anxiety and neuropeptide Y-Y1 receptors by antisense oligodeoxynucleotides. *Science* 259, 528-531.
  - (55) Decressac, M., Wright, B., David, B., Tyers, P., Jaber, M., Barker, R. A., and Gaillard, A. (2011) Exogenous neuropeptide Y promotes in vivo hippocampal neurogenesis. *Hippocampus* 21, 233-238.
  - (56) Howell, O. W., Silva, S., Scharfman, H. E., Sosunov, A. A., Zaben, M., Shatya, A., McKhann li, G., Herzog, H., Laskowski, A., and Gray, W. P. (2007) Neuropeptide Y is important for basal and seizure-induced precursor cell proliferation in the hippocampus. *Neurobiol. Dis.* 26, 174-188.
  - (57) DeCarolis, N. A., and Eisch, A. J. (2010) Hippocampal neurogenesis as a target for the treatment of mental illness: A critical evaluation. *Neuropharmacology* 58, 884-893.
  - (58) Meurs, A., Clinckers, R., Ebinger, G., Michotte, Y., and Smolders, I. (2007) Clinical potential of neuropeptide Y receptor ligands in the treatment of epilepsy. *Curr. Top. Med. Chem.* 7, 1660-1674.
  - (59) Nilsson, T., Cantera, L., and Edvinsson, L. (1996) Presence of neuropeptide Y Y<sub>1</sub> receptor mediating vasoconstriction in human cerebral arteries. *Neurosci. Lett.* 204, 145-148.
  - (60) Edvinsson, L., Ekblad, E., Håkanson, R., and Wahlestedt, C. (1984) Neuropeptide Y potentiates the effect of various vasoconstrictor agents on rabbit blood vessels. *Br. J. Pharmacol.* 83, 519-525.
  - (61) Pedrazzini, T., Seydoux, J., Künstner, P., Aubert, J.-F., Grouzmann, E., Beermann, F., and Brunner, H. R. (1998) Cardiovascular response, feeding behavior and locomotor activity in mice lacking the NPY Y1 receptor. *Nat. Med.* 4, 722-726.
  - (62) Wiest, R., Jurzik, L., Moleda, L., Froh, M., Schnabl, B., Hörsten, S. v., Schölmerich, J., and Straub, R. H. (2006) Enhanced Y1-receptor-mediated vasoconstrictive action of neuropeptide Y (NPY) in superior mesenteric arteries in portal hypertension. *J. Hepatol.* 44, 512-519.
  - (63) Crnkovic, S., Egemnazarov, B., Jain, P., Seay, U., Gattinger, N., Marsh, L. M., Bálint, Z., Kovacs, G., Ghanim, B., Klepetko, W., Schermuly, R. T., Weissmann, N., Olschewski, A.,
-

- and Kwapiszewska, G. (2014) NPY/Y1 receptor-mediated vasoconstrictory and proliferative effects in pulmonary hypertension. *Br. J. Pharmacol.* 171, 3895-3907.
- (64) Ruscica, M., Dozio, E., Boghossian, S., Bovo, G., Riano, V. M., Motta, M., and Magni, P. (2006) Activation of the Y<sub>1</sub> receptor by neuropeptide Y regulates the growth of prostate cancer cells. *Endocrinology* 147, 1466-1473.
- (65) Reubi, J. C., Gugger, M., and Waser, B. (2002) Co-expressed peptide receptors in breast cancer as a molecular basis for *in vivo* multireceptor tumour targeting. *Eur. J. Nucl. Med. Mol. Imaging* 29, 855-862.
- (66) Körner, M., and Reubi, J. C. (2006) Chapter 62 - Somatostatin and NPY, in *Handbook of Biologically Active Peptides* (Abba, J. K., Ed.) pp 435-441, Academic Press, Burlington.
- (67) Guérin, B., Dumulon-Perreault, V., Tremblay, M.-C., Ait-Mohand, S., Fournier, P., Dubuc, C., Authier, S., and Bénard, F. (2010) [Lys(DOTA)<sup>4</sup>]BVD15, a novel and potent neuropeptide Y analog designed for Y<sub>1</sub> receptor-targeted breast tumor imaging. *Bioorg. Med. Chem. Lett.* 20, 950-953.
- (68) Guérin, B., Ait-Mohand, S., Tremblay, M.-C., Dumulon-Perreault, V. r., Fournier, P., and Bénard, F. o. (2009) Total solid-phase synthesis of NOTA-functionalized peptides for PET imaging. *Org. Lett.* 12, 280-283.
- (69) Liu, M., Mountford, S. J., Zhang, L., Lee, I. C., Herzog, H., and Thompson, P. E. (2013) Synthesis of BVD15 peptide analogues as models for radioligands in tumour imaging. *Int. J. Pept. Res. Ther.* 19, 33-41.
- (70) Liu, M. (2012) in *Monash Institute of Pharmaceutical Sciences*, Monash University, Australia.
- (71) Mountford, S. J., Liu, M., Zhang, L., Groenen, M., Herzog, H., Holliday, N. D., and Thompson, P. E. (2014) Synthetic routes to the Neuropeptide Y Y1 receptor antagonist 1229U91 and related analogues for SAR studies and cell-based imaging. *Org. Biomol. Chem.* 12, 3271-3281.
- (72) Northfield, S. E., Mountford, S. J., Wielens, J., Liu, M., Zhang, L., Herzog, H., Holliday, N. D., Scanlon, M. J., Parker, M. W., Chalmers, D. K., and Thompson, P. E. (2015) Propargyloxypyrroline regio- and stereoisomers for click-conjugation of peptides: synthesis and application in linear and cyclic peptides. *Aust. J. Chem.* 68, 1365-1372.
- (73) McCrea, K. E., and Herzog, H. (2000) Radioligand binding studies: pharmacological profiles of cloned Y-receptor subtypes. *Methods Mol. Biol.* 153, 231-239.
- (74) Kilpatrick, L. E., Briddon, S. J., and Holliday, N. D. (2012) Fluorescence correlation spectroscopy, combined with bimolecular fluorescence complementation, reveals the effects of  $\beta$ -arrestin complexes and endocytic targeting on the membrane mobility of neuropeptide Y receptors. *Biochim. Biophys. Acta.* 1823, 1068-1081.
- (75) Kilpatrick, L. E., Briddon, S. J., Hill, S. J., and Holliday, N. D. (2010) Quantitative analysis of neuropeptide Y receptor association with  $\beta$ -arrestin2 measured by bimolecular fluorescence complementation. *Br. J. Pharm* 160, 892-906.

---

## CHAPTER 4      Synthesis of Fluorescently Labelled Peptidic Ligands Targeting Neuropeptide Y Y<sub>4</sub> Receptors Based On the Dimeric Y<sub>4</sub> Agonist BVD-74D Scaffold

---

---

### Table of Contents

4.1	Introduction to Y <sub>4</sub> Receptor and Its Ligands.....	4-2
4.1.1	Physiological Functions and Clinical Relevance of Y <sub>4</sub> Receptors.....	4-2
4.1.2	Y <sub>4</sub> Receptor Ligands.....	4-4
4.2	Synthesis of Dicarba-Linked Peptides Using Metathesis Reactions.....	4-8
4.3	Synthesis of Peptide Esters.....	4-10
4.4	Objectives.....	4-11
4.5	Optically Pure, Structural and Fluorescent Analogues of a Dimeric Y <sub>4</sub> Receptor Agonist Derived by an Olefin Metathesis Approach .....	4-11
4.6	Summary .....	4-23
	References.....	4-24

## 4.1 Introduction to Y<sub>4</sub> Receptor and Its Ligands

The human Y<sub>4</sub> receptor (hY<sub>4</sub>R) was first cloned by Lundell *et al.* in 1995. It was previously named the PP1 receptor owing to its high selectivity toward its endogenous ligand pancreatic polypeptide (PP). Indeed, hY<sub>4</sub>R exhibits approximately 100- and 700-fold stronger affinity to hPP than to hPYY and hNPY respectively, probably because of the relatively low amino acid sequence homology (43%) shared between hY<sub>4</sub>R and hY<sub>1</sub>R.<sup>(1)</sup> The rat rY<sub>4</sub>R possesses an overall identity of only 46% compared to rY<sub>1</sub>R and 75% to its human orthologue hY<sub>4</sub>R.<sup>(2)</sup>

Pancreatic polypeptide (**Figure 4-1**), a 36-amino acid C-terminal amidated polypeptide that belongs to the NPY peptide family, is produced by “F cells” in the pancreatic islets of Langerhans in response to vagal stimuli during meals.<sup>(3, 4)</sup> Unlike NPY, PP exhibits substantial variations (approx. 50%) in sequence across species.<sup>(2, 5)</sup>

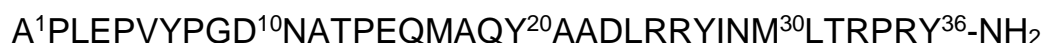


**Figure 4-1:** The amino acid sequence of human pancreatic polypeptide (PP).

### 4.1.1 Physiological Functions and Clinical Relevance of Y<sub>4</sub> Receptors

#### 4.1.1.1 Y<sub>4</sub> Receptors in Regulation of Energy Homeostasis

Y<sub>4</sub>Rs appear to co-operate with Y<sub>1</sub>Rs in regulating energy homeostasis. In contrast to Y<sub>1</sub>R, activation of the PP/Y<sub>4</sub>R signalling cascade suppresses appetite and gastric emptying rate, while it promotes energy expenditure. For instance, PP administration improved insulin resistance and hypercholesterolaemia in genetically obese *ob/ob* mice.<sup>(6)</sup> Another study using Y<sub>4</sub>R knockout mice observed an increase in body weight without changes in daily food intake.<sup>(7)</sup> Consistently in human subjects, plasma PP levels appeared to elevate in patients with anorexia nervosa and decrease in those with

obesity.(8-10) A clinical study demonstrated that PP administration induced satiety in patients with Prader-Willi Syndrome,(11) a medical condition characterised by deficiency of basal and postprandial PP, childhood-onset hyperphagia, morbid obesity and mental retardation.(12, 13) Although not fully understood, the PP/Y<sub>4</sub>R cascade has been found to inhibit expression of central orexigenic peptides such as NPY and orexin, and stimulate expression of peripheral anorexigenic peptides such as ghrelin.(6, 14, 15) Therefore, Y<sub>4</sub>R selective ligands may have significant potential as candidates for developing pharmaceuticals that address eating disorders.

Another metabolic disorder that Y<sub>4</sub>R/PP signalling system is implicated in is pancreatogenic diabetes. In contrast to the commonly known type 1 and 2 diabetes mellitus, pancreatogenic diabetes is often secondary to pancreatic tissue destruction and diminished insulin sensitivity. A typical example is chronic pancreatitis (CP), which is associated with recurring tissue inflammation and fibrosis, followed by insulin receptor down-regulation selectively in hepatocytes.(16, 17) In CP animal models, PP deficiency and compensatory over-expression of pancreatic Y<sub>4</sub>R have been observed.(18) Consistently, clinical studies showed improved insulin sensitivity and glucose tolerance following continuous PP infusion in CP patients with underlying PP deficiency.(17, 19, 20)

#### **4.1.1.2 Y<sub>4</sub> Receptors in Anxiety- and Depression-Like Behaviour**

Y<sub>4</sub>R activation is speculated to facilitate expression of anxiety and depression under unfamiliar and stressful conditions, in co-ordination with Y<sub>2</sub>R.(21) It is demonstrated that Y<sub>4</sub>R knockout mice exhibited less anxiety-related behaviour in marble burying test and light/dark test, as well as improved immobility in forced swimming and tail suspension test.(21-23) Contradictory results have been obtained by Painsipp *et al.*, who performed immune challenge on mice with either Y<sub>2</sub>R- or Y<sub>4</sub>R-knockout by single injection of

bacterial lipopolysaccharide (LPS).(24) They demonstrated that while the LPS-induced anxiety-like behaviour was short-term in  $Y_2^{-/-}$  mice, it persistently increased in  $Y_4^{-/-}$  mice. The short-term depression-related behaviour was seen only in  $Y_2^{-/-}$  but absent in  $Y_4^{-/-}$  mice; however, both genotypes developed long-term depression-related behaviour.(24) Although the reasons for these contradictions have not been fully elucidated, it can be speculated that  $Y_4R$  may be a target of prospective anxiolytics and anti-depressives that address more specific neurochemical dysfunctions.

#### **4.1.2 $Y_4$ Receptor Ligands**

As previously discussed, truncated peptidic ligands with reasonable  $Y_4R$  affinity and selectivity are ideal starting compounds to develop fluorescently labelled  $Y_4R$  ligands. The following section briefly reviews some literature documented  $Y_4R$  agonists and antagonists.

##### **4.1.2.1 Reported $Y_4$ Receptor Agonists**

A number of peptidic  $Y_4R$  agonists have been described in the literature. Berlicki *et al.* demonstrated that the truncated linear hPP and porcine NPY (pNPY) analogues  $[Nle^{30}]hPP_{25-36}$  and  $[Leu^{34}]pNPY_{25-36}$  were relatively potent  $Y_4R$  selective partial agonists. Their further work incorporating synthetic cyclic amino acids showed that the analogues  $[Nle^{30}, \beta Cpe^{34}]hPP_{25-36}$  and  $[\beta Cpe^{34}]hNPY_{25-36}$  (**Figure 4-2A, B**) possessed enhanced  $Y_4R$  affinity, however the former also substantially lost  $Y_4R$  selectivity relative to  $Y_1R$  and  $Y_2R$ . Furthermore, replacing  $\beta Cpe^{34}$  with  $\beta Cbu$  (**Figure 4-2C, D**) in these analogues resulted in slightly reduced  $Y_4R$  affinity but increased  $Y_4R$  selectivity. In summary, these findings showed various conformationally constrained amino acids at the 34-position could influence the pharmacological profiles of analogues in different manners.(25, 26)

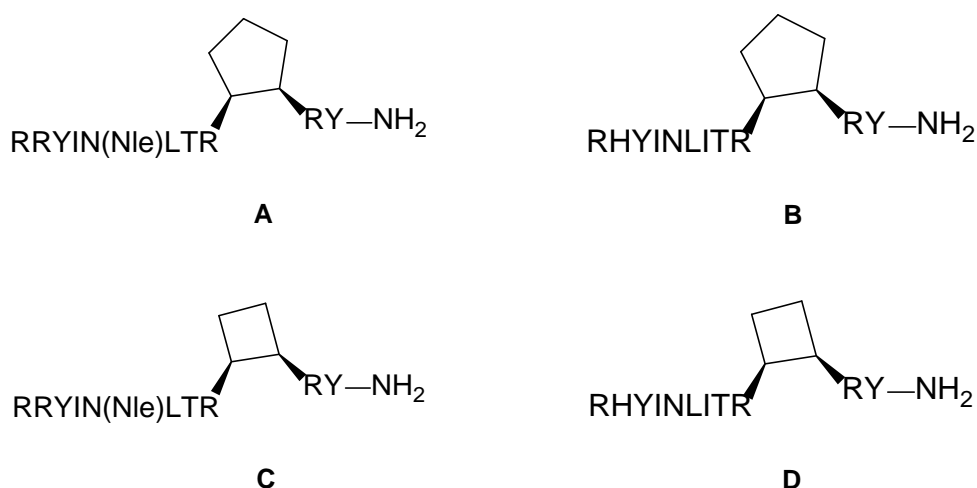


**Figure 4-2:** Cyclic amino acid containing peptide analogues reported by Berlicki *et al.*  
**A:** [Nle<sup>30</sup>,  $\beta$ Cpe<sup>34</sup>]hPP<sub>25-36</sub>; **B:** [ $\beta$ Cpe<sup>34</sup>]hNPY<sub>25-36</sub>; **C:** [Nle<sup>30</sup>,  $\beta$ Cbu<sup>34</sup>]hPP<sub>25-36</sub>; **D:** [ $\beta$ Cbu<sup>34</sup>]hNPY<sub>25-36</sub>.

Homodimeric peptides with Y<sub>4</sub>R agonism have also been reported. Daniels *et al.* produced the dimer *bis*(29/31', 29'/31)[(Glu<sup>29</sup>, Pro<sup>30</sup>, Dpa<sup>31</sup>, Tyr<sup>32</sup>, Leu<sup>34</sup>)NPY<sub>28-36</sub>] cross-linked via two lactam bridges between Glu<sup>29</sup> and Dpa<sup>31</sup> (Dpa = diaminopropionic acid). This analogue, known as GR231118 or 1229U91, is a potent Y<sub>4</sub>R agonist but also more selective towards Y<sub>1</sub>R.(27-29) Other researchers argued that GR231118 possessed equally potent Y<sub>4</sub>R agonism and Y<sub>1</sub>R antagonism.(30, 31) Balasubramaniam *et al.* reported a series of dimeric pentapeptide scaffolds. Their N-Cys disulfide-linked T-190 analogue (**Figure 4-3A**) showed Y<sub>1</sub>R antagonism and moderately potent Y<sub>4</sub>R agonism.(27, 32) Replacing the disulfide linkage with a series of stable diamino-dicarboxyl chains (**Figure 4-3B**) resulted in similarly potent full Y<sub>4</sub>R agonists with improved selectivity.(33)

Balasubramaniam *et al.* further modified these analogues by substituting Trp and Nva with Tyr and Leu respectively, and replacing the cross-linker with the cystine isostere 2,7-diaminosuberoyl group (**Figure 4-3C**). The resulting analogue BVD-74D exhibited comparably strong picomolar Y<sub>4</sub>R affinity to that of endogenous hPP ( $K_i = 0.05$  nM vs.  $K_i = 0.08$  nM). It also showed 150-fold stronger selectivity to Y<sub>4</sub>R than to Y<sub>1</sub>R, and no affinity

to Y<sub>2</sub>R and Y<sub>5</sub>R.(33) In pharmacological studies, BVD-74D showed potent inhibitory effects on food intake, comparable to endogenous PP, in fasting rats.(33)

From the structural perspective, the amino acid sequence of BVD-74D actually represents the dimerised version of the 5-amino acid C-terminal fragment of the BVD-15 scaffold. The SAR is in agreement with the findings that Arg<sup>33</sup>, Arg<sup>35</sup>, Tyr<sup>36</sup> and the C-terminal amide in PP were all crucial for Y<sub>4</sub>R binding, while the 34-position was of minor importance.(29)

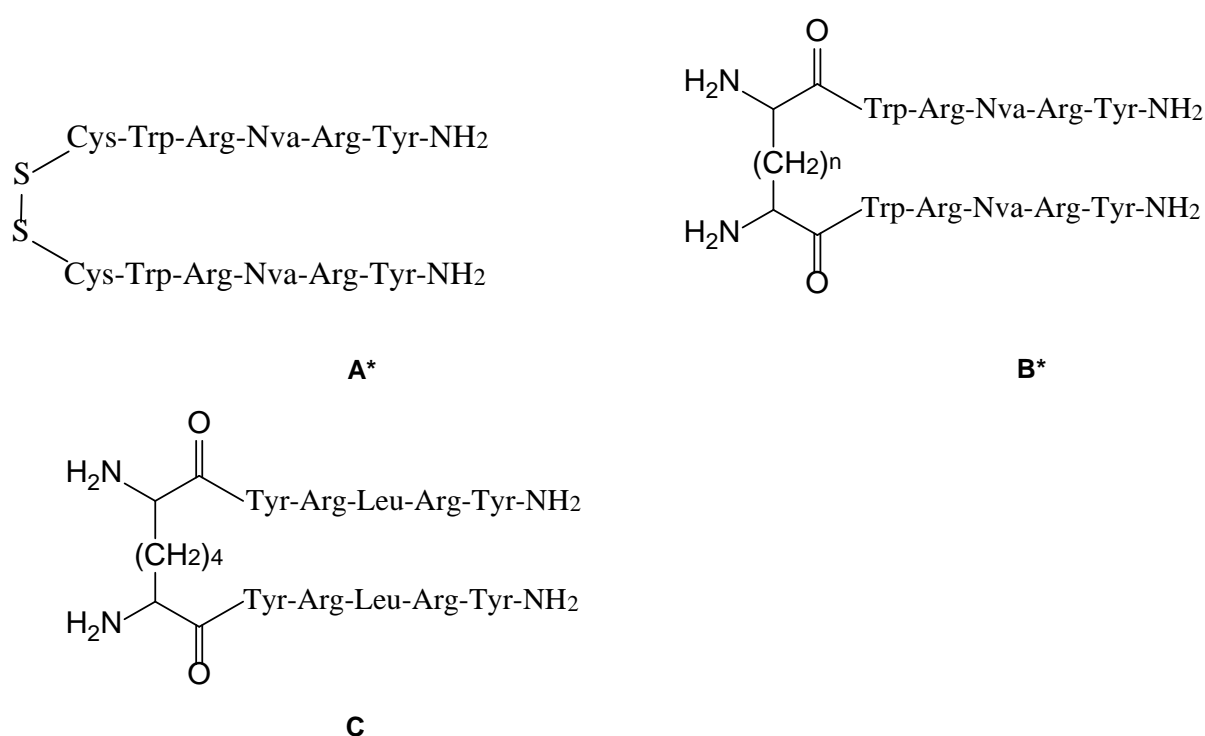


**Figure 4-3:** Dimeric peptides reported by Balasubramaniam *et al.* **A:** T-190; **B:** a series of diamino-dicarboxyl linked dimers; **C:** BVD-74D. \* Nva = norvaline

However, the literature BVD-74D is a mixture of inseparable diastereomers, consisting of both (2*S*,7*S*)- and (2*R*,7*R*)-diaminosuberoyl containing peptides, as it was synthesised using the commercially available N<sup>α</sup>-di-Boc-D/L-diaminosuberic acid (**Figure 4-4**).(33)



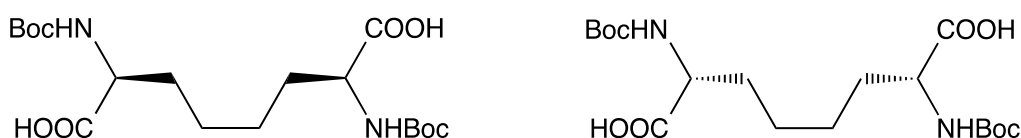


**Figure 4-4:** Structure of the stereoisomer mixture N<sup>α</sup>-di-Boc-D/L-diaminosuberic acid

#### 4.1.2.2 Reported Y<sub>4</sub> Receptor Antagonists

To date there are only a handful of Y<sub>4</sub>R antagonists documented in the literature. Ziemek *et al.* reported an acylguanidine-based small-molecule ligand (**Figure 4-5A**) with weak Y<sub>4</sub> antagonism,<sup>(34)</sup> which was subsequently modified to obtain a 20-fold increase in activity (**Figure 4-5B**). Unfortunately, further investigation was discontinued as attempts in synthesising its analogues not only failed to improve activity, but also resulted in significant cytotoxicity.<sup>(26)</sup>

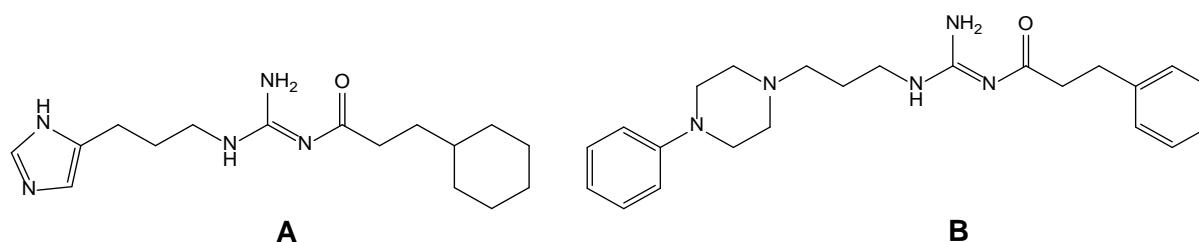


**Figure 4-5:** The Y<sub>4</sub>R antagonists reported by Ziemek *et al.*

The peptidic Y<sub>4</sub>R antagonist VD-11 *bis*(29/31', 29'/31)[(Glu<sup>29</sup>, Pro<sup>30</sup>, Dpa<sup>31</sup>, Tyr<sup>32</sup>, Leu<sup>34</sup>, (Tyr-O-CH<sub>3</sub>)<sup>36</sup>)NPY<sub>28-36</sub>] represents the C-terminal oxymethylated derivative of GR231118.<sup>(35, 36)</sup> At first, Balasubramaniam *et al.* demonstrated its competitive antagonism selectively at Y<sub>1</sub>R using radioreceptor and cAMP assays. They did not observe any Y<sub>4</sub>R antagonism, although it also showed reasonable Y<sub>4</sub>R affinity.<sup>(36)</sup> However, Parker *et al.* later found that VD-11 failed to incur Y<sub>4</sub>R internalisation and competitively inhibited Y<sub>4</sub>R activation by GR231118 in <sup>35</sup>S-GTP binding assays.<sup>(35)</sup> Therefore, the functional data of VD-11 peptide remain questionable, and the influence of

the C-terminal methyl ester on Y receptor selectivity should be further clarified, for which an efficient synthesis strategy is required.

## 4.2 Synthesis of Dicarba-Linked Peptides Using Metathesis Reactions

As described above, the literature BVD-74D peptide contains 2,7-diaminosuberoyl group as a cystine isostere and while this is perhaps the sole example of an inter-chain bridge in a peptide dimer, many cross-linked peptides have been synthesised using “dicarba” bridges as a replacement for an intra-chain disulfide bond. Such linkages are capable of modifying biological activity, mimicking naturally occurring peptide secondary structures and enhancing chemical and metabolic stability compared to disulfide bonds.(37-39) Indeed, peptide analogues based on  $\beta$ -ANP,(40) vasopressin(41) and calcitonin(42) have been previously prepared by using aminosuberic acid. The diaminosuberoyl linkage in BVD-74D, however, is more challenging to synthesise owing to its two chiral centres. This molecule has been previously prepared by alkylation of a chiral bislactimether (Schöllkopf technology) or Kolbe electrolysis of protected glutamic acid. However, the former strategy involved a complicated multistep synthetic route, while the latter may generate at least four side products, causing low yield and difficult purification.(43, 44) Another method, involving a Wittig-Horner reaction between phosphonoglycine and butanedial, required separation of chiral products.(45)

Metathesis reactions have emerged as an excellent strategy towards preparation of dicarba bridge-linked peptidomimetics. Metathesis reactions, first discovered in the 1930's, involve the exchange of two carbenes in an olefin to produce two symmetrical olefins, or two carbynes in an alkyne to give two symmetrical alkynes.(46) Since then, metathesis reactions have been the interest of many research groups and numerous efforts were taken in development of efficient catalysts. In 2005, three scientists with remarkable

contribution in this field were awarded the Nobel Prize in Chemistry. Chauvin and his group first proposed the reaction mechanism in 1971,(47) and Schrock's group in 1980-90's proved this proposal after successfully producing some highly active molybdenum- and tungsten-alkylidene based catalysts.(48-50) Based on their work, Grubb's group then described their discovery of a series of ruthenium-containing catalysts, which are commercially available and are the most popular metathesis catalysts today. Significantly, Grubbs catalysts (1<sup>st</sup> and 2<sup>nd</sup> generations) are both stable in air and compatible to many functional groups, although amines and nitriles can cause catalyst poisoning (**Figure 4-6**).(46, 51) The most recent Hoveyda-Grubbs catalyst 2<sup>nd</sup> generation is a phosphine-free derivative with similar reactivity but good solubility in water.(52)

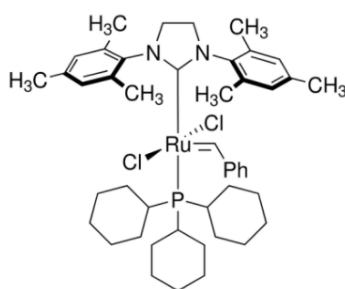


**Figure 4-6:** Structure of Grubbs catalyst 2<sup>nd</sup> generation used in this project.

Cross metathesis (CM) specifically refers to the transalkylidenation of two terminal olefins to form an unsaturated dicarba bridge, and ethene as the by-product (**Figure 4-7**). Subsequent hydrogenation can then readily achieve the desired saturated bond. The new olefins are non-stereoselective; in principle, apart from the heterodimer formed by the two different olefins, each olefin can also homo-dimerise to form six products in total (**Figure 4-8**). In synthesis of peptidomimetics, dicarba-linkages are often achieved between two allylglycine residues, where stereoselectivity is not a concern (**Figure 4-9**).(53, 54) Following this route, analogues of more complex peptides with multiple intra-molecular cycles have also been produced.(55-57)

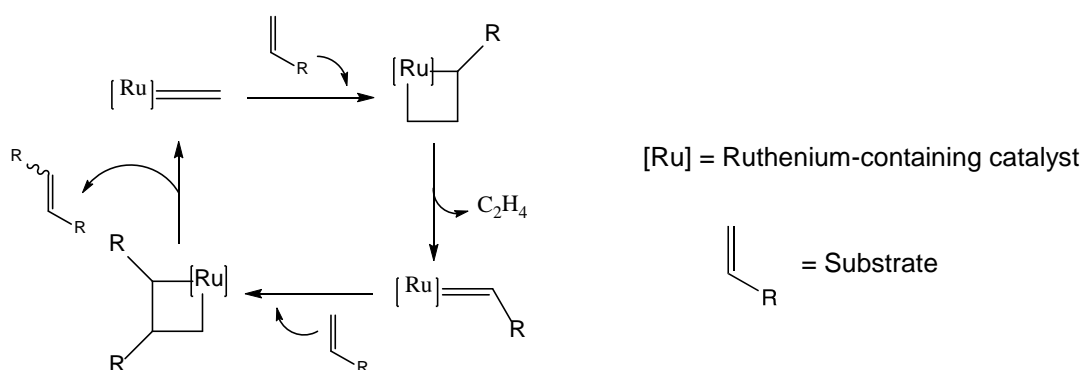


**Figure 4-7:** Mechanism of cross metathesis reactions.

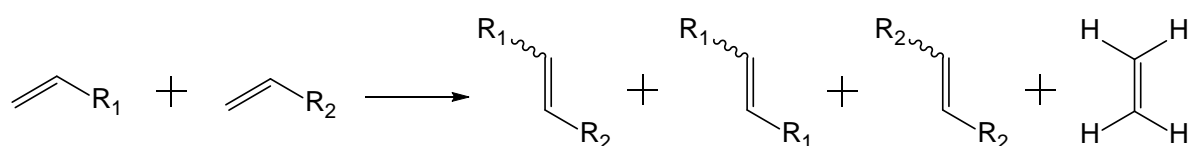


**Figure 4-8:** Cross metathesis reactions are non-selective.

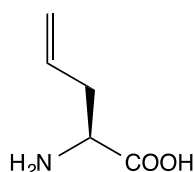


**Figure 4-9:** Structure of L-allylglycine.

### 4.3 Synthesis of Peptide Esters

Esterification is an important modification strategy that may improve certain desired properties of synthetic peptides. It is typically applied in preparing pro-drugs with increased lipophilicity that enhances membrane penetration and duration of action. Upon reaching the desired site of action, the pro-drugs can be rapidly metabolised into its active form.(58-61) Esters may also influence peptide 3D conformations and thus modify pharmacological activities. For instance, converting BVD-15 and 1229U91 scaffolds into their methyl esters has been shown to abolish their Y<sub>4</sub>R agonism.(36, 62) In addition, esters may also serve to protect against peptidases by masking the carboxylic group, thus improve peptide

metabolic stability. This can be highly favourable in formulating peptide-like drugs owing to their short plasma half-life.

Only a few strategies toward synthesising peptide esters have been reported. Balasubramaniam *et al.* reported their solid phase method using Merrifield resin; however, it required prolonged reflux at elevated temperature and potentially hazardous HF handling.(36) Turner *et al.* employed one-pot cleavage and esterification with anhydrous methanolic HCl, and successfully generated a series of peptide esters.(63) Other approaches include utilising either solution phase peptide synthesis or hydrazide resin linkages.(64-66)

#### **4.4 Objectives**

The high-affinity Y<sub>4</sub>R selective agonist BVD-74D peptide represented an ideal parent compound for conjugation of fluorophores; however, its optically pure stereoisomers had not been synthesised and thus it was unclear which stereoisomer contributed to the pharmacological profiles. In this chapter we report our work on synthesising optically pure structural and fluorescently labelled BVD-74D analogues for *in vitro* Y<sub>4</sub>R studies. Significantly, we here demonstrate our convenient and robust synthesis strategies in preparation of optically pure stereoisomers by exploiting alkene metathesis reactions between suitably protected allylglycine residues with the desired stereo-configuration.

#### **4.5 Optically Pure, Structural and Fluorescent Analogues of a Dimeric Y<sub>4</sub> Receptor Agonist Derived by an Olefin Metathesis Approach**

The complete work on synthesising optically pure BVD-74D structural and fluorescent analogues has been published in Journal of Medicinal Chemistry (full paper attached below).

# Optically Pure, Structural, and Fluorescent Analogues of a Dimeric Y<sub>4</sub> Receptor Agonist Derived by an Olefin Metathesis Approach

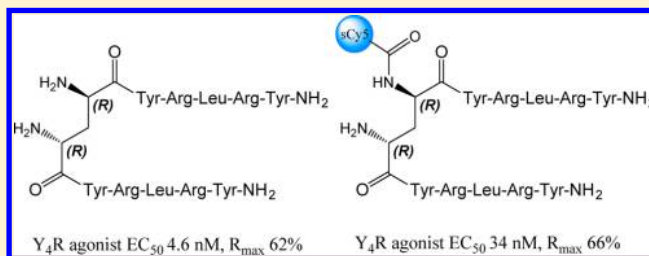
Mengjie Liu,<sup>†</sup> Simon J. Mountford,<sup>†</sup> Rachel R. Richardson,<sup>‡</sup> Marleen Groenen,<sup>‡</sup> Nicholas D. Holliday,<sup>‡</sup> and Philip E. Thompson<sup>\*,†</sup>

<sup>†</sup>Medicinal Chemistry, Monash Institute of Pharmaceutical Sciences, Monash University, 381 Royal Parade, Parkville, Victoria 3052, Australia

<sup>‡</sup>School of Life Sciences, University of Nottingham, Queen's Medical Centre, Derby Road, Nottingham NG7 2UH, United Kingdom

## Supporting Information

**ABSTRACT:** The dimeric peptide **1** (BVD-74D, as a diastereomeric mixture) is a potent and selective neuropeptide Y Y<sub>4</sub> receptor agonist. It represents a valuable candidate in developing traceable ligands for pharmacological studies of Y<sub>4</sub> receptors and as a lead compound for antiobesity drugs. Its optically pure stereoisomers along with analogues and fluorescently labeled variants were prepared by exploiting alkene metathesis reactions. The (2*R*,7*R*)-diaminosuberoyl containing peptide, (2*R*,7*R*)-**1**, had markedly higher affinity and agonist efficacy than its (2*S*,7*S*)-counterpart. Furthermore, the sulfo-Cy5 labeled (2*R*,7*R*)-**14** retained high agonist potency as a novel fluorescent ligand for imaging Y<sub>4</sub> receptors.



## INTRODUCTION

The physiological functions of three polypeptides that form the NPY peptide family, neuropeptide Y (NPY)<sup>1</sup> peptide YY (PYY),<sup>2</sup> and pancreatic polypeptide (PP),<sup>3</sup> are mediated by Y receptors, where four subtypes have been identified in human: Y<sub>1</sub>R, Y<sub>2</sub>R, Y<sub>4</sub>R, and Y<sub>5</sub>R. All subtypes belong to the rhodopsin-like G<sub>i</sub> coupled G protein-coupled receptor (GPCR) superfamily.<sup>4</sup> These Y receptor subtypes exhibit different binding affinity to the three members of the NPY peptide family. It was found that Y<sub>1</sub>R and Y<sub>2</sub>R exhibit similar affinity to NPY and PYY but poor affinity to PP. Y<sub>4</sub>R is a PP-selective subtype with lower affinity for NPY and PYY. Lastly, all three peptides are equally potent at Y<sub>5</sub>R.<sup>5</sup>

Activation of the PP/Y<sub>4</sub>R signaling system induces satiety and promotes energy expenditure. This suggests that Y<sub>4</sub>R agonists may become clinically useful antiobesity drugs, while Y<sub>4</sub>R antagonists may have potential as orexigenic agents to treat anorexia.<sup>6–9</sup> In developing such ligands, truncated peptide analogues are becoming increasingly popular. For example, [Nle<sup>30</sup>]hPP<sub>25–36</sub> and [Leu<sup>34</sup>]pNPY<sub>25–36</sub> were found to be Y<sub>4</sub>R selective partial agonists,<sup>10</sup> and a nonapeptide based on the C-terminal fragment of NPY, Ile-Asn-Pro-Ile-Tyr-Arg-Leu-Arg-Tyr-NH<sub>2</sub>, exhibits moderate Y<sub>4</sub>R agonism and Y<sub>1</sub>R competitive antagonism with similar potency.<sup>11–13</sup> Its lactam-bridged dimeric variant bis(29/31', 29/31')[(Glu<sup>29</sup>, Pro<sup>30</sup>, Dpa<sup>31</sup>, Tyr<sup>32</sup>, Leu<sup>34</sup>)-NPY<sub>28–36</sub>], also known as 1229U91, showed enhanced potency at both receptor subtypes but is in particular the most potent known Y<sub>1</sub>R antagonist.<sup>13–17</sup>

Another of several highly potent Y receptor ligands based upon dimeric C-terminal sequences is D/L-2,7-diaminooctanedioyl-bis(YRLRY-NH<sub>2</sub>), **1** (BVD-74D)<sup>18</sup> (Figure 1). This peptide exhibited comparable Y<sub>4</sub>R affinity with the native hPP (K<sub>i</sub> =

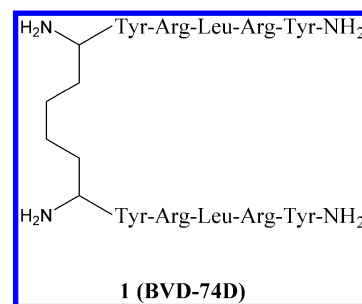


**Figure 1.** Peptide **1** reported by Balasubramaniam et al. is a diastereomeric mixture of the (2*S*,7*S*)- and (2*R*,7*R*)-diaminooctanedioyl stereoisomers.

0.05 nM vs 0.08 nM) and showed 150-fold selectivity for Y<sub>4</sub>R over Y<sub>1</sub>R, and negligible affinity to Y<sub>2</sub>R and Y<sub>5</sub>R. In fasted rat subjects, **1** showed equally potent inhibitory effects on food intake as the endogenous PP.<sup>18</sup> A later study also reported that **1** significantly reduced food intake, water intake, and weight gain in mice fed with normal and high-fat diet.<sup>19</sup> However, the reported compound is, in fact, a mixture of diastereomers composed of the (2*S*,7*S*)- and (2*R*,7*R*)-diaminooctanedioyl-containing stereoisomers<sup>18</sup> and they are inseparable by RP-HPLC. Therefore, it was unclear which stereoisomer contributed to the in vitro and in vivo pharmacological activity.

We aimed to resolve this issue and set a platform for the broader investigation of Y<sub>4</sub>R pharmacology by the synthesis of optically pure stereoisomers of **1** and related analogues that

**Received:** February 29, 2016

**Published:** June 13, 2016

probe the role of the bridging group and the role of the dimeric structure in facilitating high affinity. We hereby present our work on synthesis of a series of optically pure analogues of (S,S)-1 and (R,R)-1 along with their fluorescently labeled variants. We developed methodology for preparing the dimeric peptides utilizing Grubbs metathesis, either in the synthesis of optically pure 2,7-diaminosuberic acid building blocks or the on resin metathesis of monomeric precursor peptides.<sup>20–22</sup> Those peptide analogues were analyzed using cell-based Y<sub>4</sub>R competition binding assays and  $\beta$ -arrestin recruitment assays to identify the (R,R)-diastereomers as the high affinity constituent of 1 and the corresponding fluorescent analogues.

## RESULTS AND DISCUSSION

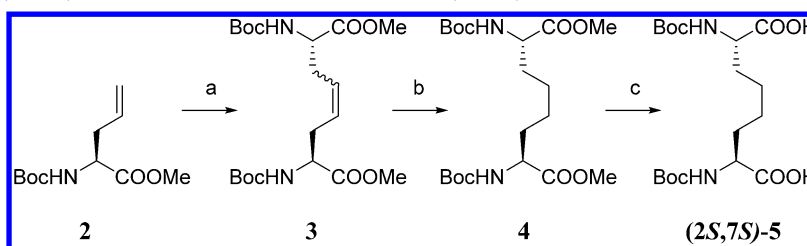
**Chemistry.** The main challenge in developing a convenient and robust strategy for synthesizing optically pure dimeric 1 analogues was to identify an optimal condition for metathesis reactions. Two different approaches were attempted. The first approach involved presynthesis of the 2,7-diaminosuberic acid unit then bis-coupling to the linear peptidyl resin, while the

second involved a solid phase cross-metathesis between two completed linear N-terminal allylglycine containing peptides.

**Synthesis of (S,S)-1 and (R,R)-1.** The synthesis of (2S,7S)-N,N-di-Boc-diaminosuberic acid, (2S,7S)-5, via metathesis was achieved by adapting the methods of Nolen et al.<sup>24</sup> and Ward et al.<sup>25</sup> (Scheme 1). The (S)-N-Boc-allylglycine methyl ester (2) was treated with Grubbs catalyst second generation in refluxing DCM overnight to obtain the desired alkene 3 in 95% yield. The intermediate 3 was then hydrogenated in the presence of 10% Pd/C, which gave 4 almost quantitatively. Finally, the desired product (2S,7S)-5 was generated by ester hydrolysis. Spectroscopic data for (2S,7S)-5 were consistent with that previously reported,<sup>23</sup> including the determined (–) optical rotation in DMF.<sup>26</sup> Experimental details are provided in the Supporting Information.

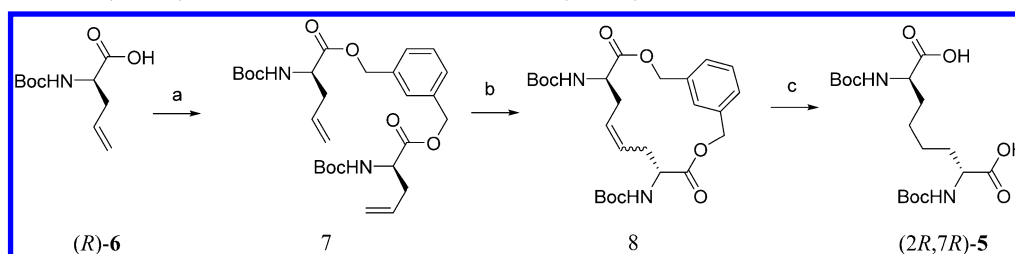
To prepare the (2R,7R)-N,N-di-Boc-diaminosuberic acid, (2R,7R)-5, we investigated the use of 1,3-benzenedimethanol as a “template” to enable selective ring-closure metathesis as reported previously (Scheme 2).<sup>27,28</sup> Esterification of Boc-D-allylglycine-OH (6) gave the diester 7, which was a substrate for RCM, and gave 8 in 54% yield. Finally, one-pot reduction

**Scheme 1.** Synthesis of (2S,7S)-N,N-Di-Boc-diaminosuberic Acid (2S,7S)-5<sup>a</sup>



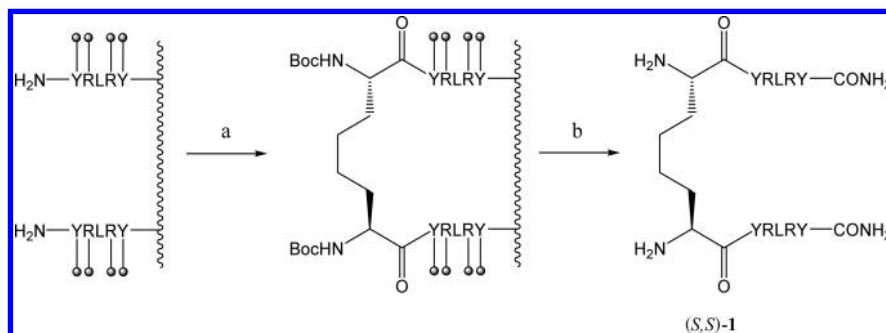
<sup>a</sup>Reagents and conditions: (a) Grubbs catalyst second generation, DCM, reflux, overnight, 95%; (b) 10% Pd/C, MeOH, H<sub>2</sub>, RT, overnight; (c) NaOH in H<sub>2</sub>O (6 mg/mL), MeOH, reflux, overnight, 50% (from 3).

**Scheme 2.** Synthesis of (2R,7R)-N,N-Di-Boc-diaminosuberic Acid (2R,7R)-5<sup>a</sup>



<sup>a</sup>Reagents and conditions: (a) 1,3-benzenedimethanol, EDCI, DMAP, DCM, RT, overnight, 56%; (b) Grubbs catalyst second generation, DCM, N<sub>2</sub>, reflux, overnight, 54%; (c) 10% Pd/C, MeOH, 1 atm H<sub>2</sub>, 53%.

**Scheme 3.** Synthesis of (S,S)-1 Using Presynthesized (2S,7S)-N,N-Di-Boc-diaminosuberic Acid 5<sup>a</sup>



<sup>a</sup>Reagents and conditions: (a) (2S,7S)-5, PyClock, DIPEA, DMF, RT, overnight; (b) reagent K, RT, 3 h.

and hydrogenolysis of **8** was achieved by treating with hydrogen in the presence of 10% Pd/C, affording (2*R*,7*R*)-**5**. Polarimetry confirmed the expected (+) optical rotation of the precursor.<sup>26</sup>

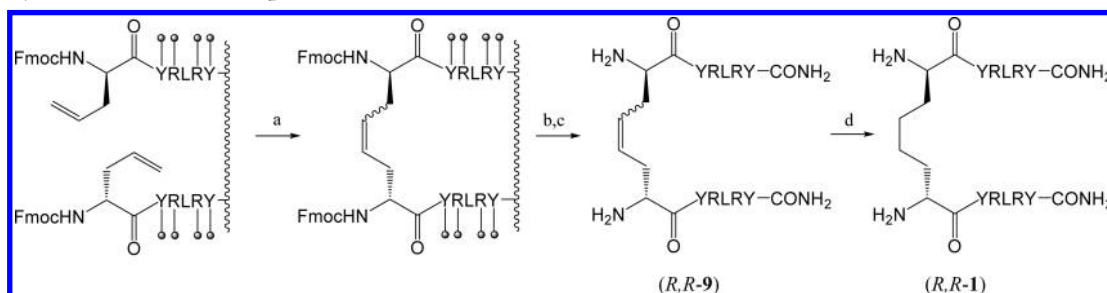
To further confirm the chiral integrity of the products, a chiral HPLC method was developed that showed that preparation of (2*S*,7*S*)-**5** and (2*R*,7*R*)-**5** was not accompanied by significant racemization either to each other or to the meso (2*R*,7*S*)-**5**<sup>29</sup> in these syntheses (see [Supporting Information](#)).

Having the protected building blocks in hand, dimeric peptide analogues (*S,S*)-**1** and (*R,R*)-**1** were prepared by conventional

solid-phase peptide synthesis ([Scheme 3](#)). After constructing the linear peptide chain on Rink amide resin, the coupling was carried out using 0.5 equiv of the Boc-protected 2,7-diaminosuberic acid (2*S*,7*S*)-**5** or (2*R*,7*R*)-**5** activated with PyClock and overnight incubation. After cleavage, the desired peptides were obtained and readily purified by RP-HPLC.

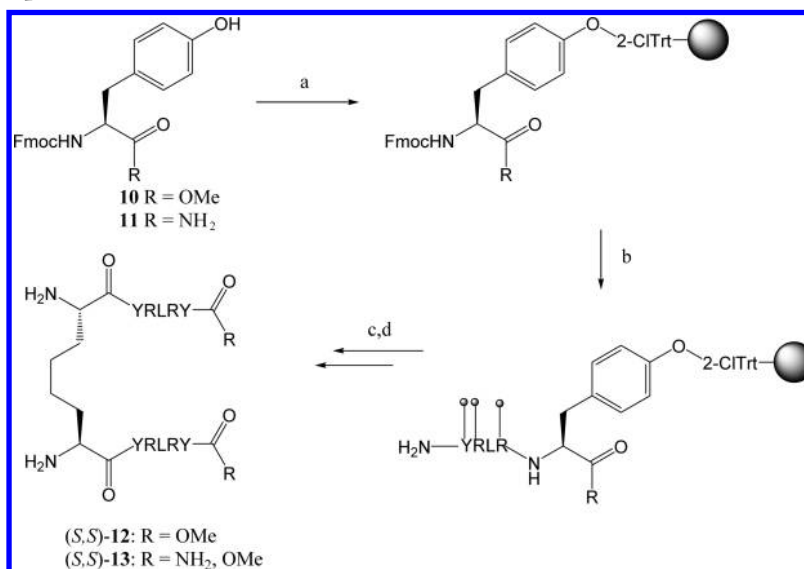
As an alternative approach, the synthesis of dimeric peptides was achieved by solid phase cross-metathesis of the corresponding resin-bound protected allylglycine containing peptides ([Scheme 4](#)). The monomeric peptide chain containing

**Scheme 4.** Synthesis of Dimeric Peptides (*R,R*)-**9** and (*R,R*)-**1** via Solid Phase Metathesis Reaction<sup>a</sup>



<sup>a</sup>Reagents and conditions: (a) Grubbs catalyst second generation, LiCl in DMF, DCM,  $\mu$ wave 100 °C, 3 h; (b) piperidine (20%) in DMF, RT, 5 min  $\times$  2; (c) reagent K, RT, 3 h; (d) Pd/C cartridge, H<sub>2</sub> (50 psi), EtOAc, 50 °C, 1 h.

**Scheme 5.** Synthesis of Peptides (*S,S*)-**12** and (*S,S*)-**13**<sup>a</sup>



<sup>a</sup>Reagents and conditions: (a) 2-chlorotriyl chloride resin, DIPEA, DCM, RT, overnight; (b) standard solid-phase synthesis; (c) **5**, PyClock, DIPEA, DMF, RT, overnight; (d) reagent K, RT, 3 h.

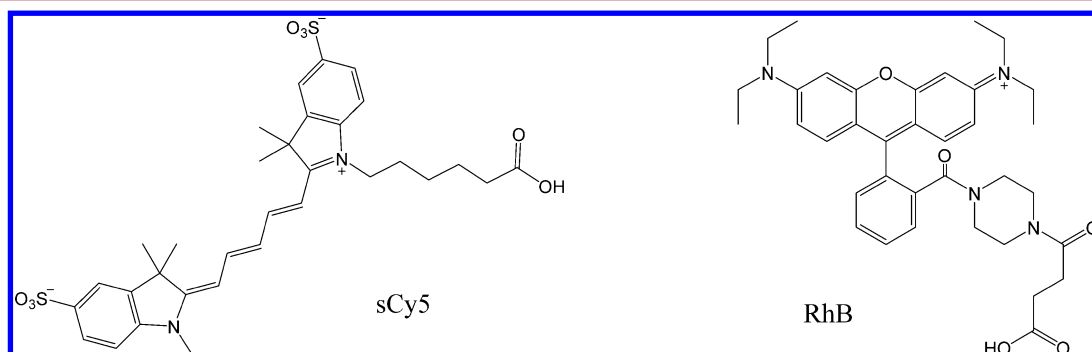


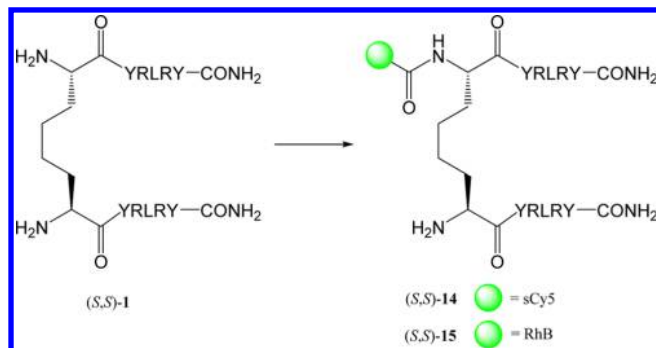
**Figure 2.** Structures of carboxy derivatized fluorophore reagents used: sulfo-Cy5 (sCy5) and rhodamine B (RhB).



either L- or D-allylglycine was first assembled following the standard Fmoc-based solid phase synthesis strategy, where the N-terminal Fmoc group was retained. The peptidyl-resin was then subject to cross-metathesis by treating with Grubbs catalyst second generation under deoxygenated conditions and microwave heating in the presence of LiCl as a chaotropic salt.<sup>21</sup> Fmoc deprotection followed by cleavage yielded the alkenyl peptides, (S,S)-9 and (R,R)-9.

The synthesis of (R,R)-1 was also achieved by hydrogenation of (R,R)-9 in the presence of 10% Pd/C in EtOAc (Scheme 4).

**Scheme 6. Example of Fluorophore Conjugation of (S,S)-1<sup>a</sup>**



<sup>a</sup>Reagents and condition: sCy5 or RhB (0.7 equiv), PyClock, DIPEA in DMF, RT, overnight.

While successful and operationally straightforward, the yield and purity of the crude peptide product was not as good as the same peptide made from presynthesized diaminosuberic acids as described above.

**Synthesis of Homo- and Heterodimeric Methyl Esters of (S,S)-1.** Having established efficient strategies for preparation of dimeric analogues with specified stereoconfiguration, we investigated the role of the C-terminal amides in Y<sub>4</sub>R interaction by replacing them as mono- or dimethyl esters. Our strategy was to utilize side chain anchoring to the resin to allow manipulation of the terminal carboxylate. Peptide anchoring to resin via the side chain of tyrosine esters has been described on both benzyl-type resins<sup>30</sup> and 2-chlorotrityl chloride resin.<sup>31</sup>

We first prepared the free phenolic tyrosine derivatives, Fmoc-Tyr-OMe (**10**)<sup>32</sup> and Fmoc-Tyr amide (**11**)<sup>33</sup> (see Supporting Information). The dimethyl ester (S,S)-12 was achieved by coupling **10** to 2-chlorotrityl chloride resin via the phenol group.<sup>31</sup> The remainder of the peptide sequence was assembled as described above with final coupling of (2S,7S)-5 and standard acidolytic cleavage (Scheme 5).

To synthesize the heterodimeric monomethyl ester (S,S)-13, **10** and **11** were anchored simultaneously to 2-chlorotrityl chloride resin as a 1:1 mixture. Standard SPPS was continued as described above, and final coupling of (2S,7S)-5 was followed by standard cleavage. The products were an approximately 2:1:1 mixture of the desired heterodimer (S,S)-13 and the

**Table 1. Synthesised Dimeric Peptides and Their Analytical Data**

code	sequence <sup>a</sup>	ESI-MS <sup>b</sup>	HPLC RT <sup>c</sup> (min)
(S,S)-1	(2S,7S)-sub(YRLRY-NH <sub>2</sub> ) <sub>2</sub>	569.75	11.21
(R,R)-1	(2R,7R)-sub(YRLRY-NH <sub>2</sub> ) <sub>2</sub>	569.85	11.16
(S,S)-9	(2S,7S)-Δsub(YRLRY-NH <sub>2</sub> ) <sub>2</sub>	569.05	11.19
(R,R)-9	(2R,7R)-Δsub(YRLRY-NH <sub>2</sub> ) <sub>2</sub>	569.10	11.34
(S,S)-12	(2S,7S)-sub(YRLRY-OMe) <sub>2</sub>	579.85	12.06
(S,S)-13	(2S,7S)-sub(YRLRY-NH <sub>2</sub> ) (YRLRY-OMe)	574.85	11.61
(S,S)-14	mono-sCy5-(2S,7S)-sub(YRLRY-NH <sub>2</sub> ) <sub>2</sub>	782.70	12.38
(R,R)-14	mono-sCy5-(2R,7R)-sub(YRLRY-NH <sub>2</sub> ) <sub>2</sub>	782.75	12.36
(S,S)-15	monoRhB-(2S,7S)-sub(YRLRY-NH <sub>2</sub> ) <sub>2</sub>	767.40	13.37
(S,S)-16	monoRhB-(2S,7S)-Δsub(YRLRY-NH <sub>2</sub> ) <sub>2</sub>	766.65	13.36
(R,R)-16	monoRhB-(2R,7R)-Δsub(YRLRY-NH <sub>2</sub> ) <sub>2</sub>	766.70	13.26

<sup>a</sup>Sub = 2,7-diaminosuberoyl linkage; Δsub = 2,7-diaminooctene-4-diyl linkage. <sup>b</sup>ESI-MS base peak corresponds to [M + 3H]<sup>3+</sup>. <sup>c</sup>HPLC retention time using a Phenomenex Luna C-8 column (100 Å, 3 μm, 100 mm × 2.00 mm). The gradient is composed of 100% H<sub>2</sub>O (0.1% TFA) for 4 min, 0–60% acetonitrile in H<sub>2</sub>O (0.1% TFA) over 10 min, and isocratic 60% acetonitrile in H<sub>2</sub>O (0.1% TFA) for 1 min.

**Table 2. Synthesized Dimeric Peptides and Their Pharmacological Data**

code	sequence <sup>a</sup>	pIC <sub>50</sub> <sup>b</sup>	R <sub>max</sub> <sup>c</sup> (% 100 nM PP)	pEC <sub>50</sub> <sup>d</sup>
PP		8.64 ± 0.12	96.3 ± 4.0	8.58 ± 0.10
(S,S)-1	(2S,7S)-sub(YRLRY-NH <sub>2</sub> ) <sub>2</sub>	7.16 ± 0.10	57.1 ± 10.9	7.08 ± 0.30
(R,R)-1	(2R,7R)-sub(YRLRY-NH <sub>2</sub> ) <sub>2</sub>	7.90 ± 0.10	61.5 ± 0.17	8.33 ± 0.17
(S,S)-9	(2S,7S)-Δsub(YRLRY-NH <sub>2</sub> ) <sub>2</sub>	6.88 ± 0.09	44.5 ± 4.8	7.52 ± 0.20
(R,R)-9	(2R,7R)-Δsub(YRLRY-NH <sub>2</sub> ) <sub>2</sub>	7.62 ± 0.11	61.0 ± 5.2	7.42 ± 0.15
(S,S)-12	(2S,7S)-sub(YRLRY-OMe) <sub>2</sub>	6.21 ± 0.11	11.3 ± 6.7 <sup>d</sup>	ND
(S,S)-13	(2S,7S)-sub(YRLRY-NH <sub>2</sub> ) (YRLRY-OMe)	7.03 ± 0.10	49.1 ± 6.8	<6.5
(S,S)-14	mono-sCy5-(2S,7S)-sub(YRLRY-NH <sub>2</sub> ) <sub>2</sub>	ND	56.6 ± 11.8	7.02 ± 0.33
(R,R)-14	mono-sCy5-(2R,7R)-sub(YRLRY-NH <sub>2</sub> ) <sub>2</sub>	ND	65.6 ± 5.7	7.48 ± 0.16
(S,S)-15	monoRhB-(2S,7S)-sub(YRLRY-NH <sub>2</sub> ) <sub>2</sub>	7.15 ± 0.09	15.9 ± 9.1 <sup>d</sup>	ND
(S,S)-16	monoRhB-(2S,7S)-Δsub(YRLRY-NH <sub>2</sub> ) <sub>2</sub>	7.16 ± 0.10	29.2 ± 4.6	8.26 ± 0.37
(R,R)-16	monoRhB-(2R,7R)-Δsub(YRLRY-NH <sub>2</sub> ) <sub>2</sub>	7.15 ± 0.09	39.3 ± 4.2	8.43 ± 0.26

<sup>a</sup>Sub = 2,7-diaminosuberoyl linkage; Δsub = 2,7-diaminooctene-4-diyl linkage. <sup>b</sup>Derived from competition binding assays using 100 nM **17** as the fluorescent ligand. <sup>c</sup>From Y<sub>4</sub>R-β-arrestin2 recruitment assays. <sup>d</sup>In the absence of significant agonist activity, the effect at 1 μM peptide is reported. ND = not determined

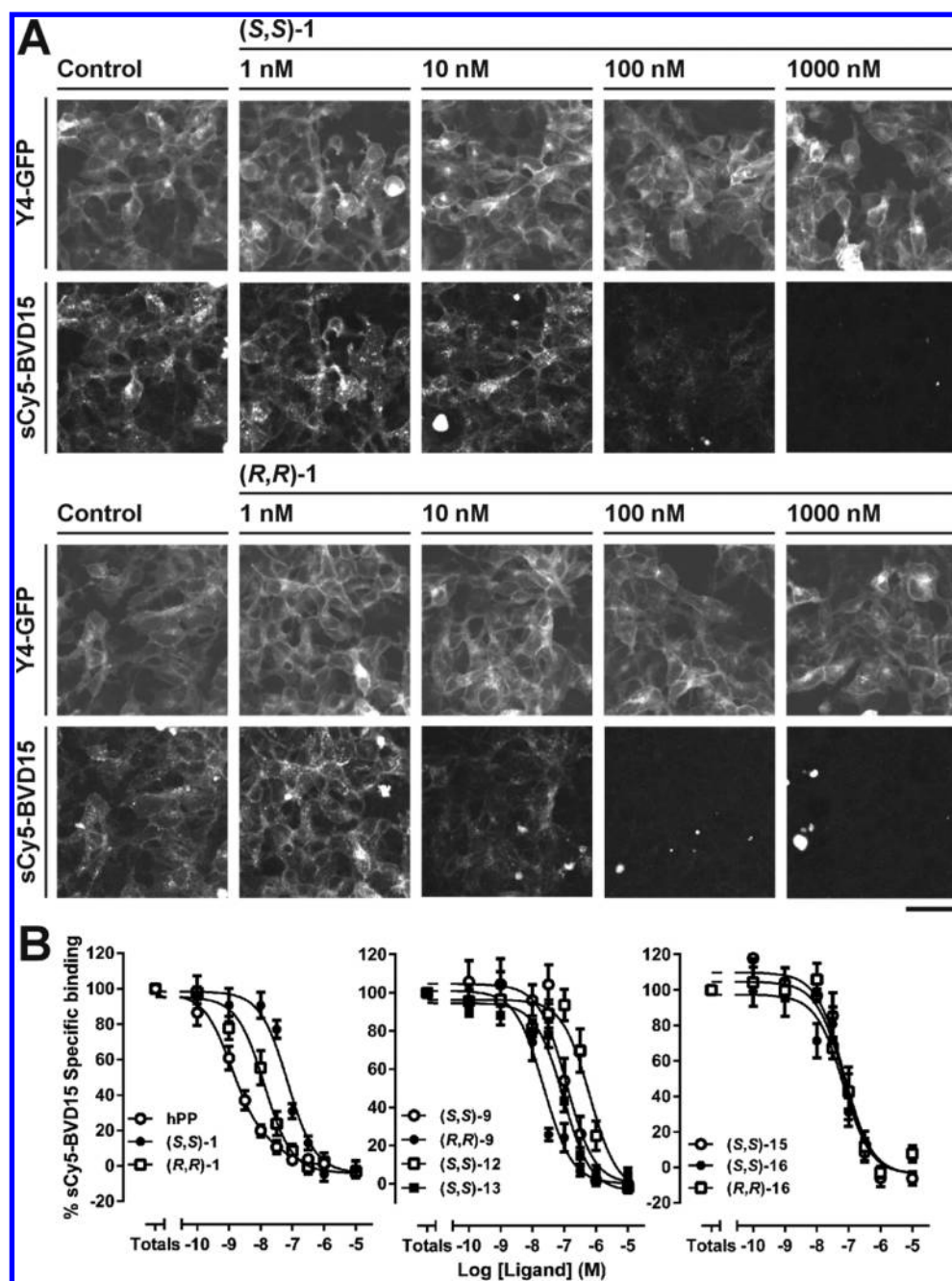


**Figure 3.** Y<sub>4</sub>R competition binding assays using high content imaging. (A) 293TR Y<sub>4</sub>-GFP cells were incubated with 100 nM, **17** in the absence (control) or presence of increasing concentrations of stereoisomers of **1**. Following 30 min at 37 °C, Y<sub>4</sub>-GFP and fluorescent ligand images were acquired on an IX Ultra plate reader. The panels show 400 × 400 regions of interest from the 1000 × 1000 pixel original plate images; scale bar 50 μm. (B) Specific binding of **17** was quantified and normalized using granularity analysis as described in the methods to obtain competition curves for peptide analogues synthesized in the current study. Graphs show pooled competition data (*n* = 5), from which the pIC<sub>50</sub> values in Table 2 were determined.

homodimers, the diamide (S,S)-**1** and dimethyl ester (S,S)-**12** (Scheme 5). The three major peptide products were readily resolved by RP-HPLC, allowing isolation of the desired product. Notable in the syntheses of compounds (S,S)-**12** and (S,S)-**13** was an excellent recovery of peptide products, indicative of more efficient cleavage from the 2-chlorotrityl chloride resin than from Rink amide resin.

**Synthesis of Fluorescently Labeled Diastereomers of (S,S)-1 and (R,R)-1.** To develop fluorescently labeled Y<sub>4</sub>R-targeting ligands for in vitro Y<sub>4</sub>R studies, (S,S)-**1**, (R,R)-**1**, (S,S)-**9**, and (R,R)-**9** were conjugated with either a rhodamine B (RhB) derivative<sup>34</sup> or the commercially available sulfo-Cy5 (sCy5)

dye (Figure 2). Following our previously reported methods for monoconjugation of dimeric peptides,<sup>35</sup> peptides (S,S)-**1** and (R,R)-**1** were treated with 0.7 mol equiv of sCy5 in the presence of PyClock and DIPEA to give the desired monolabeled analogues (S,S)-**14** and (R,R)-**14**, respectively, after purification, and peptides (S,S)-**1**, (S,S)-**9**, and (R,R)-**9** treated with the rhodamine B derivative to give (S,S)-**15**, (S,S)-**16**, and (R,R)-**16**, respectively (Scheme 6).

In summary, we have successfully developed unambiguous synthetic routes to prepare optically pure **1** and analogues through both solution and solid-phase alkene metathesis reactions. Monolabeled fluorescent analogues were conveniently

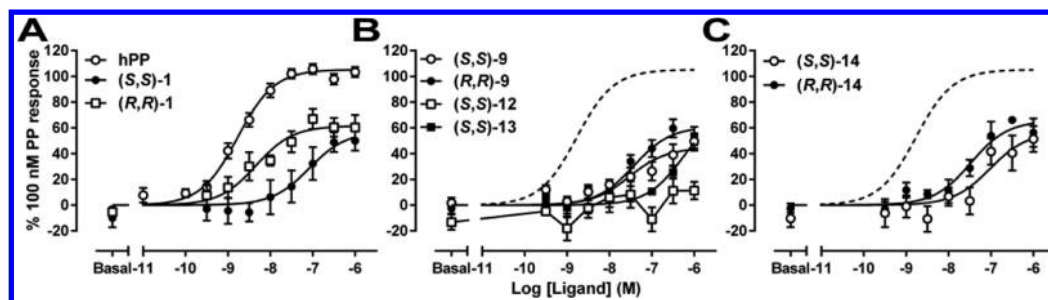


**Figure 4.**  $Y_4R$  agonism as assessed in the  $Y_4R$   $\beta$ -arrestin2 recruitment assay. The HEK293  $Y_4R$   $\beta$ -arrestin2 BiFC cell line was stimulated for 60 min with human PP or synthesized compounds, and the development of complemented YFP fluorescence following  $Y_4R$  activation was imaged and quantified using granularity analysis. (A–C) Pooled data ( $n = 4$  or greater), normalized to the 100 nM PP response, from which  $pEC_{50}$  and  $R_{max}$  values were estimated (Table 2).

prepared by standard solution phase coupling using limited molar equivalents of fluorophores. Utilizing these strategies, 11 dimeric analogues were prepared and their analytical data are summarized in Table 1.

**Pharmacology.** The pharmacological characteristics of these dimeric peptides were assessed by receptor binding and functional assays using whole-cell assay systems. This enabled binding to be assessed in physiological buffer in cells (expressing human  $Y_4R$  tagged with green fluorescent protein, GFP) rather than membranes to provide equivalence with subsequent functional measurements.

$Y_4R$  binding affinity data were obtained by competition binding against the sCy5-labeled peptide 17, ([Lys<sup>2</sup>(sCy5),Arg<sup>4</sup>]-BVD-15, 100 nM), analyzed on a high content imaging plate reader (Table 2, Figure 3).<sup>36,37</sup> The endogenous reference ligand, human PP, showed nanomolar affinity ( $IC_{50} = 2.31$  nM) in this assay. Of all the peptides, (2R,7R)-1 exhibited the highest  $Y_4R$  affinity ( $IC_{50} = 12.7$  nM) and was 5.5-fold higher in affinity than (2S,7S)-1.

The remaining analogues examined here have not been previously described (Table 2). In the alkenyl dimer series, a preference for the (R,R)-9 was again observed compared to the (S,S)-diastereomer, but overall these compounds showed 2–3-fold lower affinity for  $Y_4R$  than the corresponding diaminosuberic linked analogues 1. It can be concluded that conformational restraint due to the presence of the alkene group is not favored. Substitution of one C-terminal amide (S,S)-13 for an ester moiety did not lead to a major loss of  $Y_4R$  affinity compared to the corresponding diamide (S,S)-1 in these assays. However, replacement of both amides as in compound (S,S)-12 has a major impact with an order of magnitude drop in affinity. Mono *N*-terminal modification of (R,R)-9 with rhodamine B giving (R,R)-16 led to a 3-fold reduction in affinity, but rhodamine B addition was well tolerated in analogues (S,S)-15 and (S,S)-16. The three rhodamine B containing peptides had essentially overlapping competition curves.

The selectivity of representative peptides (R,R)-1, (S,S)-9, and (S,S)-12 was measured by  $Y_1R$ -GFP whole-cell competition binding (using the same fluorescent ligand 17 (10 nM) and confirmed at least 30-fold selectivity for  $Y_4R$  over  $Y_1R$ , the  $Y$  receptor subtype most closely related in amino acid homology.<sup>38</sup>  $Y_1R$   $pIC_{50}$  values were  $6.44 \pm 0.14$ ,  $6.31 \pm 0.30$ , and  $6.63 \pm 0.12$  for analogues (R,R)-1, (S,S)-9, and (S,S)-12 respectively ( $n = 3$ ).

The functional  $Y_4R$  agonism produced by the peptides was analyzed using a  $\beta$ -arrestin2 recruitment assay to detect  $Y_4R$  activation (Figure 4), as previously described.<sup>39,40</sup> One advantage of this assay is its limited receptor reserve, which

improves correspondence between agonist potency (as  $EC_{50}$ , the concentration of agonist that produces 50% of its maximal response) and underlying functional receptor affinities and also the likelihood that differences in agonist intrinsic efficacy are revealed through changes in relative maximum response ( $R_{max}$ ).<sup>41</sup> Thus, the reference agonist human PP stimulated  $\beta$ -arrestin2 association with an  $EC_{50}$  value (2.6 nM) very similar to its derived  $pIC_{50}$  in the whole cell  $Y_4R$  binding experiments.

Compared to PP, all the peptides were partial agonists in the  $Y_4R$ -arrestin recruitment assays, with typical  $R_{max}$  values 44–62% of that of PP (Table 2). The order of potency broadly reflected binding data in that (i) (R,R)-1 ( $EC_{50} = 4.6$  nM) was 20-fold more potent than the (S,S)-1 (Figure 4A), (ii) the alkenyl derivatives (R,R)-9 and (S,S)-9 were less potent overall than the dimers with saturated linkages (Figure 4B), and (iii) replacement of one or both C-terminal amides with ester moieties, (S,S)-13 and (S,S)-12, respectively, resulted in a loss of potency and efficacy (Figure 4B).

The functional assay enabled assessment of both RhB- and sCy5-labeled analogues as  $Y_4R$  agonists. In general, maximum responses to rhodamine analogues were reduced compared to the respective parent compounds, with compound (S,S)-15 (RhB derivative of (S,S)-1) being without significant effect in the assay (Table 2). In contrast, monolabeling with sCy5 as in (S,S)-14 and (R,R)-14, preserved the same level of maximal response exhibited by their parent peptides (Figure 4C). The sCy5-labeled (R,R)-14 was more potent, with an  $EC_{50}$  value (34 nM) approximately 7-fold lower potency than (R,R)-1.

The sCy5 derivatives (S,S)-14 and (R,R)-14 were explored further for their properties as novel  $Y_4R$  fluorescent ligands. Both compounds labeled  $Y_4R$ -GFP expressing 293TR cells in a concentration-dependent manner (with (R,R)-14 more potent), dependent on prior induction of receptor expression via tetracycline pretreatment (Figure 5). As anticipated for a ligand with agonist properties, both surface and intracellular distribution of sCy5 fluorescence was observed, likely reflecting some cointernalization of  $Y_4R$  ligand complexes from the plasma membrane following receptor activation. The presence of increasing concentrations of PP competed for the binding of (S,S)-14 or (R,R)-14.

To confirm the utility of (R,R)-14 in competition binding experiments, the fluorescence spectrum in physiological buffers was determined and found the  $\lambda_{max}$  to be the same as that of the underivatized sCy5-NHS dye (absorption max 656 nm, emission max 665 nm) with a relative quantum yield of 31% (see Supporting Information). We then used (R,R)-14 to label cells with 100 nM (R,R)-14 and determined the PP  $pIC_{50}$  was



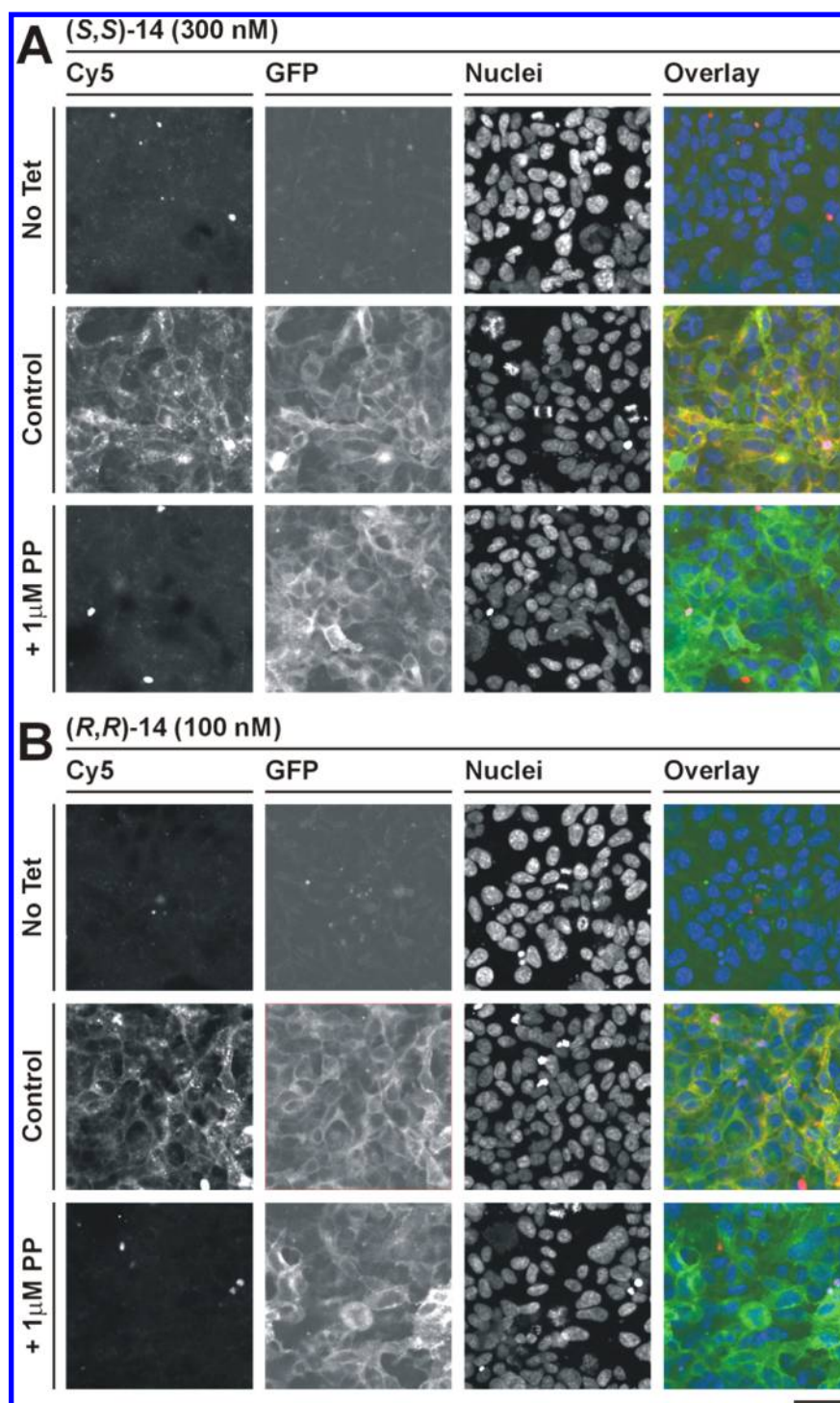


**Figure 5.** sCy5 labeled peptides as fluorescent  $Y_4R$  ligands. Representative images show binding and localization of mono-sCy5 labeled (S,S)-14 (300 nM) or (R,R)-14 (100 nM) following 30 min preincubation with 293TR  $Y_4GFP$  cells. Panels illustrate the lack of fluorescent ligand binding in controls cells without  $Y_4R$  protein expression induced by tetracycline treatment (No Tet) or in the presence of competing ligand (1  $\mu$ M PP). Examples are magnified regions of individual IX Ultra images, as described for Figure 4, representative of three independent experiments. Scale bar 50  $\mu$ m.

$8.36 \pm 0.09$  ( $IC_{50} = 4.31$  nM,  $n = 3$ ), consistent with the  $IC_{50}$  obtained using **17** (see Table 2).

The collected assay data from these studies raise interesting questions regarding the molecular mechanism governing the high potency of peptide (R,R)-1 as compared to other analogues, and therefore how dimeric analogues impart enhanced affinity generally. Set against recent studies of the  $Y_4R$ -hPP

interaction,<sup>42</sup> the simplest model is that the “first arm” of the dimer binds the receptor in the canonical fashion while the “second arm” contributes to the affinity, perhaps by mimicry of the hPP helical region, residues 14–30. An alternate view might be that the ligand binding is driven by the doubling of the local concentration of the C-terminal binding motif. The influence of the flexible bridging ligand argues against this latter explanation

although the clear preference for the presence of the (R,R)-configuration may imply a preference for a D-amino acid at that position of the truncated peptide that has not been tested in other analogues. The comparable affinity of (S,S)-1 and the half ester, half amide (S,S)-13 may also suggest that the two arms play different roles in receptor binding, where in the “second arm” the C-terminal carboxamide is not so critical. The development of synthetic routes to further interrogate the structure–activity of stereochemically defined homo- and heterodimers suggests a great opportunity for the much needed development of Y<sub>4</sub>R ligands.

## CONCLUSION

Pharmacological observations support the conclusion that the (R,R)-1 is the active principle of the original mixture of diastereomers 1, and as for the native peptides, C-terminal amidation of these compounds is required for Y<sub>4</sub>R agonist activity. As previous fluorescent ligand SAR studies have indicated,<sup>43,44</sup> the choice of rhodamine or sCy5 fluorophore influences the result Y<sub>4</sub>R properties of the labeled compounds, with mono-sCy5 labeled derivative (R,R)-14 being identified as a novel nanomolar affinity fluorescent Y<sub>4</sub>R agonist.

## EXPERIMENTAL SECTION

**Materials.** N<sup>α</sup>-Fmoc and N<sup>α</sup>-Boc protected amino acids were purchased from Auspep, Chemimpex, and Mimotopes. Unless otherwise specified, all amino acids used were of L-conformation. Rink amide resin (0.53 mequiv/g, 100–200 mesh), 2-chlorotriyl chloride resin (1.12 mequiv/g, 200–400 mesh), HCTU, and PyClock were obtained from Chemimpex. TFA was purchased from Alfa Aesar. Thioanisole, 1,2-ethanedithiol, DIPEA, piperidine, Boc anhydride, triethylamine, EDCl, DMAP, 1,3-benzenedimethanol, Fmoc-OSu, pyridine, 1,4-dioxane, and Grubbs catalyst second generation were purchased from Sigma-Aldrich. Phenol, chlorotrimethylsilane, and all solvents were obtained from Merck. The sCy5 fluorescence probe was purchased from W&J PharmaChem. The Rhodamine B analogue was purchased from Sigma-Aldrich and modified as reported.<sup>34</sup> All solvents were of analytical grade, and all chemicals were used without further purification.

Molecular mass of the compounds were determined by ESI-MS using a Shimadzu LCMS2020 instrument, incorporating a Phenomenex Luna C-8 column (100 Å, 3 μm, 100 mm × 2.00 mm). This system used 0.05% TFA in Milli-Q water as the aqueous buffer and 0.05% TFA in acetonitrile as the organic buffer. The eluting profile was a linear gradient of 0–60% acetonitrile in water over 10 min at 0.2 mL/min.

HRMS analyses were carried out on an Agilent 6224 TOF LC/MS mass spectrometer coupled to an Agilent 1290 Infinity (Agilent, Palo Alto, CA). All data were acquired and reference mass corrected via a dual-spray electrospray ionization (ESI) source. Acquisition was performed using the Agilent Mass Hunter Data Acquisition software version B.05.00 build 5.0.5042.2, and analysis was performed using Mass Hunter Qualitative Analysis version B.05.00 build 5.0.519.13.

Crude peptides were purified on a Phenomenex Luna C-8 column (100 Å, 10 μm, 250 mm × 21.2 mm) utilizing a Waters 600 semi-preparative RP-HPLC that incorporates a Waters 486 UV detector. The wavelength was set at 230 nm. This system used 0.1% TFA in Milli-Q water as the aqueous buffer, and 0.1% TFA in acetonitrile as the organic buffer. The eluting profile was a linear gradient of 0–80% acetonitrile in water over 60 min at 10 mL/min.

**Peptide Synthesis.** The purity of all reported peptides are ≥95% according to the HPLC chromatographs produced by the ESI-MS method described above.

**General Synthesis.** Linear peptide chains were synthesized on Rink amide resin or 2-chlorotriyl chloride resin (sequence dependent) using a 3-channel serial automated peptide synthesizer (“PS3”, Protein Technologies Inc.), which adopted standard Fmoc-based solid phase synthesis strategy. Fmoc deprotection was performed by 20% v/v

piperidine in DMF for 2 × 5 min. Fmoc protected amino acids (3 equiv) were coupled using DMF as solvent, and DIPEA in DMF (7% v/v) with HCTU (3 equiv) as the activating agent for 50 min.

Protected peptide resins were cleaved by treating with Reagent K (5 mL) composed of TFA–H<sub>2</sub>O–thioanisole–phenol–EDT (82.5%:5%:5%:5%:2.5%) for 3 h. The cleavage mixture was filtered, concentrated by a stream of N<sub>2</sub>, precipitated in cold Et<sub>2</sub>O, and centrifuged at 3000 rpm for 5 min. The crude product was dissolved in water–acetonitrile mixture (50%:50%) and lyophilized.

**(2S,7S)-Diaminooctanedioyl-bis(Tyr-Arg-Leu-Arg-Tyr-amide) ((S,S)-1).** The linear peptide chain was prepared by the general method described above on Rink resin (0.05 mequiv). The peptide resin was treated with (2S,7S)-N,N-di-Boc-diaminosuberic acid, (S,S)-5 (10.0 mg, 0.5 equiv), PyClock (110 mg, 4 equiv), and DIPEA (87.0 μL, 10 equiv) in DMF (5 mL) overnight. After cleavage and purification, the peptide was lyophilized to yield a white fluffy solid (3.5 mg). HPLC RT 11.21 min. ESI-MS: 569.75 (M + 3H)<sup>3+</sup>. HRMS (ESI) *m/z* calculated for [C<sub>80</sub>H<sub>124</sub>N<sub>26</sub>O<sub>16</sub> + 2H]<sup>2+</sup>, 853.4923; found, 853.4947.

**(2R,7R)-Diaminooctanedioyl-bis(Tyr-Arg-Leu-Arg-Tyr-amide) ((R,R)-1).** The (R,R) diastereomer of 1 was prepared in the same fashion as the (S,S)-diastereomer, but on 0.05 mmol scale and using (R,R)-5 yielding a fluffy white solid (13.4 mg). HPLC RT 11.16 min. ESI-MS: 569.85 (M + 3H)<sup>3+</sup>. HRMS (ESI) *m/z* calculated for [C<sub>80</sub>H<sub>124</sub>N<sub>26</sub>O<sub>16</sub> + 3H]<sup>3+</sup>, 569.6660; found, 569.6683.

Alternatively, peptide (R,R)-9 (16 mg) (see below) was dissolved in EtOAc (10 mL) then cycled through an H-Cube incorporating a 10% Pd/C cartridge at 50 °C at 1.5 mL/min under H<sub>2</sub> (50 psi). After 1 h, the solvent was removed in vacuo and the residue was purified by HPLC to yield a white fluffy solid (9.2 mg).

**(2S,7S)-Diaminooct-4-enedioyl-bis(Tyr-Arg-Leu-Arg-Tyr-amide) ((S,S)-9).** The Fmoc protected linear peptide, Fmoc-Gly(All)-Tyr-(OtBu)-Arg(Pbf)-Leu-Arg(Pbf)-Tyr(OtBu)-Rink amide resin was treated with LiCl in DMF (4.2 mg/mL, 200 μL), Grubbs catalyst second generation (0.2 equiv), and DCM (4.5 mL) in a glass microwave vessel. The mixture was charged with N<sub>2</sub> and heated in a microwave reactor at 100 °C for 3 h. After the solvent was removed by filtration, Fmoc deprotection was performed using 20% v/v piperidine in DMF (5 mL) for 2 × 5 min, and the peptide was cleaved off resin as described above to yield a white fluffy solid (10.0 mg), HPLC RT 11.19 min. ESI-MS: 569.05 (M + 3H)<sup>3+</sup>. HRMS (ESI) *m/z* calculated for [C<sub>80</sub>H<sub>122</sub>N<sub>26</sub>O<sub>16</sub> + 2H]<sup>2+</sup>, 852.9881.

**(2R,7R)-Diaminooct-4-enedioyl-bis(Tyr-Arg-Leu-Arg-Tyr-amide) ((R,R)-9).** The peptide was prepared as for (S,S)-9 above but utilizing Fmoc-D-Gly(All) to yield a white fluffy solid (5.1 mg). HPLC RT 11.34 min. ESI-MS: 569.10 (M + 3H)<sup>3+</sup>.

**(2S,7S)-Diaminooctanedioyl-bis(Tyr-Arg-Leu-Arg-Tyr dimethyl ester) ((S,S)-12).** A mixture of Fmoc-Tyr-OMe, 10 (2 equiv) and DIPEA (6 equiv) in DCM (5 mL) was added to 2-chlorotriyl resin and agitated overnight. The resin was filtered, washed with DCM × 3, MeOH × 1, and Et<sub>2</sub>O × 1 and dried in vacuo. The derivatized resin was subject to standard solid phase synthesis as described above and treated with (2S,7S)-5 as described for (S,S)-1 above. After cleavage and purification, the peptide was lyophilized to yield a white fluffy solid (40.5 mg). HPLC RT 12.06 min. ESI-MS: 579.85 (M + 3H)<sup>3+</sup>. HRMS (ESI) *m/z* calculated for [C<sub>82</sub>H<sub>126</sub>N<sub>24</sub>O<sub>18</sub> + 2H]<sup>2+</sup>, 868.4914; found, 868.4956.

**(2S,7S)-Diaminooctanedioyl-(Tyr-Arg-Leu-Arg-Tyr methyl ester) (Tyr-Arg-Leu-Arg-Tyr amide) ((S,S)-13).** (S,S)-13 was prepared as for (S,S)-12 above, except that the 2-chlorotriyl chloride resin was treated with a 50%:50% mixture of Fmoc-Tyr-OMe (10) and Fmoc-Tyr-NH<sub>2</sub> (11). After cleavage and purification, the peptide was lyophilized to yield a white fluffy solid (7.5 mg). HPLC RT 11.61 min. ESI-MS: 574.85 (M + 3H)<sup>3+</sup>. Side products of (S,S)-1 and (S,S)-12 were also identified in the product mixture. HRMS (ESI) *m/z* calculated for [C<sub>81</sub>H<sub>125</sub>N<sub>25</sub>O<sub>17</sub> + 2H]<sup>2+</sup>, 860.9920; found, 860.9956.

**Fluorescent Labeling of Peptides.** Peptides were treated with a mixture of the labeling agent (sCy5 or RhB, see Figure 2) (0.7 equiv), PyClock (2 equiv), and NMM (12 equiv) in DMF (2 mL). The mixture was stirred in darkness overnight, and DMF was removed in vacuo. The crude product was washed with TFA (1 mL), precipitated



with cold Et<sub>2</sub>O, and centrifuged at 3000 rpm for 5 min. The resulting precipitate was dissolved in water–acetonitrile (50%:50%) and lyophilized.

**Mono-sCy5-(2S,7S)-Diaminooctanedioyl-bis(Tyr-Arg-Leu-Arg-Tyr-amide) ((S,S)-14).** According to the general method for fluorescent labeling described above, (S,S)-1 (10 mg) was treated with sCy5-OH (0.7 equiv). After purification, (S,S)-14 was obtained as a fluffy blue powder (1.3 mg). HPLC RT 12.38 min. ESI-MS: 782.70 (M + 3H)<sup>3+</sup>.

**Mono-sCy5-(2R,7R)-Diaminooctanedioyl-bis(Tyr-Arg-Leu-Arg-Tyr-amide) ((R,R)-14).** According to the general method for fluorescent labeling described above, (R,R)-1 (5.9 mg) was treated with sCy5-OH (0.7 equiv). After purification, (R,R)-14 was obtained as a fluffy blue powder (1.2 mg). HPLC RT 12.36 min. ESI-MS: 782.75 (M + 3H)<sup>3+</sup>.

**Mono-RhB-(2S,7S)-Diaminooctanedioyl-bis(Tyr-Arg-Leu-Arg-Tyr-amide) ((S,S)-15).** According to the general method for fluorescent labeling described above, (S,S)-1 (10 mg) was treated with RhB-OH (0.7 equiv). After purification, (S,S)-15 was obtained as a fluffy magenta powder (0.5 mg). HPLC RT 13.37 min. ESI-MS: 767.40 (M + 3H)<sup>3+</sup>.

**Mono-RhB-(2S,7S)-Diaminooct-4-enedioyl-bis(Tyr-Arg-Leu-Arg-Tyr-amide) ((S,S)-16).** According to the general method for fluorescent labeling described above, (S,S)-9 (10 mg) was treated with RhB-OH (0.7 equiv). After purification, (S,S)-16 was obtained as a fluffy magenta powder (1.2 mg). HPLC RT 13.36 min. ESI-MS: 766.65 (M + 3H)<sup>3+</sup>.

**Mono-RhB-(2R,7R)-Diaminooct-4-enedioyl-bis(Tyr-Arg-Leu-Arg-Tyr-amide) ((R,R)-16).** According to the general method for fluorescent labeling described above, (R,R)-9 (10 mg) was treated with RhB-OH (0.7 equiv). After purification, (R,R)-16 was obtained as a fluffy magenta powder (1.4 mg). HPLC RT 13.26 min. ESI-MS: 766.70 (M + 3H)<sup>3+</sup>.

**Cell Culture.** HEK293T and 293TR cells (Invitrogen) were cultured in Dulbecco's Modified Eagle's Medium (DMEM, Sigma-Aldrich) supplemented with 10% fetal bovine serum, and passaged when confluent by trypsinization (0.25% w/v in Versene). Mixed population 293TR cell lines inducibly expressing Y receptors tagged with C-terminal GFP, and dual stable HEK293 cell lines expressing Y receptor-Yc and  $\beta$ -arrestin2-Yn (where Yc and Yn are complementary fragments of YFP) are as previously reported.<sup>35,39,40</sup>

**Y<sub>4</sub>R Competition Binding and Imaging Assays.** 293TR Y<sub>4</sub>-GFP or Y<sub>1</sub>-GFP cells were seeded at 20000 cells/well in poly-D-lysine coated 96-well imaging plates (Greiner 655090), treated as required with 1  $\mu$ g/mL tetracycline for 18–21 h and then used in experiments at confluence. Incubations were performed in HEPES-buffered saline solution (HBSS) including 0.1% BSA, the permeable nuclear dye H33342 (2  $\mu$ g/mL, Sigma), and varying concentrations of competitor ligands (10<sup>-10</sup> M to 10<sup>-5</sup> M) for 2 min, prior to the addition of fluorescent ligand at the concentration indicated. After 30 min at 37 °C, the media was replaced with HBSS/0.1% BSA and plates were immediately imaged (2 sites/well) on an IX Ultra confocal plate reader (Molecular Devices, Sunnyvale CA, USA) using laser excitation/emission filter settings appropriate for H33342 (DAPI), Y receptor-GFP (FITC), and sCy5-labeled peptides. Bound ligand fluorescence was quantified by granularity analysis (2–3  $\mu$ m diameter granules; MetaXpress 5.3, Molecular Devices) and normalized to positive (totals 100%) and negative (0%, in the presence of 100 nM PP) controls. pIC<sub>50</sub> values were then determined from the pooled data using GraphPad Prism v6 (GraphPad software, San Diego, CA).

**Y<sub>4</sub>R- $\beta$ -Arrestin Recruitment Assays.** Bimolecular fluorescence complementation (BiFC) based detection of Y receptor- $\beta$ -arrestin2 association was performed as described previously.<sup>39,40</sup> The Y<sub>4</sub>R arrestin BiFC cell lines were seeded at 40000 cells/well onto poly-D-lysine coated Greiner 655090 imaging plates and experiments performed 24 h later. Stimulation with human PP (Bachem, St. Helens, UK) or other ligands was performed in HBSS/0.1% BSA (10<sup>-10</sup> M to 10<sup>-6</sup> M, duplicate wells) for 60 min at 37 °C. Incubations were terminated by fixation with 3% paraformaldehyde in phosphate buffered saline (PBS, 10 min at 21 °C), the cells were washed once with PBS, and the cell nuclei were stained for 15 min with H33342 (2  $\mu$ g mL<sup>-1</sup> in

PBS, Sigma). H33342 was then removed by a final PBS wash. Images (four central sites/well) were acquired automatically on the IX Ultra confocal plate reader, using 405 nm/488 nm laser lines for H33342 and complemented YFP excitation, respectively.

A granularity algorithm (MetaXpress 5.3) identified internal fluorescent compartments within these images of at least 3  $\mu$ m diameter (range set to 3–12  $\mu$ m) on the basis of granule intensity thresholds set with reference to the vehicle or 100 nM PP plate controls. The response for each data point was quantified as mean granule average intensity/cell, normalized to the reference agonist response. Concentration–response curves were fitted to the pooled data by nonlinear least-squares regression (GraphPad Prism), yielding estimates of agonist potency as pEC<sub>50</sub> and maximum response (R<sub>max</sub>).

## ■ ASSOCIATED CONTENT

### Supporting Information

The Supporting Information is available free of charge on the ACS Publications website at DOI: 10.1021/acs.jmedchem.6b00310.

Experimental data relating to protected amino acid synthesis, chiral chromatography of (2S,7S)-5 and (2R,7R)-5, HPLC spectra for all peptides, and fluorescence spectra of (R,R)-14 (PDF)

## ■ AUTHOR INFORMATION

### Corresponding Author

\*Phone: +61 3 99039672. Fax: +61 3 99039582. E-mail: philip.thompson@monash.edu.

### Notes

The authors declare no competing financial interest.

## ■ ACKNOWLEDGMENTS

M.L. was supported by an Australian Postgraduate Award scholarship. R.R.R. was supported by the Nottingham-Monash Ph.D. program.

## ■ ABBREVIATIONS USED

BiFC, bimolecular fluorescence complementation; DCM, dichloromethane; DIPEA, N,N-diisopropylethylamine; DMAP, 4-dimethylaminopyridine; DMF, N,N-dimethylformamide; EDCI, 1-ethyl-3-(3-(dimethylamino)propyl)carbodiimide; EDT, 1,2-ethanedithiol; EtOAc, ethyl acetate; GFP, green fluorescent protein; HCTU, O-(6-chlorobenzotriazol-1-yl)-N,N,N,N-tetramethyluronium hexafluorophosphate; MeOH, methanol; NMM, N-methylmorpholine; Pd/C, palladium on activated carbon; PyClock, (6-chlorobenzotriazol-1-yloxy)-tripyrrrolidinophosphonium hexafluorophosphate

## ■ REFERENCES

- (1) Tatemoto, K. Neuropeptide Y: complete amino acid sequence of the brain peptide. *Proc. Natl. Acad. Sci. U. S. A.* **1982**, 79, 5485–5489.
- (2) Tatemoto, K.; Mutt, V. Isolation of two novel candidate hormones using a chemical method for finding naturally occurring polypeptides. *Nature* **1980**, 285, 417–418.
- (3) Hoffmann, J. A.; Chance, R. E. Crystallization of bovine pancreatic polypeptide. *Biochem. Biophys. Res. Commun.* **1983**, 116, 830–835.
- (4) Blomqvist, A. G.; Herzog, H. Y-receptor subtypes—how many more? *Trends Neurosci.* **1997**, 20, 294–298.
- (5) Balasubramanian, A. Neuropeptide Y (NPY) family of hormones: progress in the development of receptor selective agonists and antagonists. *Curr. Pharm. Des.* **2003**, 9, 1165–1175.
- (6) Edelsbrunner, M. E.; Painsipp, E.; Herzog, H.; Holzer, P. Evidence from knockout mice for distinct implications of neuropeptide-Y Y<sub>2</sub> and

Y<sub>4</sub> receptors in the circadian control of locomotion, exploration, water and food intake. *Neuropeptides* **2009**, *43*, 491–497.

(7) Uhe, A. M.; Szmukler, G. I.; Collier, G. R.; Hansky, J.; O'Dea, K.; Young, G. P. Potential regulators of feeding behavior in anorexia nervosa. *Am. J. Clin. Nutr.* **1992**, *55*, 28–32.

(8) Marco, J.; Zulueta, M. A.; Correas, I.; Villanueva, M. L. Reduced pancreatic polypeptide secretion in obese subjects. *J. Clin. Endocrinol. Metab.* **1980**, *50*, 744–747.

(9) Lassmann, V.; Vague, P.; Viallettes, B.; Simon, M.-C. Low plasma levels of pancreatic polypeptide in obesity. *Diabetes* **1980**, *29*, 428–430.

(10) Berlicki, L.; Kaske, M.; Gutiérrez-Abad, R.; Bernhardt, G.; Illa, O.; Ortuño, R. M.; Cabrele, C.; Buschauer, A.; Reiser, O. Replacement of Thr<sup>32</sup> and Gln<sup>34</sup> in the C-terminal neuropeptide Y fragment 25–36 by *cis*-cyclobutane and *cis*-cyclopentane  $\beta$ -amino acids shifts selectivity toward the Y<sub>4</sub> receptor. *J. Med. Chem.* **2013**, *56*, 8422–8431.

(11) Leban, J. J.; Heyer, D.; Landavazo, A.; Matthews, J.; Aulabaugh, A.; Daniels, A. J. Novel modified carboxy terminal fragments of neuropeptide Y with high affinity for Y<sub>2</sub>-type receptors and potent functional antagonism at the Y<sub>1</sub>-type receptor. *J. Med. Chem.* **1995**, *38*, 1150–1157.

(12) Balasubramaniam, A.; Dhawan, V. C.; Mullins, D. E.; Chance, W. T.; Sheriff, S.; Guzzi, M.; Prabhakaran, M.; Parker, E. M. Highly selective and potent neuropeptide Y (NPY) Y<sub>1</sub> receptor antagonists based on [Pro(30), Tyr(32), Leu(34)]NPY(28–36)-NH<sub>2</sub> (BW1911U90). *J. Med. Chem.* **2001**, *44*, 1479–1482.

(13) Parker, E. M.; Babij, C. K.; Balasubramaniam, A.; Burrier, R. E.; Guzzi, M.; Hamud, F.; Mukhopadhyay, G.; Rudinski, M. S.; Tao, Z.; Tice, M.; Xia, L.; Mullins, D. E.; Salisbury, B. G. GR231118 (1229U91) and other analogues of the C-terminus of neuropeptide Y are potent neuropeptide Y Y<sub>1</sub> receptor antagonists and neuropeptide Y Y<sub>4</sub> receptor agonists. *Eur. J. Pharmacol.* **1998**, *349*, 97–105.

(14) Daniels, A. J.; Matthews, J. E.; Slepatis, R. J.; Jansen, M.; Viveros, O. H.; Tadepalli, A.; Harrington, W.; Heyer, D.; Landavazo, A.; Leban, J. J. High-affinity neuropeptide Y receptor antagonists. *Proc. Natl. Acad. Sci. U. S. A.* **1995**, *92*, 9067–9071.

(15) Gehlert, D. R.; Schober, D. A.; Beavers, L.; Galski, R.; Hoffman, J. A.; Smiley, D. L.; Chance, R. E.; Lundell, I.; Larhammar, D. Characterization of the peptide binding requirements for the cloned human pancreatic polypeptide-preferring receptor. *Mol. Pharmacol.* **1996**, *50*, 112–118.

(16) Matthews, J. E.; Jansen, M.; Lyster, D.; Cox, R.; Chen, W.-J.; Koller, K. J.; Daniels, A. J. Pharmacological characterization and selectivity of the NPY antagonist GR231118 (1229U91) for different NPY receptors. *Regul. Pept.* **1997**, *72*, 113–119.

(17) Schober, D. A.; Gackenhaimer, S. L.; Heiman, M. L.; Gehlert, D. R. Pharmacological characterization of [<sup>125</sup>I]-1229U91 binding to Y<sub>1</sub> and Y<sub>4</sub> neuropeptide Y/peptide YY receptors. *J. Pharmacol. Exp. Ther.* **2000**, *293*, 275–280.

(18) Balasubramaniam, A.; Mullins, D. E.; Lin, S.; Zhai, W.; Tao, Z.; Dhawan, V. C.; Guzzi, M.; Knittel, J. J.; Slack, K.; Herzog, H.; Parker, E. M. Neuropeptide Y (NPY) Y<sub>4</sub> receptor selective agonists based on NPY(32–36): development of an anorectic Y<sub>4</sub> receptor selective agonist with picomolar affinity. *J. Med. Chem.* **2006**, *49*, 2661–2665.

(19) Li, J.-B.; Asakawa, A.; Terashi, M.; Cheng, K.; Chaolu, H.; Zoshiki, T.; Ushikai, M.; Sheriff, S.; Balasubramaniam, A.; Inui, A. Regulatory effects of Y<sub>4</sub> receptor agonist (BVD-74D) on food intake. *Peptides* **2010**, *31*, 1706–1710.

(20) Robinson, A. J.; Elaridi, J.; Van Lierop, B. J.; Mujcinovic, S.; Jackson, W. R. Microwave-assisted RCM for the synthesis of carbocyclic peptides. *J. Pept. Sci.* **2007**, *13*, 280–285.

(21) Van Lierop, B. J.; Bornschein, C.; Jackson, W. R.; Robinson, A. J. Ring-closing metathesis in peptides - the sting is in the tail! *Aust. J. Chem.* **2011**, *64*, 806–811.

(22) Elaridi, J.; Patel, J.; Jackson, W. R.; Robinson, A. J. Controlled synthesis of (S,S)-2,7-diaminosuberlic acid: a method for regioselective construction of dicarba analogues of multicystine-containing peptides. *J. Org. Chem.* **2006**, *71*, 7538–7545.

(23) Passarella, D.; Peretto, B.; Blasco y Yepes, R.; Cappelletti, G.; Cartelli, D.; Ronchi, C.; Snaith, J.; Fontana, G.; Danieli, B.; Borlak, J. Synthesis and biological evaluation of novel thiocolchicine-podophyllotoxin conjugates. *Eur. J. Med. Chem.* **2010**, *45*, 219–226.

(24) Nolen, E. G.; Fedorka, C. J.; Blicher, B. Synthesis of orthogonally protected S,S-2,6-diaminopimelic acid via olefin cross-metathesis. *Synth. Commun.* **2006**, *36*, 1707–1713.

(25) Ward, M. D.; Zhu, Z. Compounds as L-cystine crystallization inhibitors and uses thereof. US 2012/0316236, Dec 13, 2012.

(26) Hiebl, J.; Blanka, M.; Guttman, A.; Kollmann, H.; Leitner, K.; Mayrhofer, G.; Rovenszky, F.; Winkler, K. A detailed investigation of the preparation of 2,7-diaminosuberlic acid and 2,5-diaminoadipic acid derivatives using Kolbe electrolysis. *Tetrahedron* **1998**, *54*, 2059–2074.

(27) Williams, R. M.; Liu, J. Asymmetric synthesis of differentially protected 2,7-diaminosuberlic acid, a ring-closure metathesis approach. *J. Org. Chem.* **1998**, *63*, 2130–2132.

(28) Aguilera, B.; Wolf, L. B.; Nieczypor, P.; Rutjes, F. P. J. T.; Overkleeft, H. S.; van Hest, J. C. M.; Schoemaker, H. E.; Wang, B.; Mol, J. C.; Furstner, A.; Overhand, M.; van der Marel, G. A.; van Boom, J. H. Synthesis of diaminosuberlic acid derivatives via ring-closing alkyne metathesis. *J. Org. Chem.* **2001**, *66*, 3584–3589.

(29) Hiebl, J.; Kollmann, H.; Rovenszky, F.; Winkler, K. One step synthesis of orthogonally protected diaminodicarboxylic acids by mixed kolbe electrolysis. *Bioorg. Med. Chem. Lett.* **1997**, *7*, 2963–2966.

(30) Cabrele, C.; Langer, M.; Beck-Sickinger, A. G. Amino acid side chain attachment approach and its application to the synthesis of tyrosine-containing cyclic peptides. *J. Org. Chem.* **1999**, *64*, 4353–4361.

(31) Rizzi, L.; Cendic, K.; Vaiana, N.; Romeo, S. Alcohols immobilization onto 2-chlorotriethylchloride resin under microwave irradiation. *Tetrahedron Lett.* **2011**, *52*, 2808–2811.

(32) Adamson, J. G.; Blaskovich, M. A.; Groenevelt, H.; Lajoie, G. A. Simple and convenient synthesis of tert-butyl ethers of Fmoc-serine, Fmoc-threonine, and Fmoc-tyrosine. *J. Org. Chem.* **1991**, *56*, 3447–3449.

(33) Combs, A. P.; Yue, E. W.; Bower, M.; Ala, P. J.; Wayland, B.; Douthy, B.; Takvorian, A.; Polam, P.; Wasserman, Z.; Zhu, W.; Crawley, M. L.; Pruitt, J.; Sparks, R.; Glass, B.; Modi, D.; McLaughlin, E.; Bostrom, L.; Li, M.; Galya, L.; Blom, K.; Hillman, M.; Gonneville, L.; Reid, B. G.; Wei, M.; Becker-Pasha, M.; Klabe, R.; Huber, R.; Li, Y.; Hollis, G.; Burn, T. C.; Wynn, R.; Liu, P.; Metcalf, B. Structure-based design and discovery of protein tyrosine phosphatase inhibitors incorporating novel isothiazolidinone heterocyclic phosphotyrosine mimetics. *J. Med. Chem.* **2005**, *48*, 6544–6548.

(34) Nguyen, T.; Francis, M. B. Practical synthetic route to functionalized rhodamine dyes. *Org. Lett.* **2003**, *5*, 3245–3248.

(35) Mountford, S. J.; Liu, M.; Zhang, L.; Groenen, M.; Herzog, H.; Holliday, N. D.; Thompson, P. E. Synthetic routes to the Neuropeptide Y Y<sub>1</sub> receptor antagonist 1229U91 and related analogues for SAR studies and cell-based imaging. *Org. Biomol. Chem.* **2014**, *12*, 3271–3281.

(36) Stoddart, L. A.; Vennart, A. J.; Denman, J. L.; Briddon, S. J.; Kellam, B.; Hill, S. J. Fragment screening at adenosine-A<sub>3</sub> receptors in living cells using a fluorescence-based binding assay. *Chem. Biol.* **2012**, *19*, 1105–1115.

(37) Liu, M. J.; Mountford, S. J.; Zhang, L.; Lee, I. C.; Herzog, H.; Thompson, P. E. Synthesis of BVD15 peptide analogues as models for radioligands in tumour imaging. *Int. J. Pept. Res. Ther.* **2013**, *19*, 33–41.

(38) Michel, M. C.; Beck-Sickinger, A.; Cox, H.; Doods, H. N.; Herzog, H.; Larhammar, D.; Quirion, R.; Schwartz, T.; Westfall, T. XVI. International union of pharmacology recommendations for the nomenclature of neuropeptide Y, peptide YY, and pancreatic polypeptide receptors. *Pharmacol. Rev.* **1998**, *50*, 143–150.

(39) Kilpatrick, L. E.; Briddon, S. J.; Hill, S. J.; Holliday, N. D. Quantitative analysis of neuropeptide Y receptor association with  $\beta$ -arrestin2 measured by bimolecular fluorescence complementation. *Br. J. Pharmacol.* **2010**, *160*, 892–906.

(40) Kilpatrick, L. E.; Briddon, S. J.; Holliday, N. D. Fluorescence correlation spectroscopy, combined with bimolecular fluorescence

complementation, reveals the effects of  $\beta$ -arrestin complexes and endocytic targeting on the membrane mobility of neuropeptide Y receptors. *Biochim. Biophys. Acta, Mol. Cell Res.* **2012**, 1823, 1068–1081.

(41) Stott, L. A.; Hall, D. A.; Holliday, N. D. Unravelling intrinsic efficacy and ligand bias at G protein coupled receptors: A practical guide to assessing functional data. *Biochem. Pharmacol.* **2016**, 101, 1–12.

(42) Pedragosa-Badia, X.; Sliwoski, G. R.; Dong Nguyen, E.; Lindner, D.; Stichel, J.; Kaufmann, K. W.; Meiler, J.; Beck-Sickinger, A. G. Pancreatic polypeptide is recognized by two hydrophobic domains of the human Y<sub>4</sub> receptor binding pocket. *J. Biol. Chem.* **2014**, 289, 5846–5859.

(43) Baker, J. G.; Middleton, R.; Adams, L.; May, L. T.; Briddon, S. J.; Kellam, B.; Hill, S. J. Influence of fluorophore and linker composition on the pharmacology of fluorescent adenosine A1 receptor ligands. *Br. J. Pharmacol.* **2010**, 159, 772–786.

(44) Briddon, S.; Kellam, B.; Hill, S. Design and use of fluorescent ligands to study ligand–receptor interactions in single living cells. In *Receptor Signal Transduction Protocols*; Willars, G. B., Challiss, R. A. J., Eds.; Humana Press: Totowa, NJ, 2011; Vol. 746, pp 211–236.

(45) Kuhn, K. K.; Ertl, T.; Dukorn, S.; Keller, M.; Bernhardt, G.; Reiser, O.; Buschauer, A. High Affinity Agonists of the Neuropeptide Y (NPY) Y<sub>4</sub> Receptor Derived from the C-terminal Pentapeptide of Human Pancreatic Polypeptide (hPP): Synthesis, Stereochemical Discrimination and Radiolabeling. *J. Med. Chem.* **2016**, DOI: [10.1021/acs.jmedchem.6b00309](https://doi.org/10.1021/acs.jmedchem.6b00309).

#### ■ NOTE ADDED IN PROOF

Buschauer and coworkers describe the synthesis of the diastereomers of **1** and using complementary assays also identified (*R,R*)-**1** as the active constituent.<sup>45</sup> Further they have prepared a range of analogues that contribute to the SAR understanding of these dimeric peptides and described radiolabelled analogues with excellent Y<sub>4</sub> potency and selectivity that complement our fluorescently labeled analogue (*R,R*)-**14**.



## 4.6 Summary

This chapter has depicted chemical synthesis and pharmacological analysis of a group of optically pure, structural and fluorescently labelled Y<sub>4</sub>R peptidic ligands derived from the homodimeric Y<sub>4</sub>R agonist BVD-74D peptide.

The optically pure analogues were obtained by bis-coupling the linear resin-bound peptides with the pre-synthesised 2,7-diaminosuberic acid units, which were robustly synthesised by alkene metathesis between two suitably protected allylglycine residues with the desired stereo-configuration. Particularly, we have found that a N<sup>α</sup>-Boc combined with a C-methyl ester enabled resistance to harsh synthesis conditions and also selective deprotection prior to peptide synthesis. On the other hand, the solid phase metathesis approach was less preferable owing to its lower yield and crude product purity. With the dimeric peptides in hand, mono-labelled analogues could be effectively prepared by using the desired fluorophore as the limiting reagent.

Competition binding assays have revealed that the (*R,R*)-stereoisomer of BVD-74D exhibited the strongest Y<sub>4</sub>R affinity, whereas the (*S,S*)-stereoisomer, the alkenyl-linked dimers and peptide methyl esters were all less favourable. In functional assays, all analogues appeared to be partial agonists, where the unlabelled (*R,R*)-BVD-74D and its mono-sCy5 labelled variant both showed higher efficacy and potency compared to their (*S,S*)-counterparts. The capability of mono-sCy5 labelled (*R,R*)-BVD-74D as a specific fluorescent Y<sub>4</sub>R ligand in competition binding experiments has been confirmed using living whole cells. The rhodamine B-labelled analogues exhibited weaker Y<sub>4</sub>R agonism and non-specific binding thus were not pursued further. To conclude, mono-sCy5-(*R,R*)-BVD-74D represents a novel fluorescently labelled peptide suitable for pharmacological studies and development of new ligands for Y<sub>4</sub>R.

## References

- (1) Lundell, I., Blomqvist, A. G., Berglund, M. M., Schober, D. A., Johnson, D., Statnick, M. A., Galski, R. A., Gehlert, D. R., and Larhammar, D. (1995) Cloning of a human receptor of the NPY receptor family with high affinity for pancreatic polypeptide and peptide YY. *J. Biol. Chem.* 270, 29123-29128.
- (2) Lundell, I., Statnick, M., Johnson, D., Schober, D., Starbäck, P., Gehlert, D., and Larhammar, D. (1996) The cloned rat pancreatic polypeptide receptor exhibits profound differences to the orthologous receptor. *Proc. Natl. Acad. Sci.* 93, 5111-5115.
- (3) Orci, L., Malaisse-Lagae, F., Baetens, D., and Perrelet, A. (1978) Pancreatic-polypeptide-rich regions in human pancreas. *Lancet* 312, 1200-1201.
- (4) Schwartz, T. W., Stadil, F., Chance, R. E., Rehfeld, J. F., Larson, L. I., and Moon, N. (1976) Pancreatic-polypeptide response to food in duodenal-ulcer patients before and after vagotomy. *Lancet* 307, 1102-1105.
- (5) Blomqvist, A. G., Söderberg, C., Lundell, I., Milner, R. J., and Larhammar, D. (1992) Strong evolutionary conservation of neuropeptide Y: sequences of chicken, goldfish, and *Torpedo marmorata* DNA clones. *Proc. Natl. Acad. Sci. USA* 89, 2350-2354.
- (6) Asakawa, A., Inui, A., Yuzuriha, H., Ueno, N., Katsuura, G., Fujimiya, M., Fujino, M. A., Nijima, A., Meguid, M. M., and Kasuga, M. (2003) Characterization of the effects of pancreatic polypeptide in the regulation of energy balance. *Gastroenterology* 124, 1325-1336.
- (7) Edelsbrunner, M. E., Painsipp, E., Herzog, H., and Holzer, P. (2009) Evidence from knockout mice for distinct implications of neuropeptide-Y Y<sub>2</sub> and Y<sub>4</sub> receptors in the circadian control of locomotion, exploration, water and food intake. *Neuropeptides* 43, 491-497.
- (8) Uhe, A. M., Szmukler, G. I., Collier, G. R., Hansky, J., O'Dea, K., and Young, G. P. (1992) Potential regulators of feeding behavior in anorexia nervosa. *Am. J. Clin. Nutr.* 55, 28-32.
- (9) Marco, J., Zulueta, M. A., Correas, I., and Villanueva, M. L. (1980) Reduced pancreatic polypeptide secretion in obese subjects. *J. Clin. Endocrinol. Metab.* 50, 744-747.
- (10) Lassmann, V., Vague, P., Vialettes, B., and Simon, M.-C. (1980) Low plasma levels of pancreatic polypeptide in obesity. *Diabetes* 29, 428-430.
- (11) Berntson, G. G., Zipf, W. B., O'Dorisio, T. M., Hoffman, J. A., and Chance, R. E. (1993) Pancreatic polypeptide infusions reduce food intake in Prader-Willi syndrome. *Peptides* 14, 497-503.
- (12) Cassidy, S. B. (1997) Prader-Willi syndrome. *J. Med. Genet.* 34, 917-923.
- (13) Cassidy, S. B., and Driscoll, D. J. (2008) Prader-Willi syndrome. *Eur. J. Hum. Genet.* 17, 3-13.

- 
- (14) Ueno, N., Inui, A., Iwamoto, M., Kaga, T., Asakawa, A., Okita, M., Fujimiya, M., Nakajima, Y., Ohmoto, Y., Ohnaka, M., Nakaya, Y., Miyazaki, J.-I., and Kasuga, M. (1999) Decreased food intake and body weight in pancreatic polypeptide-overexpressing mice. *Gastroenterology* 117, 1427-1432.
- (15) Asakawa, A., Inui, A., Kaga, T., Katsuura, G., Fujimiya, M., Fujino, M. A., and Kasuga, M. (2003) Antagonism of ghrelin receptor reduces food intake and body weight gain in mice. *Gut* 52, 947-952.
- (16) Andersen, D. K. (2007) Mechanisms and emerging treatments of the metabolic complications of chronic pancreatitis. *Pancreas* 35, 1-15.
- (17) Seymour, N. E., Volpert, A. R., Lee, E. L., Andersen, D. K., and Hernandez, C. (1995) Alterations in hepatocyte insulin binding in chronic pancreatitis: Effects of pancreatic polypeptide. *Am. J. Surg.* 169, 105-110.
- (18) Seymour, N. E., Spector, S. A., Andersen, D. K., Elm, M. S., and Whitcomb, D. C. (1998) Overexpression of hepatic pancreatic polypeptide receptors in chronic pancreatitis. *J. Surg. Res.* 76, 47-52.
- (19) Brunicardi, F., Chaiken, R., Ryan, A., Seymour, N., Hoffmann, J., Lebovitz, H., Chance, R., Gingerich, R., Andersen, D., and Elahi, D. (1996) Pancreatic polypeptide administration improves abnormal glucose metabolism in patients with chronic pancreatitis. *J. Clin. Endocrinol. Metab.* 81, 3566-3572.
- (20) Rabiee, A., Galiatsatos, P., Salas-Carrillo, R., Thompson, M. J., Andersen, D. K., and Elahi, D. (2011) Pancreatic polypeptide administration enhances insulin sensitivity and reduces the insulin requirement of patients on insulin pump therapy. *J. Diabetes Sci. Technol.* 5, 1521-1528.
- (21) Tasan, R. O., Lin, S., Hetzenauer, A., Singewald, N., Herzog, H., and Sperk, G. (2009) Increased novelty-induced motor activity and reduced depression-like behavior in neuropeptide Y (NPY)-Y<sub>4</sub> receptor knockout mice. *Neuroscience* 158, 1717-1730.
- (22) Painsipp, E., Wultsch, T., Edelsbrunner, M. E., Tasan, R. O., Singewald, N., Herzog, H., and Holzer, P. (2008) Reduced anxiety-like and depression-related behavior in neuropeptide Y Y<sub>4</sub> receptor knockout mice. *Genes, Brain and Behav.* 7, 532-542.
- (23) Steru, L., Chermat, R., Thierry, B., and Simon, P. (1985) The tail suspension test: a new method for screening antidepressants in mice. *Psychopharmacology* 85, 367-370.
- (24) Painsipp, E., Herzog, H., and Holzer, P. (2010) Evidence from knockout mice that neuropeptide-Y Y<sub>2</sub> and Y<sub>4</sub> receptor signalling prevents long-term depression-like behaviour caused by immune challenge. *J. Psychopharmacol.* 24, 1551-1560.
- (25) Berlicki, Ł., Kaske, M., Gutiérrez-Abad, R., Bernhardt, G., Illa, O., Ortuño, R. M., Cabrele, C., Buschauer, A., and Reiser, O. (2013) Replacement of Thr<sup>32</sup> and Gln<sup>34</sup> in the C-terminal neuropeptide Y fragment 25–36 by *cis*-cyclobutane and *cis*-cyclopentane β-amino acids shifts selectivity toward the Y<sub>4</sub> receptor. *J. Med. Chem.* 56, 8422-8431.

- 
- (26) Kaske, M. (2012) in *Naturwissenschaftlichen Fakultät IV – Chemie und Pharmazie*, der Universität Regensburg, Germany.
- (27) Parker, E. M., Babij, C. K., Balasubramaniam, A., Burrier, R. E., Guzzi, M., Hamud, F., Gitali, M., Rudinski, M. S., Tao, Z., Tice, M., Xia, L., Mullins, D. E., and Salisbury, B. G. (1998) GR231118 (1229U91) and other analogues of the C-terminus of neuropeptide Y are potent neuropeptide Y Y<sub>1</sub> receptor antagonists and neuropeptide Y Y<sub>4</sub> receptor agonists. *Eur. J. Pharmacol.* 349, 97-105.
- (28) Daniels, A., Matthews, J., Slepetis, R., Jansen, M., Viveros, O., Tadepalli, A., Harrington, W., Heyer, D., Landavazo, A., and Leban, J. (1995) High-affinity neuropeptide Y receptor antagonists. *Proc. Natl. Acad. Sci.* 92, 9067-9071.
- (29) Gehlert, D., Schober, D., Beavers, L., Gadski, R., Hoffman, J., Smiley, D., Chance, R., Lundell, I., and Larhammar, D. (1996) Characterization of the peptide binding requirements for the cloned human pancreatic polypeptide-preferring receptor. *Mol. Pharmacol.* 50, 112-118.
- (30) Matthews, J. E., Jansen, M., Lyerly, D., Cox, R., Chen, W.-J., Koller, K. J., and Daniels, A. J. (1997) Pharmacological characterization and selectivity of the NPY antagonist GR231118 (1229U91) for different NPY receptors. *Regul. Pept.* 72, 113-119.
- (31) Schober, D. A., Gackenhimer, S. L., Heiman, M. L., and Gehlert, D. R. (2000) Pharmacological characterization of 125I-1229U91 binding to Y<sub>1</sub> and Y<sub>4</sub> neuropeptide Y/peptide YY receptors. *J. Pharmacol. Exp. Ther.* 293, 275-280.
- (32) Balasubramaniam, A., Zhai, W., Sheriff, S., Tao, Z., Chance, W. T., Fischer, J. E., Eden, P., and Taylor, J. (1996) Bis(31/31'){[Cys31,Trp32,Nva34]NPY- (31-36)}: A Specific NPY Y-1 Receptor Antagonist. *J. Med. Chem.* 39, 811-813.
- (33) Balasubramaniam, A., Mullins, D. E., Lin, S., Zhai, W., Tao, Z., Dhawan, V. C., Guzzi, M., Knittel, J. J., Slack, K., Herzog, H., and Parker, E. M. (2006) Neuropeptide Y (NPY) Y<sub>4</sub> receptor selective agonists based on NPY(32-36): development of an anorectic Y<sub>4</sub> receptor selective agonist with picomolar affinity. *J. Med. Chem.* 49, 2661-2665.
- (34) Ziemek, R., Schneider, E., Kraus, A., Cabrele, C., Beck-Sickinger, A. G., Bernhardt, G., and Buschauer, A. (2007) Determination of affinity and activity of ligands at the human neuropeptide Y Y<sub>4</sub> receptor by flow cytometry and aequorin luminescence. *J. Recept. Signal Transduct. Res.* 27, 217-233.
- (35) Parker, M. S., Sah, R., Sheriff, S., Balasubramaniam, A., and Parker, S. L. (2005) Internalization of cloned pancreatic polypeptide receptors is accelerated by all types of Y<sub>4</sub> agonists. *Regul. Pept.* 132, 91-101.
- (36) Balasubramaniam, A., Dhawan, V. C., Mullins, D. E., Chance, W. T., Sheriff, S., Guzzi, M., Prabhakaran, M., and Parker, E. M. (2001) Highly selective and potent neuropeptide Y (NPY) Y<sub>1</sub> receptor antagonists based on [Pro(30), Tyr(32), Leu(34)]NPY(28-36)-NH<sub>2</sub> (BW1911U90). *J. Med. Chem.* 44, 1479-1482.

- (37) Stymiest, J. L., Mitchell, B. F., Wong, S., and Vederas, J. C. (2005) Synthesis of oxytocin analogues with replacement of sulfur by carbon gives potent antagonists with increased stability. *J. Org. Chem.* 70, 7799-7809.
- (38) Carotenuto, A., D'Addona, D., Rivalta, E., Chelli, M., Papini, A. M., Rovero, P., and Ginanneschi, M. (2005) Synthesis of a dicarba-analog of octreotide keeping the type II'  $\beta$  -turn of the pharmacophore in water solution. *Lett. Org. Chem.* 2, 274-279.
- (39) Andrews, M. J. I., and Tabor\*, A. B. (1997) Synthesis of an orthogonally-protected bifunctional amino acid for conformationally constrained peptides. *Tetrahedron Lett.* 38, 3063-3066.
- (40) Kambayashi, Y., Nakajima, S., Ueda, M., and Inouye, K. (1989) A dicarba analog of beta-atrial natriuretic peptide (beta-ANP) inhibits guanosine 3',5'-cyclic monophosphate production induced by alpha-ANP in cultured rat vascular smooth muscle cells. *FEBS Lett.* 248, 28-34.
- (41) Hase, S., Morikawa, T., and Sakakibara, S. (1969) Synthesis of a biologically active analog of deamino-8-arginine-vasopressin which does not contain a disulphide bond. *Experientia* 25, 1239-1240.
- (42) čeřovský, V., Wünsch, E., and Brass, J. (1997) Enzymatic semisynthesis of dicarba analogs of calcitonin. *Eur. J. Biochem.* 247, 231-237.
- (43) Kremminger, P., and Undheim, K. (1997) Asymmetric synthesis of unsaturated and bis-hydroxylated (S,S)-2,7-Diaminosuberic acid derivatives. *Tetrahedron* 53, 6925-6936.
- (44) Hiebl, J., Blanka, M., Guttman, A., Kollmann, H., Leitner, K., Mayrhofer, G., Rovenszky, F., and Winkler, K. (1998) A detailed investigation of the preparation of 2,7-diaminosuberic acid and 2,5-diaminoadipic acid derivatives using Kolbe electrolysis. *Tetrahedron* 54, 2059-2074.
- (45) Hiebl, J., Kollmann, H., Rovenszky, F., and Winkler, K. (1999) Enantioselective synthesis of diamino dicarboxylic acids. *J. Org. Chem.* 64, 1947-1952.
- (46) Astruc, D. (2005) The metathesis reactions: from a historical perspective to recent developments. *New J. Chem.* 29, 42-56.
- (47) Jean-Louis Hérisson, P., and Chauvin, Y. (1971) Catalyse de transformation des oléfines par les complexes du tungstène. II. Télomérisation des oléfines cycliques en présence d'oléfines acycliques. *Makromol. Chem.* 141, 161-176.
- (48) Schrock, R., Rocklage, S., Wengrovius, J., Rupprecht, G., and Fellmann, J. (1980) Preparation and characterization of active niobium, tantalum and tungsten metathesis catalysts. *J. Mol. Catal.* 8, 73-83.
- (49) Schrock, R. R., Murdzek, J. S., Bazan, G. C., Robbins, J., DiMare, M., and O'Regan, M. (1990) Synthesis of molybdenum imido alkylidene complexes and some reactions involving acyclic olefins. *J. Am. Chem. Soc.* 112, 3875-3886.

- 
- (50) Wengrovius, J. H., Schrock, R. R., Churchill, M. R., Missert, J. R., and Youngs, W. J. (1980) Multiple metal-carbon bonds. 16. Tungsten-oxo alkylidene complexes as olefins metathesis catalysts and the crystal structure of  $W(O)(CHCMe_3(PEt_3)Cl_2$ . *J. Am. Chem. Soc.* 102, 4515-4516.
- (51) Wolf, J., Stürer, W., Grünwald, C., Werner, H., Schwab, P., and Schulz, M. (1998) Ruthenium trichloride, tricyclohexyl-phosphane, 1-alkynes, magnesium, hydrogen, and water - ingredients of an efficient one-pot synthesis of ruthenium catalysts for olefin metathesis. *Angew. Chem. Int. Ed. Engl.* 37, 1124-1126.
- (52) Hong, S. H., and Grubbs, R. H. (2006) Highly active water-soluble olefin metathesis catalyst. *J. Am. Chem. Soc.* 128, 3508-3509.
- (53) Stymiest, J. L., Mitchell, B. F., Wong, S., and Vederas, J. C. (2003) Synthesis of biologically active dicarba analogues of the peptide hormone oxytocin using ring-closing metathesis. *Org. Lett.* 5, 47-49.
- (54) Miller, S. J., Blackwell, H. E., and Grubbs, R. H. (1996) Application of ring-closing metathesis to the synthesis of rigidified amino acids and peptides. *J. Am. Chem. Soc.* 118, 9606-9614.
- (55) Robinson, A. J., Elaridi, J., van Lierop, B. J., Mujcinovic, S., and Jackson, W. R. (2007) Microwave-assisted RCM for the synthesis of carbocyclic peptides. *J. Pept. Sci.* 13, 280-285.
- (56) van Lierop, B. J., Bornschein, C., Jackson, W. R., and Robinson, A. J. (2011) Ring-closing metathesis in peptides - the sting is in the tail! *Aust. J. Chem.* 64, 806-811.
- (57) Elaridi, J., Patel, J., Jackson, W. R., and Robinson, A. J. (2006) Controlled synthesis of (S,S)-2,7-diaminosuberic acid: A method for regioselective construction of dicarba analogues of multicystine-containing peptides. *J. Org. Chem.* 71, 7538-7545.
- (58) Doh, H.-J., Cho, W.-J., Yong, C.-S., Choi, H.-G., Kim, J. S., Lee, C.-H., and Kim, D.-D. (2003) Synthesis and evaluation of Ketorolac ester prodrugs for transdermal delivery. *J. Pharm. Sci.* 92, 1008-1017.
- (59) Beaumont, K., Webster, R., Gardner, I., and Dack, K. (2003) Design of ester prodrugs to enhance oral absorption of poorly permeable compounds: challenges to the discovery scientist. *Curr. Drug. Met.* 4, 461-485.
- (60) Zablocki, J. A., Tjoeng, F. S., Bovy, P. R., Miyano, M., Garland, R. B., Williams, K., Schretzman, L., Zupec, M. E., Rico, J. G., Lindmark, R. J., Toth, M. V., McMackins, D. E., Adams, S. P., Panzer-Knodle, S. G., Nicholson, N. S., Taite, B. B., Salyers, A. K., King, L. W., Champion, J. G., and Feigen, L. P. (1995) A novel series of orally active antiplatelet agents. *Bioorg. Med. Chem.* 3, 539-551.
- (61) Sawada, K., Terada, T., Saito, H., Hashimoto, Y., and Inui, K.-I. (1999) Recognition of L-amino acid ester compounds by rat peptide transporters PEPT1 and PEPT2. *J. Pharmacol. Exp. Ther.* 291, 705-709.

- (62) Jois, S. D. S., and Balasubramaniam, A. (2003) Conformation of neuropeptide Y receptor antagonists: structural implications in receptor selectivity. *Peptides* 24, 1035-1043.
- (63) Turner, R. A., Weber, R. J., and Lokey, R. S. (2010) Direct conversion of resin-bound peptides to C-terminal esters. *Org. Lett.* 12, 1852-1855.
- (64) Millington, C. R., Quarrell, R., and Lowe, G. (1998) Aryl hydrazides as linkers for solid phase synthesis which are cleavable under mild oxidative conditions. *Tetrahedron Lett.* 39, 7201-7204.
- (65) Xue, C.-B., Caldwell, G. A., Becker, J. M., and Naider, F. (1989) Total synthesis of the lipopeptide  $\alpha$ -mating factor of *saccharomyces cerevisiae*. *Biochem. Biophys. Res. Co.* 162, 253-257.
- (66) Ludolph, B., Eisele, F., and Waldmann, H. (2002) Solid-phase synthesis of lipidated peptides. *J. Am. Chem. Soc.* 124, 5954-5955.

## CHAPTER 5 Conclusion and Future Directions

---

---

This thesis has explored the synthesis of several fluorescent natural and modified peptides for use in the *in vitro* imaging of GPCRs. At a fundamental level it is built on the idea that the activity and thus utility of the fluorescent peptide will hinge on the location and nature of the fluorophore and the chemistry of the linkage to the peptide, and highlights the importance of developing a range of chemistries to achieve useful compounds. Ligands with promising pharmacological properties have been identified, which enable the application of these ligands in receptor optical imaging.

The thesis has been presented as studies of increasing chemical complexity from the relatively straightforward N-terminal acylation of linear peptides through to the development of orthogonal approaches to peptide labelling and “fluorophore scanning” and finally the synthesis of a complex labelled peptide dimer structure utilising metathesis chemistry that is orthogonal to both peptide synthesis and conjugation.

In Chapter 2 the development of fluorescently labelled analogues based on two neuropeptides, ghrelin and kisspeptin was described. The human ghrelin analogue [Lys(RhB)<sup>19</sup>]hGhrelin<sub>1-19</sub> was synthesised utilising an orthogonal protection strategy adapted from McGirr *et al.*(1) to facilitate the introduction of a side-chain fatty acid and fluorophore. The resulting analogue showed highly specific human GHS-R1a binding and comparably strong agonism to the endogenous peptide, and continues to be used to identify the receptor in native tissue systems. In addition, the principles have been applied in the first attempts to prepare a fluorescent version of the cyclic ghrelin analogues. The array of effects that ghrelin and its analogues show appear to



be mediated by more than one receptor and our attention is turning to fluorescent versions of these derivatives, such as the cyclic peptide AZP531 (2) in the hope that they might allow identification of the receptor targets.

Both human and tilapia kisspeptin analogues were prepared, where the fluorescent labels were incorporated in solution phase without orthogonal protection. Human kisspeptin-10 tolerated a N-terminal rhodamine B conjugation, but not a Cy5.5 labelling. Moreover, a Pop<sup>4</sup> residue also sacrificed GPR54 agonism. By modifying the predicted tilapia Kiss1 and Kiss2 sequences, we have found that a N-terminal rhodamine B on tilapia Kiss2 retained agonism in nanomolar range. This analogue has displayed potential as a novel fluorescent ligand for mapping tilapia GPR54 in GnRH neurons during our preliminary imaging studies. On the other hand, Kiss1 and its analogues were all inactive.

In Chapter 3 the preparation of Y<sub>1</sub>R-targeting fluorescent peptides derived from the NPY 9-amino acid fragment BVD-15 is described. In a scanning type strategy, the 2-, 3- and 4-positions were examined as potential conjugation sites. Labelling at the 3-position was achieved by CuAAC reactions between Pop and the azide-bearing coumarin and rhodamine B derivatives. Labelling proceeded rapidly with high yield in solution phase, and most peptide conjugates exhibited strong Y<sub>1</sub>R affinity. The 2- and 4-position labelled analogues incorporated cyanine and rhodamine B derivatives via either an ordinary Lys (amide) or an azide-bearing Lys (triazole). We have found that [Lys<sup>2</sup>(sCy5), Arg<sup>4</sup>]BVD-15 displayed highly specific Y<sub>1</sub>R and Y<sub>4</sub>R binding, and competitive Y<sub>1</sub>R antagonism and Y<sub>4</sub>R partial agonism. The usefulness of [Lys<sup>2</sup>(sCy5), Arg<sup>4</sup>]BVD-15 in Y<sub>1</sub>R and Y<sub>4</sub>R competition binding assays have been demonstrated using whole cell imaging experiments.

Chapter 4 described preparation of Y<sub>4</sub>R-targeting fluorescent peptides derived from the selective Y<sub>4</sub>R agonist BVD-74D and also showed the utility of the [Lys<sup>2</sup>(sCy5), Arg<sup>4</sup>]BVD-15 from Chapter 3 in performing the studies. Robust synthetic routes were developed towards the two optically pure stereoisomers of BVD-74D by exploiting metathesis between suitably protected allylglycine residues. N-terminal mono-labelling was achieved in solution using limited equivalence of the fluorophore. We have found that the (*R,R*)-stereoisomer exhibited stronger Y<sub>4</sub>R affinity and agonism comparing to the (*S,S*)-counterpart. Their sCy5-labelled variants essentially retained Y<sub>4</sub>R agonism, while the (*R,R*)-stereoisomer showed greater efficacy and potency. The suitability of mono-sCy5-(*R,R*)-BVD-74D as a fluorescent Y<sub>4</sub>R ligand was also confirmed by imaging studies.

In summary, we have successfully demonstrated effective peptide synthesis and fluorescence conjugation strategies, which have resulted in promising ligands suitable for *in vitro* receptor imaging studies. Importantly, these results may serve as valuable guides in developing future fluorescent ligands for imaging studies of other Y receptor subtypes, or any therapeutically useful GPCRs.

The work here offers a number of opportunities and ideas for further research. Not least the work may find application in the search for new treatments for obesity, a disease in which Y receptor ligands have great potential. Obesity has become a major global health concern, as the associated comorbidities, e.g. type II diabetes, hypertension, stroke and cardiovascular diseases,(3) place heavy burden on the social community and healthcare system. In Australia, the prevalence of overweight and obesity in the past decade has increased from 56.3% in 1995 to 62.8% in 2011-12.(4) Unfortunately, the treatment options for obesity are limited (**Table 1**). There is

an urgent need for new anti-obesity pharmaceuticals that are both safer and more effective.

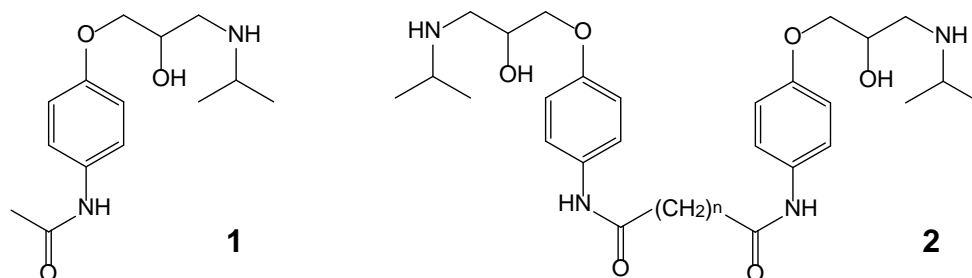
**Table 1:** Past and currently approved treatment options for obesity (summarised from reference (5))

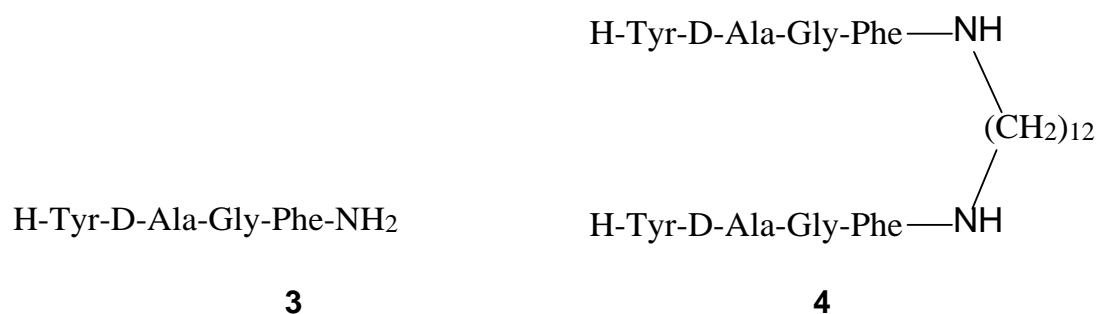
Treatment options	Disadvantages	Reference
Life style changes (e.g. exercise, dieting)	No marked or sustainable effects	(6, 7)
Psychological therapies	Cannot be delivered on mass scale; less effective in long-term	(8)
Surgery (reserved for morbid obesity)	Associated mortality and complications, needs for re-operation	(9)
Centrally acting sympathomimetics	Cardiovascular risk, abuse	(10)
Fenfluramine, dexfenfluramine	Cardiac valvulopathy	(11)
Sibutramine	Cardiovascular risk	(12, 13)
Rimonabant	Psychiatric disorders	(14, 15)
Orlistat (only long-term anti-obesity agent approved in Europe)	Gastrointestinal side-effects (generally mild)	(16)

In searching for targets of anti-obesity drugs, there has been interest in each of the human isoforms, Y<sub>1</sub>R antagonist and Y<sub>4</sub>R agonists among them. In the course of our work we have uncovered new SAR around the target peptides that offer opportunities for new therapeutic development, and in the fluorescent ligands, a means to efficiently screen for new compounds. We are also interested in NPY Y<sub>2</sub>R and Y<sub>5</sub>R, both of which also play important roles in regulation of feeding behaviour. Activation of Y<sub>2</sub>R was found to suppress food intake,(17, 18) and activation of Y<sub>5</sub>R appeared to promote food intake and reduce energy expenditure.(19) These findings support the speculation that in addition to Y<sub>1</sub>R and Y<sub>4</sub>R ligands, Y<sub>2</sub>R agonists and Y<sub>5</sub>R antagonists hold significance as promising lead compounds in developing anti-obesity drugs.

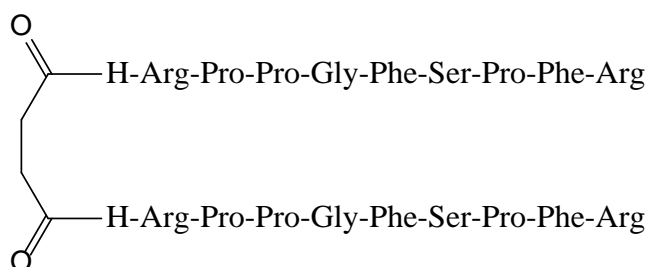
Fluorescently labelled peptides targeting Y<sub>2</sub>R and Y<sub>5</sub>R could be valuable tools in understanding the location, regulation and mechanism of action of those receptors. Our success in adapting dimeric analogues based on 1229U91 (Y<sub>1</sub>R) and BVD-74D

(Y<sub>4</sub>R) has emphasised the value of the “bivalent ligand” approach in our future work. By definition, “bivalent ligands” refer to molecules containing two pharmacophores covalently linked by a spacer.<sup>(20)</sup> This approach has been attracting increasing attention, as the dimeric derivatives often display improved pharmacological or pharmacokinetic properties over their corresponding monomer. For example, the bivalent analogue (**2**) showed over 160-fold stronger  $\beta$ -receptor affinity over its monomer practolol (**1**), and the  $\beta_1/\beta_2$  selectivity could be altered by manipulating the spacer length.<sup>(21)</sup> While the monomeric peptide (**3**) showed preferential binding to opioid  $\mu$  receptors, its dimeric variant (**4**) exhibited nanomolar affinity to the  $\delta$  subtype and 92-fold  $\delta$  selectivity over  $\mu$  receptors.<sup>(22)</sup> As another interesting example, the dimeric peptide succinyl-*bis*-bradykinin (**6**) only exhibited 9% potency of its monomer bradykinin (**5**) in an enzyme-free tissue preparation, but was almost equally potent when metabolic enzymes were present.<sup>(23)</sup> Similarly, our previous stability studies demonstrated that the dimeric peptide 1229U91 possessed a markedly longer half-life in human plasma (approx. 320 min) than the monomeric [Lys<sup>4</sup>]BVD-15 (< 0.5 min) (unpublished data). The enhanced metabolic stability holds significance, as short duration of action caused by enzymatic degradation is an ongoing issue in developing peptide-based drugs, especially in orally available formulations.





**5**



**6**

Inspired by this approach, we have taken particular note of the literature dimeric Y<sub>5</sub>R agonist BWX-46 bis(31/31')(Cys<sup>31</sup>,Nva<sup>34</sup>)NPY<sub>27-36</sub>-NH<sub>2</sub> (**Figure 1**). This peptide showed comparable Y<sub>5</sub>R affinity to NPY (IC<sub>50</sub> = 0.85 nM vs. 0.54 nM respectively) but markedly stronger Y<sub>5</sub>R selectivity.(24) It also stimulated food intake in rats following injection into the hypothalamus. The authors observed lack of stimulation at lower dose, and explained it by the poor *in vivo* stability of the disulfide linkage. Accordingly, we have recently synthesised BWX-46 and its analogues and they are now being assayed in cell-based Y<sub>5</sub>R binding assays. If these analogues retain Y<sub>5</sub>R activity, they may offer ideal starting compounds for developing novel bioavailable Y<sub>5</sub>R ligands (including fluorescently labelled analogues).

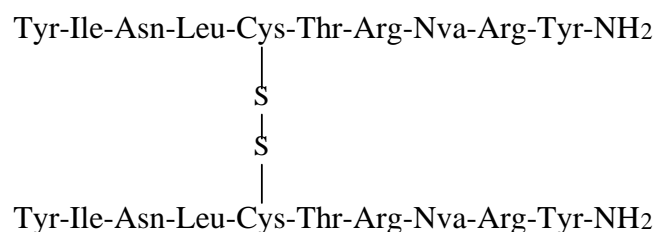


**Figure 1:** BWX-46 reported by Balasubramaniam *et al.*

Finally, although to date there is no dimeric Y<sub>2</sub>R ligand reported, it is reasonable to speculate that the selective Y<sub>2</sub>R ligands hNPY<sub>3-36</sub> and hPYY<sub>3-36</sub> may be good starting points to derive such ligands. (18, 25)

## References

- (1) McGirr, R., McFarland, M. S., McTavish, J., Luyt, L. G., and Dhanvantari, S. (2011) Design and characterization of a fluorescent ghrelin analog for imaging the growth hormone secretagogue receptor 1a. *Regul. Pept.* 172, 69-76.
- (2) Granata, R., Settanni, F., Julien, M., Nano, R., Togliatto, G., Trombetta, A., Gallo, D., Piemonti, L., Brizzi, M. F., Abribat, T., van Der Lely, A.-J., and Ghigo, E. (2012) Des-acyl ghrelin fragments and analogues promote survival of pancreatic  $\beta$ -cells and human pancreatic islets and prevent diabetes in streptozotocin-treated rats. *J. Med. Chem.* 55, 2585-2596.
- (3) Flegal, K. M., Graubard, B. I., Williamson, D. F., and Gail, M. H. (2007) Cause-specific excess deaths associated with underweight, overweight, and obesity. *JAMA* 298, 2028-2037.
- (4) Australian Bureau of Statistics. (2013).
- (5) Rodgers, R. J., Tschöp, M. H., and Wilding, J. P. H. (2012) Anti-obesity drugs: past, present and future. *Dis. Model. Mech.* 5, 621-626.
- (6) Dansinger, M. L., Gleason, J., Griffith, J. L., Selker, H. P., and Schaefer, E. J. (2005) Comparison of the atkins, ornish, weight watchers, and zone diets for weight loss and heart disease risk reduction: A randomized trial. *JAMA* 293, 43-53.
- (7) LeBlanc, E. S., O'Connor, E., Whitlock, E. P., Patnode, C. D., and Kapka, T. (2011) Effectiveness of primary care-relevant treatments for obesity in adults: a systematic evidence review for the U.S. preventive services task force. *Ann. Intern. Med.* 155, 434-447.
- (8) Wing, R. R., Tate, D. F., Gorin, A. A., Raynor, H. A., and Fava, J. L. (2006) A self-regulation program for maintenance of weight loss. *N. Engl. J. Med.* 355, 1563-1571.
- (9) Field, B. C. T., Chaudhri, O. B., and Bloom, S. R. (2009) Obesity treatment: novel peripheral targets. *Br. J. Clin. Pharmacol.* 68, 830-843.
- (10) Call, T. D., Hartneck, J., Dickinson, A., Hartman, C. W., and Bartel, A. G. (1982) Acute cardiomyopathy secondary to intravenous amphetamine abuse. *Ann. Intern. Med.* 97, 559-560.
- (11) Connolly, H. M., Crary, J. L., McGoon, M. D., Hensrud, D. D., Edwards, B. S., Edwards, W. D., and Schaff, H. V. (1997) Valvular heart disease associated with fenfluramine-phentermine. *N. Engl. J. Med.* 337, 581-588.
- (12) James, W. P. T., Caterson, I. D., Coutinho, W., Finer, N., Van Gaal, L. F., Maggioni, A. P., Torp-Pedersen, C., Sharma, A. M., Shepherd, G. M., Rode, R. A., and Renz, C. L. (2010) Effect of sibutramine on cardiovascular outcomes in overweight and obese subjects. *N. Engl. J. Med.* 363, 905-917.

- 
- (13) Scheen, A. J. (2011) Sibutramine on cardiovascular outcome. *Diabetes Care* 34, S114-S119.
- (14) European Medicines Agency Press Office. (2008), London.
- (15) Moreira, F. A., and Crippa, J. A. S. (2009) The psychiatric side-effects of rimonabant. *Rev. Bras. Psiquiatr.* 31, 145-153.
- (16) Hennes, S., and Perry, C. M. (2006) Orlistat: a review of its use in the management of obesity. *Drugs* 66, 1625-1656.
- (17) DeCarr, L. B., Buckholz, T. M., Milardo, L. F., Mays, M. R., Ortiz, A., and Lumb, K. J. (2007) A long-acting selective neuropeptide Y<sub>2</sub> receptor PEGylated peptide agonist reduces food intake in mice. *Bioorg. Med. Chem. Lett.* 17, 1916-1919.
- (18) Batterham, R. L., Cowley, M. A., Small, C. J., Herzog, H., Cohen, M. A., Dakin, C. L., Wren, A. M., Brynes, A. E., Low, M. J., Ghatei, M. A., Cone, R. D., and Bloom, S. R. (2002) Gut hormone PYY<sub>3-36</sub> physiologically inhibits food intake. *Nature* 418, 650-654.
- (19) Hwa, J. J., Witten, M. B., Williams, P., Ghibaudi, L., Gao, J., Salisbury, B. G., Mullins, D., Hamud, F., Strader, C. D., and Parker, E. M. (1999) Activation of the NPY Y<sub>5</sub> receptor regulates both feeding and energy expenditure. *Am. J. Physiol.* 277, R1428-R1434.
- (20) Halazy, S. (1999) G-protein coupled receptors bivalent ligands and drug design. *Expert Opin. Ther. Pat.* 9, 431-446.
- (21) Kizuka, H., and Hanson, R. N. (1987)  $\beta$ -Adrenoceptor antagonist activity of bivalent ligands. 1. Diamide analogs of practolol. *J. Med. Chem.* 30, 722-726.
- (22) Shimohigashi, Y., Costa, T., Chen, H.-C., and Rodbard, D. (1982) Dimeric tetrapeptide enkephalins display extraordinary selectivity for the  $\delta$  opiate receptor. *Nature* 297, 333-335.
- (23) Vevrek, R. J., and Stewart, J. M. (1983) in *Peptides: Proceedings of the Eighth American Peptide Symposium* (Hurby, V. J., and Rich, D. H., Eds.) pp 381-384, Pierce Chemical Co., Rockford, IL, USA.
- (24) Balasubramaniam, A., Sheriff, S., Zhai, W., and Chance, W. T. (2002) Bis(31/31'){[Cys<sup>31</sup>, Nva<sup>34</sup>]NPY(27-36)-NH<sub>2</sub>}: a neuropeptide Y (NPY) Y<sub>5</sub> receptor selective agonist with a latent stimulatory effect on food intake in rats. *Peptides* 23, 1485-1490.
- (25) Grandt, D., Schmiczek, M., Rascher, W., Feth, F., Shively, J., Lee, T. D., Davis, M. T., Reeve Jr, J. R., and Michel, M. C. (1996) Neuropeptide Y 3-36 is an endogenous ligand selective for Y<sub>2</sub> receptors. *Regul. Pept.* 67, 33-37.



## **Appendix – Co-authored Publications**

# Propargyloxypyrroline Regio- and Stereoisomers for Click-Conjugation of Peptides: Synthesis and Application in Linear and Cyclic Peptides

Susan E. Northfield,<sup>A</sup> Simon J. Mountford,<sup>A</sup> Jerome Wielens,<sup>A,B</sup>  
Mengjie Liu,<sup>A</sup> Lei Zhang,<sup>C</sup> Herbert Herzog,<sup>C</sup> Nicholas D. Holliday,<sup>D</sup>  
Martin J. Scanlon,<sup>A</sup> Michael W. Parker,<sup>B,E</sup> David K. Chalmers,<sup>A</sup>  
and Philip E. Thompson<sup>A,F</sup>

<sup>A</sup>Medicinal Chemistry, Monash Institute of Pharmaceutical Sciences, 381 Royal Parade, Parkville, Vic. 3052, Australia.

<sup>B</sup>ACRF Rational Drug Discovery Centre, St Vincent's Institute of Medical Research, Fitzroy, Vic. 3065, Australia.

<sup>C</sup>Neuroscience Research Program, Garvan Institute of Medical Research, St Vincent's Hospital, Darlinghurst, NSW 2010, Australia.

<sup>D</sup>Institute of Cell Signalling, School of Life Sciences, University of Nottingham, Queen's Medical Centre, Nottingham NG7 2UH, UK.

<sup>E</sup>Department of Biochemistry and Molecular Biology, Bio21 Molecular Science and Biotechnology Institute, The University of Melbourne, Parkville, Vic. 3010, Australia.

<sup>F</sup>Corresponding author. Email: [philip.thompson@monash.edu](mailto:philip.thompson@monash.edu)

The use of the click reaction for the introduction of conjugate groups, such as affinity or fluorescent labels, to a peptide for the study of peptide biochemistry and pharmacology is widespread. However, the nature and location of substituted 1,2,3-triazoles in peptide sequences may markedly affect conformation or binding as compared with native sequences. We have examined the preparation and application of propargyloxypyrroline (Pop) residues as a precursor to such peptide conjugates. Pop residues are available in a range of regio- and stereoisomers from hydroxypyrroline precursors and are readily prepared in Fmoc-protected form. They can be incorporated routinely in peptide synthesis and broadly retain the conformational properties of the parent proline containing peptides. This is exemplified by the preparation of biotin- and fluorophore-labelled peptides derived from linear and cyclic peptides.

Manuscript received: 26 March 2015.

Manuscript accepted: 15 May 2015.

Published online: 24 June 2015.

## Introduction

The ability to readily label and/or conjugate peptides is an important facet of biological chemistry research.<sup>[1]</sup> Such conjugates can be used for tagging bioactive peptides with specific labels to track and identify binding targets, or they can be used to alter physicochemical properties for improved pharmacological activity.<sup>[2]</sup> The positions at which peptides can be usefully functionalised are critically dependent on what region of the peptide is necessary for activity. In linear peptides, conjugates can be added to either the N- or C-terminus, or from one of the amino acid side-chains, commonly a lysine or tyrosine, but these regions should not be part of the key pharmacophore. Conjugates can also be attached using a range of linking chains, varying in length and/or polarity, to distance them from the bioactive peptide. When dealing with head-to-tail cyclic peptides, the choice of where to introduce conjugates is more limited as there is no free terminus available at which to functionalise, and local structural changes can have a marked

impact on cyclic peptide conformation. A position in the peptide must be identified where a conjugate could be incorporated without disrupting the binding or activity of the parent peptide sequence.

Proline provides unique conformational restraint as compared with the other natural amino acids, driven by its cyclic structure and the presence of a tertiary amide bond. Proline is also frequently reported as a tool to induce reverse-turns in cyclic peptides.<sup>[3]</sup> This function can place the proline residue in a conformation protruding away from the peptide binding/activity site, making proline an attractive residue at which to incorporate functionality (Fig. 1). Proline derivatisation, or 'editing' as it has recently been termed, has been shown to be a diverse approach to peptide derivatisation.<sup>[4]</sup> Zondlo et al. have described a range of diverse modifications to proline that allow for further derivatisation. This report on an array of substituted prolines notes the influence substitution might have on *cis-trans* isomerisation and even peptide conformation.

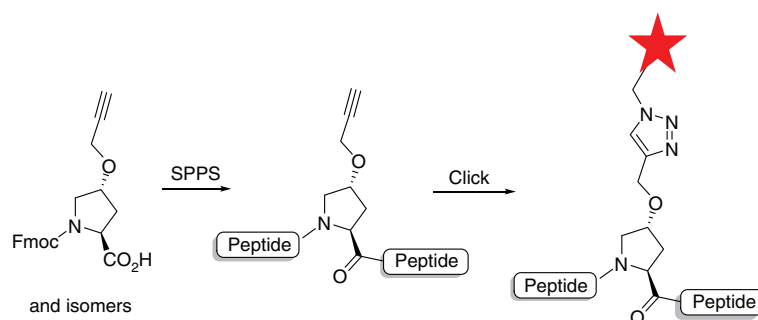


**Fig. 1.** ‘Exposed’ proline residues in cyclic or linear peptides can be modified to include ‘handles’ for side-chain conjugation. Proline residues appended with a propargyloxy handle are incorporated in place of proline in peptides. Labels (star) are introduced using standard conditions for copper-catalysed azide–alkyne conjugation (CuAAC) reactions (SPPS: solid phase peptide synthesis).

Similarly, we envisaged that introduction of a propargyloxy group yielding propargyloxypyrrolidine (Pop) residues might fulfil a similar role in the development of peptide conjugates undergoing click reactions. The click reaction is one of the most widely used methods of introducing conjugates into azido or alkyne-containing peptides.<sup>[5]</sup> The use of click reactions using Pop derivatives as substrates has included the synthesis of macrocyclic peptides<sup>[6]</sup> and also as a way of immobilising proline as an asymmetric catalyst for aldol reactions.<sup>[7]</sup> We anticipated using hydroxyproline stereoisomers as precursors, to gain access to a range of isomeric Pop-containing peptides. The resultant triazolylmethoxy conjugates would supply a useful spacer away from the peptide chain, minimising the impact of the conjugate on the peptide structure.

We report here on the synthesis of a range of Fmoc-protected Pop regio- and stereoisomers and their incorporation into two classes of peptide of interest in our laboratories. The first were derivatives of the  $Y_1$  receptor antagonist peptide, BVD15, and the second were cyclic hexapeptides incorporating a Lys–Ile–Asp–Asn (KIDN) pharmacophore motif of lens epithelium-derived growth factor (LEDGF), a key protein for the activity of HIV integrase (IN).

We and others have had an on-going interest in the development of conjugates of peptides that bind to the  $Y_1$  G-protein coupled receptors,<sup>[8]</sup> and we had reported modification of a proline residue by Ctp (Fig. 2) in the dimeric  $Y_1$  antagonist, 1229U91 but with significant loss of activity.<sup>[9]</sup> Another prominent starting point has been the 10-residue peptide  $Y_1$  antagonist, BVD-15,<sup>[10]</sup> which has been more amenable to conjugation.<sup>[8,9]</sup> We decided to investigate the use of conjugates built around a variety of Pop isomers.

In our second application of the building blocks we focussed on a series of cyclic hexapeptides based upon the reverse turn motif of LEDGF, a protein that binds at the dimer interface of IN.<sup>[11]</sup> The interaction is essential for efficient integration of HIV DNA into the host chromosome, and consequently for successful viral replication.<sup>[12]</sup> These hexapeptides contain the tetrapeptide sequence Lys–Ile–Asp–Asn (KIDN) linked by a dipeptide scaffold comprised of one or two proline residues to support a reverse-turn pharmacophore at the tetrapeptide portion. In X-ray structures of peptide–IN complexes, the dipeptide scaffold projected away from the protein binding site and was not taking part in any binding interactions. This presented an opportunity for us to incorporate additional functionality to our peptides.

## Results and Discussion

### Synthesis of Fmoc-Pop Stereoisomers

Fmoc-protected Pop derivatives were prepared from their corresponding hydroxyproline isomers, including the commonly occurring amino acid (2*S*,4*R*)-hydroxyproline (or *trans*-4-hydroxy-L-proline). A selection of isomers were synthesised using a common synthetic strategy (Scheme 1). For example, (2*S*,4*R*)-hydroxyproline (**i**) was Boc-protected (**v**), and then treated with propargyl bromide under basic conditions to give the Boc-(2*S*,4*R*)-Pop (**ix**). Deprotection and then reprotection of  $N\alpha$  gives the key building block Fmoc-(2*S*,4*R*)-4-propargyloxypyrrolidine (**xiii**) in 25 % overall yield. Note that the preparation of **ix** was recently reported and the sensitivity of the alkylation to selected base and solvent conditions was highlighted.<sup>[13]</sup> The three step synthesis could be carried out without purification of intermediates, carrying through the crude products at each step. In the final step, Fmoc-OSu was limited to 1.0 molar equivalent, limiting the formation of Fmoc- $\beta$ -Alanine-OH,<sup>[14]</sup> which had proved difficult to separate from **xiii**.

In the same manner, we prepared the *N*-Fmoc-protected *O*-propargyl derivatives of (2*R*,4*R*)-, [**xiv**, *cis*-4-hydroxy-D-proline] (2*S*,4*S*)- (**xv**, *cis*-4-hydroxy-L-proline), and (2*S*,3*R*)-hydroxyproline (**xvi**, *cis*-3-hydroxy-L-proline) stereoisomers from the corresponding building blocks giving a collection of Fmoc-protected amino acids on a gram scale for incorporation into peptides using standard solid phase peptide synthesis (SPPS) protocols (see Supplementary Material).

### Synthesis of NPY Analogues

Three parent  $Y_1$  antagonists Lys<sup>4</sup>-BVD15 (**1**), Arg<sup>4</sup>-BVD15 (**2**), and a cyclic peptide, c(Glu<sup>2</sup>,Dap<sup>4</sup>)-BVD15, **3** and their Pop-containing analogues **4–9** were prepared. The synthesis of linear peptides **1**, **2**, and **4–7** was achieved using standard Fmoc-based SPPS protocols using Rink Amide resin. Cleavage using trifluoroacetic acid (TFA) yielded the products in good recovery and purity.<sup>[9]</sup> Peptides **3** and **8** were prepared by solid phase synthesis of the linear Fmoc-precursor and solution phase Glu to Dap cyclisation. Peptide **9** was prepared similarly but with an *N*-terminal 4-fluorobenzoic acid group. Cyclisation was carried out in DMF (1 mg mL<sup>−1</sup> peptide) using PyClock (2 equiv.) coupling reagent and *N*-methylmorpholine (NMM) (12 equiv.) as activating base. We have previously reported the use of PyClock as a cyclisation reagent for the dimeric forms of the peptides, 1229U91,<sup>[9]</sup> but the formation of the dimeric product is suppressed by using NMM instead of diisopropylethylamine

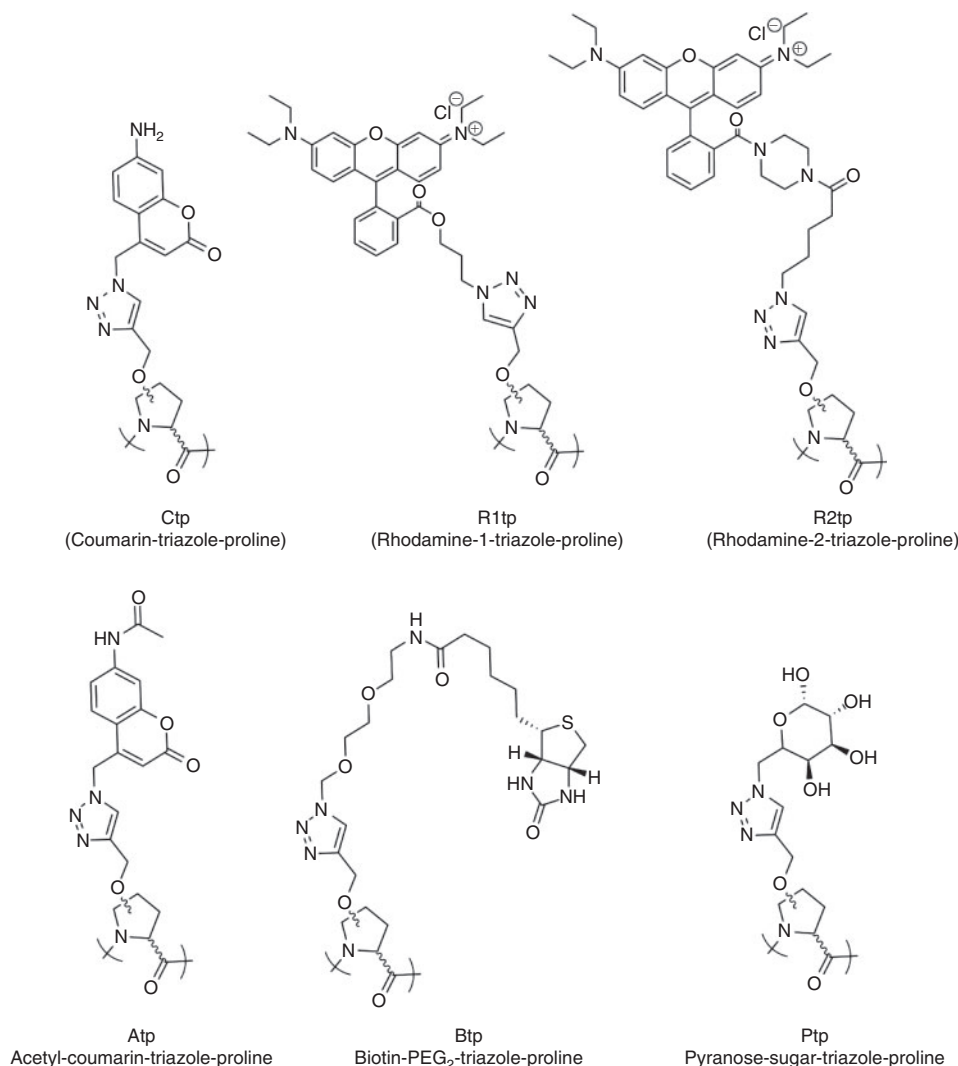
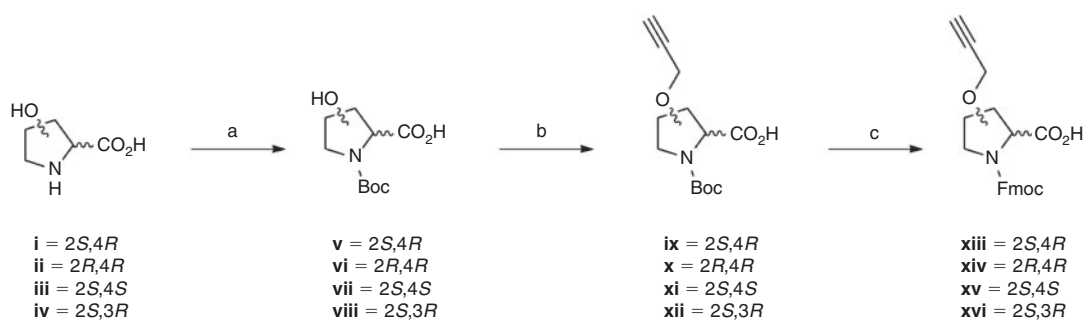


**Fig. 2.** Structures of labels incorporated in the NPY and LEDGF analogues.



**Scheme 1.** Synthetic scheme for the synthesis of Fmoc-propargyloxypyrroline residues **xiii–xvi**. (a) Boc-anhydride, triethylamine, MeOH reflux overnight; (b) NaH, DMF, propargyl bromide, 0°C, 2 h; (c) 1 : 1 trifluoroacetic acid/dichloromethane, room temp 30 min, then Fmoc-OSu, dioxan, 0°C, pH 10, 60 min, room temperature overnight.

(DIPEA) as base. For peptides **3** and **8**, the N-terminal Fmoc group was removed and the peptides precipitated in diethyl ether. The recovered products were used directly for click chemistry and reverse phase (RP)-HPLC purification.

With the precursors in hand, conjugation reactions were performed. Peptides **4–7** were conjugated with 7-amino-4-azidomethylcoumarin to yield the products **10–15**. Peptide **4**

was also conjugated with azido-functionalised rhodamine fluorophores to give **16** and **17** (Fig. 2 and Table 1).

Click reactions were carried out by one of two methods, depending on the solubility of the peptide and azide reagents involved. Reactions were performed at room temperature, in the presence of copper sulfate, sodium ascorbate, and stabilising ligand. Using a DMF solvent system, 1 mg mL<sup>-1</sup> of peptide was

treated with a 4-fold excess of azide-conjugate including the copper-stabilising ligand TBTA (tris[(1-benzyl-1*H*-1,2,3-triazol-4-yl)methyl]amine). Alternately, an aqueous phosphate buffer system could be applied.<sup>[15]</sup> In this method peptides at a concentration of 20 mg mL<sup>-1</sup> in phosphate buffer (pH 7) were additionally treated with aminoguanidine hydrochloride and stabilising ligand THPTA (tris(3-hydroxypropyltriazolyl-methyl)amine). Coupling reactions were very efficient, and the peptides were subsequently purified by RP-HPLC. While successfully prepared using crude Pop-containing peptides, the complexity of the product mixture suggests that purification of the precursor peptides is advisable.

### Analysis of NPY Analogues

The labelled products of these studies were screened for Y<sub>1</sub> receptor affinity in competition binding studies using membrane preparations from Y<sub>2</sub>Y<sub>4</sub> knockout mice as described previously.<sup>[9]</sup> The conjugates **10–15** showed dose-dependent competition with radiolabelled NPY for receptor binding and comparable to the parent sequences in most cases with 50 % inhibitory concentration (IC<sub>50</sub>) values of between 0.6 and 6 nM (Table 1, Fig. S1 in the Supplementary Material). This showed that the receptor was relatively unaffected by the peptide substitutions irrespective of the position or chirality of the alkoxy substituent. Compound **15** was the exception with a relatively poor affinity, the combination of FBz group and coumarin (Fig. 2) both proving deleterious to affinity.

Two rhodamine derivatives **16** and **17** were also prepared, noting that these analogues could be potentially of use in receptor imaging using the fluorescence excitation properties

of the rhodamine group. These were assayed in a recombinant Y<sub>1</sub>-293TR cell system and compared again to the parent peptide **1**. The affinity of these conjugates proved comparable to **1** with IC<sub>50</sub> values of 10 and 18 nM respectively (Table 1, Fig. S2 in the Supplementary Material). While still a reasonably strong affinity, we have developed superior conjugates through other routes, which will be reported elsewhere.

### Synthesis of Head-to-Tail Cyclic LEDGF Mimics

The second series of peptides we chose to study using Pop-derived conjugates were designed to mimic the binding loop of LEDGF that binds to IN. Inhibitors of LEDGF–IN binding are postulated to be potential inhibitors of HIV DNA integration into host cells, and the binding loop of LEDGF comprises a tetrapeptide Lys–Ile–Asp–Asn motif.<sup>[12a,16]</sup> We had developed cyclic hexapeptides including turn-inducing dipeptide units of one or two proline residues. Crystal structures of these peptides bound to IN showed preservation of the tetrapeptide pharmacophore and that the Pro residues protruded away from the protein binding pocket, providing a potential conjugation point. While showing a modest binding affinity (*K<sub>d</sub>* ~1 mM as measured by surface plasmon resonance (SPR) and HSQC NMR), these peptides show strong conformational mimicry of the native protein.

Pop residues were included in three cyclic peptides based upon three parent cyclic hexapeptides for which we had determined crystal structures: cyclo[Asn–D-Pro–Pro–Lys–Ile–Asp] **18**, cyclo[Asn–D-Val–Pro–Lys–Nle–Asp] **19**, cyclo[Asn–D-Val–Pro–Lys–D-Ile–Asp], and **20** (PDB ID: 3WNG and 3WNH) (Northfield et al., in preparation). In the first example, D-proline of **18** was replaced with *cis*-4-propargyloxy-D-proline (**xiv**) to

**Table 1.** Conjugated NPY-derived peptides, incorporating functionality using click chemistry

FBz = 4-Fluorobenzoyl. For other abbreviations see Fig. 2

Peptide	Sequence	ESI-MS <sup>A</sup> [ <i>m/z</i> ]	IC <sub>50</sub> [nM] Y <sub>2</sub> Y <sub>4</sub> KO <sup>E</sup>
Precursor peptides			
<b>1</b>	Ile–Asn–Pro–Lys–Tyr–Arg–Leu–Arg–Tyr (Lys <sup>4</sup> -BVD15)	611.7 <sup>B</sup>	0.9
<b>2</b>	Ile–Asn–Pro–Arg–Tyr–Arg–Leu–Arg–Tyr (Arg <sup>4</sup> -BVD15)	625.7 <sup>B</sup>	1.3
<b>3</b>	Ile–cyc[Glu–Pro–Dap]–Tyr–Arg–Leu–Arg–Tyr (c[Glu <sup>2</sup> ,Dap <sup>4</sup> ]-BVD15)	589.2 <sup>B</sup>	0.9
<b>4</b>	Ile–Asn– <i>trans</i> -4-L-Pop–Lys–Tyr–Arg–Leu–Arg–Tyr	638.6 <sup>B</sup>	1.0
<b>5</b>	Ile–Asn– <i>trans</i> -4-L-Pop–Arg–Tyr–Arg–Leu–Arg–Tyr	652.7 <sup>B</sup>	
<b>6</b>	Ile–Asn– <i>cis</i> -4-L-Pop–Lys–Tyr–Arg–Leu–Arg–Tyr	638.8 <sup>B</sup>	
<b>7</b>	Ile–Asn– <i>cis</i> -3-L-Pop–Lys–Tyr–Arg–Leu–Arg–Tyr	638.8 <sup>B</sup>	
<b>8</b>	Ile–cyc[Glu– <i>trans</i> -4-L-Pop–Dap]–Tyr–Arg–Leu–Arg–Tyr	616.3 <sup>B</sup>	
<b>9</b>	FBz–Ile–cyc[Glu– <i>trans</i> -4-L-Pop–Dap]–Tyr–Arg–Leu–Arg–Tyr	677.4 <sup>B</sup>	
Final products			
<b>10</b>	Ile–Asn– <i>trans</i> -4-L-Ctp–Lys–Tyr–Arg–Leu–Arg–Tyr	498.3 <sup>C</sup>	0.6
<b>11</b>	Ile–Asn– <i>trans</i> -4-L-Ctp–Arg–Tyr–Arg–Leu–Arg–Tyr	507.8 <sup>C</sup>	6.0
<b>12</b>	Ile–Asn– <i>cis</i> -4-L-Ctp–Lys–Tyr–Arg–Leu–Arg–Tyr	498.4 <sup>C</sup>	1.9
<b>13</b>	Ile–Asn– <i>cis</i> -3-L-Ctp–Lys–Tyr–Arg–Leu–Arg–Tyr	498.3 <sup>C</sup>	0.9
<b>14</b>	Ile–cyc[Glu– <i>trans</i> -4-L-Ctp–Dap]–Tyr–Arg–Leu–Arg–Tyr	724.3 <sup>B</sup>	1.9
<b>15</b>	FBz–Ile–cyc[Glu– <i>trans</i> -4-L-Ctp–Dap]–Tyr–Arg–Leu–Arg–Tyr	785.5 <sup>B</sup>	41
			IC <sub>50</sub> [nM] Y <sub>1</sub> -HEK293 <sup>F</sup>
<b>1</b>			7.9
<b>16</b>	Ile–Asn– <i>trans</i> -4-L-R <sup>1</sup> tp–Arg–Tyr–Arg–Leu–Arg–Tyr	685.7 <sup>D</sup>	10
<b>17</b>	Ile–Asn– <i>trans</i> -4-L-R <sup>2</sup> tp–Arg–Tyr–Arg–Leu–Arg–Tyr	649.0 <sup>D</sup>	18

<sup>A</sup>ESI-MS = electrospray ionisation–mass spectrometry.

<sup>B</sup>ESI-MS base peak corresponds to [M + 2H]<sup>2+</sup>.

<sup>C</sup>ESI-MS base peak corresponds to [M + 3H]<sup>3+</sup>.

<sup>D</sup>ESI-MS base peak corresponds to [M + TFA + 3H]<sup>3+</sup> ([M + 3H]<sup>3+</sup> peaks were observed at lower intensity).

<sup>E</sup>Inhibition of [<sup>125</sup>I]-NPY (25 pM) binding to brain membrane homogenates.

<sup>F</sup>Inhibition of [<sup>125</sup>I]-PYY (15 pM) binding to Y<sub>1</sub> transfected 293TR cells.



give **21**, and in **19** and **20** L-proline was replaced with *trans*-4-propargyloxy-L-proline (**xiii**) to give **22** and **23** respectively (Table 2).

The synthesis of the peptides was achieved with Fmoc-based SPPS of side-chain protected linear precursors followed by solution phase cyclisation and then side-chain deprotection. The linear hexapeptide chains were prepared from Fmoc-Asp (OtBu)-chlorotrityl resin, followed by solution head-to-tail

**Table 2.** Conjugated LEDGF-derived peptides, incorporating functionality using click chemistry

Peptide	Sequence	ESI-MS <sup>A</sup> [Da]
Precursors		
<b>18</b>	cyclic[Asn-D-Pro-Pro-Lys-Ile-Asp]	665.6
<b>19</b>	cyclic[Asn-D-Val-Pro-Lys-Nle-Asp]	667.5
<b>20</b>	cyclic[Asn-D-Val-Pro-Lys-D-Ile-Asp]	667.5
<b>21</b>	cyclic[Asn- <i>cis</i> -4-D-Pop-Pro-Lys-Ile-Asp]	719.5
<b>22</b>	cyclic[Asn-D-Val- <i>trans</i> -4-L-Pop-Lys-Nle-Asp]	721.6
<b>23</b>	cyclic[Asn-D-Val- <i>trans</i> -4-L-Pop-Lys-D-Ile-Asp]	721.6
Final products		
<b>24</b>	cyclic[Asn- <i>cis</i> -4-D-Ctp-Pro-Lys-Ile-Asp]	935.4
<b>25</b>	cyclic[Asn- <i>cis</i> -4-D-Atp-Pro-Lys-Ile-Asp]	977.4
<b>26</b>	cyclic[Asn- <i>cis</i> -4-D-Btp-Pro-Lys-Ile-Asp]	1119.6
<b>27</b>	cyclic[Asn-D-Val- <i>trans</i> -4-L-Actp-Lys-Nle-Asp]	979.5
<b>28</b>	cyclic[Asn-D-Val- <i>trans</i> -4-L-Btp-Lys-Nle-Asp]	1121.6
<b>29</b>	cyclic[Asn-D-Val- <i>trans</i> -4-L-Ptp-Lys-Nle-Asp]	926.6
<b>30</b>	cyclic[Asn-D-Val- <i>trans</i> -4-L-Btp-Lys-D-Ile-Asp]	1121.6

<sup>A</sup>ESI-MS peaks correspond to  $m/z$ :  $[M + H]^+$ .

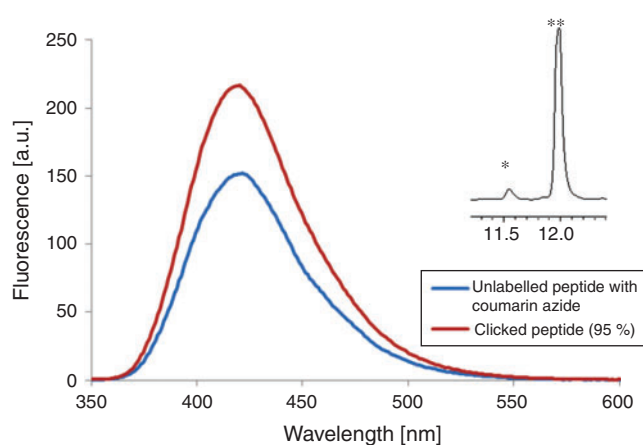


**Fig. 3.** Formation of labelled peptide **25** from **21**. (a) Reaction mixture in absence (blue) or presence (red) of catalyst after 48 h reaction time. (b) Reverse phase-HPLC trace of mixture showing **21** (\*) and **25** (\*\*).

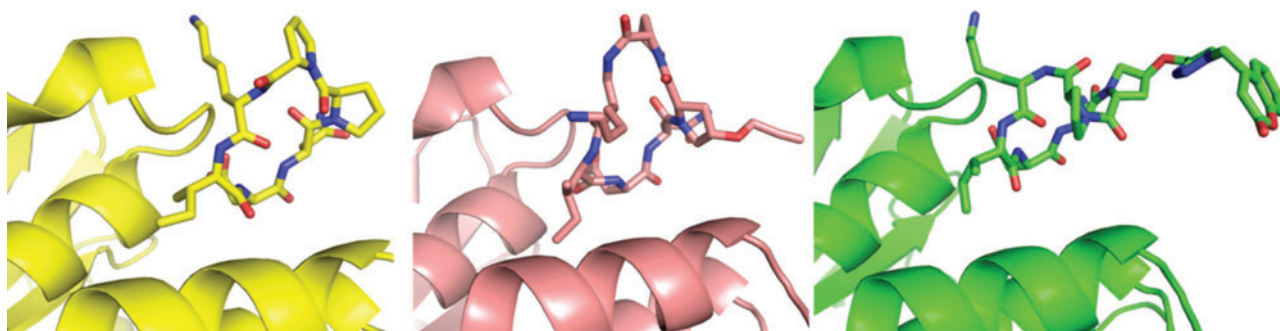


**Fig. 4.** Crystal structures of peptides **18**, **21**, and **24** (left to right) in complex with core domain of HIV integrase (IN).

cyclisation of the linear peptides using diphenylphosphoryl azide (DPPA) as the cyclisation reagent and finally side-chain cleavage. The sequences showed some propensity for racemisation in the cyclisation step, but the D-Asp-containing diastereomers were in general minor components and readily separated from the desired compounds. The recovered yields for cyclisation of Pop-containing peptides **21–23** ranged from 30 to 70 %, and were comparable to those obtained in the synthesis of the parent proline-containing sequences **18–20**. This demonstrated that substituting L-Pro for *trans*-4-L-Pop and D-Pro for *cis*-4-D-Pop did not have a detrimental effect on peptide cyclisation.

The Pop-substituted cyclic peptides were purified by semi-preparative RP-HPLC, then used as substrates for click reactions with a variety of azido-compounds: 7-amino-4-azidomethylcoumarin, 7-acetylamino-4-azidomethylcoumarin, Biotin-PEG<sub>2</sub>-azide, and azido-6-deoxy- $\alpha$ -D-galactopyranose (Fig. 2, Table 2). All of the selected conjugates were successfully coupled to one or more of the cyclic peptides **21–23**, under standard conditions within 8 h using the same DMF click chemistry method described for the NPY analogue conjugation above. An interesting feature of the coupling of the 4-azido-methyl-7-acetamidocoumarin in the synthesis of peptide **25** was the increase in fluorescence with progression of the reaction over a 48 h period, while the spectrum of the same mixture in the absence of the catalyst was unchanged (Fig. 3). While modest, the ability to distinguish substrates from products by fluorescence might be useful in performing click reactions in more complex media.

#### Analysis of Cyclic LEDGF Mimics

With the conjugated peptides in hand we examined the effect the substitution had on the peptide conformation at the LEDGF binding site of IN. The peptides showed comparable, albeit weak affinity for IN to the parent hexapeptides, **18** and **19**, and we obtained crystal structures of respective labelled derivatives peptide **24** and peptide **28**, and the propargyloxy derivatives **21** and **22** bound to the core domain of IN.

The crystal structures all show well resolved density at the tetrapeptide sequence, allowing for comparison of the homologous series at the key pharmacophore (Fig. 4). The density of the prosthetic structures was poorly resolved suggesting that the labels are flexible and do not interact with the IN protein.

Peptides **18**, **21**, and **24** differ only in the presence of the substituent at the *cis*-4-position of the D-proline residue. Peptide **18** and the coumarin conjugate **24** show a close overlay of the tetrapeptide pharmacophore. In peptide **21** however the lysine residue has moved substantially and cannot be said to be mimicking the native structure. In both cases, the proline motif has undergone some conformational change, although the

resolution at those residues is not sufficient to identify the cause. In the case of the cyclic peptide structures **19**, **28**, and **22** again the conformation of the conjugate **28** more closely resembled the native Pro-containing peptide **19** than the Pop counterpart **22** (Fig. 3 in the Supplementary Material).

## Conclusions

In commencing this work, we reasoned that the incorporation of (1*H*-1,2,3-triazol-4-yl)methoxy substituents on proline would be a successful strategy in order to produce conjugated versions of proline-containing peptides, especially as compared with the corresponding products from commonly used propargylglycine. Proline is a structurally rigid amino acid and so an additional substituent might not be expected to impact the native peptide conformation, and the linker group is also relatively remote from the peptide backbone. Except in the case of proline isomerases and proline specific proteases, proline does not generally play a direct role in ligand binding events and so can be a benign place to make a residue replacement. Furthermore, the use of varied stereochemistry or regiochemistry of substituents projecting from the proline ring allows conjugates to be directed away from the peptide pharmacophore or the target protein binding site, but may also influence levels of *cis* or *trans* amide conformers. The Pop stereoisomers can be readily obtained from commercially available starting materials and incorporated in peptide sequences using standard Fmoc-SPPS protocols. The pharmacological and biophysical data we have obtained in these two examples supports the approach for both small linear and cyclic peptides. Given the absence of N- or C-terminal residues, the ability to link through proline seems prospectively valuable in head-to-tail cyclic peptides especially. However, the data also provide the caveat that irrespective of the linking handle, the nature of the prosthetic group can have a marked effect on the binding affinity or conformation adopted by these conjugates.

## Experimental

*N*<sup>z</sup>-Fmoc-protected amino acids were purchased from Auspep and ChemImpex. Rink amide resin and *O*-(1*H*-6-chlorobenzo-triazol-1-yl)-*N,N,N',N'*-tetramethyluronium hexafluorophosphate (HCTU) were purchased from ChemImpex. Piperidine and TFA were purchased from Auspep. *N,N*-DIPEA, DMF, and dichloromethane (DCM), were purchased from Merck. Diphenylphosphorylazide (DPPA) and triisopropylsilane (TIPS) were purchased from Sigma–Aldrich. Fluorobenzoic acid was purchased from Alfa Aesar. 7-Amino-4-(azidomethyl)-2*H*-chromen-2-one<sup>[17]</sup> was a gift from Dr Bim Graham (Monash Institute of Pharmaceutical Sciences). The Rhodamine B derivatives were prepared in-house. All chemicals were used without further purification.

<sup>1</sup>H NMR spectra were routinely recorded at 300 MHz using a 300 MHz Bruker Advance DPX-300 spectrometer or at 400 MHz using a 400 MHz Bruker Ultrashield–Advance III NMR spectrometer, with *TOPSPIN* v2.1 software, at 298 K. <sup>13</sup>C NMR spectra were recorded at 101 MHz using a 400 MHz Bruker Ultrashield–Advance III NMR spectrometer, with *TOPSPIN* v2.1 software, at 298 K. Liquid chromatography mass spectra were acquired on a Shimadzu 2020 LCMS system incorporating a photodiode array detector coupled directly into an electrospray ionisation source and a single quadrupole mass analyser. Standard RP-HPLC was carried out at room temperature employing a Phenomenex Luna C8 (100 × 2.0 mm internal diameter, I.D.) column eluting with a gradient of either 0–64 %

acetonitrile (ACN) in 0.05 % aqueous TFA over 10 min or 0–100 % B over 15 min (Buffer B is 100 % ACN + 0.1 % TFA) at a flow rate of 0.2 mL min<sup>−1</sup> unless stated otherwise. Mass spectra were obtained in positive mode with a scan range of *m/z* 200–2000. Semi-preparative RP-HPLC was performed using a Waters Associates liquid chromatography system (Model 600 controller and Waters 486 Tuneable Absorbance Detector) using a gradient of 0–64 % ACN in 0.1 % TFA over 20 min or 30 min at a flow rate of 10 mL min<sup>−1</sup> on a Phenomenex Luna C8 100 Å, 10 µm (50 × 21.2 mm I.D.) or a Phenomenex Luna C8 100 Å, 10 µm (250 × 21.2 mm I.D.) column.

## Chemical Synthesis

### (2*S*,4*R*)-1-(Tert-butoxycarbonyl)-4-hydroxypyrrolidine-2-carboxylic Acid (Boc-*trans*-L-4-hydroxyproline, **v**)

To a stirred solution of *trans*-L-4-hydroxyproline **i** (2.0 g, 15.3 mmol) in MeOH (36.0 mL) was added Et<sub>3</sub>N (4.0 mL, 28.7 mmol) and Boc anhydride (6.7 g, 30.5 mmol) and the reaction was refluxed for 3.5 h, cooled to room temperature, and stirred for 20 h. Solvent was removed under vacuum and the residue cooled to 0 °C. Following the addition of NaH<sub>2</sub>PO<sub>4</sub> (150 mg), the solution was acidified to pH 2 with 0.5 M HCl. The mixture was stirred at 0 °C for 30 min before extracting the product with EtOAc (4 × 20 mL). The combined organic layers were dried with MgSO<sub>4</sub> and filtered. The solvent was removed under vacuum yielding **v** as a white foam (3.23 g, 14 mmol, 92 %).

$\delta_{\text{H}}$  (CD<sub>3</sub>OD, 400 MHz) 4.40 (dd, *J* 5.5, 3.4, CH, 1H), 4.32 (dt, *J* 12.9, 8.0, CH, 1H), 3.54 (dt, *J* 11.4, 4.0, 0.5 × CH<sub>2</sub>, 1H), 3.44 (dt, *J* 11.4, 1.9, 0.5 × CH<sub>2</sub>, 1H), 2.27 (dddd, *J* 12.3, 7.7, 2.8, 1.8, 0.5 × CH<sub>2</sub>, 1H), 2.06 (ddd, *J* 13.2, 8.6, 4.5, 0.5 × CH<sub>2</sub>, 1H), 1.45 (s, Boc, 9H).  $\delta_{\text{C}}$  (CD<sub>3</sub>OD, 101 MHz) 176.75 and 176.37 (pair of rotamers, Cq), 156.54 and 156.02 (pair of rotamers, Cq), 81.72 and 81.42 (pair of rotamers, Cq), 70.68 and 70.06 (pair of rotamers, CH), 59.39 and 58.91 (pair of rotamers, CH), 55.85 and 55.51 (pair of rotamers, CH<sub>2</sub>), 40.07 and 39.4 (pair of rotamers, CH<sub>2</sub>), 28.71 and 28.53 (pair of rotamers, 3 × CH<sub>3</sub>). *m/z* (LC-MS) 277.35 (100 %, [M + 2Na]<sup>+</sup>).

### (2*S*,4*R*)-1-(Tert-Butoxycarbonyl)-4-(prop-2-yn-1-yloxy)pyrrolidine-2-carboxylic Acid (Boc-*trans*-L-4-propargyloxyproline, **ix**)

A solution of Boc-*trans*-L-4-hydroxyproline, **v** (2.80 g, 12.13 mmol) in dry DMF (30 mL) was added to a suspension of NaH (0.93 g, 38.75 mmol) in dry DMF (10 mL) under nitrogen at 0 °C. After 15 min, 1.5 equivalents of propargyl bromide (80 % in toluene) was added dropwise to the reaction (1.68 mL, 18.85 mmol). The reaction was stirred at 0 °C for 2 h and then quenched with H<sub>2</sub>O and lyophilised in H<sub>2</sub>O/ACN. The reaction was taken up in EtOAc and the pH adjusted to 2 with 10 % citric acid. The aqueous layer was extracted with EtOAc (3 × 20 mL). The combined organic layers were dried with MgSO<sub>4</sub> and filtered. Solvent was removed under vacuum to yield **ix** as a brown solid (2.97 g, 11.0 mmol, 91 %) which was directly carried on to the next step.

$\delta_{\text{H}}$  (CD<sub>3</sub>OD, 400 MHz) 4.37–4.31 (m, CH, 1H), 4.31–4.21 (m, CH, 1H), 4.19 (d, *J* 2.4, CH<sub>2</sub>, 2H), 3.64–3.57 (m, 0.5 × CH<sub>2</sub>, 1H), 3.57–3.50 (m, 0.5 × CH<sub>2</sub>, 1H), 2.94–2.77 (m, CH, 1H), 2.44 (ttdd, *J* 14.3, 11.5, 3.0, 1.6, 0.5 × CH<sub>2</sub>, 1H), 2.13–2.04 (m, 0.5 × CH<sub>2</sub>, 1H), 1.45 (s, Boc, 9H).  $\delta_{\text{C}}$  (CD<sub>3</sub>OD, 101 MHz) 178.33 and 175.54 (pair of rotamers, Cq), 156.04 and 155.93 (pair of rotamers, Cq), 81.64 and 80.9 (pair of rotamers, Cq),

79.31 (CH), 76.2 and 75.85 (pair of rotamers, CH), 75.04 (Cq), 57.90 and 57.87 (pair of rotamers, CH), 56.58 and 56.51 (pair of rotamers, CH<sub>2</sub>), 51.93 and 51.18 (pair of rotamers, CH<sub>2</sub>), 36.57 and 34.57 (pair of rotamers, CH<sub>2</sub>), 28.45 and 28.33 (pair of rotamers, 3 × CH<sub>3</sub>). *m/z* (LCMS) 315.35 (80%, [M + 2Na]<sup>+</sup>).

(2*S*,4*R*)-1-(((9*H*-Fluoren-9-yl)methoxy)carbonyl)-4-(prop-2-yn-1-yloxy)pyrrolidine-2-carboxylic Acid (Fmoc-*trans*-L-4-Propargyloxypyrroline-OH, **xiii**)

Boc-*trans*-L-propargyloxypyrroline **ix** (2.97 g, 11.01 mmol) was treated with 1 : 1 TFA/DCM (10 mL) at room temperature over 45 min and solvent removed under vacuum. The reaction was diluted with H<sub>2</sub>O (10 mL) and adjusted to pH 9 with Na<sub>2</sub>CO<sub>3</sub>. To the reaction solution 1.4 equiv. of Fmoc-OSu (5.20 g, 16.18 mmol) in dioxane (22 mL) was added at 0°C and stirred for 1 h. The reaction was then brought to room temperature and stirred overnight. Dioxane was removed under vacuum and the reaction acidified to pH 3 with 1 M HCl. Product was extracted with EtOAc (3 × 20 mL), washed with brine, and dried with MgSO<sub>4</sub>. Solvent was removed under vacuum to yield a yellow foam. Purification was achieved by flash chromatography (0–2% MeOH in chloroform) yielding **xiii** as a white powder (1.31 g, 3.35 mmol, 30%).

$\delta_{\text{H}}$  (CD<sub>3</sub>OD, 400 MHz) 7.8 (t, *J* 7.5, 2H), 7.63 (td, *J* 7.5, 2.4, 2H), 7.39 (td, *J* 7.4, 4.0, 2H), 7.35–7.28 (m, 2H), 4.46–4.18 (m, 6H), 4.15 (dd, *J* 4.7, 2.4, 1H), 3.64–3.5 (m, 2H), 2.89 (t, *J* 2.4, 1H), 2.57–2.4 (m, 1H), 2.22–2.05 (m, 1H).  $\delta_{\text{C}}$  (CD<sub>3</sub>OD, 101 MHz) 175.98 and 175.75 (pair of rotamers, Cq), 156.71 and 156.62 (pair of rotamers, Cq), 145.31, 145.29, 145.12, 145.05 (rotamers, Cq), 142.64, 142.61, 142.56, 142.49 (rotamers, Cq), 128.88 (CH), 128.25 (CH), 126.28, 125.25, 126.16, 126.15 (rotamers, CH), 121.03 and 120.98 (pair of rotamers, CH), 80.58 and 80.57 (pair of rotamers, Cq), 77.92 and 77.15 (pair of rotamers, CH), 76.27 and 77.26 (pair of rotamers, CH), 69.32 and 68.75 (pair of rotamers, CH<sub>2</sub>), 59.26 and 59.01 (pair of rotamers, CH), 57.25 and 57.21 (pair of rotamers, CH<sub>2</sub>), 53.21 and 52.78 (pair of rotamers, CH<sub>2</sub>), 48.39 and 48.33 (pair of rotamers, CH), 37.6 and 36.6 (pair of rotamers, CH<sub>2</sub>). *m/z* (LCMS) 392.30 (100%, [M + H]<sup>+</sup>). HRMS *m/z* 392.1494; C<sub>23</sub>H<sub>22</sub>NO<sub>5</sub><sup>+</sup> [M + H]<sup>+</sup> requires 392.1492.

Compounds **xiv**, **xv**, and **xvi** were prepared in the same manner. Full details are provided in the Supplementary Material.

BVD15 analogues **1–9** were prepared as previously reported. Peptide syntheses were performed on Rink amide resin (0.3–0.7 mequiv. g<sup>−1</sup>, 100–200 mesh, 0.1 mmol scale) using conventional Fmoc-based solid phase peptide synthesis. Fmoc-protected amino acids in 3-fold molar excess were coupled using DMF as solvent, a 6-fold molar excess of DIPEA in DMF (70 mL L<sup>−1</sup>) with a 3-fold molar excess of HCTU as the activating agent for 50 min. Fmoc deprotection was carried out by treatment with 20% piperidine in DMF for 10 min.

Peptide cleavage from the resin was performed using a cocktail containing TFA/TIPS/DMB (92.5 : 2.5 : 5%; DMB = 1,3-dimethoxybenzene) for 3 h.<sup>[18]</sup> The cleavage mixture was filtered, concentrated by a stream of nitrogen, precipitated by cold diethyl ether, and centrifuged. The resulting crude product was dissolved by water/ACN (1 : 1) and lyophilised overnight.

The click reactions to prepare peptides **10–15** involved dissolving the corresponding peptide-alkyne **5–9** (1 equiv.) in H<sub>2</sub>O and adding a solution of the azidocoumarin<sup>[17]</sup> (4 equiv.) in DMF to give a 1 : 3 ratio of H<sub>2</sub>O to DMF. Copper sulfate (10 equiv.), TBTA (10 equiv.), and sodium ascorbate (10 equiv.)

were then added and the reaction mixed for 3 h. Peptides **16** and **17** were prepared in the same fashion but using the appropriate azido-substituted rhodamine B derivatives. Peptides were purified by reverse-phase preparative HPLC. Purity of fractions was assessed using electrospray ionisation-mass spectrometry (ESI-MS) (Table 1) and analytical HPLC (Fig. S5 in the Supplementary Material).

### Synthesis of Cyclic LEDGF Analogues

Cyclic peptides **18–23** were synthesised on 2-chlorotrityl chloride (2CTC) resin on a 0.1 mequiv. scale. Couplings were performed using 3 equiv. of Fmoc-protected amino acid, 3 equiv. of HCTU, and 6 equiv. of DIPEA in DMF (0.1 M in amino acid) for 50 min. Fmoc deprotection was carried out with 30% (v/v) piperidine in DMF (2 × 5 min). After each coupling and deprotection step, the resin was washed six times with DMF. Peptides were cleaved from the resin using 1% (v/v) TFA in DCM. Head-to-tail cyclisation of side-chain protected peptide was performed in DMF (4 mM final concentration of peptide) with 3 equiv. of DPPA and 4 equiv. of DIPEA. Following removal of the solvent, side-chain protecting groups were removed in 95 : 5 TFA/TIPS. After cyclisation, the peptides were purified by reverse-phase preparative HPLC. Purity of fractions was assessed using ESI-MS (Table 2) and analytical HPLC.

### Synthesis of Peptides 24–30

A solution of the Pop-containing peptide (1 mg mL<sup>−1</sup> in H<sub>2</sub>O) was treated with a 4-fold excess of the azido derivative (1 mg mL<sup>−1</sup> in DMF). One equivalent of sodium ascorbate (1 mg mL<sup>−1</sup> in H<sub>2</sub>O), one equivalent of TBTA (1 mg mL<sup>−1</sup> in DMF), and one equivalent of copper sulfate (1 mg mL<sup>−1</sup> in H<sub>2</sub>O) were subsequently added to the reaction. The reaction was left at room temperature and progression monitored by LCMS. When no remaining unlabelled peptide was observed, the reaction was diluted in 1 : 1 ACN/H<sub>2</sub>O and lyophilised before purification by RP-HPLC. Purity of fractions was assessed using ESI-MS (Table 2) and analytical HPLC (Fig. S5 in the Supplementary Material).

In the case of peptide **29**, the click reaction was performed using 1,2 : 3,4-di-*O*-isopropylidene-6-azido-6-deoxy- $\alpha$ -D-galactopyranose.<sup>[19]</sup> The resultant acetonide (*m/z* 1006.7, [M + H]<sup>+</sup>) was deprotected by treatment with 90% TFA overnight, diluted in 1 : 1 ACN/H<sub>2</sub>O, and lyophilised before purification by RP-HPLC to yield the free galactopyranose **29**.

### Competition Binding Studies

Competition binding assays were carried out as described previously.<sup>[9]</sup> In brief, receptor binding assays to measure Y<sub>1</sub>R affinity of the ligands **10–15** (described below) were performed on crude membranes prepared from the brains of Y<sub>2</sub>R- and Y<sub>4</sub>R-deficient mice (Y<sub>2</sub>−/−Y<sub>4</sub>−/−), where Y<sub>1</sub>R accounts for the majority of remaining Y receptors. Peptides **16** and **17** were assayed using 293TR Y<sub>1</sub> receptor GFP membranes.

For mouse brain preparations, equal volumes (25  $\mu$ L) of non-radioactive ligands and <sup>125</sup>I-human polypeptide YY (<sup>125</sup>I-hPYY, 2200 Ci mmol<sup>−1</sup>; PerkinElmer Life Science Products, Boston, MA, USA) were added into each assay. The final concentration of <sup>125</sup>I-hPYY in the assay was 25 pM. The binding of <sup>125</sup>I-hPYY competed with Y<sub>1</sub>R ligands of interest at increasing concentrations ranging from 10<sup>−12</sup> to 10<sup>−6</sup> M over 2 h. Non-radioactive human PYY (Auspep, Parkville, Vic., Australia) at 10<sup>−6</sup> M was used as the non-specific binding control.



Using membranes from the 293TR Y<sub>1</sub> receptor-sfGFP cell competition binding assays were performed for 90 min at 21°C in buffer (25 mM HEPES, 2.5 mM CaCl<sub>2</sub>, 1.0 mM MgCl<sub>2</sub>, 0.1 % bovine serum albumin, 0.1 mg mL<sup>-1</sup> bacitracin; pH 7.4), increasing concentrations of unlabelled ligands (10<sup>-12</sup> to 10<sup>-6</sup> M, duplicate), and [<sup>125</sup>I]PYY (15 pM). Non-specific binding in these experiments comprised less than 5 % of total counts, and was subtracted from the data.

In both sets of data, IC<sub>50</sub> values were calculated from displacement curves (repeated 2–4 times for each peptide, fitted using non-linear least-squares regression in *GraphPad Prism 5.01* (Graphpad software, San Diego, CA, USA).

### X-Ray Crystallography

Crystal structures of the cyclic hexapeptides bound to IN were determined as previously described.<sup>[20]</sup> The coordinates of the four IN<sub>CORE4H123</sub>/cyclic LEDGF peptide complexes have been deposited in the protein database (PDB) with the accession numbers 4Y1C and 4Y1D.

### Supplementary Material

Detailed synthesis procedures as well as additional supplementary figures showing dose–response curves for Y<sub>1</sub>R binding by peptides **1–4** and **10–17**, structures of peptides **19, 22**, and **28** complexed with IN, NMR data for Pop derivatives **v–xvi**, and RP-HPLC traces of peptides **10–17** and **24–30** are available on the Journal's website.

### Acknowledgements

This work was supported by CRC for Biomedical Imaging Development (CRC-BID), Australia, and the Australian Research Council (ARC) Linkage project (LP0775192). This research was partly undertaken on the MX2 beamline at the Australian Synchrotron, Victoria, Australia and the authors thank the beamline staff for their assistance. Funding from the Victorian Government Operational Infrastructure Support Scheme to St Vincent's Institute is gratefully acknowledged. M.W.P. is a National Health and Medical Research Council of Australia Research Fellow. SEN and ML were supported by an Australian Post-graduate scholarship.

### References

- [1] R. J. Pieters, D. T. S. Rijkers, R. M. J. Liskamp, *QSAR Comb. Sci.* **2007**, *26*, 1181. doi:10.1002/QSAR.200740075
- [2] C. Hein, X.-M. Liu, D. Wang, *Pharm. Res.* **2008**, *25*, 2216. doi:10.1007/S11095-008-9616-1
- [3] (a) M. MacDonald, J. Aube, *Curr. Org. Chem.* **2001**, *5*, 417. doi:10.2174/1385272013375517  
(b) C. M. Deber, B. Brodsky, A. Rath, in *Encyclopedia of Life Sciences* **2010** (John Wiley & Sons, Ltd: Chichester).
- [4] A. K. Pandey, D. Naduthambi, K. M. Thomas, N. J. Zondlo, *J. Am. Chem. Soc.* **2013**, *135*, 4333. doi:10.1021/JA3109664
- [5] M. Meldal, C. W. Tornøe, *Chem. Rev.* **2008**, *108*, 2952. doi:10.1021/CR0783479
- [6] G. Chouhan, K. James, *Org. Lett.* **2011**, *13*, 2754. doi:10.1021/OL200861F
- [7] D. Font, C. Jimeno, M. A. Pericàs, *Org. Lett.* **2006**, *8*, 4653. doi:10.1021/OL061964J
- [8] B. Guérin, V. Dumulon-Perreault, M.-C. Tremblay, S. Ait-Mohand, P. Fournier, C. Dubuc, S. Authiera, F. Bénard, *Bioorg. Med. Chem. Lett.* **2010**, *20*, 950. doi:10.1016/J.BMCL.2009.12.068
- [9] S. J. Mountford, M. Liu, L. Zhang, M. Groenen, H. Herzog, N. D. Holliday, P. E. Thompson, *Org. Biomol. Chem.* **2014**, *12*, 3271. doi:10.1039/C4OB00176A
- [10] M. Liu, S. J. Mountford, L. Zhang, I. C. Lee, H. Herzog, P. E. Thompson, *Int. J. Pept. Res. Ther.* **2013**, *19*, 33. doi:10.1007/S10989-012-9330-Z
- [11] A. Engelman, P. Cherepanov, *PLoS Pathog.* **2008**, *4*, e1000046. doi:10.1371/JOURNAL.PPAT.1000046
- [12] (a) W. Thys, K. Busschots, M. McNeely, A. Voet, F. Christ, Z. Debyser, *HIV Ther.* **2009**, *3*, 171. doi:10.2217/17584310.3.2.171  
(b) S. Hare, P. Cherepanov, *Viruses* **2009**, *1*, 780. doi:10.3390/V1030780
- [13] V. Mihalj, F. Foschi, M. Penso, G. Pozzi, *Eur. J. Org. Chem.* **2014**, *2014*, 5351. doi:10.1002/EJOC.201402429
- [14] M. Obkircher, C. Stähelin, F. Dick, *J. Pept. Sci.* **2008**, *14*, 763. doi:10.1002/PSC.1001
- [15] V. Hong, S. I. Presolski, C. Ma, M. G. Finn, *Angew. Chem. Int. Ed.* **2009**, *48*, 9879. doi:10.1002/ANIE.200905087
- [16] Z. Hayouka, M. Hurevich, A. Levin, H. Benyamini, A. Iosub, M. Maes, D. E. Shalev, A. Loyter, C. Gilon, A. Friedler, *Bioorg. Med. Chem.* **2010**, *18*, 8388. doi:10.1016/J.BMC.2010.09.046
- [17] M. A. Kamaruddin, P. Ung, M. I. Hossain, B. Jarasrassamee, W. O'Malley, P. Thompson, D. Scanlon, H.-C. Cheng, B. Graham, *Bioorg. Med. Chem. Lett.* **2011**, *21*, 329. doi:10.1016/J.BMCL.2010.11.005
- [18] P. Stathopoulos, S. Papas, V. Tsikaris, *J. Pept. Sci.* **2006**, *12*, 227. doi:10.1002/PSC.706
- [19] S. B. Ferreira, A. C. R. Sodero, M. F. C. Cardoso, E. S. Lima, C. R. Kaiser, F. P. Silva Jr, V. F. Ferreira, *J. Med. Chem.* **2010**, *53*, 2364. doi:10.1021/JM901265H
- [20] J. Wielens, S. J. Headey, J. J. Deadman, D. I. Rhodes, G. T. Le, M. W. Parker, D. K. Chalmers, M. J. Scanlon, *ChemMedChem* **2011**, *6*, 258. doi:10.1002/CMDC.201000483

# Beta amino acid-modified and fluorescently labelled kisspeptin analogues with potent KISS1R activity

M. A. Camerino,<sup>a</sup> M. Liu,<sup>a</sup> S. Moriya,<sup>b</sup> T. Kitahashi,<sup>b</sup> A. Mahgoub,<sup>a</sup>  
S. J. Mountford,<sup>a</sup> D. K. Chalmers,<sup>a</sup> T. Soga,<sup>b</sup> I. S. Parhar<sup>b</sup> and P. E. Thompson<sup>a\*</sup>

Kisspeptin analogues with improved metabolic stability may represent important ligands in the study of the kisspeptin/KISS1R system and have therapeutic potential. In this paper we assess the activity of known and novel kisspeptin analogues utilising a dual luciferase reporter assay in KISS1R-transfected HEK293T cells. In general terms the results reflect the outcomes of other assay formats and a number of potent agonists were identified among the analogues, including  $\beta^2$ -hTyr-modified and fluorescently labelled forms. We also showed, by assaying kisspeptin in the presence of protease inhibitors, that proteolysis of kisspeptin activity within the reporter assay itself may diminish the agonist outputs. Copyright © 2016 European Peptide Society and John Wiley & Sons, Ltd.

**Keywords:** kisspeptin; KISS1R agonist; beta amino acids; fluorescent peptides

## Introduction

Kisspeptin (*aka* metastin) and its cognate receptor, KISS1R (GPR54), have been identified in various vertebrate species [1–3] including humans [4]. Kisspeptin was found to present as several forms (KP-10, 13, 15, and KP-54) derived from a precursor peptide, which share a functionally important *N*-terminal core region. Kisspeptin's activity [5] is dictated through the KISS1 receptor (GPR54) and is a pivotal element in the neuroendocrine network governing gonadotropin secretion and is thus essential for the physiological functions of gonadotropin-releasing hormone (GnRH). Thus KISS1R agonists may be useful for the treatment of infertility, hypogonadism, and delayed puberty, and functional antagonists would be useful for the treatment of hormone – dependent cancers (prostate, breast, endometrial), ovarian hyperstimulation, contraception and precocious puberty.[6–8] However, despite recent publications, much remains unknown about the physiological role(s) and mechanisms of actions of the 'kisspeptin family of peptides' and associated receptors in veterinary and aquaculture settings. The dearth of information about how kisspeptin interacts with GPR54 is due to, in-part, limited access to appropriate kisspeptin 'mimics' for use as biological probes and suitable biological assays.

Like most proteins and peptides, the utility of kisspeptin and its peptide analogues either clinically or as pharmacological tools will be compromised by limiting physicochemical properties. Typically this means poor oral bio-availability and its short biological half-life, thus mimics or antagonists necessarily need to avoid these shortcomings. Approaches to novel GPR54 ligands (agonists and antagonists) are still in their infancy but include the following: (i) HTS for small molecules GPR54 agonists and antagonists [9–11] and (ii) Peptide analogues designed with unnatural amino acid substitutions (Table 1).[12] Among these, a series of agonist compounds have been described including d-Tyr<sup>1</sup>-KP10,[13] other analogues by workers at Takeda (TAK series)[14] and *N*-terminally modified

pentapeptides (FTM series) from Tomita et al.[12] Just one peptide antagonist has been reported known as Peptide 234.[15] Most recently, a triazol-linked family of analogues has been described including peptide 'Beltramo 3' (Table 1).[16]

While giving promise to the idea of the development of therapeutic agents targeting GPR54, these few reports leave us with little information about the interaction between kisspeptin and GPR54. Structural information of kisspeptins is limited to conformational studies of kisspeptin-13 that suggests a helical conformation of the peptide in solution, [9] while in contrast certain modifications are consistent with favouring turn conformers. [14] In the long term, the identification of GPR54-dependent biological functions will be well served by developing a better understanding of the bioactive conformation and how it interacts with the receptor. This has been made more significant with the apparent affinity of kisspeptin peptides for the more recently identified neuropeptide FF receptors.[17] Peptidomimetic kisspeptin analogues (agonists and antagonists) are essential tools to improve our knowledge in this area.

The *in vitro* study of GPR54 agonism has been achieved via a number of different assay formats. The majority of studies have employed calcium flux in transfected-CHO cells as measured in the FLIPR assay protocols. [12] Other assays have examined ERK1/2 phosphorylation. [13] Reporter genes have also been employed. First, Niida reported a LacZ-based system in yeast, [18] while Lee et al. utilised a c-fos-Luciferase system. [1] Kuohung

\* Correspondence to: P. E. Thompson, Medicinal Chemistry, Monash Institute of Pharmaceutical Sciences, Monash University, 381 Royal Parade, Parkville 3052 Australia. E-mail: philip.thompson@monash.edu

<sup>a</sup> Medicinal Chemistry, Monash Institute of Pharmaceutical Sciences, Monash University, 381 Royal Parade, Parkville 3052, Australia

<sup>b</sup> Brain Research Institutes, Monash University Malaysia, Jalan Lagoon Selatan, Bandar Sunway, Selangor, 47500, Malaysia

**Table 1.** Reported KISS1R ligands

Name	Sequence	Reference
Kisspeptin-10	H-Tyr-Asn-Trp-Asn-Ser-Phe-Gly-Leu-Arg-Phe-NH <sub>2</sub>	
[dY]1-KP10	H-d-Tyr-Asn-Trp-Asn-Ser-Phe-Gly-Leu-Arg-Phe-NH <sub>2</sub>	[13]
KISS1-305	d-Tyr-d-Pya(4)-Asn-Ser-Phe-azaGly-Leu-Arg(Me)-Phe-NH <sub>2</sub> <sup>a</sup>	[14]
TAK448	Ac-d-Tyr-Hyp-Asn-Thr-Phe-azaGly-Leu-Arg(Me)-Trp-NH <sub>2</sub>	[14]
TAK663	Ac-d-Tyr-d-Trp-Asn-Thr-Phe-azaGly-Leu-Arg(Me)-Trp-NH <sub>2</sub>	[14]
FTM-080	FBz-Phe-Gly-Leu-Arg-Phe-NH <sub>2</sub>	[12]
FTM-145	FBz-Phe-Gly = Leu-Arg-Phe-NH <sub>2</sub> <sup>b</sup>	[12]
Beltramo 3	Ac-Tyr-Asn-Trp-Asn-Ser-Phe-Glyψ[Tz]Leu-Arg-Phe-NH <sub>2</sub> <sup>c</sup>	[16]
Peptide 234	Ac-d-Ala-Asn-Trp-Asn-Gly-Phe-Gly-d-Trp-Arg-Phe-NH <sub>2</sub>	[15]

<sup>a</sup>d-Pya(4) refers to d-4-pyridinylalanine<sup>b</sup>Gly = Leu refers to an alkenyl replacement for the conventional carboxamide;<sup>c</sup>Glyψ[Tz]Leu refers to a triazolyl replacement for the conventional carboxamide. See references for details.

et al. described a number of assays developed for high throughput screening purposes including the use of an IP3 sensitive IP-One HTRF™ assay. [11] It is worth noting that each of these assays has a marked difference in the kinetics of the outputs and so the degree of exposure of the cells to test compounds also differs.

Here we assessed kisspeptin analogues via an alternate *in vitro* reporter assay. We transiently transfected HEK293T cell line with a human GPR54 construct (hGPR54) and monitored the activity of GPR54 using the dual luciferase reporter assay, in which the expression of firefly luciferase gene is activated by the induction of the serum response element (SRE)–mitogen-activated protein (MAP) kinase signal transduction pathway.

We have used this assay to evaluate the activity of a range of synthetic analogues of KP10. These include analogues possessing a range of novel structural motifs: peptides incorporating unusual amino acids, fluorescent KP10 analogues and cyclic peptides. [19] Kisspeptins have been shown to be degraded by serum proteases via the cleavage of the terminal Tyr-Asn and Arg-Phe bonds but also endopeptidase cleavage after Trp<sup>47</sup> Phe<sup>50</sup> and Gly<sup>51</sup>. [20,21] As such a particular priority of this approach was to target modifications that protect the products from proteolytic degradation. We decide to examine the β<sup>2</sup>-homoamino acid class, which might offer reduced peptidase susceptibility. Introduction of β-amino acid homologues of DNA-encoded α-amino acids has resulted in an array of interesting pharmacological and structural outcomes in peptide science, although β<sup>2</sup>-homoamino acids have been less well studied than their β<sup>3</sup>-homoamino acid counterparts. [22–24] We also compiled a range of fluorescent ligands, targeting a variety of fluorophores, linking chemistries and positional substitution. [25] Such ligands as well as providing useful tools for studying KISS1R pharmacology contribute to the SAR understanding of kisspeptin-related peptides.

## Materials and Methods

### Chemistry

N<sup>ε</sup>-Fmoc-protected amino acids were purchased from Auspep and ChemImpex. Rink amide resin and *O*-(1*H*-6-chlorobenzotriazol-1-yl)-*N,N,N',N'*-tetramethyluronium hexafluorophosphate (HCTU) were purchased from ChemImpex. 6-Chloro-benzotriazole-1-yl-oxy-tris-pyrrolidinophosphonium hexafluorophosphate (PyClock) was purchased from Merck. Methylbenzhydrylamine (MBHA) resin, piperidine and trifluoroacetic acid (TFA) were purchased from

Auspep. *N,N*-diisopropylethylamine (DIPEA), DMF, DCM, were purchased from Merck. Triisopropylsilane (TIPS) was purchased from Sigma-Aldrich. 4-Fluorobenzoic acid was purchased from Alfa Aesar. Rhodamine B isothiocyanate was obtained from Sigma-Aldrich. The azidopentanoylpiperazine-rhodamine B derivative was prepared in-house. [26,27] Cy5.5 carboxylic acid was obtained from Lumiprobe (Cat# 27090) (Florida). All chemicals were used without further purification.

Liquid Chromatography Mass Spectra (LCMS) were acquired on a Shimadzu 2020 LCMS system incorporating a photodiode array detector coupled directly into an electrospray ionisation source and a single quadrupole mass analyser. RP-HPLC was carried out at room temperature employing a Phenomenex Luna C8 (100 × 2.0 mm I.D.) column eluting with a gradient of 0–100% ACN in 0.05% aqueous TFA over 15 min at a flow rate of 0.2 ml/min. Mass spectra were obtained in positive mode with a scan range of 200–2000 m/z. Semi-preparative reverse-phase HPLC was performed using a Waters Associates liquid chromatography system (Model 600 controller and Waters 486 Tuneable Absorbance Detector) using a gradient of 0.80% ACN in 0.1% TFA over 20 min or 30 min at a flow rate of 10 ml/min on a Phenomenex Luna C8 100 Å, 10 μm (250 × 21.2 mm I.D.) or Phenomenex Luna C8 100 Å, 10 μm (100 × 21.2 mm I.D.) column.

Except where otherwise stated peptide syntheses were performed on Rink amide resin (0.3–0.7 meq/g, 100–200 mesh, 0.1 mmol scale) using conventional Fmoc-based solid phase peptide synthesis. Fmoc-protected amino acids in threefold molar excess were coupled using DMF as solvent; sixfold molar excess of diisopropylethylamine in DMF (70 ml/l) with threefold molar excess of HCTU as the activating agent for 50 min. Fmoc deprotection was carried out by treatment with 20% piperidine in DMF for 10 min. Peptide cleavage off resin was performed using a cocktail containing TFA/TIPS/DMB (92.5%:2.5%:5%) for 2 h [28]. The cleavage mixture was filtered, concentrated by a stream of nitrogen, precipitated by cold diethyl ether and centrifuged. The resulting crude product was dissolved in water/acetonitrile (1 : 1) and lyophilised overnight.

### β<sup>2</sup>-Homoamino Acid Containing Peptides

#### Boc-β<sup>2</sup>-homoamino acid synthesis

##### General procedure for the Knoevenagel condensation

To a solution of methyl cyanoacetate **I** (1.3 eq.) and piperidine (seven drops) in MeOH (50 ml) was added the aldehyde (1 eq.)

and the reaction mixture refluxed for 16 h. The reaction was cooled to room temperature and the product precipitated out by addition of H<sub>2</sub>O (50 ml), filtered and washed (H<sub>2</sub>O, 10 ml) to give the product. Purification where necessary by column chromatography.

**Methyl 2-cyano-3-phenylacrylate (IIa)** [29,30]. From benzaldehyde (2.20 ml, 24.9 mmol). White solid (3.56 g, 96%). *R<sub>f</sub>* 0.66 (25% EtOAc in hexane). <sup>1</sup>H-NMR: (CDCl<sub>3</sub>, 300 MHz) δ 8.26 (1H, s, CH); 7.99 (2H, d, *J* = 9.0 Hz, Ar. H); 7.56–7.47 (3H, m, Ar. H); 3.93 (3H, s, COOMe). Mp: 85–87 °C, lit [30] 87–89 °C.

**Methyl 2-cyano-4-methylpent-2-enoate (IIb)**. From isobutyraldehyde (1.50 ml, 16.4 mmol). Clear oil (0.905 g, 36%). *R<sub>f</sub>* 0.84 (CHCl<sub>3</sub>). <sup>1</sup>H-NMR: (CDCl<sub>3</sub>, 400 MHz) δ 7.43 (1H, d, *J* = 10.6 Hz, CH); 3.82 (3H, s, COOMe); 2.99–2.90 (1H, m, CH); 1.11 (6H, d, *J* = 6.6 Hz, 2 × CH<sub>3</sub>).

**Methyl 3-(4-hydroxyphenyl)-2-isocyanoacrylate (IIc)** [31]. From *p*-hydroxybenzaldehyde (2.40 g, 19.7 mmol). White solid (3.25 g, 81%). <sup>1</sup>H-NMR: (CDCl<sub>3</sub>, 300 MHz) δ 8.21 (1H, s, CH); 7.96 (2H, d, *J* = 8.7 Hz, Ar. H); 6.91 (2H, d, *J* = 9.0 Hz, Ar. H); 3.87 (3H, s, COOMe). Mp: 213–214 °C, lit [31] 208–210 °C.

**Methyl 3-(1H-indol-3-yl)-2-isocyanoacrylate (IId)** [32,33]. From 3-indolecarboxaldehyde (3.60 g, 24.9 mmol). White solid (3.35 g, 75%). *R<sub>f</sub>* 0.61 (50% EtOAc in hexane). <sup>1</sup>H-NMR: (CDCl<sub>3</sub>, 300 MHz) δ 9.15 (1H, br s, NH); 8.64 (2H, m, Ar. H and CH); 7.87–7.84 (1H, m, Ar. H); 7.50–7.48 (1H, m, Ar. H); 7.34 (2H, m, Ar. H); 3.93 (1H, s, COOMe). ESI-MS (+): *m/z* = 227.1 [M + H]<sup>+</sup>, ESI-MS (–) 225.1 [M – H]<sup>–</sup>. Mp: 186.5–188.5 °C, lit [34] 165.9 °C.

#### General procedure for one-pot reduction and Boc protection

To a solution of the alkene (1 eq.) in MeOH (300 ml) in a 500 ml round bottomed flask fitted with a drying tube, was added CoCl<sub>2</sub>·6H<sub>2</sub>O (0.5 eq.) and Boc<sub>2</sub>O (3 eq.). The mixture was cooled to 0 °C and NaBH<sub>4</sub> (14 eq.) added slowly over 2 h. The reaction was warmed to room temperature and stirred for 16–24 h. To the reaction mixture was added diethylenetriamine (1 eq.) and stirred for 30 min. The solvent was evaporated *in vacuo* and the purple residue taken up in EtOAc. The organic layer was washed with saturated aq. NaHCO<sub>3</sub>, and dried over Na<sub>2</sub>SO<sub>4</sub>. The solvent was removed *in vacuo* and the residue purified by flash chromatography using 0–25% EtOAc in hexane to give product.

**Boc-(±)-β<sup>2</sup>-homophenylalanine-methyl ester (IIIa)** [35]. From **IIa** (0.500 g, 0.27 mmol). Pale yellow oil (0.185 g, 26%). *R<sub>f</sub>* 0.74 (25% EtOAc in hexane). <sup>1</sup>H-NMR: (CDCl<sub>3</sub>, 300 MHz) δ 7.28–7.23 (5H, m, Ar. H); 4.94 (1H, s, NH); 3.62 (3H, s, COOMe); 3.37–3.20 (2H, m, CH<sub>2</sub> and CH); 2.97–2.75 (3H, m, CH<sub>2</sub> and CH); 1.41 (9H, s, Boc).

**Boc-(±)-β<sup>2</sup>-homoleucine-methyl ester (IIIb)**. From **IIb** (0.679 g, 4.43 mmol). Pale yellow oil (0.321 g, 28%). <sup>1</sup>H-NMR: (CDCl<sub>3</sub>, 300 MHz) δ 4.89 (1H, br. s, NH), 3.66 (3H, s, COOMe), 3.29 (1H, dd, *J* = 11.8, 5.6 Hz, CH<sub>2</sub>), 3.25–2.59 (3H, m, CH<sub>2</sub> and CH), 1.39 (1H, s, 0.5 × CH<sub>2</sub>), 1.29–1.20 (6H, m, 2 × CH<sub>3</sub>); 0.87 (9H, d, *J* = 6.1 Hz, Boc). ESI-MS (+): *m/z* = 260.4 [M + H]<sup>+</sup>, 282.4 (M + Na)<sup>+</sup>.

**Boc-(±)-β<sup>2</sup>-homotyrosine-methyl ester (IIIc)**. From **IIc** (1.72 g, 8.48 mmol). Pale yellow oil (0.548 g, 16%). *R<sub>f</sub>* 0.54 (50% EtOAc in hexane). <sup>1</sup>H-NMR: (CDCl<sub>3</sub>, 600 MHz) δ 6.99 (2H, d, *J* = 8.1 Hz, Ar. H); 6.71 (2H, d, *J* = 7.5 Hz, Ar. H); 3.66 (3H, s, COOMe); 3.35 (1H, m, 0.5 × CH<sub>2</sub>); 3.23 (1H, m, CH); 2.90–2.88 (2H, m, 0.5 × CH<sub>2</sub> and 0.5 × CH<sub>2</sub>); 2.72 (1H, dd, *J* = 9.9, 15.6 Hz, 0.5 × CH<sub>2</sub>); 1.43 (9H, s, Boc).

Di-Boc-(±)-β<sup>2</sup>-homotyrosine-methyl ester was also obtained pale yellow oil (0.319 g, 9%). *R<sub>f</sub>* 0.79 (50% EtOAc in hexane). <sup>1</sup>H-NMR (CDCl<sub>3</sub>, 600 MHz) δ 7.15 (2H, d, *J* = 12.0 Hz, Ar. H); 7.06 (2H, d,

*J* = 6.0 Hz, Ar. H); 3.62 (3H, s, COOMe); 3.37–3.35 (1H, m, 0.5 × CH<sub>2</sub>); 3.28–3.26 (1H, m, CH); 2.94–2.89 (2H, m, 0.5 × CH<sub>2</sub> and 0.5 × CH<sub>2</sub>); 2.80–2.78 (1H, m, 0.5 × CH<sub>2</sub>); 1.54 (9H, s, Boc); 1.42 (9H, s, Boc).

**Boc-(±)-β<sup>2</sup>-homotryptophan-methyl ester (IIId)**. From **IId** (1.00 g, 4.40 mmol). Brown oil (0.898 g, 61%). *R<sub>f</sub>* 0.22 (25% EtOAc in hexane). <sup>1</sup>H-NMR: (CDCl<sub>3</sub>, 300 MHz) δ 7.85 (1H, d, *J* = 9.0 Hz, Ar. H); 7.34 (1H, d, *J* = 9.0 Hz, Ar. H); 7.18 (1H, t, *J* = 9.0 Hz, Ar. H); 7.11 (1H, t, *J* = 9.0 Hz, Ar. H); 7.01 (1H, s, Ar. H); 3.67 (3H, s, COOMe); 3.45–3.29 (2H, m, CH<sub>2</sub>); 3.20–3.10 (1H, m, CH); 3.04–2.92 (2H, m, CH<sub>2</sub>); 1.43 (9H, s, Boc). ESI-MS (+): *m/z* = 333.5 [M + H]<sup>+</sup>, 665.8 [M + 2H]<sup>2+</sup>.

#### General procedure for the ester hydrolysis

To a solution of the Boc protected methyl-ester (1 eq.) in THF (5 ml) was added a solution of lithium hydroxide (1.2 eq.) in 5 ml of H<sub>2</sub>O. The reaction mixture was stirred at room temperature for 16 h or heated with stirring under microwave irradiation (100 °C, Power = 105 W) for 40 min. The organic solvent was removed *in vacuo*, the residue acidified with 1 M HCl to pH 2 and extracted with ethyl acetate (3 × 10 ml). The combined organic layers were washed with brine (10 ml), dried over Na<sub>2</sub>SO<sub>4</sub> and the solvent removed *in vacuo* to give the product.

**Boc-(±)-β<sup>2</sup>-homophenylalanine (IVa)** [36–39]. From **IIIa** (0.636 mg, 2.17 mmol). Yellow solid (0.623 g, > 99%). <sup>1</sup>H-NMR: (CD<sub>3</sub>OD, 300 MHz) δ 7.34–7.20 (5H, m, Ar. H); 3.46–3.20 (2H, m, CH<sub>2</sub>); 3.14–2.71 (3H, m, CH and CH<sub>2</sub>); 1.46 (9H, s, Boc). ESI-MS (–): *m/z* = 278.5 [M – H]<sup>–</sup>, 557.7 (2M – H)<sup>–</sup>. Mp: 94–96 °C.

**Boc-(±)-β<sup>2</sup>-homoleucine (IVb)** [37]. From **IIIb** (0.321 mg, 1.24 mmol). Pale yellow oil (0.301 g, 99%). <sup>1</sup>H-NMR: (CD<sub>3</sub>OD, 300 MHz) δ 3.47–3.13 (2H, m, CH<sub>2</sub>); 2.77–2.61 (1H, m, CH); 1.91–1.69 (2H, m, CH<sub>2</sub>); 1.47 (9H, s, Boc); 0.94 (6H, d, *J* = 6.48 Hz, 2 × CH<sub>3</sub>). ESI-MS (–): *m/z* = 244.2 [M – H]<sup>–</sup>.

**Boc-(±)-β<sup>2</sup>-homotyrosine (IVc)**. From **IIIc** (319 mg, 1.03 mmol). Yellow oil (0.186 g, 61%). <sup>1</sup>H-NMR: (CD<sub>3</sub>OD, 600 MHz) δ 7.00 (2H, d, *J* = 6.8 Hz, Ar. H); 6.71 (2H, d, *J* = 6.9 Hz, Ar. H); 3.43–3.33 (1H, m, 0.5 × CH<sub>2</sub>); 3.24–3.22 (1H, m, 0.5 × CH<sub>2</sub>); 3.13–3.08 (1H, m, CH); 2.77–2.75 (1H, m, 0.5 × CH<sub>2</sub>); 2.66–2.63 (1H, m, 0.5 × CH<sub>2</sub>); 1.43 (9H, s, Boc). ESI-MS (+): 318.3 (M + Na)<sup>+</sup>, ESI-MS (–): *m/z* = 294.9 [M – H]<sup>–</sup>.

**Boc-(±)-β<sup>2</sup>-homotryptophan (IVd)** [40]. From **IIId** (0.856 mg, 2.57 mmol). Yellow oil (0.679 g, 83%). <sup>1</sup>H-NMR: (CDCl<sub>3</sub>, 300 MHz) δ 7.55 (1H, d, *J* = 7.7 Hz, Ar. H); 7.08 (3H, dt, *J* = 7.0, 14.6 Hz, Ar. H); 6.95 (1H, s, Ar. H); 3.46–3.22 (2H, m, CH<sub>2</sub>); 3.14 (1H, dd, *J* = 4.9, 13.2 Hz, CH); 3.03–2.82 (2H, m, CH<sub>2</sub>); 1.41 (9H, s, Boc). ESI-MS (–): *m/z* = 317.2 [M – H]<sup>–</sup>.

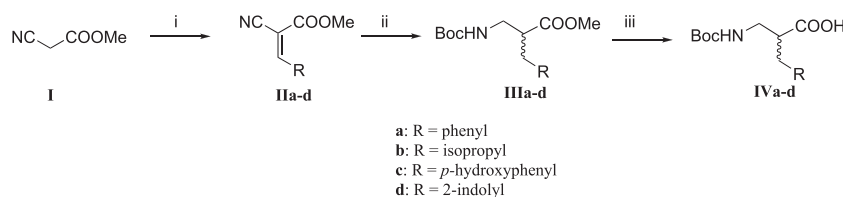
#### β<sup>2</sup>-Homoamino Acid Containing Peptide Synthesis

β<sup>2</sup>-Homoamino acid containing peptides were prepared on MBHA resin by a mixed Boc/Fmoc-based synthesis strategy, such that after coupling with Boc-protected β<sup>2</sup>-homoaminoacids, deprotection was performed with 100% trifluoroacetic acid. The TFA-stable Fmoc-Arg(Mtr) was used for introduction of arginine. Peptides were cleaved from the resin using a mixture of trifluoromethane sulfonic acid and TFA as previously described.[19]

#### Peptide Labelling

Rhodamine linked amide **12** was prepared by treatment of kisspeptin with a rhodamine B derivative activated with PyClock and NMM in DMF for three hours. The solvent was removed *in vacuo*, the residue dissolved in a minimum volume of TFA,





**Scheme 1.** Reagents and conditions; i, R-CHO, piperidine, MeOH, reflux 16 h; ii,  $\text{CoCl}_2 \cdot 6\text{H}_2\text{O}$ ,  $\text{Boc}_2\text{O}$ ,  $\text{NaBH}_4$ , 24 h; iii,  $\text{LiOH}$ ,  $\text{THF}/\text{H}_2\text{O}$ , RT, 16 h or mw, 100 nm, 40 min.

precipitated with ether and centrifuged to yield the crude product which was purified by RP-HPLC. RhB-KP10 **12** RT 14.94 min

Cy5.5 linked amide **13** was prepared by treatment of kisspeptin with Cy5.5 carboxylic acid activated with PyCLOCK and NMM in DMF for three hours. The solvent was removed *in vacuo*, the residue dissolved in a minimum volume of TFA, precipitated with ether and centrifuged to yield the crude product which was purified by RP-HPLC. Cy5.5-KP10 **13** RT 12.8 min

Rhodamine thioureas **14** and **16** were prepared by treating a solution of the peptide (0.015 mmol) in methanol with rhodamine B isothiocyanate (8 mg, 0.15 mmol) and 0.1 M  $\text{Na}_2\text{CO}_3$  was added until a pH of 9 was attained. The reaction was stirred overnight at RT, then diluted with water (40 ml) and freeze dried. The residue was purified by RP-HPLC.

**14** was obtained as two regioisomers RT 14.7, 15.1 min.

**16** was obtained as two regioisomers RT 14.5, 14.9 min.

The triazolo-linked rhodamine B peptide **15** was prepared by involved dissolving the corresponding peptide-alkyne (1 eq.) in  $\text{H}_2\text{O}$  and adding a solution of the azido substituted rhodamine B derivative (4 eq.) in DMF to give a 1 : 3 ratio of  $\text{H}_2\text{O}$  to DMF. Copper sulfate (10 eq.), TBTA (10 eq.) and sodium ascorbate (10 eq.) were then added and the reaction mixed for 3 h. [27] Peptides were purified by reverse-phase preparative HPLC.

### Dual Luciferase Reporter Gene Assay

Full CDS region of human GPR54 mRNA (GenBank accession number NM\_032551) was amplified from FirstChoice PCR-Ready Human Brain cDNA (Ambion, Austin, TX) and cloned into a pcDNA3.1(+) expression vector (Invitrogen, Carlsbad, CA) to prepare the GPR54 expression construct (pcGPR54). HEK293-T cells were maintained in Dulbecco's modified Eagle's medium (DMEM; GIBCO, Alckland, NZ) supplemented with 10% fetal bovine serum (FBS), 0.1 x penicillin–streptomycin solution (iDNA, Kuala Lumpur, Malaysia) under 5%  $\text{CO}_2$ . One day before transfection, cells were plated in 24-well plates in the media without penicillin–streptomycin. Cotransfection of pcGPR54 (100 ng/well), pSRE-Luc (100 ng/well; Stratagene, La Jolla, CA), and pRL-TK vectors (25 ng/well; Promega, Madison, WI) was carried out with Lipofectamine 2000 transfection reagent (Invitrogen) overnight according to the manufacturer's instructions. The cells were serum starved in the media with 0.5% FBS for 18–20 h, and then treated with the vehicle or GPR54 analogues in the media for 6 h. The cells were harvested and the luciferase activity in the cell extracts was determined using Dual-Luciferase Reporter Assay System (Promega) in a single-tube luminometer (Sirius; Berthold Detection Systems GmbH, Pforzheim, Germany) according to the manufacturer's instruction.

### Data Analysis

Luciferase induction as a percentage of maximal compound activity was calculated by setting the highest induction of each compound

at 100%. Data analysis including the calculation of half effective concentration ( $\text{EC}_{50}$ ) and a fit sigmoidal graph was performed using Origin 6.0 software (Microcal Software, Inc., Northampton, MA). All data are presented as mean  $\pm$  SEM.

### Protease Inhibitor Assay

To examine the effect of protein degradation during the assay, dual luciferase reporter gene assay was conducted with the addition of Protease Inhibitor Cocktail (Sigma-Aldrich, St. Louis, MO). Different doses (0, 1, 2, and 5  $\mu\text{l}$ ) of the protease inhibitor was applied to 500  $\mu\text{l}$  media and HEK293-T cells transfected with the vectors were incubated with different doses of KP-10 in the media for 6 h. The cells were harvested and the luciferase activity in the cell extracts was determined using Dual-Luciferase Reporter Assay System (Promega) in a single-tube luminometer (Sirius) according to the manufacturer's instruction.

## Results

### (a) Synthetic Analogues of KP-10

A variety of kisspeptin analogues were prepared as assay controls. This included a kisspeptin 10 (**1**), the d-Tyr analogue (**2**), a simplified analogue of TAK448 (**3**), an analogue of FTM-080, (**4**) and Peptide 234 (**5**). (Table 1) These peptides were synthesised using standard Fmoc solid phase peptide synthesis procedures on Rink amide resin.

In addition, we evaluated some novel peptides containing  $\beta^2$ -homoamino acids. The Boc-protected amino acids were prepared according to the general methods described by Patay[41] and Caddick.[42] The first step of this synthesis (Scheme 1) was the Knoevenagel condensation between methylcyanoacetate (**I**), and the aldehydes in the presence of piperidine and methanol, to give the alkenes in 36–95% yield. One pot reduction and *N*-Boc protection of alkenes **IIa–d** were performed using cobalt-boride, which was formed *in situ* from sodium borohydride and cobalt chloride hexahydrate. Base-catalysed hydrolysis of the methyl esters **IIIa–d** under thermal or microwave heating (100  $^\circ\text{C}$ , 105 W) with lithium hydroxide gave the Boc- $\beta^2$ -homoamino acids, Boc- $\beta^2$ -hTyr, Boc- $\beta^2$ -hPhe, Boc- $\beta^2$ -hLeu, and Boc- $\beta^2$ -hTrp (**IVa–d**) in good yields. All spectroscopic data were consistent with proposed structures and literature values, where available.

A KP10 analogue containing a  $\beta^2$ -homotyrosine at the *N*-terminus was prepared as well as analogues of the linear hexapeptides FTM 180 and **4**. The  $\beta$ -amino acids were coupled as Boc-protected derivatives. In examples that contained mid-sequence substitutions, were synthesised using a mixed Fmoc and Boc protection strategy on MBHA resin. The yields of purified peptide in these cases were quite low, in part due to poor yield of the  $\beta^2$ -amino acid coupling, but in addition, residual trifluoromethanesulfonic acid created problems in isolation of the

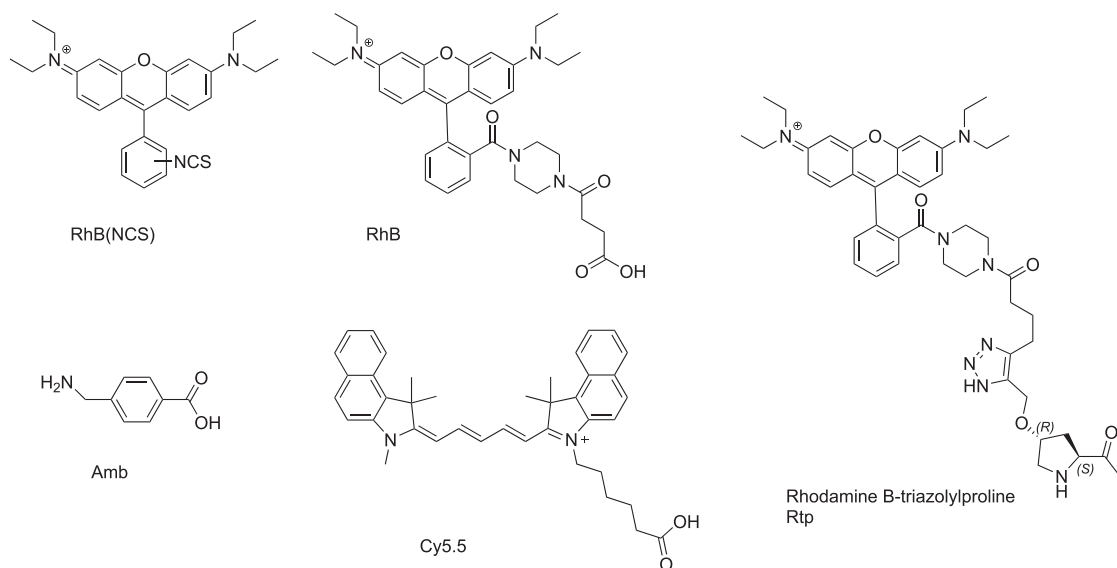


**Figure 1.** Chemical structure of fluorophores utilised in this study.

product from crude cleavage reaction mixtures. The products were all obtained as pairs of diastereomers, consistent with the racemic nature of the precursor  $\beta^2$ -homoamino acids and the mixtures could not be separated by HPLC. In the case of peptide **3**, the purification from other impurities resulted in partial resolution of the diastereomers yielding a 1 : 4 mixture of the diastereomeric pair.

We also prepared fluorescently labelled analogues where the fluorophore was appended either through the amino terminus (**12–14**) or by introduction of an appending ligand to replace Asn<sup>4</sup> (**15–16**). (Figure 1) While this residue is important for activity as shown by alanine replacement, we reasoned that the carboxamide side chain might be mimicked by thiourea or triazole functions, utilising linkage methods we have described in other work.[27] The fluorescent rhodamine B thiourea derivatives **14** and **16** were prepared by coupling with either rhodamine B isothiocyanate either in solution or on resin. Two regioisomeric products were obtained corresponding to the two regioisomers of the parent rhodamine isothiocyanate. The *N*-terminal rhodamine **12** and Cy5.5 carboxamides **13** were prepared by reacting with the corresponding PyClock-activated esters. The triazolyl linked rhodamine was prepared by coupling the propargyloxypyrrolidine derivative with an azido functionalised rhodamine using the copper-assisted alkyne-azide cycloaddition reaction.[27]

#### Biological assays

##### (a) Powerful Luciferase induction by kisspeptin of KISS1R transfected HEK293T cells

The specificity of the reporter gene assay system was confirmed by comparing hGPR54 construct (hGPR54 in a pGEM-T Easy vector) with a control plasmid. Treatment with human KP-10 (**1**) increased relative (Firefly/*Renilla*) luciferase activity in a dose-response manner (Figure 2A), while no induction was seen in the HEK293T cells without hGPR54 expression, indicating that the assay system exclusively detects the activation of exogenous GPR54 and is thus useful in the evaluation of kisspeptin analogues in the present study. The induction of luciferase activity was time dependent and shown to be maximal at 6 h of incubation. The EC<sub>50</sub> of KP-10 was determined to be  $13 \pm 1.9$  nM, in general accord with the results obtained under other assay formats.[12,13]

Reported compounds **2** and **4** were also found to be potent agonists, giving EC<sub>50</sub> values in the low nanomolar range and consistent with literature reports (Peptide **2** EC<sub>50</sub> 3.6 nM (receptor binding)[13]; Peptide **4** EC<sub>50</sub> 3.1 nM Fliper assay[12]). Compound **3**, a simplified analogue of TAK448[14] has not been previously reported and was shown to be a particularly potent agonist, with an EC<sub>50</sub> of 0.24 nM in the reporter assay. (Figure 2B–D)

It should be noted that one feature of the assays with these transiently transfected cells was that the degree of induction varied from experiment to experiment, although the EC<sub>50</sub> stayed relatively constant. However, it was also noticed that the level of induction for analogues **2–3** was greater than that for kisspeptin itself in the same batch of treatment. We hypothesised that this was not due to any difference in intrinsic efficacy but due to improved stability of these compounds compared with kisspeptin in the assay conditions and this was investigated further as described later. As such the reported EC<sub>50</sub> values for a peptide are referenced against the maximum induction for that same peptide. (Table 1, Figure 2)

The assay system should also be suitable to evaluate potential antagonism of GPR54, with incubation of test compounds in the presence of established agonists such as KP-10. The reported antagonist 'Peptide 234' (Ac-d-Ala-Asn-Trp-Asn-Gly-Phe-Gly-d-Trp-Arg-Phe-NH<sub>2</sub>)[15] was tested in the assay but showed no antagonism of the KP-10 response. This was both with in-house synthesised samples and the samples obtained from the laboratory that described the peptide (R. Millar, The Queens Medical Research Institute, Edinburgh).[15] These samples did display phenotypic behaviours indicative of reported GPR54 antagonism in mouse models (data not shown). The reason for these conflicting results is unknown – the problem may be due to a technical aspect of the luciferase assay system or it may relate to an off-target effect of Peptide 234 that results in indirect but functional antagonism of Kisspeptin responses.

In the study of the modified kisspeptin analogues it was observed that both  $\beta^2$ -homoamino acid and fluorescent labelling could have dramatic effects on KISS1R agonist activity.

The kisspeptin 10 analogue bearing an *N*-terminal  $\beta^2$ -hTyr substitution **6** was a potent KISS1R agonist with an EC<sub>50</sub> of 0.41 nM. (Figure 2E) This shows the tolerance the receptor has for the *N*-

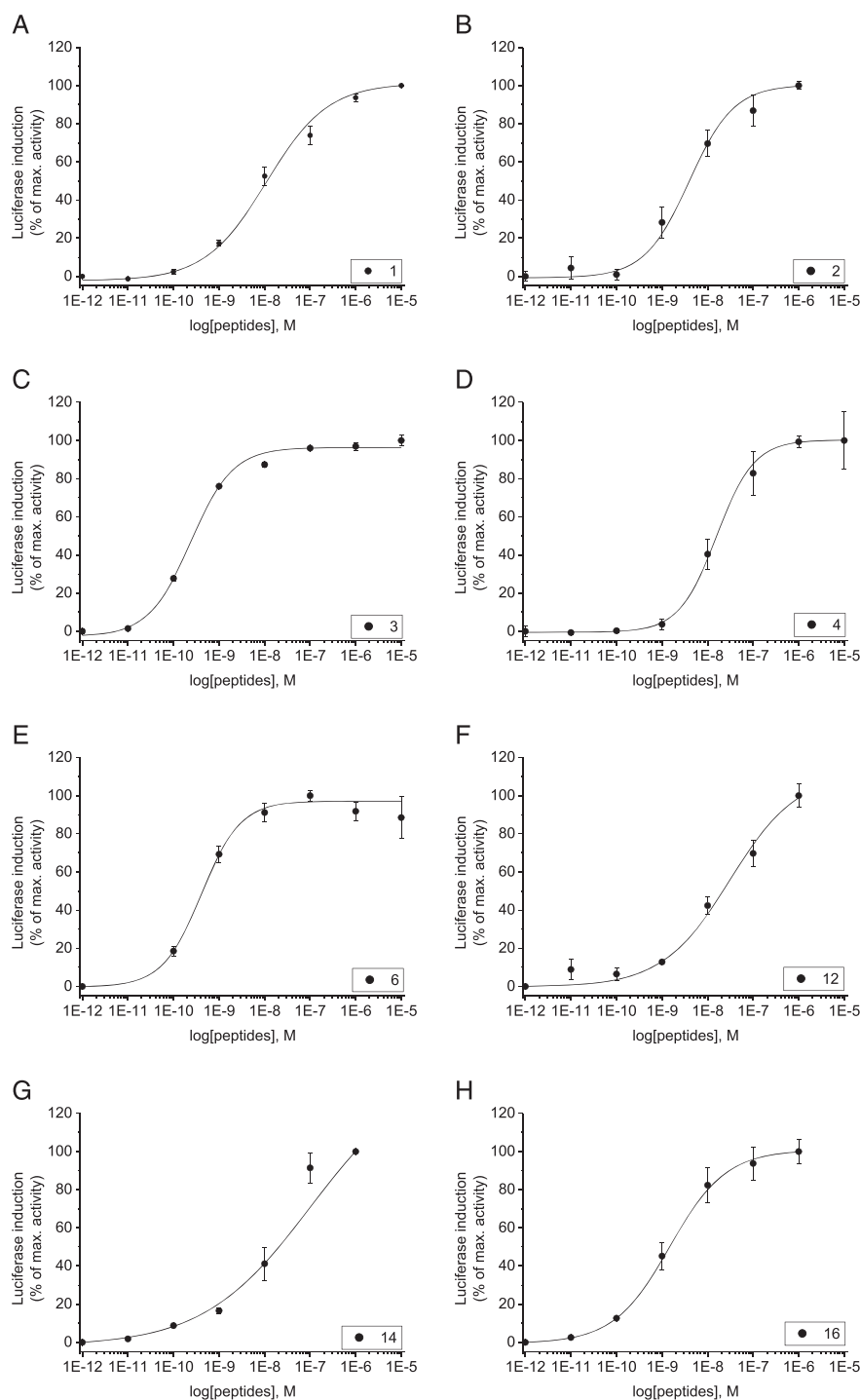


**Figure 2.** Dose response curves for luciferase induction by test peptides upon GPR-54 transfected HEK293-T cells. See Materials and Methods for details.

terminal modifications consistent with the potent activity of analogues **2** and **3**.

On the other hand, the  $\beta$ -amino acid containing analogues of FTM80 and **3** were much less active but agonist activity was seen at high concentrations of certain ligands. The compounds showed some differences in EC<sub>50</sub> that must correspond to the ability to adopt the bioactive conformation found with the parent peptide. Compound **8**, where a glycine was replaced by a  $\beta$ -alanine ( $\beta^2$ -hGly), showed the strongest activity in this series with an EC<sub>50</sub> of 0.6  $\mu$ M. This is consistent with other studies where this region of

the peptide has been amenable to certain structural changes – such as FTM145, which has a non-peptide replacement for the Phe-Gly linkage and the triazolo linked peptide Beltramo 3 (Table 1). [16,43] Note also that a series of previously published [19] cyclic peptides that adopt stable helical structures also showed no agonist efficacy in these assays (data not shown). (Figure 3)

Finally, the fluorescently labelled ligands showed a quite marked and surprising structure-activity profile. The inclusion of the rhodamine label at the N-terminus of KP-10, as amide **12** or thiourea **14** had little effect upon the observed potency with EC<sub>50</sub> values of 30

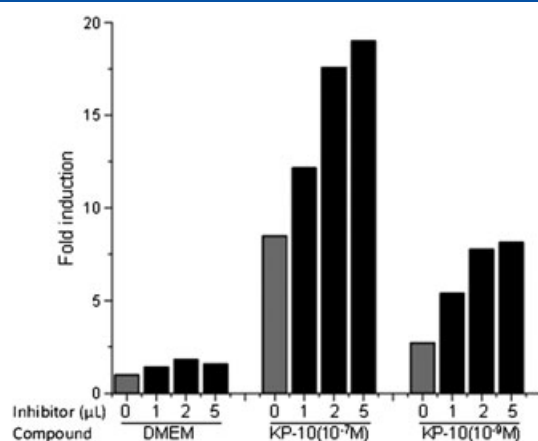


**Figure 3.** Comparison of luciferase induction of GPR-54 transfected HEK293-T cells by vehicle (DMEM), KP-10 (100 nM) and KP10 (1 nM) in the presence of 0, 1, 2 or 5  $\mu$ L of protease inhibitor cocktail.

and 10 nM, respectively. The inclusion of the Cy5.5 label **11** completely abolished activity. This form of the Cy5.5 label has a non-sulfated benzo[e]indol-2-ylidene rendering it quite hydrophobic, which may impact on the binding affinity. (Table 2)

Introduction of a rhodamine label replacing the asparagine residue of the TAK-488 analogues resulted in a potent inhibitor **16** ( $EC_{50}$  = 1 nM) albeit less potent than the parent molecule. The introduction of a triazolyl-proline at the same position in dTyr-KP10 **15** abolished activity, a likely consequence of the conformational effect of the proline-like residue as the precursor peptide was similarly inactive (data not shown).

The variation in the extent of luciferase induction by the variety of peptide agonists described earlier was further examined. While there might be a number of mechanisms to explain 'partial' agonism displayed by KP-10, one hypothesis was that the peptide was being degraded over the course of the incubation period, such that the actual concentration of agonist was diminishing across time. As such the synthetic analogues that possessed modified

amino acids might be more resistant to proteases in particular and so express agonist efficacy throughout the incubation period.

To test this hypothesis, the assay of KP-10 activity was repeated but in this case with increasing amounts of a protease inhibitor cocktail present in the culture media. The level of induction increased by over 150% at both 1 nM and 100 nM concentrations suggesting that protease activity was diminishing the full expression of agonist activity in the reporter assay.

## Discussion

The development of new ligands for KISS1R is being pursued by a number of groups, as the potential for therapeutic agonists and antagonists is evident from numerous studies. In our pursuit of such ligands we have developed a functional assay format that is robust and straightforward, giving a clear dose dependent readout of agonist activity. Three reported agonists gave  $EC_{50}$  values consistent with those reported by others. The activity of peptide **2** has not been described, and showed it to be a potent agonist of GPR54. Notably, this increased potency was achieved by the introduction of D-amino acid, d-Tyr or the  $\beta$ -amino acid,  $\beta^2$ hTyr at the N-terminus with relatively little change to the C-terminal sequence, although it may reflect either increased binding affinity or be due to an increased stability in the time course assay. This is consistent with the reported improvement of *in vivo* potency of d-Tyr<sup>1</sup>-KP-10.[13] We have also shown that agonist potency can be retained with the inclusion of fluorophores, also providing other potentially useful tools for studying the kisspeptin/GPR54 system. Kaneda et al. recently described alternate fluorescently labelled kisspeptin analogues through N-terminal derivatization of KP-14 and KP-52. The retention of agonist activity with the tetramethylrhodamine and rhodamine green labels is consistent with our data here.[25]

We also examined the use of  $\beta$ -amino acids as a means of constraining the short pentapeptide agonists in the hope that it may confer metabolic stability while also retaining a bioactive conformation. The changes to the structure proved very deleterious to

**Table 2.** LC-MS and  $EC_{50}$  data for KISS1R peptides

Number	Sequence	ESI-MS m/z	$EC_{50}$ /(nM)
1 (KP-10)	H-Tyr-Asn-Trp-Asn-Ser-Phe-Gly-Leu-Arg-Phe-NH <sub>2</sub>	1302.8	13 $\pm$ 1.9
2	H-d-Tyr-Asn-Trp-Asn-Ser-Phe-Gly-Leu-Arg-Phe-NH <sub>2</sub>	652.2 <sup>a</sup>	5.3 $\pm$ 1.23
3	Ac-d-Tyr-Hyp-Asn-Thr-Phe-Gly-Leu-Arg-Trp-NH <sub>2</sub>	1210.4	0.24 $\pm$ 0.012
4	Amb-Phe-Gly-Leu-Arg-Phe- NH <sub>2</sub>	771.6	16 $\pm$ 5.6
5	Ac-d-Ala-Asn-Trp-Asn-Gly-Phe-Gly-d-Trp-Arg-Phe-NH <sub>2</sub>	1295.6	—
6	H- $\beta^2$ hTyr-Asn-Trp-Asn-Ser-Phe-Gly-Leu-Arg-Phe-NH <sub>2</sub>	1300.8	0.41 $\pm$ 0.065
7	FBz- $\beta^2$ hPhe-Gly-Leu-Arg-Phe- NH <sub>2</sub>	774.6	Inactive
8	FBz-Phe- $\beta$ Ala-Leu-Arg-Phe- NH <sub>2</sub>	774.7	600 $\pm$ 140
9	Amb-Phe-Gly- $\beta^2$ hLeu-Arg-Phe- NH <sub>2</sub>	786.0	>1000 <sup>b</sup>
10	FBz-Phe-Gly-Leu-Arg- $\beta^2$ hPhe- NH <sub>2</sub>	774.3	Inactive
11	FBz-Phe-Gly-Leu-Arg- $\beta^2$ hTrp- NH <sub>2</sub>	812.9	>1000 <sup>b</sup>
12	RhB-Tyr-Asn-Trp-Asn-Ser-Phe-Gly-Leu-Arg-Phe-NH <sub>2</sub>	948.9 <sup>a</sup>	31 $\pm$ 19.2
13	Cy5.5-Tyr-Asn-Trp-Asn-Ser-Phe-Gly-Leu-Arg-Phe-NH <sub>2</sub>	934.7 <sup>a</sup>	Inactive
14	RhB(NHCS)-Tyr-Asn-Trp-Asn-Ser-Phe-Gly-Leu-Arg-Phe-NH <sub>2</sub>	902.10 <sup>a</sup>	10 $\pm$ 11.0
15	H-d-Tyr-Asn-Trp-Rtp-Ser-Phe-Gly-Leu-Arg-Phe-NH <sub>2</sub> <sup>c</sup>	989.0 <sup>a</sup>	Inactive
16	Ac-d-Tyr-Hyp-Dap( $\gamma$ SCNH-RhB)-Thr-Phe-Gly-Leu-Arg-Trp-NH <sub>2</sub>	842.2 <sup>a</sup>	1.0 $\pm$ 0.49

<sup>a</sup>ESI-MS m/z = (M + 2H)<sup>2+</sup>;

<sup>b</sup>Luciferase induction still rising at maximum concentration (10  $\mu$ M) tested;

<sup>c</sup>Rtp = rhodamine-triazolylproline (Figure 1) [27]



agonist efficacy, although in one case agonist activity was obtained at high concentrations. In principle, these changes can be compared with FTM145, a recently described peptidomimetic, where the Gly-Leu dipeptide unit was replaced by an *E*-alkene dipeptide isostere retaining the affinity of the parent peptide. However its EC<sub>50</sub> of 300 nM was substantially poorer than the parent peptide.[43]

One of the interesting results identified across the course of these experiments was that the degree of agonist-induced luciferase activity was lower for kisspeptin than some other synthetic analogues irrespective of the EC<sub>50</sub> of the compound. This an important feature to note as in some respects it can confound the results of single point assays in screening programmes. The luciferase activity acquired over a 6 h incubation of agonist will represent a combination of accumulated acute receptor activation events. Time-dependent loss of agonist due to degradation processes would be expected to result in lower luciferase expression even with a full agonist. The present results show that incubating the cells with a conventional protease inhibitor mixture yielded a significant rise of luciferase-related activity suggesting that proteolytic activity was responsible for the reduced induction of the native peptide. The use of these cell based assays might well be coupled to the use of competition binding assays, possibly utilising the fluorescently labelled kisspeptin analogues described here, to assist in attribution of the activity in compound screens. Equally, an *in vitro* assay that identifies protease susceptibility as part of the readout could be a useful tool in peptide optimization.

## Acknowledgements

The authors would like to thank the Director General of Health Malaysia for his permission to publish this article and the Director of the Institute for Medical Research for his support. This study was supported by Ministry of Health Malaysia, JPP07-034 (to I.S.P.). The provision of Australian Post-graduate Awards (to M.A.C and M.L.) is acknowledged.

## References

- 1 Lee DK, Nguyen T, O'Neill GP, Cheng R, Liu Y, Howard AD, Coulombe N, Tan CP, Tang-Nguyen AT, George SR, O'Dowd BF. Discovery of a receptor related to the galanin receptors. *FEBS Lett.* 1999; **446**: 103–107.
- 2 Parhar IS, Ogawa S, Sakuma Y. Laser-captured single digoxigenin-labeled neurons of gonadotropin-releasing hormone types reveal a novel G protein-coupled receptor (Gpr54) during maturation in cichlid fish. *Endocrinology* 2004; **145**: 3613–3618.
- 3 Stafford LJ, Xia C, Ma W, Cai Y, Liu M. Identification and characterization of mouse metastasis-suppressor KISS1 and its G-protein-coupled receptor. *Cancer Res.* 2002; **62**: 5399–5404.
- 4 Kotani M, Dethieux M, Vandenbogaerde A, Communi D, Vanderwinden JM, Le Poul E, Brezillon S, Tyldesley R, Suarez-Huerta N, Vandeput F, Blanpain C, Schiffmann SN, Vassart G, Parmentier M. The metastasis suppressor gene KISS-1 encodes kisspeptins, the natural ligands of the orphan G protein-coupled receptor GPR54. *J. Biol. Chem.* 2001; **276**: 34631–34636.
- 5 Tena-Sempere M. GPR54 and kisspeptin in reproduction. *Hum. Reprod. Update* 2006; **12**: 631–639.
- 6 Kirby HR, Maguire JJ, Colledge WH, Davenport AP. International union of basic and clinical pharmacology. LXXVII. Kisspeptin receptor nomenclature, distribution, and function. *Pharmacol. Rev.* 2010; **62**: 565–578.
- 7 Silveira LG, Latronico AC, Seminara SB. Kisspeptin and clinical disorders. *Adv. Exp. Med. Biol.* 2013; **784**: 187–199.
- 8 Cho SG, Li D, Tan K, Siwko SK, Liu M. KISS1 and its G-protein-coupled receptor GPR54 in cancer development and metastasis. *Cancer Metastasis Rev.* 2012; **31**: 585–591.
- 9 Orsini MJ, Klein MA, Beavers MP, Connolly PJ, Middleton SA, Mayo KH. Metastin (KISS-1) mimetics identified from peptide structure-activity relationship-derived pharmacophores and directed small molecule database screening. *J. Med. Chem.* 2007; **50**: 462–471.
- 10 Sasaki S, Baba A. Pyridylphenol Compound and Use Thereof. *International Patent Application.* 2007; **PCT/JP2006/316129**.
- 11 Kuohung W, Burnett M, Mukhtyar D, Schuman E, Ni J, Crowley WF, Glicksman MA, Kaiser UB. A high-throughput small-molecule ligand screen targeted to agonists and antagonists of the G-protein-coupled receptor GPR54. *J. Biomol. Screen.* 2010; **15**: 508–517.
- 12 Tomita K, Niida A, Oishi S, Ohno H, Cluzeau J, Navenot J-M, Wang Z-x, Peiper SC, Fujii N. Structure-activity relationship study on small peptidic GPR54 agonists. *Bioorg. Med. Chem.* 2006; **14**: 7595–7603.
- 13 Curtis AE, Cooke JH, Baxter JE, Parkinson JR, Bataveljic A, Gbatei MA, Bloom SR, Murphy KG. A kisspeptin-10 analog with greater *in vivo* bioactivity than kisspeptin-10. *Am. J. Physiol. Endocrinol. Metab.* 2010; **298**: E296–E303.
- 14 Matsui H, Asami T. Effects and therapeutic potentials of kisspeptin analogs: regulation of the hypothalamic-pituitary-gonadal axis. *Neuroendocrinology* 2014; **99**: 49–60.
- 15 Roseweir AK, Kauffman AS, Smith JT, Guerriero KA, Morgan K, Pielecka-Fortuna J, Pineda R, Gottsch ML, Tena-Sempere M, Moenter SM, Terasawa E, Clarke IJ, Steiner RA, Millar RP. Discovery of potent kisspeptin antagonists delineate physiological mechanisms of gonadotropin regulation. *J. Neurosci.* 2009; **29**: 3920–3929.
- 16 Beltramo M, Robert V, Galibert M, Madinier JB, Marceau P, Dardente H, Decourt C, De Roux N, Lomet D, Delmas AF, Caraty A, Aucagne V. Rational Design of Triazololipeptides Analogs of Kisspeptin Inducing a Long-Lasting Increase of Gonadotropins. *J. Med. Chem.* 2015; **58**: 3459–3470.
- 17 Oishi S, Misu R, Tomita K, Setsuda S, Masuda R, Ohno H, Naniwa Y, Ieda N, Inoue N, Ohkura S, Uenoyama Y, Tsukamura H, Maeda K, Hirasawa A, Tsujimoto G, Fujii N. Activation of Neuropeptide FF receptors by kisspeptin receptor ligands. *ACS Med Chem Lett.* 2011; **2**: 53–57.
- 18 Niida A, Wang Z, Tomita K, Oishi S, Tamamura H, Otaka A, Navenot JM, Broach JR, Peiper SC, Fujii N. Design and synthesis of downsized metastin (45–54) analogs with maintenance of high GPR54 agonistic activity. *Bioorg. Med. Chem. Lett.* 2006; **16**: 134–137.
- 19 Camerino MA, Kong DCM, Chalmers DK, Thompson PE. Solid phase synthesis and circular dichroism analysis of (i – i + 4) cyclic lactam analogues of kisspeptin. *Int J Pept Res Ther.* 2008; **14**: 323–331.
- 20 Asami T, Nishizawa N, Ishibashi Y, Nishibori K, Horikoshi Y, Matsumoto H, Ohtaki T, Kitada C. Trypsin resistance of a decapeptide KISS1R agonist containing an N-omega-methylarginine substitution. *Bioorg. Med. Chem. Lett.* 2012; **22**: 6328–6332.
- 21 Asami T, Nishizawa N, Ishibashi Y, Nishibori K, Nakayama M, Horikoshi Y, Matsumoto S, Yamaguchi M, Matsumoto H, Tarui N, Ohtaki T, Kitada C. Serum stability of selected decapeptide agonists of KISS1R using pseudopeptides. *Bioorg. Med. Chem. Lett.* 2012; **22**: 6391–6396.
- 22 Seebach D, Gardiner J. Beta-peptidic peptidomimetics. *Acc. Chem. Res.* 2008; **41**: 1366–1375.
- 23 Lukaszuk A, Demagdt H, Szemenyei E, Toth G, Tymecka D, Misicka A, Karoyan P, Vanderheyden P, Vauquelin G, Tourwe D. Beta-homo-amino acid scan of angiotensin IV. *J. Med. Chem.* 2008; **51**: 2291–2296.
- 24 Johnson LM, Barrick S, Hager MV, McFedries A, Homan EA, Rabaglia ME, Keller MP, Attie AD, Saghatelian A, Bisello A, Gellman SH. A potent alpha/beta-peptide analogue of GLP-1 with prolonged action *in vivo*. *J. Am. Chem. Soc.* 2014; **136**: 12848–12851.
- 25 Kaneda M, Misu R, Ohno H, Hirasawa A, Ieda N, Uenoyama Y, Tsukamura H, Maeda K, Oishi S, Fujii N. Design and synthesis of fluorescent probes for GPR54. *Bioorg. Med. Chem.* 2014; **22**: 3325–3330.
- 26 Nguyen T, Francis MB. Practical synthetic route to functionalized rhodamine dyes. *Org. Lett.* 2003; **5**: 3245–3248.
- 27 Northfield SE, Mountford SJ, Wielens J, Liu MJ, Zhang L, Herzog H, Holliday ND, Scanlon MJ, Parker MW, Chalmers DK, Thompson PE. Propargyloxypyrrolone regio- and stereoisomers for click-conjugation of peptides: synthesis and application in linear and cyclic peptides. *Aust J Chem.* 2015; **68**: 1365–1372.
- 28 Stathopoulos P, Papas S, Tsikaris V. C-terminal N-alkylated peptide amide resulting from the linker decomposition of the Rink amide resin. A new cleavage mixture prevents their formation. *J. Pept. Sci.* 2006; **12**: 227–232.
- 29 Motokura K. An acidic layered clay is combined with a basic layered clay for One-Pot sequential reactions. *J. Am. Chem. Soc.* 2005; **127**: 9674–9675.
- 30 Moussaoui Y. Catalyzed Knoevenagel reactions on inorganic solid supports: Application to the synthesis of coumarin compounds. *Comptes Rendus Chimie* 2007; **10**: 1162–1169.

- 31 Kaupp G. Solvent-free Knoevenagel condensations and Michael additions in the solid state and in the melt with quantitative yield. *Tetrahedron* 2003; **59**: 3753–3760.
- 32 Matsuoka M, Kitao T, Nakatsu K. Synthetic design of organic nonlinear optical materials: cyanovinylheteroaromatics and related compounds. *Springer Proc Phys.* 1989; **36**: 228–231.
- 33 McNab H, Tyas RG. A thermal cascade route to pyrroloisindolones and pyrroloimidazolones. *J. Org. Chem.* 2007; **72**: 8760–8769.
- 34 Blanco-Ania D, Valderas-Cortina C, Hermkens PHH, Slidregt LAJM, Scheeren HW, Rutjes FPJT. Synthesis of dihydrouracils spiro-fused to pyrrolidines: druglike molecules based on the 2-arylethyl amine scaffold. *Molecules* 2010; **15**: 2269–2301.
- 35 Peddie V, Pietsch M, Bromfield KM, Pike RN, Duggan PJ, Abell AD. Fluorinated beta 2- and beta 3-amino acids: synthesis and inhibition of alpha -chymotrypsin. *Synthesis* 2010; **11**: 1845–1859.
- 36 Chi Y, English EP, Pomerantz WC, Horne SW, Joyce LA, Alexander LR, Fleming WS, Hopkins EA, Gellman SH. Practical synthesis of enantiomerically pure b<sup>2</sup>-amino acids via proline-catalyzed diastereoselective aminomethylation of aldehydes. *J. Am. Chem. Soc.* 2007; **129**: 6050–6055.
- 37 Moumne R, Denise B, Guitot K, Rudler H, Lavielle S, Karoyan P. New scalable asymmetric aminomethylation reaction for the synthesis of β<sup>2</sup>-amino acids. *Eur. J. Org. Chem.* 2007; **12**: 1912–1920.
- 38 Tessier A, Lahmar N, Pytkowicz J, Brigaud T. Highly Diastereoselective Synthetic Route to Enantiopure β<sup>2</sup>-Amino Acids and γ-Amino Alcohols Using a Fluorinated Oxazolidine (Fox) as Chiral Auxiliary. *J. Org. Chem.* 2008; **73**: 3970–3973.
- 39 Wozniak D, Szymanska A, Oldziej S, Lankiewicz L, Grzonka Z. Application of Oppolzer's sultam in the synthesis of cyclic α-amino acids and β-amino acids. *Polish J. Chem.* 2006; **80**: 265–277.
- 40 Moumne R, Larregola M, Boutadla Y, Lavielle S, Karoyan P. Aminomethylation of chiral silyl enol ethers: access to beta(2)-homotryptophane and beta(2)-homolysine derivatives. *Tetrahedron Lett.* 2008; **49**: 4704–4707.
- 41 Caddick S, Judd DB, Lewis AKD, Reich MT, Williams MRV. A generic approach for the catalytic reduction of nitriles. *Tetrahedron* 2003; **59**: 5417–5423.
- 42 Pataj Z, Ilisz I, Berkecz R, Forro E, Fulop F, Peter A. Comparison of Separation Performances of Amylose- and Cellulose-Based Stationary Phases in the High-Performance liquid Chromatographic Enantioseparation of Stereoisomers of beta-lactams. *Chirality* 2010; **22**: 120–128.
- 43 Tomita K, Oishi S, Cluzeau J, Ohno H, Navenot JM, Wang ZX, Peiper SC, Akamatsu M, Fujii N. SAR and QSAR studies on the n-terminally acylated pentapeptide agonists for GPR54. *J. Med. Chem.* 2007; **50**: 3222–3228.

## Synthetic routes to the Neuropeptide Y Y<sub>1</sub> receptor antagonist 1229U91 and related analogues for SAR studies and cell-based imaging†

Cite this: *Org. Biomol. Chem.*, 2014, **12**, 3271

Simon J. Mountford,<sup>a</sup> Mengjie Liu,<sup>a</sup> Lei Zhang,<sup>b</sup> Marleen Groenen,<sup>c</sup> Herbert Herzog,<sup>b</sup> Nicholas D. Holliday<sup>c</sup> and Philip E. Thompson<sup>\*a</sup>

Received 23rd January 2014,  
Accepted 2nd April 2014

DOI: 10.1039/c4ob00176a

www.rsc.org/obc

The potent Y<sub>1</sub> receptor antagonist, 1229U91 has an unusual cyclic dimer structure that makes syntheses of analogue series quite challenging. We have examined three new routes to the synthesis of such peptides that has given access to novel structural variants including heterodimeric compounds, ring size variants and labelled conjugates. These compounds, including a fluorescently labelled analogue **VIII** show potent antagonism that can be utilised in studying Y<sub>1</sub> receptor pharmacology.

### Introduction

Neuropeptide Y (NPY) is a 36-amino acid C-terminal amidated polypeptide first isolated from porcine brain in 1982.<sup>1</sup> NPY shares a high degree of homology in amino acid sequence with pancreatic polypeptide (PP) and peptide YY (PYY). It is a peptide neurotransmitter implicated in various physiological processes at the central nervous system<sup>2</sup> (e.g. stimulation of feeding behaviour and inhibition of anxiety) and the peripheral nervous system<sup>3</sup> (e.g. vasoconstriction, insulin release, renal secretion, gastrointestinal secretion). These effects, together with those of the gastrointestinal hormones PYY and PP, are mediated in man by G-protein coupled receptor subtypes, Y<sub>1</sub>, Y<sub>2</sub>, Y<sub>4</sub> and Y<sub>5</sub>.<sup>4,5</sup>

The important roles of NPY in both human physiology and pathophysiology have led to considerable efforts to develop subtype specific NPY receptor agonists and antagonists, which may be prospective clinical candidates for various indications such as cancer,<sup>6</sup> obesity<sup>7</sup> and epilepsy.<sup>8</sup> The utility of labelled ligands in imaging applications has also been recognized.<sup>9,10</sup>

Both small-molecule and peptide-based antagonists have been described for the Y<sub>1</sub> receptor however they are associated with a number of shortcomings. For example, the small-molecule ligand BIBP3226 possesses high selectivity and moderate Y<sub>1</sub> affinity but also has CNS toxicity.<sup>11,12</sup> It has been

utilised as a pharmacological tool in over 100 studies.<sup>13</sup> Optimisation of BIBP3226 into the more active BIBO3304 gave a 10-fold increase in affinity towards Y<sub>1</sub>-receptors however it is still burdened with cross-reactivity towards Neuropeptide FF receptors.<sup>14,15</sup>

Truncated NPY analogues have received increasing attention since 1995, when Leban *et al.* described the C-terminal decapeptide, Tyr-Ile-Asn-Leu-Ile-Tyr-Arg-Leu-Arg-Tyr-NH<sub>2</sub>.<sup>16</sup> Based on this sequence the subsequent peptide (Ile-Asn-Pro-Ile-Tyr-Arg-Leu-Arg-Tyr-NH<sub>2</sub>, known as BW1911U90 or BVD15), had a 10-fold increase in Y<sub>1</sub> activity and a 4-fold decrease in Y<sub>2</sub> affinity.<sup>16</sup> It also had agonist activity at Y<sub>4</sub> receptors with similar affinity to Y<sub>1</sub>.<sup>17,18</sup> Other peptides similar to BW1911U90 have also been described recently such as the Y<sub>1</sub>-selective agonist [Pro,<sup>30</sup>Nle,<sup>31</sup>Bpa,<sup>32</sup>Leu<sup>34</sup>]NPY(28–36),<sup>19</sup> the Y<sub>1</sub> selective [Lys(DOTA)<sup>4</sup>]BVD15<sup>20</sup> and analogous NOTA derivative<sup>21</sup> and the click chemistry radiolabelled analogue <sup>18</sup>F-ALK-BVD15.<sup>22</sup>

Another potent Y<sub>1</sub> receptor antagonist known as 1229U91 (or GR231118) was described by Daniels in 1995.<sup>23</sup> It is a homodimer based on BW1911U90 whereby Glu<sup>2</sup> and Dap<sup>4</sup> have been included in order to form a lactam bridge between two sequences (Fig. 1). It has been demonstrated that 1229U91 exhibits a higher affinity and more potent competitive antagonism at Y<sub>1</sub> receptors than BW1911U90. It also showed extended activity *in vivo* attributed to the stability of the cyclic peptide.<sup>18,24</sup> It was subsequently found to be an agonist at Y<sub>4</sub> receptors while showing a much weaker affinity towards Y<sub>2</sub> receptors.<sup>18,25–27</sup> Only a limited number of other dimer variants have previously been described.<sup>17,23,28–30</sup> They include modifications to the C-terminus residues and the use of disulfide bridges, diaminopimelic acid or other lactam bridge conformations to interconnect the monomer sequences.

<sup>a</sup>Medicinal Chemistry, Monash Institute of Pharmaceutical Sciences, 381 Royal Parade, Parkville, VIC 3052, Australia. E-mail: philip.thompson@monash.edu; Fax: +61 3 9903 9582; Tel: +61 3 9903 9672

<sup>b</sup>Neuroscience Research Program, Garvan Institute of Medical Research, St. Vincent's Hospital, Darlinghurst, NSW 2010, Australia

<sup>c</sup>Cell Signalling Research Group, School of Life Sciences, University of Nottingham, Queen's Medical Centre, Nottingham NG7 2UH, UK

†Electronic supplementary information (ESI) available. See DOI: 10.1039/c4ob00176a

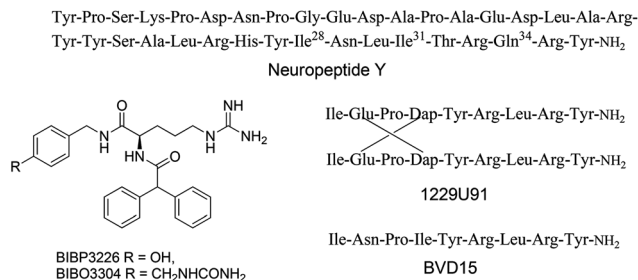


Fig. 1 Y1 receptor ligands.

The challenges associated with unambiguous synthesis of 1229U91 analogues are not trivial. The discovery of 1229U91 looks somewhat serendipitous as the product would normally be associated with a side-reaction in intramolecular cyclisation.<sup>28,31</sup> The original method to prepare 1229U91 was described by Daniels using Boc-based chemistry. The use of base sensitive side chain protecting groups 9-Fc and Fmoc on the Glu and Dap residues respectively allowed for selective deprotection and then on-resin cyclisation using BOP reagent.<sup>28</sup> Lew *et al.* described a solution phase cyclodimerisation of an *N*-Fmoc-protected (but side-chain deprotected) linear precursor yielding a 75:25 ratio of dimer to monomer.<sup>31</sup> The ability to achieve efficient and clean cyclisation in the absence of protecting groups for Tyr and Arg residues was a somewhat surprising but attractive element to this synthesis although Balasubramaniam reported that in their hands they found that this method was inferior to the original on-resin BOC method.<sup>17</sup> Note that both these approaches would best suit symmetrical cyclic dimers.

We identified a need for more versatile synthetic routes to 1229U91 analogues to explore structure activity relationships and/or incorporate labelling agents. Herein we report the development of such routes in preparing 1229U91 and a series of novel analogues. The methods have extended the existing solution phase and solid phase cyclodimerisation routes to allow for preparation of homo- and/or heterodimers in useful yields, but also an unambiguous synthesis of cyclic dimers that avoids concomitant competing intramolecular cyclisation.

These products have been tested in competition binding assays and functional studies, to yield high affinity functional antagonists of the Y<sub>1</sub> receptor, one of which incorporates a fluorescent rhodamine substitution that can be used in cell imaging studies.

## Results and discussion

### Chemistry

**First Fmoc-based solid phase synthesis of 1229U91 and analogues.** We first adapted the reported on-resin cyclisation method to Fmoc SPPS for the preparation of homodimers (Scheme S1†). An orthogonal protecting group strategy included Dap(Aloc) and Glu(OAll) residues while standard

side chain protecting groups on Tyr and Arg residues were left intact. The N-terminal Ile was Boc-protected. The OAll and Aloc were selectively removed by Pd(PPh<sub>3</sub>)<sub>4</sub> catalysed allyl transfer in CHCl<sub>3</sub>-AcOH-NMM under N<sub>2</sub> for 2 h.<sup>32</sup> The cyclisation was then performed by treating the partially deprotected resin with PyClock/DIPEA in DMF for 6 h. Cleavage from the resin with TFA yielded the crude peptide. Under these conditions, the isolated yield was 5% and the cyclic dimer was almost exclusively favoured over the cyclic monomer. We also prepared the N-terminal truncated sequence **I** in this way obtaining a 5% overall yield.

While the solid phase route above is an efficient method for the synthesis of homodimeric cyclic peptides, it appeared limited from the perspective of generating heterodimers with mixed monomer sequences. To include those as possible products we turned to the solution phase route, to see if we could extend the utility of that pathway.

**Solution phase synthesis of dimeric peptides.** The first element of the syntheses that follow was the preparation of a series of partially protected monomeric, linear peptides that would become the substrates for solution phase cyclisation reactions. Some of these contain either modified amino acids or allow for later incorporation of the conjugates shown in Fig. 2. These syntheses were performed by conventional solid phase peptide synthesis on Rink Amide resin. The syntheses in general gave rise to the desired products with no identifiable deletion or side products. The isolated peptides are summarized in Table 1 (see also Fig. S4†).

We first utilised peptide **1** as monomer to examine the solution phase conditions described by Lew *et al.* We found that using PyBOP as cyclisation reagent and DIPEA as base we achieved the same ratio of cyclic dimer/monomer (80:20) as reported (Fig. 3a). The recoveries after cyclisation and then Fmoc-deprotection were quite poor, leading to overall a very low yield of 1229U91 (<1%). The yield was improved substantially by not isolating the Fmoc-protected cyclisation product, but treating reaction mixture directly with piperidine and then retrieving the final product directly by semi-preparative RP-HPLC. In this way yields of 4% (based on 0.1 mmol resin loading) could be obtained.

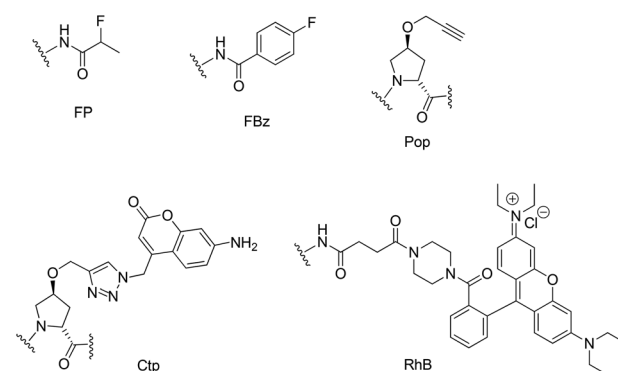


Fig. 2 Structures of conjugate groups.



Table 1 Protected linear monomer precursors

#	Sequence	(M + 2H) <sup>2+</sup>
1	Fmoc-Ile-Glu-Pro-Dap-Tyr-Arg-Leu-Arg-Tyr-CONH <sub>2</sub>	709.4
2	Fmoc-Ile-Glu-Pop-Dap-Tyr-Arg-Leu-Arg-Tyr-CONH <sub>2</sub>	736.5
3	Fmoc-Ile-Glu-Pro-Lys-Tyr-Arg-Leu-Arg-Tyr-CONH <sub>2</sub>	730.5
4	FBz-Ile-Glu-Pro-Dap-Tyr-Arg-Leu-Arg-Tyr-CONH <sub>2</sub>	659.3
5	Fmoc-Ile-Glu(O-AlI)-Pro-Dap-Tyr-Arg-Leu-Arg-Tyr-CONH <sub>2</sub>	729.4
6	Fmoc-Ile-Glu-Pro-Dap(Alloc)-Tyr-Arg-Leu-Arg-Tyr-CONH <sub>2</sub>	751.5
7	Fp-Ile-Glu(O-AlI)-Pro-Dap-Tyr-Arg-Leu-Arg-Tyr-CONH <sub>2</sub>	655.4
8	Fmoc-Ile-Glu-Pro-Lys(Alloc)-Tyr-Arg-Leu-Arg-Tyr-CONH <sub>2</sub>	772.5
9	Fmoc-Ile-Glu(O-AlI)-Pro-Lys-Tyr-Arg-Leu-Arg-Tyr-CONH <sub>2</sub>	750.2

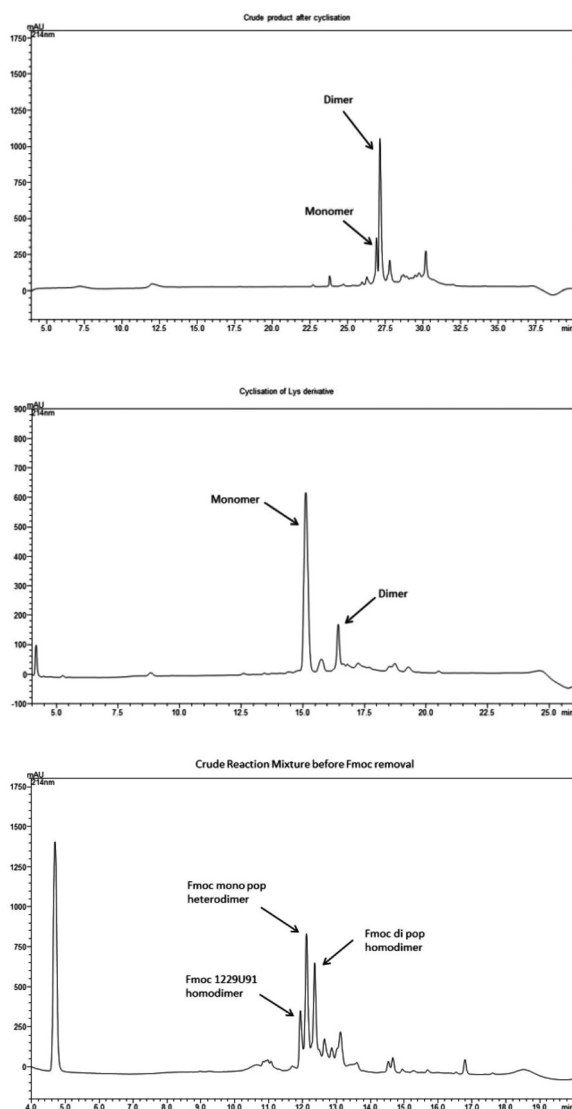


Fig. 3 HPLC traces of crude products from cyclisation reactions with PyBOP of (a) protected peptide 1, (b) protected peptide 3 and (c) mixture of protected peptides 1 and 2.

We examined other parameters to see if the ratio of dimer to monomer could be increased. Intramolecular and intermolecular amide bond formation will be competing events

and should be influenced by changes to the coupling agent or base. No enhancement of the proportion of dimer was seen by changing the base from DIPEA to TMP (Fig. S2a†) (although the reaction mixture had fewer other impurities) or by replacing PyBOP with the slightly more reactive coupling reagent PyClock.

When the same reaction was attempted with peptide 2 where the proline residues had been replaced with an alkyne derivatised proline (Pop), the dialkynyl dimer **II** was obtained, with the 80 : 20 dimer/monomer ratio maintained. In contrast, using linear peptide 3 where the Dap residue was replaced with Lys, the proportion of the desired dimer **III** to the corresponding cyclic monomer **IIIa** was reversed (15 : 85) (Fig. 3b). This example showed the sequence dependence that can dictate the outcome of these competing reactions.

**Synthesis of Heterodimers (non-orthogonal).** This solution phase protocol was also used to prepare heterodimeric analogues of 1229U91. It was envisaged that a mixture of two analogous but independent sequences could be reacted under similar conditions to give a mixture of the heterodimer and the two possible homodimeric products. These could potentially be separated by HPLC.

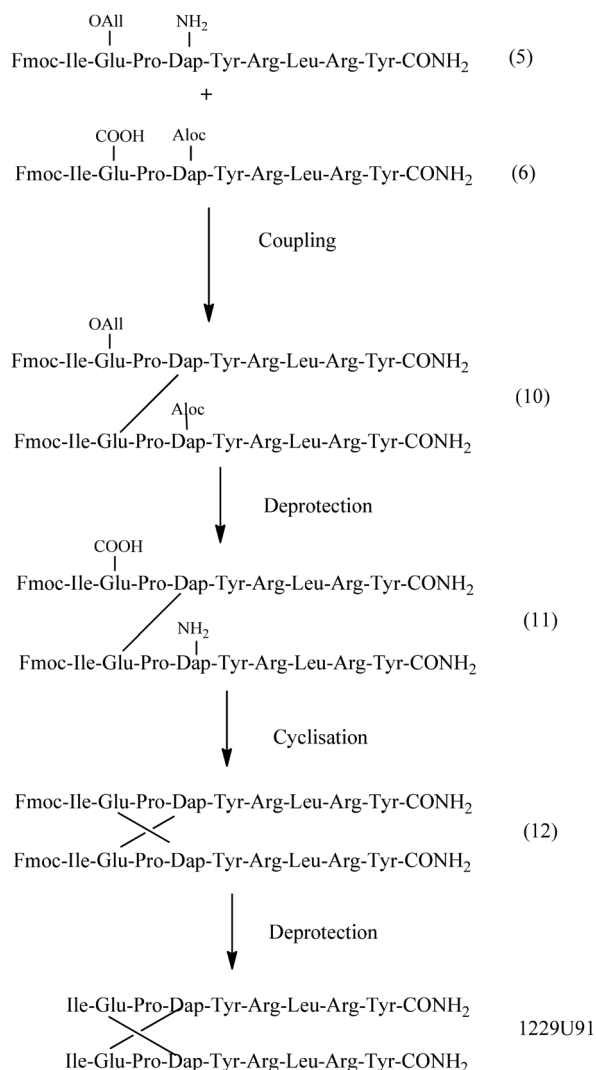
First, a mono-Pop containing analogue **IV** was prepared. A 1 : 1 mixture of the purified linear peptides 1 and 2 was treated with PyBOP and DIPEA yielding the expected mix of products (Fig. 3c). Deprotection of the Fmoc groups with piperidine and purification of the complex mixture allowed for isolation of the mono Pop heterodimer **IV** as well as the homodimer **II** by HPLC. Compound **IV** was then utilised as an intermediate in the synthesis of the fluorescently labelled product **IX** described later.

A second heterodimeric peptide was prepared by inclusion of an amino terminal fluorobenzoyl group in one of the monomers 4. When monomer 4 and monomer 1 were coupled (Fig. S2b†) followed by deprotection, the mono- and di-labelled FBz derivatives **V** and **VI** were retrieved by HPLC.

In summary, the use of Fmoc-based solid phase synthesis with solution cyclisation can be used to retrieve useful amounts of both homo- and hetero-dimeric peptides.

**Solution phase formation of cyclic dimers via orthogonal protection.** Despite the improvements instituted in the syntheses above, these studies also identified a need for more chemoselective, sequence-independent methods if we were to expand our studies to include a variety of modified sequences, heterodimers or conjugates. The competition between cyclic dimer and monomer formation results from competition between an intermolecular coupling (followed by cyclic lactam formation) in the dimer case and intramolecular cyclisation for the cyclic monomer. In addition, with heterodimer formation we had competition between self- and hetero-coupling which may also be sequence dependent. We decided to examine orthogonal protection strategies to prevent these competing events.

Starting with the synthesis of 1229U91 itself (Scheme 1), two different protected peptides were prepared. In one the Glu side chain was protected with *O*-allyl ester (OAlI) 5 and in the



**Scheme 1** Strategy for orthogonal stepwise synthesis of 1229U91.

other the Dap was protected as the allyl carbamate (Alloc) **6**. The two sequences were then coupled by forming an amide bridge between the unprotected Dap and Glu side chains to give the branched intermediate **10**. This was in turn deprotected *via* Pd(0) catalysed allyl transfer, cyclised and Fmoc deprotected to give 1229U91.

Note that the coupling of the two fragments was successful, but only after a key modification to the standard methods was made. It was necessary to use TMP as the base as it allowed for the acid fragment to be pre-activated without substrate degradation, as was observed in the case of DIPEA. The optimal conditions were that the acidic fragment peptide and PyClock (4 eq.) were dissolved in DMF. TMP (22 eq.) was added followed by the addition of the amino fragment (Final concentration 0.1 M in DMF). After 30 min, analysis by LCMS showed conversion to the desired side chain linked product (Fig. S2a†).

Where DIPEA was used only small amount of the desired bridged sequence was observed (Fig. S2b†). It was observed

that **6** degraded under the reaction conditions. The same proved true for a protected test peptide Fmoc-Ile-Glu-Pro-Dap-(Boc)-CONH<sub>2</sub>. Switching the base to TMP minimized this degradation.

To complete the synthesis, selective deprotection of both the Alloc and OAll groups was achieved using Pd(0) catalysed allyl transfer. The catalyst, Pd(PPh<sub>3</sub>)<sub>4</sub>, dissolved in CHCl<sub>3</sub>-AcOH-NMM was added under a N<sub>2</sub> atm to the peptide and mixed for 2 h. A small amount of product contained incomplete removal of the OAll group. Cyclisation of the purified peptide was achieved using PyClock (3 eq.) and TMP (24 eq.) in DMF (1 mg mL<sup>-1</sup>) followed by Fmoc deprotection to give the target peptide 1229U91.

The method above was then used to prepare two analogues of 1229U91. The first was a N-2-fluoropropyl substituted analogue **VII**. The Glu(OAll) protected peptide **7** was coupled to the Dap-protected fragment **6** (1 eq.) to give the branched product **13**. The allyl deprotection step was achieved again with Pd(PPh<sub>3</sub>)<sub>4</sub> in CHCl<sub>3</sub>-AcOH-NMM under N<sub>2</sub> atm for 2 h. Cyclisation of the purified peptide in DMF (1 mg mL<sup>-1</sup>) using PyClock (3 eq.) and TMP (24 eq.) followed by Fmoc deprotection gave a 7% overall yield of **VII** after purification.

This method was also used to prepare the dimeric Lys-containing analogue **III** which was difficult to achieve by the conventional methods described above, due to preferential monomeric cyclisation. The linear peptide **8** (1 eq.) was activated with PyClock (3 eq.) in a solution of DMF and TMP (24 eq.) followed by the addition of the amino fragment **9** (1 eq.) (final peptide conc. in DMF, 66.5 mM) to give the coupled product **16** (Fig. S3a†). In this case, complete Pd catalysed removal of the protecting groups was best achieved using the conditions of Thiuret with phenyl silane (Fig. S3c†) as compared to Pd(PPh<sub>3</sub>)<sub>4</sub> in CHCl<sub>3</sub>-AcOH-NMM (Fig. S3b†). Cyclisation of the crude material was achieved using PyClock (3 eq.) and TMP in DMF. The solution phase Fmoc deprotection was performed using 10% piperidine in DMF, followed by preparative HPLC to give the desired product **III**. The 12% isolated yield was a improvement over the minority product (<2%) obtained *via* direct cyclisation above.

**Post-synthesis modification.** With the development of reliable methods for the synthesis of 1229U91 (and other derivatives) at reasonable scales labeling of these peptides has also been achieved as a “post-synthesis” step.

For example, the fluorescently labeled rhodamine derivative **VIII** was prepared by reacting purified 1229U91 with a limiting amount (*e.g.* 0.7 eq.) of an NHS-activated Rhodamine B derivative,<sup>33</sup> in a solution of DMF and DIPEA. The reaction was monitored by LCMS and the resultant mixture of the desired mono-labeled product, di-labeled product and unreacted 1229U91 was then purified by HPLC allowing for isolation of the mono-labeled derivative **VIII** in 26% yield.

Secondly, we were successful in introducing a triazolocoumarin to the peptide using click chemistry upon the propargyloxy derivative of 1229U91 **IV** to prepare **IX**. The reaction between the purified peptide and 7-amino-4-(azidomethyl)-2H-chromen-2-one<sup>34</sup> in a solution of DMF and H<sub>2</sub>O was initiated

Table 2 1229U91 and analogues

Cmd #	Dimer sequence	ESI-MS <sup>a</sup>	IC <sub>50</sub> /nM Y <sub>2</sub> Y <sub>4</sub> KO <sup>c</sup>	95% Confidence limits
1229U91	Ile-Glu-Pro-Dap-Tyr-Arg-Leu-Arg-Tyr	823.5	0.10	0.49–0.021
I	Ile-Glu-Pro-Dap-Tyr-Arg-Leu-Arg-Tyr Glu-Pro-Dap-Tyr-Arg-Leu-Arg-Tyr	748.1	7.32	2.9–16
II	Ile-Glu-Pop-Dap-Tyr-Arg-Leu-Arg-Tyr Ile-Glu-Pop-Dap-Tyr-Arg-Leu-Arg-Tyr	859.4	0.11	0.057–0.22
III	Ile-Glu-Pro-Lys-Tyr-Arg-Leu-Arg-Tyr Ile-Glu-Pro-Lys-Tyr-Arg-Leu-Arg-Tyr	851.6	0.12	0.049–0.30
IV	Ile-Glu-Pop-Dap-Tyr-Arg-Leu-Arg-Tyr Ile-Glu-Pro-Dap-Tyr-Arg-Leu-Arg-Tyr	841.4	n.d.	
V	FBz-Ile-Glu-Pro-Dap-Tyr-Arg-Leu-Arg-Tyr Ile-Glu-Pro-Dap-Tyr-Arg-Leu-Arg-Tyr	864.1	0.13	0.039–0.44
VI	FBz-Ile-Glu-Pro-Dap-Tyr-Arg-Leu-Arg-Tyr FBz-Ile-Glu-Pro-Dap-Tyr-Arg-Leu-Arg-Tyr	904.8	4.12	0.82–21
VII	FP-Ile-Glu-Pro-Dap-Tyr-Arg-Leu-Arg-Tyr Ile-Glu-Pro-Dap-Tyr-Arg-Leu-Arg-Tyr	848.1	0.53	0.094–3.0
VIII	RhB-Ile-Glu-Pro-Dap-Tyr-Arg-Leu-Arg-Tyr Ile-Glu-Pro-Dap-Tyr-Arg-Leu-Arg-Tyr	766.2 <sup>b</sup>	0.08	0.016–0.43
IX	Ile-Glu-Ctp-Dap-Tyr-Arg-Leu-Arg-Tyr Ile-Glu-Pro-Dap-Tyr-Arg-Leu-Arg-Tyr	913.4	19.2	8.3–44

<sup>a</sup> ESI-MS base peak corresponds to  $[M + TFA + 3H]^{3+}$ . Note  $[M + 3H]^{3+}$  peaks were observed at lower intensity. See Fig. S5. <sup>b</sup> ESI-MS ion base peak corresponds to  $[M + TFA + 4H]^{4+}$ . <sup>c</sup> Inhibition of  $^{125}I$ -NPY (25 pM) binding to brain membrane homogenates.

by standard CuAAC conditions. The reaction was complete in 3 h when 10 eq. of copper sulfate, sodium ascorbate and TBTA were used.

In summary, the work described above has provided us with methods that can serve for the synthesis of a wide variety of 1229U91 analogues shown in Table 2 (see also Fig. S5†). Collectively we now have the means to prepare compounds bearing multiple modifications with variation in ring size and unambiguous synthesis of heterodimers provided by the orthogonal protection of monomeric precursors.

### Pharmacology

With the compounds described above in hand we were able to assess the influence of the various structural changes on Y<sub>1</sub> receptor affinity. To do this competition assays against [ $^{125}I$ ]-PYY binding to brain homogenates from Y<sub>2</sub>Y<sub>4</sub>-receptor knock-out mice were utilised. Such homogenates are a native tissue source of Y<sub>1</sub> receptors free from significant Y-receptor cross-reactivity.<sup>35</sup> The results are shown in Table 2.

The compounds assayed all showed high affinity for Y<sub>1</sub> receptors with IC<sub>50</sub> values in the low nanomolar range or better. Notably, compounds **II**, **III**, **V** and **VIII** all show comparable affinity to 1229U91 itself. Some key results stood out for us from this work. Firstly, the equivalent affinities of **III** and 1229U91 is of interest as **III** is anticipated to adopt a markedly different ring structure, with 6 extra methylene units in the cyclic portion of the molecule. It was also of interest that the bis-Pop ligand **II** retained high affinity, suggesting that the ring structure could tolerate a range of changes.

Second, the tolerance for a range of prosthetic labeling groups was demonstrated, for example by inclusion of fluoro-benzoyl (**V**) and 2-fluoropropyl (**VII**) as potential labeling

conjugates for  $^{18}F$ -radioimaging. The difference between **V** and **VI**, where a second label is detrimental to affinity suggests that care would need to be taken in generating such compounds as a final step in synthesis.

In the murine binding assay, in which low levels of native Y<sub>1</sub> receptor expression are limiting, we observed strong but inconsistent competition data with the rhodamine conjugate (**VIII**). However this compound was investigated successfully in transfected cell membranes and functional assays (see below). Disappointingly given the apparent tolerance for substitution by the propargyloxy groups in **II**, the “click” product **IX** had 100 fold reduced affinity compared to 1229U91.

Compounds **III** and **VIII** stood out as warranting further investigation; compound **VIII** because of the utility that a fluorescent ligand would have in studies of Y<sub>1</sub> pharmacology, and **III** because of potential to understand more of the SAR governing Y<sub>1</sub> binding and in particular selectivity with respect to Y<sub>4</sub> receptors given the reported agonism at Y<sub>4</sub> shown by 1229U91.

These two compounds were thus studied in assays using rat Y<sub>1</sub>- and human Y<sub>4</sub>-transfected HEK293 cells. In [ $^{125}I$ ]PYY competition binding studies using rat Y<sub>1</sub>-GFP transfected cell membranes (as described in Kilpatrick *et al.*,<sup>36</sup> compound **III** was confirmed as a high affinity ligand with a K<sub>i</sub> similar to 1229U91 itself (Table 2). Furthermore compound **VIII** also showed a clear concentration-dependent competition for specific [ $^{125}I$ ]PYY binding, with a K<sub>i</sub> in the low nM range, 24 fold lower affinity than 1229U91 (Table 2, ESI Fig. S7†). Nevertheless, compound **VIII** represents a novel template for Y<sub>1</sub> receptor fluorescent ligands, with equivalent affinity to previously reported NPY or argininamide (BIBP3226) analogues.<sup>37–39</sup>

**Table 3** Studies of 1229U91, III and VIII in rat Y<sub>1</sub>-transfected HEK293

	pK <sub>i</sub> <sup>a</sup>	pK <sub>b</sub>
1229U91	9.9 ± 0.06	9.5 ± 0.1
III	10.2 ± 0.12	8.4 ± 0.1
VIII	8.5 ± 0.02	8.6 ± 0.2

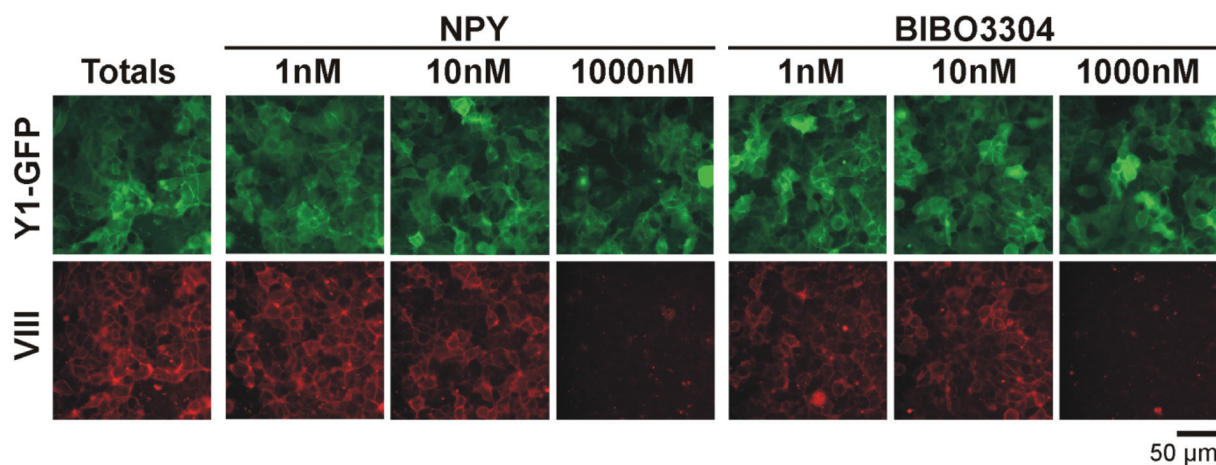
<sup>a</sup> Inhibition of [<sup>125</sup>I]PYY (25 pM) binding to recombinant 293TR Y1 receptor-sfGFP cell line.

We used an assay of NPY-stimulated Y receptor association with β-arrestin2 to examine the functional effects of III and VIII, as we have previously reported for 1229U91.<sup>40</sup> Both III and VIII were Y<sub>1</sub> receptor antagonists in this assay (Table 3, ESI Fig. S7†), with estimated affinities in the nM range (pK<sub>b</sub> 8.4–8.6; Table 3).

The fluorescently labelled compound VIII was also examined as a tracer for competition binding studies using live cell imaging with fluorescent platereaders.<sup>41</sup> VIII labelled Y<sub>1</sub>-GFP transfected HEK293 cells using concentrations as low as 1 nM, with the ligand colocalised with plasma membrane Y<sub>1</sub>-GFP fluorescence (Fig. 4). There was no evidence of significant ligand or receptor internalisation under the experimental conditions used. Specific binding of VIII to the Y<sub>1</sub> receptor was clearly demonstrated by its concentration dependent displacement using either an unlabelled agonist (NPY) or non-peptide antagonist (BIBO3304). NPY and BIBO3304 IC<sub>50</sub> values were 27 and 14 nM respectively, consistent with expectations for a whole cell binding assay. In contrast, little fluorescent binding of compound VIII (100 nM) to Y<sub>4</sub>-GFP cells was observed, demonstrating its relative selectivity for the Y<sub>1</sub> receptor.

When studied in the equivalent Y<sub>4</sub> receptor arrestin recruitment assay, no antagonism of PP activity was observed by

### A: Y1-GFP 1 nM VIII



### B: Y1-GFP displacements 1 nM VIII

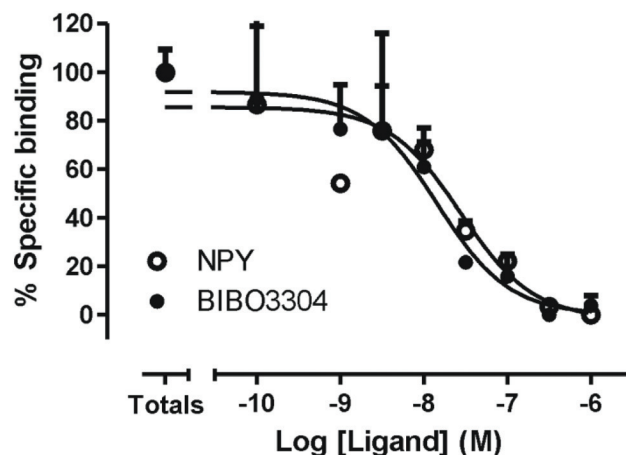


**Fig. 4** Use of compound VIII as fluorescent ligand to label Y<sub>1</sub> receptors. Living 293TR cells expressing the Y<sub>1</sub>-GFP receptor were incubated with 1 nM compound VIII in the absence (totals) or presence of increasing concentrations of NPY or BIBO3304, for 30 min at 37 °C. (A) illustrates representative images acquired on a Molecular Devices IX Micro platereader, monitoring localisation of the Y<sub>1</sub>-GFP receptor (FITC channel) and bound compound VIII (TRITC channel). (B) represents a single representative experiment performed in triplicate, in which compound VIII binding and its displacement by NPY or BIBO3304 was quantified from the images using a granularity algorithm.



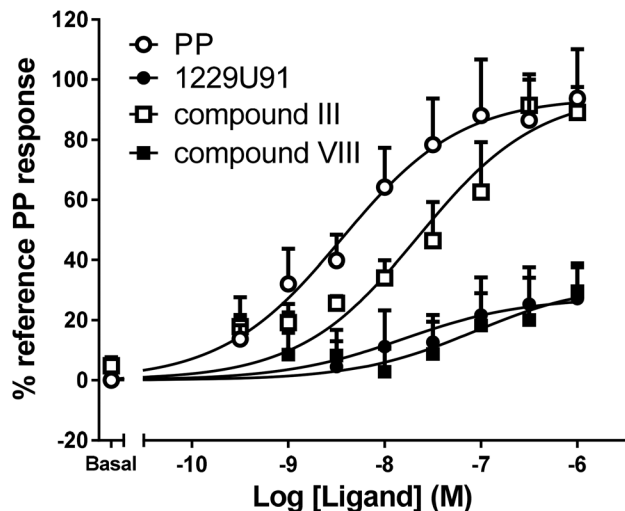


Fig. 5 Concentration response curve for  $Y_4$  receptor agonist activity, measured in the  $\beta$ -arrestin2 recruitment assay. Pooled data are combined from 4 experiments.

these ligands, but rather agonist responses (Fig. 5). 1229U91 and fluorescent compound **VIII** were relatively low efficacy partial agonists, compared to human PP. The difference from previous reports of full 1229U91 agonism can be attributed to the absence of receptor reserve and lack of signal amplification when measuring receptor–arrestin interaction directly here, in contrast to downstream second messenger pathways (16, 17). However compound **III** was a full  $Y_4$  agonist with an  $EC_{50}$  of 22 nM in this assay, just an order of magnitude less potent than PP itself ( $EC_{50}$  3.6 nM). Thus in contrast to interactions with the  $Y_1$  binding site, the markedly different ring structure adopted by **III** compared with 1229U91 appears to significantly enhance its ability to stabilise an active  $Y_4$  receptor conformation.

## Conclusions

By expanding the available synthetic approaches for the synthesis of side-chain bridged dimers related to 1229U91, we are in a position to fully interrogate the quite remarkable pharmacology of this ligand. As well as the apparent  $Y_1$  potency and selectivity that has been identified over many years of study, the stability *in vivo* first identified by Hegde and co-workers places 1229U91 in a special category of pharmacologically-active peptides. In this work we have been able to develop syntheses that can accommodate the preparation of modified heterodimers, cyclic homodimers with altered ring size and/or conjugated derivatives. In doing so we have developed **VIII**, a rhodamine conjugated analogue of 1229U91 that shows very comparable  $Y_1$  antagonist properties, and which can be used in  $Y_1$  receptor imaging studies; and **III**, a  $Y_1$  antagonist which also displayed enhanced  $Y_4$  agonism. These compounds and their analogues could find application in future studies of  $Y$  receptor pharmacology.

## Experimental section

$N^{\alpha}$ -Fmoc-protected amino acids were purchased from Auspep and ChemImpex. Rink amide resin and HCTU were purchased from ChemImpex. Piperidine, TFA and PyBOP were purchased from Auspep. DIPEA, phenylsilane, 4-methylmorpholine and tetrakis(triphenylphosphine)palladium were obtained from Sigma-Aldrich. DMF, DCM, chloroform, acetic acid, and PyClock were purchased from Merck. Fluorobenzoic acid was purchased from Alfa Aesar. Collidine was obtained from Ajax Chemicals. 4-Nitrophenyl-2-fluoropropionate was a gift from Peter McCallum Cancer Research Centre and 7-amino-4-(azido-methyl)-2H-chromen-2-one<sup>34</sup> was a gift from Dr Bim Graham (Monash Institute of Pharmaceutical Sciences). Fmoc-L-*trans*-4-propargyloxypyrrolidine (Pop) and the Rhodamine B derivative<sup>33</sup> were prepared in-house. All chemicals were used without further purification.

RP-HPLC was performed on a Phenomenex Luna C-8 column (100 Å, 10  $\mu$ m, 250  $\times$  50.0 mm) utilising a Waters 600 semi-preparative HPLC incorporating a Waters 486 UV detector. Eluting profile was a linear gradient of 0–80% acetonitrile in water over 60 min at a flow rate of 20 ml min<sup>-1</sup>. Peptide identity and purity was confirmed by ESI-MS, using a Shimadzu LCMS2020 instrument, incorporating a Phenomenex Luna C-8 column (100 Å, 3  $\mu$ m, 100  $\times$  2.00 mm). Eluting profile was a linear gradient of 100% water for 4 min, followed by 0–64% acetonitrile in water over 10 min and isocratic 64% acetonitrile for 1 min, at a flow rate of 0.2 ml min<sup>-1</sup>. All peptides assayed were of >95% purity.

### Solid phase synthesis

Peptide syntheses were performed on a Protein Technologies PS3 synthesiser following the conventional Fmoc-based solid phase peptide synthesis strategy using Rink amide resin (*ca.* 0.7 meq g<sup>-1</sup>, 100–200 mesh, 0.1 mmol scale). Fmoc-protected amino acids in 3-fold molar excess were coupled using DMF as solvent, 70 ml L<sup>-1</sup> DIPEA in DMF with 3-fold molar excess of HCTU as the activating agent for 50 minutes. Fmoc deprotection was carried out by treatment with 20% piperidine in DMF for 10 minutes. Occasionally amino acids were incorporated into the sequence by a manual procedure. The amino acid (1.5 eq.) was dissolved in DMF and added to a suspension of HOBt (1.5 eq.) in DCM. After stirring for 2 min DIC (1.5 eq.) was added and the mixture stirred for further 10 min before adding to the vessel containing pre-swollen resin (1 eq.) and agitated for 2 h.

Peptide cleavage from resin was performed using a cocktail containing TFA–TIPS–DMB (92.5% : 2.5% : 5%) for 3 hours.<sup>42</sup> The cleavage mixture was filtered, concentrated by a stream of nitrogen, precipitated by cold diethyl ether and centrifuged. The resulting crude product was dissolved in water–acetonitrile (1 : 1) and lyophilised overnight.

The on-resin linear sequence used in the preparation of peptides **5** and **6** were N-terminus labelled by dissolving fluorobenzoic acid (3 eq.) in DMF and adding to a suspension of HOBt (3 eq.) in DCM. After stirring for 2 min DIC (3 eq.) was

added and the mixture stirred for further 10 min before adding to the vessel containing pre-swollen resin (1 eq.) and agitating for 2 h.

The on-resin linear sequence used in the preparation of peptide 7 was N-terminus labelled by dissolving 4-nitrophenyl 2-fluoropropionate (1.5 eq.) in DIPEA (12 eq.) and DMF and adding to the vessel containing pre-swollen resin (1 eq.) and agitating for 2 h.

### Orthogonal deprotection methods

**Mtt and O-2-PhiPr removal.** Adapting the method originally described by Aletras,<sup>43</sup> the peptide-resin was allowed to swell in DMF, washed with DCM and then treated with 1% TFA and 5% TIPS in DCM for 10 × 2 min. The resin was then washed with DCM (×3), 10% DIPEA in DMF (×3) and DMF (×3).

#### Allyl and Aloc removal

**Solid phase.** Following the method described by Kates,<sup>44</sup> a solution of Pd(PPh<sub>3</sub>)<sub>4</sub> (3 eq.) dissolved in CHCl<sub>3</sub>-MeOH-NMM (37:2:1) under a nitrogen atmosphere was added to a flask containing the peptide-resin and shaken for 2 h. The resin was filtered, and washed with 0.5% DIPEA in DMF (×3) and sodium diethyldithiocarbamate (0.5% w/w) in DMF.

**Solution phase.** Pd(PPh<sub>3</sub>)<sub>4</sub> (3–6 eq.) was dissolved in a mixture of CHCl<sub>3</sub>-MeOH-NMM (37:2:1) under a nitrogen atmosphere and then added to a solution of the crude peptide in CHCl<sub>3</sub>-MeOH-NMM (37:2:1) and stirred for 2 h. The solvent was removed *in vacuo*, the residue acidified with a small amount of TFA and the peptide precipitated with cold ether and isolated.

**Solid phase.** Following the method described by Thieriet,<sup>32</sup> the peptidyl resin was allowed to swell in DMF and was then washed and suspended in DCM under a nitrogen atmosphere. PhSiH<sub>3</sub> (24 eq.) in DCM was added to the resin suspension. A solution of Pd(PPh<sub>3</sub>)<sub>4</sub> (0.25 eq.) dissolved in DCM under a nitrogen atmosphere was then added to the peptide solution and mixed for 30 min. The resin was washed with DCM (×3), DMF (×3) and DCM (×3). The resin was then suspended in DCM and the allyl deprotection step repeated.

**Solution phase.** The crude cleaved peptide was dissolved in MeOH, placed under a nitrogen atmosphere and PhSiH<sub>3</sub> (24 eq.) added. A solution of Pd(PPh<sub>3</sub>)<sub>4</sub> (1 eq.) dissolved in DCM under a nitrogen atmosphere was then added to the peptide solution and mixed for 2 h. The solvents were removed *in vacuo*, the residue acidified with a small amount of TFA and the peptide precipitated with cold ether and isolated.

**ivDde and ODmab removal.** According to the method outlined by Chan,<sup>45</sup> the peptide-resin was allowed to swell in DMF, filtered, and then treated with 2% hydrazine monohydrate in DMF (3 × 3 min) and then washed with DMF.

### Solid phase cyclisation methods

**Method for 1229U91 on-resin.** The linear protected peptide resin Boc-Ile-Glu(OAll)-Pro-Dap(Aloc)-Tyr(*t*Bu)-Arg(Pbf)-Leu-Arg-(Pbf)-Tyr(*t*Bu)-Rink resin was OAll/Aloc deprotected using the Thieriet method as described above. The resin was then allowed to swell in DMF before a solution of PyClock (3 eq.) in

DMF was added followed by DIPEA (10 eq.). The resin was agitated for 6 h and then washed with DMF (×3), MeOH (×3) and Et<sub>2</sub>O (×3). Peptide cleavage from resin was performed as described above and the crude peptide purified by RP-HPLC.

Peptide **I** was prepared in the same way, except using Boc-Glu(OAll)-Pro-Dap(Aloc)-Tyr(*t*Bu)-Arg(Pbf)-Leu-Arg(Pbf)-Tyr(*t*Bu)-Rink resin. After Fmoc-based SPPS, the N-terminus of the unprotected Glu residue was Boc-protected by adding Boc anhydride (3 eq.), dissolved in DIPEA (6 eq.) and DMF, to the pre-swelled resin (0.1 eq.) and mixed for 2 h.

### Solution phase cyclisation methods

1229U91 was prepared by treating linear peptide **1** (0.1 M) in DMF with PyBOP (2 eq.) and DIPEA (12 eq.) and the reaction mixture was stirred for 2 h. A solution of 20% piperidine in DMF was then added stirring continued for a further 30 min. The solvent was removed *in vacuo* and the residue triturated with cold ether after which the residue was purified by RP-HPLC or extracted with 1:1 ACN-H<sub>2</sub>O and the extract purified by RP-HPLC.

In the same way, peptide **2** was reacted to yield peptide **II**. When peptide **3** was treated in this way compound **III** was obtained as a minor component. The cyclic monomeric peptide, cyclo(Glu,Lys)-Ile-Glu-Pro-Lys-Tyr-Arg-Leu-Arg-Tyr (**IIIa**) was obtained as the major component.

In the same way, an equimolar mixture of **1** and **2** was treated to give a mixture of products **IV**, **II** and **1229U91** which were isolated by RP-HPLC.

An equimolar mixture of **1** and **4** was treated to give a mixture of products **V**, **VI** and **1229U91** which were isolated by RP-HPLC.

**Solution phase formation of cyclic dimers via orthogonal protection.** The partially protected peptide **6** (1 eq.) and PyClock (4 eq.) were dissolved in DMF (100 mg mL<sup>-1</sup>). TMP (24 eq.) was added followed by the partially protected peptide **5** (1 eq.). The reaction mixture was stirred at ambient temperature for 2 h. Volatile components were removed *in vacuo* and the resulting residue was treated with a small volume of TFA precipitated with cold Et<sub>2</sub>O to yield crude peptide **10**. Selective deprotection of the OAll/Aloc groups was performed by the method of Thieriet as described above to give peptide **11**. Cyclisation of **11** was achieved by dissolving the peptide in DMF (5 mg mL<sup>-1</sup>) and TMP (24 eq.) and PyClock (4 eq.) were added and the mixture stirred for 6 h. Volatile components were removed *in vacuo* and the resulting residue was treated with a small volume of TFA and precipitated with cold Et<sub>2</sub>O to yield crude peptide **12**. Finally peptide **12** was dissolved in a solution of 10% piperidine in DMF and mixed for 1 h. Volatile components were removed *in vacuo* and the resulting residue was treated with a small volume of TFA and crude peptide was precipitated with cold Et<sub>2</sub>O. The precipitate was purified by RP-HPLC to give **1229U91**.

In the same way, peptide **VII**, was prepared by coupling linear precursors **6** and **7** to give **13** followed by OAll/Aloc deprotection, and cyclisation and Fmoc-deprotection. Peptide **III** was prepared in the same way from linear peptides **8** and **9**.

## Conjugation methods

Compound **VIII** was achieved by dissolving purified 1229U91 (1 eq.) in DMF and DIPEA (12 eq.) and adding a solution of the NHS-activated Rhodamine B derivative<sup>33</sup> (0.7 eq.) in DMF which was stirred for 2 h.

The click reaction to prepare peptide **IX** involved dissolving the purified peptide **IV** (1 eq.) in H<sub>2</sub>O and adding a solution of the azidocoumarin<sup>34</sup> (4 eq.) in DMF to give a 1 : 3 ratio of H<sub>2</sub>O to DMF. Copper sulfate (10 eq.), TBTA (10 eq.) and sodium ascorbate (10 eq.) were then added and the reaction mixed for 3 h.

## Receptor binding methods

**Preparation of membranes from mouse brain.** To test the Y<sub>1</sub>R affinity of the synthesised ligands, receptor binding assays (described below) were performed on crude membranes prepared from the brains of Y<sub>2</sub>R- and Y<sub>4</sub>R-deficient mice (Y<sub>2</sub>-/-Y<sub>4</sub>-/-), where Y<sub>1</sub>R accounts for the majority of remaining Y receptors. Membranes were prepared following modified membrane extraction protocol published elsewhere.<sup>46</sup> In brief, fresh frozen Y<sub>2</sub>-/-Y<sub>4</sub>-/- mouse brains were cut into small cubes and homogenised in ice-cold homogenisation buffer (50 mM Tris-HCl, 10 mM NaCl, 5 mM MgCl<sub>2</sub>, 2.5 mM CaCl<sub>2</sub>, pH = 7.4, supplemented with 1 mg mL<sup>-1</sup> bacitracin (250 000 U; Calbiochem-Novabiochem., La Jolla, CA, USA) prior to use on ice with a glass homogeniser (Wheaton, USA) using 30 strokes. Subsequently, the homogenates were centrifuged at 32 000g for 15 minutes at 4 °C. The resulting pellet was re-suspended in ice-cold homogenisation buffer and re-homogenised using 30 strokes on ice, followed by centrifugation at 32 000g for 15 minutes at 4 °C to obtain the final pellet. The final pellet was re-suspended in ice-cold homogenisation buffer and flash frozen in liquid nitrogen. The protein concentration of the suspension was determined using Bradford protein assay (Quick Start™ Bradford Protein Assay, Bio-Rad Laboratories Pty., Ltd, Hercules, CA, USA).

## Cell culture

HEK293 T and 293TR cells (Invitrogen) were cultured in Dulbecco's modified Eagle's medium (DMEM, Sigma-Aldrich) supplemented with 10% foetal bovine serum, and passaged when confluent by trypsinisation (0.25% w/v in Versene). Mixed population 293TR cell lines inducibly expressing Y receptors tagged with C terminal GFP, and dual stable HEK293 cell lines expressing Y receptor-Yc and β-arrestin2-Yn (where Yc and Yn are complementary fragments of YFP), have both been described elsewhere.<sup>36,47</sup>

## [<sup>125</sup>I]PYY radioligand binding assays

Competition assays were performed on Y<sub>2</sub>-/-Y<sub>4</sub>-/- mouse brain membrane preparations or 293TR Y1 receptor GFP membranes following procedures published previously.<sup>36,46,47</sup> Briefly, for mouse brain preparations, equal volumes (25 μL) of non-radioactive ligands and <sup>125</sup>I-human polypeptide YY (<sup>125</sup>I-hPYY, 2200 Ci mmol<sup>-1</sup>; PerkinElmer Life Science Products, Boston,

MA, USA) were added into each assay. The final concentration of <sup>125</sup>I-hPYY in the assay was 25 pM. The binding of <sup>125</sup>I-hPYY was competed by Y<sub>1</sub>R ligands of interest at increasing concentrations ranging from 10<sup>-12</sup> M to 10<sup>-6</sup> M. Non-radioactive human PYY (Auspep, Parkville, VIC, Australia) at 10<sup>-6</sup> M was used as the non-specific binding control. The reaction was initiated by the addition of 50 μL of membrane suspension containing 30 μg of protein into the assay mixture and incubated for 2 hours at room temperature. After the incubation, each sample was layered with 200 μL of pre-cooled (4 °C) horse serum and centrifuged at 13 000g for 4 minutes to separate of bound from free <sup>125</sup>I-PYY. The supernatant solution was removed and resultant pellet was harvested and counted for radioactivity using a γ-counter (Wallac 1470 WIZARD® Gamma Counter; PerkinElmer Life Sciences, Turku, Finland).

Using membranes from the 293TR Y1 receptor-sfGFP cell line (after tetracycline induction, prepared as Kilpatrick<sup>36,47</sup>), competition binding assays were performed for 90 min at 21 °C in buffer (25 mM HEPES, 2.5 mM CaCl<sub>2</sub>, 1.0 mM MgCl<sub>2</sub>, 0.1% bovine serum albumin, 0.1 mg mL<sup>-1</sup> bacitracin; pH 7.4), increasing concentrations of unlabelled ligands (10<sup>-12</sup> M to 10<sup>-6</sup> M, duplicate) and [<sup>125</sup>I]PYY (15 pM). Membrane bound radioligand was separated by filtration through Whatman GF/B filters soaked in 0.3% polyethyleneimine on a Brandel cell harvester, and retained radioactivity was quantified using a gamma-counter (Packard Cobra II, Perkin Elmer, Waltham MA, U.S.A.). Non-specific binding in these experiments comprised less than 5% of total counts, and was subtracted from the data.

In both sets of data, IC<sub>50</sub> values were calculated from displacement curves (repeated 2–4 times for each peptide, fitted using non-linear least squares regression in GraphPad Prism 5.01 (Graphpad software, San Diego CA, U.S.A.). The assays using membrane preparations from Y2Y4 knockout animals gave a less uniform distribution of results than the recombinant cell assay data. The IC<sub>50</sub> values and 95% confidence interval measure was selected as more suitable to describe the variability of this data set. In the recombinant cell assay data, the Cheng–Prusoff equation was used to convert IC<sub>50</sub> measurements to pK<sub>i</sub> values (±SEM).

## Functional analysis of Y receptor–arrestin recruitment

This analysis used bimolecular fluorescence complementation (BiFC) based detection of Y receptor – β-arrestin2 association, as described previously (Kilpatrick refs). Y1 arrestin or Y2 arrestin BiFC cell lines were seeded at 40 000 cells per well onto poly-D-lysine coated 96 well black clear bottomed plates (655090, Greiner Bio-One, Gloucester, U.K.), and experiments were performed once cells reached confluence at 24 h. Medium was replaced with DMEM/0.1% bovine serum albumin (BSA), and if appropriate cells were pretreated for 20 min at 37 °C with 1229U91 analogues (3–100 nM). NPY, PP (Bachem, St. Helens, U.K.) or other ligands were then added for 60 min (10<sup>-11</sup> M–3 × 10<sup>-6</sup> M, triplicate wells). Incubations were terminated by fixation with 3% paraformaldehyde in phosphate buffered saline (PBS, 10 min at 21 °C), the cells



were washed once with PBS and the cell nuclei were stained for 15 min with the permeable dye H33342 ( $2 \mu\text{g ml}^{-1}$  in PBS, Sigma). H33342 was then removed by a final PBS wash. Images (4 central sites per well) were acquired automatically on an IX Ultra confocal platereader (Molecular Devices, Sunnyvale CA, U.S.A.), equipped with a Plan Fluor 40 $\times$  NA0.6 extra-long working distance objective and 405 nm/488 nm laser lines for H33342 and sfGFP excitation respectively.

An automated granularity algorithm (MetaXpress 5.1, Molecular Devices) identified internal fluorescent compartments within these images of at least 3  $\mu\text{m}$  diameter (range set to 3–18  $\mu\text{m}$ ). For each experiment, granules were classified on the basis of intensity thresholds which were set manually with reference to the negative (vehicle) or positive (1  $\mu\text{M}$  NPY, or 100 nM PP) plate controls. The response for each data point was quantified as mean granule average intensity per cell, from assessment of 12 images (4 sites per well in triplicate), normalised to the reference agonist response. Concentration response curves were fitted to the pooled data by non-linear least squares regression (Graphpad Prism), and antagonist  $\text{pK}_\text{b}$  values were calculated from agonist curve shifts using the Gaddum equation ( $\text{pK}_\text{b} = \log[\text{CR} - 1] - \log[\text{B}]$ , where  $[\text{B}]$  is the antagonist concentration, and CR is the  $\text{EC}_{50}$  ratio for the agonist response in the presence and absence of antagonist).

### Fluorescent imaging of compound VIII

293TR Y1-GFP or Y4-GFP cells were seeded at 20 000 cells per well in poly-D-lysine coated 96 well imaging plates (Greiner 655090), treated with  $1 \mu\text{g ml}^{-1}$  tetracycline for 18–21 h and then used in experiments at confluence. Cells were incubated in HEPES-buffered saline solution (HBSS) including 0.1% BSA, H33342 ( $2 \mu\text{g ml}^{-1}$ ) and varying concentrations of competitor ligands ( $10^{-10}$  M to  $10^{-6}$  M) for 2 min, prior to the addition of compound VIII at a final concentration of 1 nM (Y1-GFP) or 100 nM (Y4-GFP). Incubations were continued for 30 min at 37  $^{\circ}\text{C}$ , after which the media was replaced with HBSS/0.1% BSA (to remove free compound VIII). The cells were immediately imaged (2 sites per well) on a Molecular Devices IX Micro epifluorescence platereader using excitation/emission filter sets appropriate for H33342 (DAPI), Y receptor-GFP (FITC), and the rhodamine ligand (TRITC). Read time was less than 10 min, and repeated “total” wells at the end of the read confirmed stable binding of the fluorescent ligand over this period. Bound ligand fluorescence was quantified by granularity analysis (2–3  $\mu\text{m}$  diameter granules; count per cell using MetaXpress), and normalised to positive (totals 100%) and negative (0%, presence of 1  $\mu\text{M}$  NPY) controls. NPY and BIBO3304  $\text{IC}_{50}$  values were then determined using Graphpad Prism, as for radioligand binding.

### Acknowledgements

This work was supported by CRC for Biomedical Imaging Development (CRC-BID), Australia. ML was supported by an Australian Post-graduate Award scholarship.

### References

- 1 K. Tatemoto, *Proc. Natl. Acad. Sci. U. S. A.*, 1982, **79**, 5485–5489.
- 2 J. G. Wettstein, B. Earley and J. L. Junien, *Pharmacol. Ther.*, 1995, **65**, 397–414.
- 3 S. P. Sheikh, *Am. J. Physiol. Gastrointest. Liver Physiol.*, 1991, **261**, G701–G715.
- 4 A. G. Blomqvist and H. Herzog, *Trends Neurosci.*, 1998, **20**, 294–298.
- 5 C. Cabrele and A. G. Beck-Sickinger, *J. Pept. Sci.*, 2000, **6**, 97–122.
- 6 M. Ruscica, E. Dozio, M. Motta and P. Magni, *Curr. Top. Med. Chem.*, 2007, **7**, 1682–1691.
- 7 N. Sato, Y. Ogino, S. Mashiko and M. Ando, *Expert Opin. Ther. Pat.*, 2009, **19**, 1401–1415.
- 8 R. C. Alfred Meurs, G. Ebinger, Y. Michotte and I. Smolders, *Curr. Top. Med. Chem.*, 2007, **7**, 1660–1674.
- 9 Y. Dumont, P. Gaudreau, M. Mazzuferi, D. Langlois, J. G. Chabot, A. Fournier, M. Simonato and R. Quirion, *Br. J. Pharmacol.*, 2005, **146**, 1069–1081.
- 10 M. Keller, G. Bernhardt and A. Buschauer, *ChemMedChem*, 2011, **6**, 1566–1571.
- 11 Y. Dumont, J.-A. St-Pierre and R. Quirion, *NeuroReport*, 1996, **7**, 901–904.
- 12 H. N. Doods, H. A. Wieland, W. Engel, W. Eberlein, K.-D. Willim, M. Entzeroth, W. Wienen and K. Rudolf, *Regul. Pept.*, 1996, **65**, 71–77.
- 13 A. Brennauer, S. Dove and A. Buschauer, *Neuropeptide Y and related peptides*, Springer, Berlin Heidelberg, 2004.
- 14 H. A. Wieland, W. Engel, W. Eberlein, K. Rudolf and H. N. Doods, *Br. J. Pharmacol.*, 1998, **125**, 549–555.
- 15 C. Mollereau, H. Mazarguil, D. Marcus, I. Quelven, M. Kotani, V. Lannoy, Y. Dumont, R. Quirion, M. Detheux, M. Parmentier and J.-M. Zajac, *Eur. J. Pharmacol.*, 2002, **451**, 245–256.
- 16 J. J. Leban, D. Heyer, A. Landavazo, J. Matthews, A. Aulabaugh and A. J. Daniels, *J. Med. Chem.*, 1995, **38**, 1150–1157.
- 17 A. Balasubramaniam, V. C. Dhawan, D. E. Mullins, W. T. Chance, S. Sheriff, M. Guzzi, M. Prabhakaran and E. M. Parker, *J. Med. Chem.*, 2001, **44**, 1479–1482.
- 18 E. M. Parker, C. K. Babij, A. Balasubramaniam, R. E. Burrier, M. Guzzi, F. Hamud, G. Mukhopadhyay, M. S. Rudinski, Z. Tao, M. Tice, L. Xia, D. E. Mullins and B. G. Salisbury, *Eur. J. Pharmacol.*, 1998, **349**, 97–105.
- 19 D. Zwanziger, D. L. Ilka Bóshme and A. G. Beck-Sickinger, *J. Pept. Sci.*, 2009, **15**, 856–866.
- 20 B. Guérin, V. Dumulon-Perreault, M.-C. Tremblay, S. Ait-Mohand, P. Fournier, C. Dubuc, S. Authier and F. Bénard, *Bioorg. Med. Chem. Lett.*, 2010, **20**, 950–953.
- 21 B. Guérin, S. Ait-Mohand, M.-C. Tremblay, V. Dumulon-Perreault, P. Fournier and F. Bénard, *Org. Lett.*, 2010, **12**, 280–283.

- 22 M. Pourghiasian, J. Inkster, N. Hundal, F. Mesak, B. Guérin, S. Ait-Mohand, T. Ruth, M. Adam, K.-S. Lin and F. Bénard, *J. Nucl. Med.*, 2011, **52**, 1682.
- 23 A. J. Daniels, J. E. Matthews, R. J. Slepatis, M. Jansen, H. Viveros, A. Tadepalli, W. Harrington, D. Heyer, A. Landavazo, J. J. Leban and A. Spaltenstein, *Proc. Natl. Acad. Sci. U. S. A.*, 1995, **92**, 9067–9071.
- 24 S. S. Hegde, D. W. Bonhaus, W. Stanley, R. M. Eglen, T. M. Moy, M. Loeb, S. G. Shetty, A. Desouza and J. Krstenansky, *J. Pharmacol. Exp. Ther.*, 1995, **275**, 1261–1266.
- 25 J. E. Matthews, M. Jansen, D. Lyerly, R. Cox, W.-J. Chen, K. J. Koller and A. J. Daniels, *Regul. Pept.*, 1997, **72**, 113–119.
- 26 L. H. Pheng, Y. Dumont, A. Fournier, J.-G. Chabot, A. Beaudet and R. Quirion, *Br. J. Pharmacol.*, 2003, **139**, 695–704.
- 27 C. Walther, K. Morl and A. G. Beck-Sickinger, *J. Pept. Sci.*, 2011, **17**, 233–246.
- 28 A. J. Daniels, D. Heyer, A. Landavazo, J. J. Leban and A. Spaltenstein, Preparation of peptides as Neuropeptide Y antagonists, WO 94/00486, 1994.
- 29 A. Balasubramaniam, W. Zhai, S. Sheriff, Z. Tao, W. T. Chance, J. E. Fischer, P. Eden and J. Taylor, *J. Med. Chem.*, 1996, **39**, 811–813.
- 30 D. Chatenet, R. Cescato, B. Waser, J. Rivier and J. C. Reubi, *Biopolymers*, 2011, **96**, 469–469.
- 31 M. J. Lew, R. Murphy and J. A. Angus, *Br. J. Pharmacol.*, 1996, **117**, 1768–1772.
- 32 N. Thieriet, J. Alsina, E. Giralt, F. Guibé and F. Albericio, *Tetrahedron Lett.*, 1997, **38**, 7275–7278.
- 33 T. Nguyen and M. B. Francis, *Org. Lett.*, 2003, **5**, 3245–3248.
- 34 M. A. Kamaruddin, P. Ung, M. I. Hossain, B. Jarasrassamee, W. O'Malley, P. Thompson, D. Scanlon, H. C. Cheng and B. Graham, *Bioorg. Med. Chem. Lett.*, 2011, **21**, 329–331.
- 35 K. E. McCrea and H. Herzog, *Methods Mol. Biol.*, 2000, **153**, 231–239.
- 36 L. E. Kilpatrick, S. J. Briddon and N. D. Holliday, *Biochim. Biophys. Acta*, 2012, **1823**, 1068–1081.
- 37 M. Keller, D. Erdmann, N. Pop, N. Pluym, S. Teng, G. Bernhardt and A. Buschauer, *Bioorg. Med. Chem. Lett.*, 2011, **19**, 2859–2878.
- 38 E. Schneider, M. Keller, A. Brennauer, B. K. Hoefelschweiger, D. Gross, O. S. Wolfbeis, G. Bernhardt and A. Buschauer, *ChemBioChem*, 2007, **8**, 1981–1988.
- 39 M. Fabry, M. Langer, B. Rothen-Rutishauser, H. Wunderli-Allenspach, H. Hocker and A. G. Beck-Sickinger, *Eur. J. Biochem.*, 2000, **267**, 5631–5637.
- 40 L. E. Kilpatrick, S. J. Briddon, S. J. Hill and N. D. Holliday, *Br. J. Pharmacol.*, 2010, **160**, 892–906.
- 41 L. A. Stoddart, A. J. Vernal, J. L. Denman, S. J. Briddon, B. Kellam and S. J. Hill, *Chem. Biol.*, 2012, **19**, 1105–1115.
- 42 R. Rink, A. Arkema-Meter, I. Baudoin, E. Post, A. Kuipers, S. A. Nelemans, M. H. J. Akanbi and G. N. Moll, *J. Pharmacol. Toxicol. Methods*, 2010, **61**, 210–218.
- 43 A. Aletras, K. Barlos, D. Gatos, S. Koutsogianni and P. Mamos, *Int. J. Pept. Protein Res.*, 1995, **45**, 488–496.
- 44 S. A. Kates, S. B. Daniels and F. Albericio, *Anal. Biochem.*, 1993, **212**, 303–310.
- 45 W. C. Chan, B. W. Bycroft, D. J. Evans and P. D. White, *J. Chem. Soc., Chem. Commun.*, 1995, 2209–2210.
- 46 S. M. Okarvi, *Eur. J. Nucl. Med.*, 2001, **28**, 929–938.
- 47 L. E. Kilpatrick and N. D. Holliday, *Methods Mol. Biol.*, 2012, **897**, 109–138.